

QUANTITATIVE COMPARISON ON THE PERFORMANCE OF AN INFILTRATION (IT) DRAIN SYSTEM



Master of Science Thesis
Faculty of Civil Engineering & Geosciences
MSc. Hydraulics Engineering

Author
Neo Hong Chuan
Student number: 4066618
14 June 2011

Author

Neo Hong Chuan, BSc
Delft University of Technology
Specialisation Hydraulics Engineering
Student number: 4066618
neo.hong.chuan@gmail.com

Graduation committee
Delft University of Technology



Prof. dr. ir. N.C. van de Giesen
Faculty Civil Engineering & Geosciences
Department of Water Resources
Management
N.C.vandeGiesen@tudelft.nl

Dr.ir. P.J. Visser
Faculty Civil Engineering & Geosciences
Department of Hydraulics Engineering
P.J.Visser@tudelft.nl

Delft University of Technology and
Deltares, Dutch research institute



Dr.ir. F.H.M. van de Ven
Faculty Civil Engineering & Geosciences
Department of Water Resources
Management
Deltares: department of Urban Water
Management
Frans.vandeVen@deltares.nl

ir. A.J.J. Vergroesen
Faculty Civil Engineering & Geosciences
Department of Water Resources
Management
Deltares: department of Hydrology
Toine.Vergroesen@deltares.nl

Preface

“One cannot reflect in streaming water. Only those who know internal peace can give it to others. - Lao Tzu”

This thesis report is the final result of the Master of Science graduation project within the Double-Degree Programme (DDP) between Faculty of Civil Engineering (Hydraulics Engineering and Water Resources Management track) in National University of Singapore (NUS) and Hydraulics Engineering specialisation study program at the Faculty of Civil Engineering & Geosciences of the Delft University of Technology (TUD). While some would argue that the marriage between two diverse backgrounds is fraught with challenges, that brought me here into this programme as I believe diversity brings strength and robust solutions to ever-changing situations, which would reduce our vulnerabilities.

This investigation was made possible with all the kind assistance and advice from various parties and individuals from Singapore and Netherlands. They include Public Utilities Board (PUB), Singapore Delft Water Alliance (SDWA), National University of Singapore (NUS), Delft University of Technology (TUD), Tauw, Eindhoven Municipality, Deltares (Water Management and Hydrology) and many other helpful individuals.

In this preface, I would like to thank those who have helped me in one way or another. First and foremost, I am grateful to PUB and my supervisors for sponsoring and supporting my postgraduate studies in this DDP. This lays my very first foundation slab towards this Masters programme.

Next, I would like to thank TUD, Tauw (Amsterdam & Eindhoven), Eindhoven Municipality and Deltares for providing me the opportunity to conduct this challenging investigation in Prinsejagt. The experience and lessons learnt during this project are both extraordinary and unforgettable.

My special gratitude goes to my primary supervisor and committee member Toine Vergroesen. He was instrumental in advising me on my investigation approach and suggesting ways to overcome any site and time constraints that I faced from time to time. His guidance and knowledge of site investigation studies and suggestions have very much contributed towards the structure of my thesis.

Moreover, I would also like to extend my sincerest appreciation toward my other committee members, Nick van de Giesen, Frans van de Ven, Paul Visser and May Chui Ting Fong (NUS) for their valuable feedback and advice during the entire thesis. Frans van de Ven's enthusiasm on infiltration system had inspired me to take up this Low-impact Development-related study. During the three-committee meetings, their encouragements and support were a major driving force for me to continue with the investigation.

Eelco Verschelling, from Deltares, has kindly shared his insights on infiltration drains modelling. During the site measurement phase (between February and May 2011), I received fantastic assistance from Tauw's Floris Boogaard and his fellow colleagues (namely Hans and Barry who even accompanied me to site for measurements at times). Tauw had

carried out previous investigation on the IT system in Prinsejagt in 2003 after it was recently installed; this provides a baseline condition for my investigation, and most of all, a first-hand experience on how the investigation and the site-setup could be carried out.

Apart from sharing their expertise (equipment and knowledge), they introduced me to Luuk Postmes (Eindhoven Municipal) who subsequently gave us the green light to proceed with the investigation studies at Prinsejagt. Much gratitude is expressed towards Luuk Postmes, who has provided me much of his valuable advice on the infiltration system installed, and his gracious support in mobilizing the site preparation prior to the actual monitoring scheme. I would like to acknowledge the support of Tauw, Deltares, Eindhoven municipality and Ben Murreau, from Wavin, for the closed-loop test carried out in short notice.

Special thanks go to TUD's Wim Luxemburg, Stijn Jong and Betty Rothfusz (Nick's secretary) for providing me with the logistics and administrative support throughout my measurement period. Furthermore, I would like to thank Ms Helena Nijdam, resident of Serlioweg no. 12, for her kindness in allowing us to site our rain gauge within her premise.

Lastly, and most importantly, I am thankful to my friends, family and dear wife for their support throughout this period. Their unwavering faith in me gave me strength and fighting spirit to overcome the challenges I encountered during my entire study and research period.

Delft, June 2011
Hong Chuan

Executive summary

The hydrological effects of urbanization affect the rainfall-runoff regime of many cities in the world. While traditional stormwater drainage systems are often able to effectively serve the function of flood control, they increase downstream peak flows and do not provide a habitat to support a healthy aquatic ecosystem.

The Low Impact Development (LID) is an alternative approach in managing stormwater runoff. Its main philosophy is to replicate the pre-development hydrological properties of water catchment. It seeks to first infiltrate, filter, store and retaining the surface runoff near to its source before draining it to downstream. Some examples of LIDs include green roofs, permeable pavement, vegetated swales, infiltration drains, bioretention cells (also known as rain gardens).

One type of LIDs, infiltration drains, has been used in Netherlands quite extensively. While infiltration drains seem to be a viable solution to reduce the flooding problem in the Netherlands, it is important to find out its current performance after years of operation. Existing researches or studies of infiltration drain system concentrate on its performance when it is newly installed. Studies that look into performance of an existing system that has been put into operation for quite some time are still quite rare.

In order to investigate the effectiveness of infiltration drain systems after they have been used for some time, a case study in Prinsejagt, Eindhoven will be used. Data from previous studies is available to allow for comparison on the performance of infiltration drains after ~10 years of installation.

The main research goal and main research question is to determine the percentage reduction in exfiltration rate at the measurement site as compared to initial readings derived from previous research. My secondary research goals are 1) How can we describe the processes involved in the performance of an infiltration drain system? 2) How does the infiltration drains develop after 10 years of usage? Do they clog every year? 3) How can we forecast the performance of the infiltration drain for its useful lifespan and perhaps introduce a maintenance plan to restore its performance?

Methodology

To achieve the above goals, the research focuses on determining the percentage reduction in exfiltration rate at the measurement site as compared to initial readings derived from previous research. It involves the monitoring of water levels at the same locations of the infiltration (IT) drain system in Prinsejagt (as carried out the previous monitoring scheme in 2003) and to carry out IT drain model simulations. In addition, closed-loop tests were conducted at four selected stretches of infiltration pipes to ascertain the exfiltration properties of the particular stretch of pipe. Our research approach consisted of two main components: qualitative and quantitative. First, we explain about the phenomenon observed at our monitoring site qualitatively before applying quantitative approaches (like graphical, curve-fitting and simulation methods) to assess the percentage reduction in exfiltration rates at the monitoring locations. Graphical approach gives quick but rough estimates; Curve-fitting is relatively accurate and straightforward to apply; simulation requires us to derive the differential equation first (to explain the physical phenomenon

within the infiltration pipe) before we can proceed with the calibration of model, the differential equations are solved and approximated using Runge Kuta 4 method on an Excel spreadsheet. Using the simulation results, we arrived at a projected clogging rate in which we used to predict the future system exfiltration rate.

Results

From the 2003 and 2011 water level trends, the monitoring locations exhibit system behaviour and there is linear relationship of the water level trend among the respective locations. Moreover, it was found that the groundwater level plays a significant role in influencing the performance of the infiltration drain system in 2011. At groundwater level of NAP+15.85m or above, less than 25% of the infiltration drain system can start to exfiltrate its water; this groundwater interference reduces tremendously the system exfiltration rate [L^3/T]. Therefore, both the system behaviour (of the infiltration drains) coupled with the influence of groundwater level determine the overall performance of the infiltration drain system at Prinsejagt. Moreover, we compiled a system K-values curve for different groundwater level.

Each of the quantitative analysis approaches gave slightly different percentage reduction in average exfiltration rates for location A. Graphical method gives a range of 47% reduction, while the curve-fitting tells us that the percentage drop is 30%. We verified that a linear mathematical function can adequately describe the water level trends to an accuracy of 0.01m RMSE for all monitoring locations. Simulation results give us a 10% drop in exfiltration rate. Using a 'clogging' model, we derived the IT drain system curve for the maximum exfiltration rate over its useful lifespan. It is believed that by Year 2021, the maximum exfiltration will drop to $49.7m^3/day$ which is a 20% drop in performance as compared to the initial $62.2m^3/day$ in 2003.

Lastly, the K-values of the four closed-loop tests which are between 0.0039 to 0.05m/day, this difference in the K values at the individual pipe section could be attributed to differences in localised conditions (soil profiles, groundwater level and degree of clogging).

Conclusions and recommendations

A minimum 10% reduction in the exfiltration rate is noted. Regular maintenance to clear any accumulated sediment inside IT drains should be done and it is recommended that once the maintenance works is done (e.g. using pressure-jet), monitoring on the infiltration drain system performance should commence so as to determine its effectiveness in increasing the overall system permeability.

Moreover, water quality monitoring in IT drain system could be implemented to prevent any contamination to groundwater resources. In lowering the pipe invert level of the entire IT system, the IT system performance can be enhanced during low groundwater period.

Of all the three approaches, we would recommend to use the curve-fitting method to get a quick insight of the reduction in exfiltration rates.

Contents

Preface.....	iii
Executive summary	v
List of Figures	ix
List of Tables	xii
1 Introduction.....	1
1.1 Urbanisation and Water.....	1
1.2 Urban water management and Low impact Development (LID)	1
1.3 Scope of the research	2
1.4 Main research goals and main research question.....	2
1.5 Research approach	3
1.6 Structure of report.....	3
2 Literature review.....	5
3 Prinsejagt Case Study Site	7
3.1 Introduction to Prinsejagt case study	7
3.2 Why this site was selected	9
3.3 Physical site setup and scope of investigation	9
4 Qualitative Description on the Experimental Findings	16
4.1 Introduction.....	16
4.2 Overview of the infiltration drain system	16
4.3 Water level trends	18
4.4 System behaviour at all monitoring locations in 2003 and 2011.....	35
4.5 Experimental results from the closed-loop test.....	38
4.6 Additional analysis to study the characteristics of the infiltration system.....	41
5 Quantitative comparison of exfiltration rates in 2003 and 2011.....	43
5.1 Introduction.....	43
5.2 Graphical method	44
5.3 Analysis of average rate of water level drop using Graphical method	48
5.4 Curve-fitting method.....	49
5.5 Selection of mathematical function to be used for curve-fitting analysis.....	54
5.6 Analysis of average rate of water level drop using Curve-fitting method.....	56
6 Excel simulation using the derived differential equation (dh/dt)	58

6.1	Introduction.....	58
6.2	Derivation of differential equation.....	58
6.3	Simulation of closed-loop test results	63
7	Analysis of results	74
7.1	Introduction.....	74
7.2	Comparison and analysis of results for the three approaches	74
7.3	Forecast of the system exfiltration rate trend	75
8	Conclusion	78
8.1	Answers to our Primary research objective	78
8.2	Answers to our Secondary research objectives	80
9	Recommendations and Discussion	82
9.1	Improvement to existing research.....	82
9.2	Proposed new areas of research	82
9.3	Proposed improvement measures for the Prinsejagt measurement site	83
	Literature List.....	87
Appendix 1	Verification of water levels at the monitoring locations during site visits....	88
Appendix 2	The locations and details of the selected stretch of infiltration pipes for closed-loop test are indicated in map below.	90
Appendix 3	Diver & rain gauge specifications and short description of infiltration pipe	91
Appendix 4	Daily precipitation and potential evapotranspiration plot (10 – 20 May 2011), details on groundwater monitoring locations and general soil profile at Prinsejagt monitoring site	96
Appendix 5	The highlighted locations show where the “lower-than-normal” invert level of infiltration drains (betw NAP+14.8 – NAP+15.4m).....	99
Appendix 6	Graphical method for location C, E & F	100
Appendix 7	Scatter plots between all monitoring locations for monitoring period in 2003 and 2011	103
Appendix 8	Water trends of closed-loop test at locations: Point 2 and Point 4.....	110
Appendix 9	ln (dh/dt) vs ln (h) plots for 3 to 13 November 2003 for Locations A - F....	111
Appendix 10	Definitions on the statistics used to determine the goodness-of-fit:.....	117
Appendix 11	For remaining curve-fitting of rain events using 3 different mathematical functions for Location A	120
Appendix 12	Curve-fitting using linear function at Locations B, C, D, E, F and Pt7	130
Appendix 13	Summary of the equations of water level trends derived from curve-fitting method	151

List of Figures

Figure 1: Google map of the Prinsejagt catchment area, located in 51028'01.90" N, 5027'44.63" E	7
Figure 2: Average precipitation south of Netherlands (figure extracted from (Boogaard, 2006))	8
Figure 3: Map of Eindhoven and the measurement site at Prinsejagt	8
Figure 4: Schematic diagram of a diver installed inside a manhole to measure the water level the infiltration drain	9
Figure 5: Schematic diagram on the closed-loop test	11
Figure 6: Photos on the procedure of closed-loop test Clockwise from top-left - 1. Installing of isolation plug; 2. Pressuring the plug to at least 3 bars (Right picture); 3. Pumping water into the manhole once the affected pipe has been isolated, then lower in the diver (measuring device).....	11
Figure 7: Locations of 6 measurement points (A – F) excluding the surface water monitoring location, and the 5 selected stretches of infiltration pipe for closed-loop test (1-5)	12
Figure 8: Groundwater level trend for September to November 2003 (above) and February to May 2011 period (below).....	13
Figure 9: Groundwater level trends at WL021 (groundwater monitoring point) from end 1998 till May 2011	14
Figure 10: Sobek representation on the respective invert level of infiltration drains	16
Figure 11: Graph on the ratio of the length of IT pipeline with respect to its invert level [m above NAP]	17
Figure 12 Water levels at monitoring location A including lowest invert level of connected infiltration pipes and overflow weir level, from 25 September to 13 November 2003	18
Figure 13: Water levels at monitoring location B including lowest invert level of connected infiltration pipes and overflow weir level, from 25 September to 13 November 2003.....	18
Figure 14: Water levels at monitoring location C including lowest invert level of connected infiltration pipes and overflow weir level, from 25 September to 13 November 2003.....	19
Figure 15: Water levels at monitoring location D including lowest invert level of connected infiltration pipes, from 25 September to 13 November 2003	19
Figure 16: Water levels at monitoring location E including lowest invert level of connected infiltration pipes, from 25 September to 13 November 2003.....	20
Figure 17: Water levels at monitoring location F including lowest invert level of connected infiltration pipes, from 25 September to 13 November 2003.....	20
Figure 18: Water levels at monitoring location A including the groundwater level and invert levels of connected infiltration pipes from 10 February to 20 May 2011.....	22
Figure 19: Schematic diagram of the pipe connectivity at monitoring location A.....	22
Figure 20: Existing condition of one of the 300mm diameter infiltration pipe at location A.....	23
Figure 21: Water levels at monitoring location B including the groundwater level and invert levels of connected infiltration pipes from 10 February to 20 May 2011.....	24
Figure 22: Schematic diagram of the pipe connectivity at monitoring location B.....	24
Figure 23: Existing condition of the 400mm diameter infiltration pipe at location B.....	25

Figure 24: Water levels at monitoring location C including the groundwater level and invert levels of connected infiltration pipes from 10 February to 20 May 2011.....	26
Figure 25: Schematic diagram of the pipe connectivity at monitoring location C.....	26
Figure 26: Existing condition of the 500mm diameter infiltration pipe at location C.....	27
Figure 27: Water levels at monitoring location D including the groundwater level and invert levels of connected infiltration pipes from 10 February to 20 May 2011.....	28
Figure 28: Schematic diagram of the pipe connectivity at monitoring location D.....	28
Figure 29: Existing condition of the 250mm diameter infiltration pipe at location D.....	29
Figure 30: Water levels at monitoring location E including the groundwater level and invert levels of connected infiltration pipes from 10 February to 20 May 2011.....	30
Figure 31: Schematic diagram of the pipe connectivity at monitoring location E.....	30
Figure 32: Existing condition of 400mm diameter infiltration pipe at location E.....	31
Figure 33: Water levels at monitoring location F including the groundwater level and invert levels of connected infiltration pipes from 10 February to 20 May 2011.....	32
Figure 34: Schematic diagram of the pipe connectivity at monitoring location F.....	32
Figure 35: Existing condition of one of the 300mm diameter infiltration pipe at location F..	33
Figure 36: Water levels at monitoring location 7 (surface water near monitoring location B) including the groundwater level from 10 February to 20 May 2011.....	34
Figure 37: Existing condition of surface water system (near monitoring location B).....	34
Figure 38: Water level trends at all the monitoring locations during 25 September to 13 November 2003 (top) and 10 February to 20 May 2011 (bottom).....	35
Figure 39: Scatter plot of water levels at locations A and B for entire 2003 monitoring period (top) Scatter plot of water levels at location A and B for entire 2011 monitoring period (below).....	36
Figure 40: Zoom in view of silt accumulated up to almost the pipe crown level at location Point 1.....	38
Figure 41: Water level trend at location Point 3.....	39
Figure 42: Water level trend at location Point 5.....	39
Figure 43: Schematic view of the infiltration pipe and the surrounding soil.....	40
Figure 44: General trend of water level development in the infiltration drain system.....	41
Figure 45: Graphical method used at Location A for 10 October – 2 November 2003 period	45
Figure 46: Graphical method used at Location A for 3 – 27 April 2011 period.....	45
Figure 47: Graphical method used at Location B for 10 October – 2 November 2003 period.....	46
Figure 48: Graphical method used at Location B for 3 – 27 April 2011 period.....	46
Figure 49: Graphical method used at Location D for 10 October – 2 November 2003 period.....	47
Figure 50: Graphical method used at Location D for 3 – 27 April 2011 period.....	47
Figure 51: Curve-fitting method for Location A during 18 to 24 October 2003.....	51
Figure 52: Curve-fitting method for Location A during 29 April to 7 May 2011.....	53
Figure 53: Symbols used and their definitions for differential equation.....	59
Figure 54: Schematic diagram of connectivity of manhole and IT pipes location A.....	61

Figure 55: (left) Radial flow pattern, K1; (right) modified and reduced radial flow pattern, K2.....	63
Figure 56: Plot of simulated and measured water levels at location Point 2.....	64
Figure 57: Plot of simulated and measured water levels at location Point 3.....	64
Figure 58: Plot of simulated and measured water levels at location Point 4.....	64
Figure 59: Plot of simulated and measured water levels at location Point 5.....	64
Figure 60: Plot of simulated and measured water levels at location A (18 – 29 March 2011).....	67
Figure 61: Plot of simulated and measured water levels at location A (3 – 10 April 2011).....	67
Figure 62: Plot of simulated and measured water levels at location A (12 – 26 April 2011).....	67
Figure 63: Plot of simulated and measured water levels at location A (29 April – 7 May 2011).....	67
Figure 64: Relation of K1 and K2 with different groundwater levels during 2011 monitoring period.....	68
Figure 65: System exfiltration rate [L^3/T] at various system water level for different groundwater level conditions.....	69
Figure 66: Plot of maximum exfiltration rate for different groundwater levels observed in 2011.....	70
Figure 67: Plot of simulated and measured water levels at location A (15 – 21 October 2003).....	71
Figure 68: Plot of simulated and measured water levels at location A (29 April – 7 May 2011).....	71
Figure 69: Difference in the system exfiltration rate [m^3/hr] between 2003 and 2011 for the respective water levels in the infiltration system.....	72
Figure 70: Prediction of the progress of K values over time using the ‘clogging’ model.....	76
Figure 71: System exfiltration rate in 2003, 2011 and predicted system exfiltration rate for 2021.....	76
Figure 72: System exfiltration rate that can be derived by lowering the overall pipe invert level for the infiltration system by 0.2m for 2011 scenario.....	84
Figure 73: Prediction of maximum system exfiltration rate over time.....	85

List of Tables

Table 1: Factsheet about Prinsejagt catchment	7
Table 2: Comparison of average rate of water drop between 2003 and 2011 data.....	48
Table 3: Assessment of mathematical functions for various events occurring at Location A	54
Table 4: Percentage reduction of exfiltration rates at the respective monitoring locations .	56
Table 5: Percentage reduction of exfiltration rates at the respective monitoring locations after factoring the influence of groundwater level	57
Table 6: K1, K2 and RMSE values obtained for closed-loop tests	65
Table 7: Summary of K1 and K2 values for various groundwater level at location A	68
Table 8: Comparison table of K2 values obtained from simulation for 2003 and 2011 data .	71
Table 9: Comparison of K values of closed-loop test and location A (system)	73
Table 10: Comparison on the values of average rate of water level drop obtained from the three approaches	74

1 Introduction

1.1 Urbanisation and Water

Water is the primary source of life. It covers more than 80% of the Earth's surface yet a mere 10% is clean enough for direct consumption. Water is used for food production, transportation, energy production, domestic (drinking, washing, bathing) and industries (for cooling and other processes) and even in cultural festivals (for example in Thailand).

There is a close link between the survival of a city to its ability to secure clean and adequate water supply and manage the water resources in a sustainable fashion.

From United Nations estimates (UN, 2010), urbanization is expected to continue rising in both the more developed and the less developed regions and, by 2050, the world population is expected to be 69% urban.

Without adequate planning and sound policy, rapid urbanization may lead to water issues like water shortage, flooding, and contamination of water sources within cities. The severity of the water issue is further compounded by climate change bringing higher frequency of floods, droughts, storms and other unexpected extreme events. Therefore, there is an urgent need for us to transform the way we plan, build and manage our cities in order to make them liveable and sustainable. The creative forces of humanity have to be harnessed to combat the complexity of climate change and cities have to protect citizens from both the excesses and shortages of water.

1.2 Urban water management and Low impact Development (LID)

City developments (urbanization) will most often lead to increased proportion of non-pervious surfaces, and this non-pervious surface causes more surface runoff. If not managed properly, this will lead to higher frequencies of flooding which is undesirable. The conventional approach to flood management is to convey away the surface runoff, as fast as possible, downstream during rainstorms through stormwater drainage. However, by passing the surface runoff (load) downstream, we also increase the risk of flooding downstream when the drainage network downstream also experiences a heavy rainstorm.

The Low Impact Development (LID) is an alternative approach in managing stormwater runoff. Its main philosophy is to replicate the pre-development hydrological properties of water catchments. It seeks to first infiltrate, filter, store and retain the surface runoff near to its source before draining it downstream. It uses natural features to protect water quality.

Although flooding can still occur in undeveloped natural environment, these natural environments that consist of mainly permeable surface allow more easily precipitation to

infiltrate into the soil and be stored before being discharged into the surface water. Urbanisation alters the hydrological conditions of the environment as more impervious surfaces are introduced (like residential and commercial buildings, roads). The permeable surfaces (vegetated flood plains, natural parks) help to reduce the peak flows during storm events. In addition, more contaminants may be carried along with the higher peak flow and cause pollution to the precious water resources. Some of the common LIDs include green roofs, permeable pavement, vegetated swales, infiltration drains, bioretention cells (also known as rain gardens).

While LID seems to be a viable solution to reduce the flooding problem, we want to investigate its performance after the LID (in particular infiltration drain system) has been put into operation for some time. A case study in Prinsejagt, Eindhoven will be used.

1.3 Scope of the research

This Msc thesis will focus on making quantitative comparison on the performance of an infiltration (IT) drain system when it was newly installed and the current performance. This research is a collaboration involving various parties like Deltares, Gemeente Eindhoven, Tauw and Wavin (in carrying out closed loop test).

Existing researches or studies of IT drain concentrate on its performance when it is newly installed; Studies that look into performance of an existing system which has been put into operation for quite some time are still quite rare. It is useful to study the performance of IT drains after they have been put into use for some time, in order to determine the effectiveness of IT drains over the long-term. The selected measurement site of my case-study is Prinsejagt. It is located within the Eindhoven municipal and data of previous measurement from this site is also available. Measurements will be taken to ascertain the current exfiltration properties of the infiltration drain system, further make comparisons on the profile of IT drains performance over time and perhaps even make suggestions as to when replacement or maintenance should be carried out in order to prevent any gross underperformance of the IT drain system.

1.4 Main research goals and main research question

1. To determine the percentage reduction in exfiltration rate at the measurement site as compared to initial readings derived from previous research (Boogaard, 2006)

Secondary research goals:

2. How can we describe the processes involved in the performance of an infiltration drain system?
3. How does the infiltration drains develop after 10 years of usage? Do they clog every year?
4. How can we forecast the performance of the infiltration drain for its useful lifespan and perhaps introduce a maintenance plan to restore its performance?

1.5 Research approach

Through the problem description, research goals, research scope and research approach, we define our general direction and approach of this research.

The literature review will help to provide us with an overview of the infiltration drain knowledge; concept and modelling techniques that could be deployed to evaluate the initial and current performance of the IT drain system. The Prinsejagt case study is selected to be our monitoring site for this study.

The available 2003 data will be analysed and used to generate infiltration drain models to describe the processes involved. Through this, we can assess the performance of the infiltration drain when it is recently installed. Then, we adopt the same approach (as data for 2003) with the collected 2011 data, in our analysis to obtain the current performance of infiltration drain now. These two data are subsequently compared against each other to determine the percentage of reduction in exfiltration performance.

Once we obtain satisfactory results on the processes within an infiltration drain, we will attempt to predict the future performance of the infiltration drain and also the schedule to carry out maintenance or replacement of pipes. Furthermore, we will check for any vulnerable areas that could be improved and suggest recommendations to improve the adaptive capacity of the Prinsejagt catchment.

1.6 Structure of report

Chapter 2 of this thesis contains the literature review as it presents an overview of the infiltration drain system.

Chapter 3 introduces us to the Prinsejagt case study and also talks about the experiments (periodic monitoring and closed-loop test) conducted together with an overview of the existing groundwater level monitoring.

Chapter 4 looks into the qualitative description on the experimental findings in 2003 and 2011 for the periodic monitoring and closed-loop test experiments. Moreover, additional analysis will be done to study and explain the characteristics of the infiltration drain system.

Chapter 5 seeks to compare quantitatively the difference in exfiltration rates between 2003 and 2011 experimental data using graphical and curve-fitting methods.

Chapter 6 contains description of the simulation conducted using a derived differential equation for firstly the closed-loop test; and secondly at one of the monitoring locations. We will subsequently seek to estimate the system exfiltration rate and make comparison between the 2003 and 2011 findings.

Chapter 7 gives the summary of the results obtained from the three approaches (graphical, curve-fitting and simulation) before we proceed to forecast the trend of system exfiltration rate for the next 10 years.

Chapter 8 provides the conclusion of the thesis findings.

The last chapter, Chapter 9 will provide the recommendations and discussion of the thesis research.

2 Literature review

Low Impact Developments (like Infiltration drain system) are often installed to reduce the surface runoff and also to manage drainage at its source. It allows surface runoff from impervious surface like roofs, roads to be stored underground temporarily before it infiltrates slowly into the surrounding soils (Woods-Ballard, 2007).

While there are extreme rain events that will eventually lead to flood of urban areas, Low Impact Development (LID) helps to reduce the degree of uncertainty brought in by climate change and its prediction by increasing the adaptive capacity of the urban environment to cope with more varied weather conditions (Annette Semadeni-Davies, 2008). This brings to the city/water planner some flexibility and valuable time to respond to these changes. Next, LID can help to reduce the peak flow experienced at downstream of the drainage system by retaining as much runoff at the current site, it minimises the need of the drainage system (downstream) to handle its upstream load. In addition, it helps to reduce the stormwater discharge to the sewer system hereby minimising the risk of combined sewer overflows. This is good water management practice as it reduces the risk of flooding downstream and combined sewer overflows. Moreover, with some simple filtration or treatment installed at the site, it can improve the water quality before discharging it to surface water or groundwater. Also, LID can act as a means to aid groundwater recharge by increasing the infiltration rates as compared to the impervious surfaces (van de Ven, 2010).

Studies show that the performance of infiltration systems will decrease over time due to clogging effects from entry of sediment (Revitt, 2003). Several field monitoring exercises were conducted at infiltration facilities to estimate the reduction in performance ((Lindsey, 1992) and (Dechesne, 2005)). Most of the clogging models are empirical ((Dechesne, 2004) and (Endo, 2009)) or derived from estimated amount of sediment particles entering the infiltration system (Siriwardene, 2007). To date, very few monitoring investigations focus on the infiltration drain systems that have been put into operation for 10 years or above.

While the advantages of LID are more widely recognised in recent times, the effectiveness of LID (in particular infiltration drain system) after it has been put into operation for some time (for example, 10 years) have not been investigated and understood adequately. This impedes the momentum or adoption rate of LID. In early 1990, Warnaaars et al. carried out monitoring for two infiltration trenches installed in a housing area in Nørrebro in central Copenhagen (Warnaaars, 1999). They monitored and assessed the performance of the infiltration system and further observed that during the short 3 year period of operation there were already signs of reduced performance.

In 2003, Boogaard et al. conducted ~2 months of monitoring for the infiltration drain system at Prinsejagt, Eindhoven after the infiltration drain system was put in operation for approximately 3 years (Boogaard, 2006). The objective of the monitoring is to determine the

performance of the infiltration system in relation to its local rainfall and groundwater level pattern. In their report, it was concluded that the longer emptying time of the infiltration drain system as compared to its design calculations could be due to higher groundwater tables, silting up of the infiltration drain system or lower permeability of soil. However, they are unable to determine whether there is any decrease in performance of the infiltration drain system since there was no baseline to compare with.

Bergman et al. recently conducted an investigation in 2009 to verify whether the reduction in performance of the infiltration system (in the earlier research done by (Warnaars, 1999)) is still happening and to determine the extent of clogging. They also presented a new, physically based, time-dependent clogging model for the prediction of future performance of the infiltration system (Bergman, 2010).

3 Prinsejagt Case Study Site

3.1 Introduction to Prinsejagt case study

Our measurement site at Prinsejagt, Figure 1, covers an area of approximately 24 hectares and is located in the northern part of Eindhoven city. Within the measurement site, the runoff from roof and road surfaces are disconnected to the infiltration drain system and there are three overflow points in this infiltration drain system where excess water can be discharged to the surface water located in the outskirts of this Prinsejagt area. Currently, the surface water in Prinsejagt measurement site does not have any external connection.

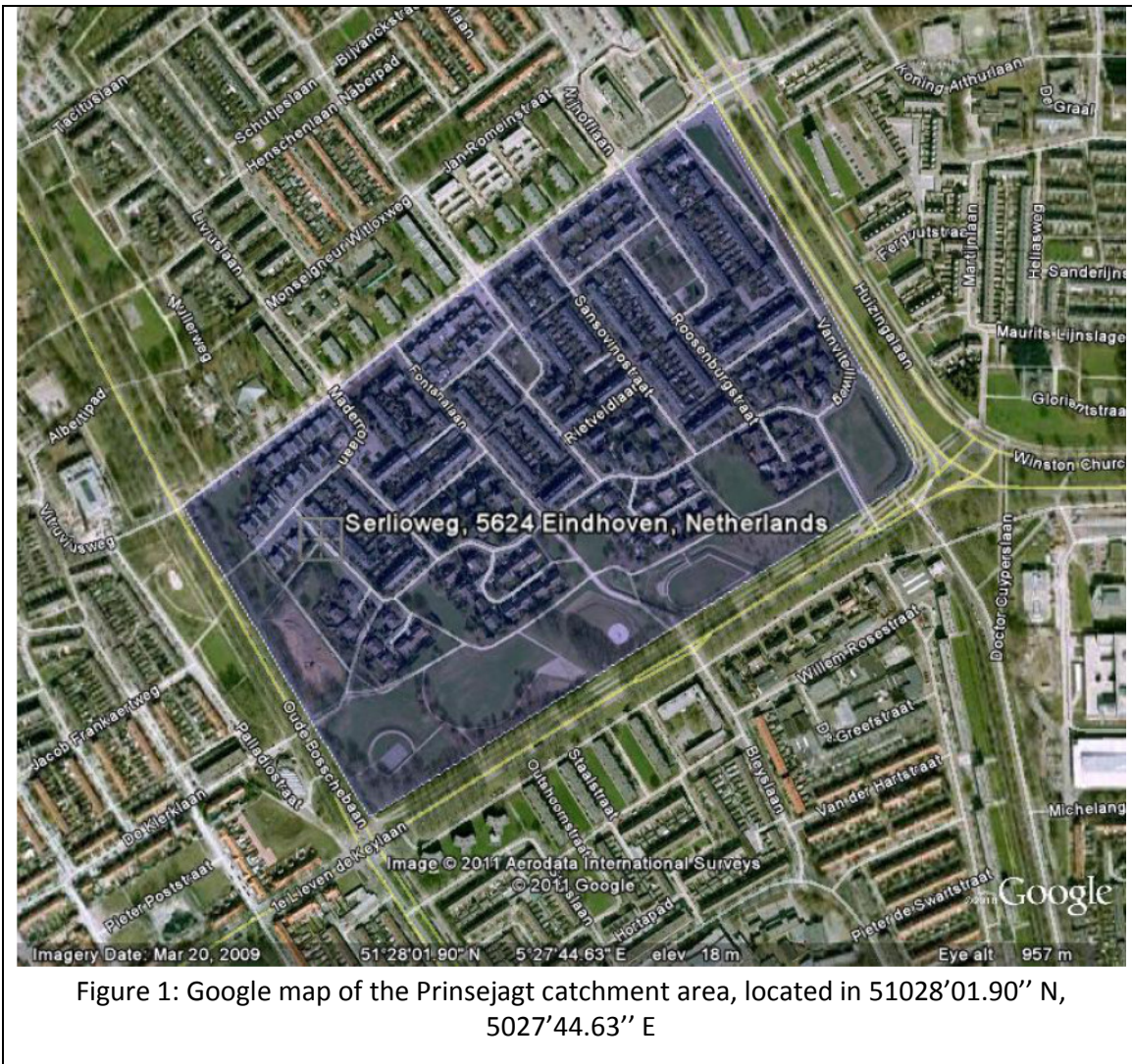


Table 1: Factsheet about Prinsejagt catchment

Gross area [m ²]	Impervious surface area [m ²]	Roof area [m ²]	Road area [m ²]
240000	68400	28600	39600

In the design of the infiltration drain system, it was assumed that the system could achieve a permeability of 1.5m/day and a recovery of 310m³. This would mean that for a total area of impervious surface of 68400m², the infiltration drain system can take in 4.53mm of rainfall daily before it starts to discharge water through its overflow facilities to the open surface water. The designed overflow level is set at NAP+16.40m level. The KNMI average annual rainfall (from KNMI data of 1971 to 2000) is around 775mm (Figure 2).

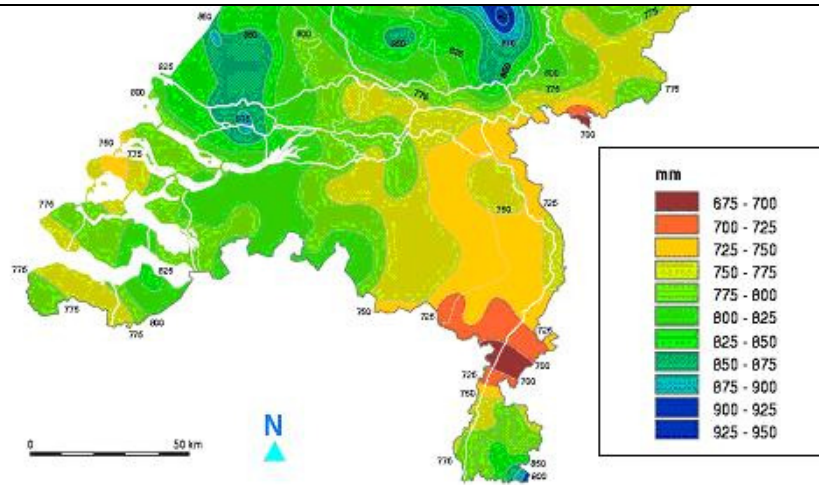


Figure 2: Average precipitation south of Netherlands (figure extracted from (Boogaard, 2006))

Rainfall monitoring stations in Eindhoven include a KNMI meteorological station location (within 5km radius) near the Eindhoven airport, Sportpark Woensel (within 1km radius) and Wastewater Treatment plant, RWZI (within 3km radius) where the last two locations measure rainfall on a daily basis. For their respective locations, please refer to Figure 3 below.

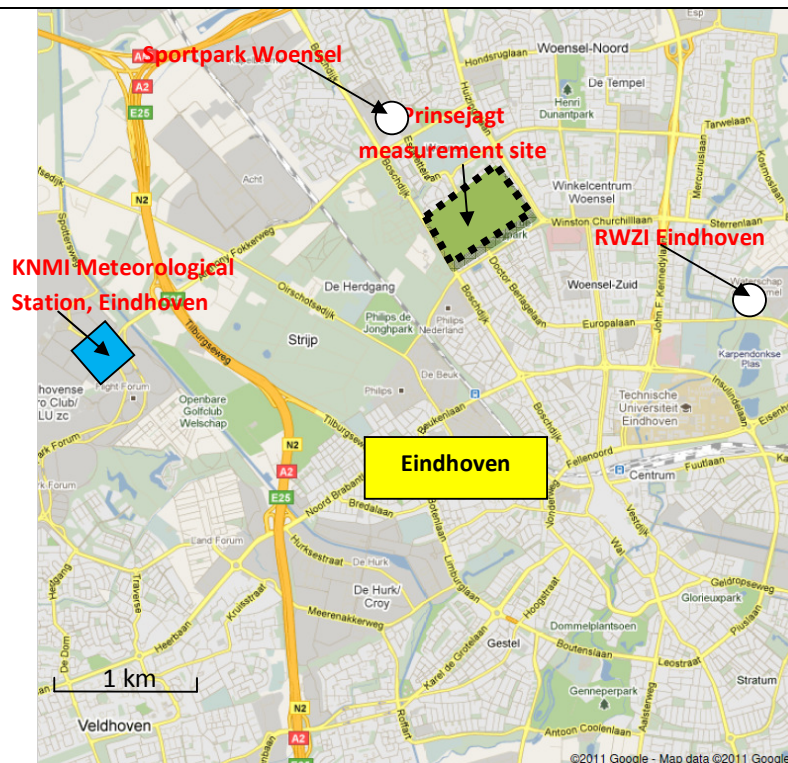


Figure 3: Map of Eindhoven and the measurement site at Prinsejagt

3.2 Why this site was selected

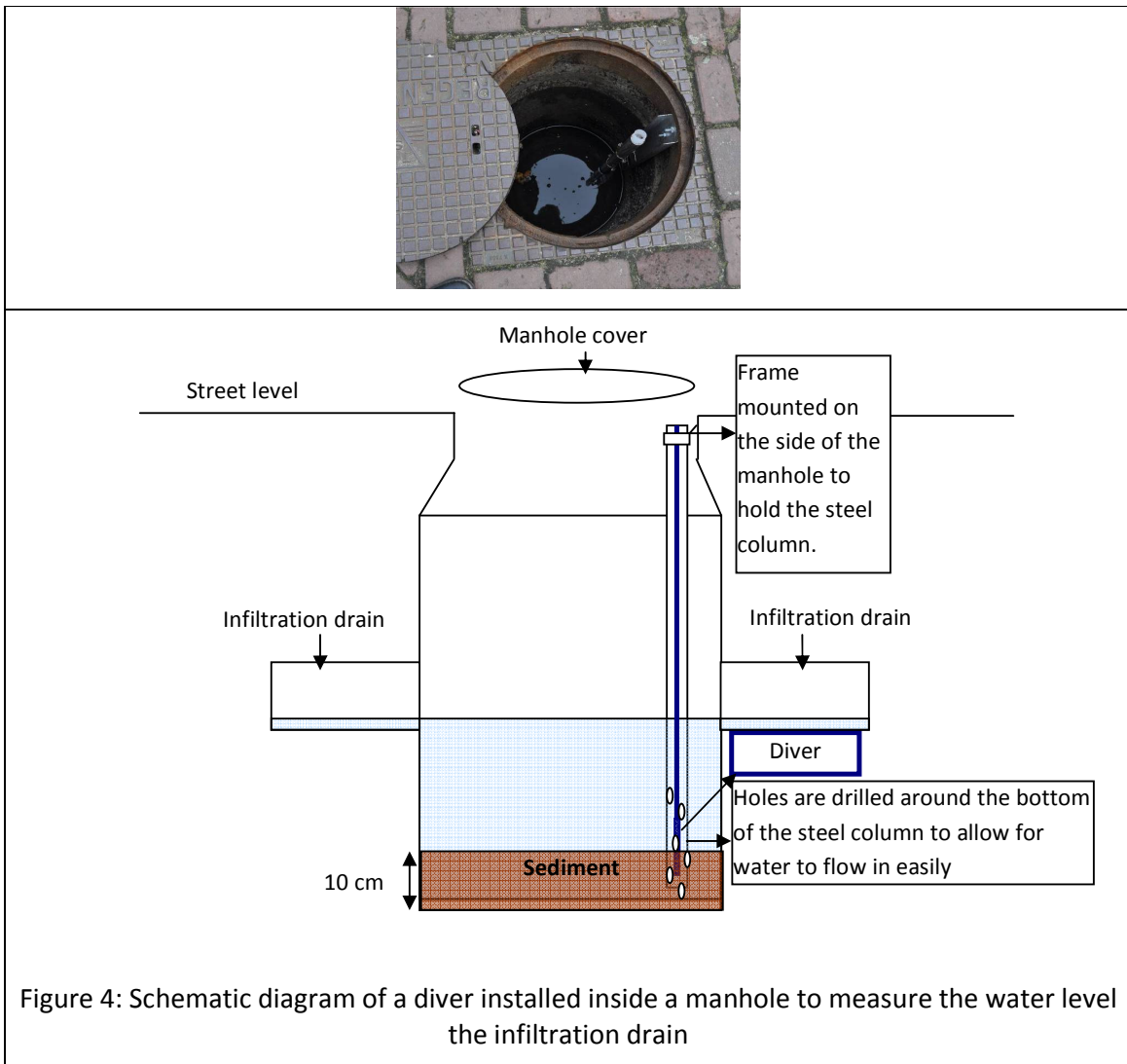
Data from previous studies in 25 September – 13 November 2003 (of ~ 2 months) is available to allow for comparison on the performance of infiltration drains after ~10 years of installation. No or little research has been done to determine the performance of infiltration drains after they have been put into use for more than 5 years.

3.3 Physical site setup and scope of investigation

We conducted two different types of experiment for our monitoring site. One is the periodic monitoring of water levels at the locations A-F and Point 7; and the other one is the closed-loop test for 5 selected sections of infiltration pipe.

Periodic monitoring at locations A-F and Pt 7

The duration of the period monitoring is approximately 3 months, from 10 February to 20 May 2011. In order to allow direct comparison of our 2011 results to the previous 2003 results, divers/loggers were installed at the six monitoring locations (same location as previous measurement taken in 2003) to measure their respective water levels in the system; and an additional diver was installed to monitor surface water level downstream of Location B. Please refer to Figure 4 for details of installation.



Verification of water levels at the monitoring locations

During all the four site visits, the water levels at the monitoring locations are taken and verified with the readings registered by divers. Moreover, efforts have been put in to ascertain the pipe crown and pipe invert levels, including the manhole bottom levels. These measurements have been verified to be in line with the as-constructed drawings provided by the municipality authorities. The detailed findings can be found in Appendix 1.

A point to note is that there will be some systematic or random errors involved when conducting site measurement. Nevertheless, it acts as a form of counter-check against the water level readings registered at the divers at the respective monitoring locations (A-F and Pt 7). The difference in water level (between the divers reading and site measurement) is within acceptable range of -0.09 to 0.03m for all monitoring locations (except for monitoring location F where it consistently records a difference of more than -0.1m, this could be due to error arising from different ground settlement at different site locations).

Closed-loop test

The duration of the closed-loop test is from 17 to 20 May 2011. The main objective of this test is to find out the exfiltration rate of the selected stretch of infiltration drain only. Before conducting the test, we have to plug the other sections of infiltration drains that are also connected to the selected manhole. This experiment is different from our periodic monitoring done at Locations A to F, we conduct the test in a relatively controlled environment by eliminating the possibility of water flowing toward the other infiltration drains when we fill the manhole with water to at least 0.5m above the pipe crown level (of the selected infiltration pipe). Doing so gives us an adequate level of certainty about the exfiltration capability for this particular stretch of infiltration pipe. Five sections of infiltration pipe at different locations within the Prinsejagt catchment area were selected for this test. They are located in various premises of Prinsejagt. The locations and details of the selected stretch of infiltration pipes can be found in Appendix 2.

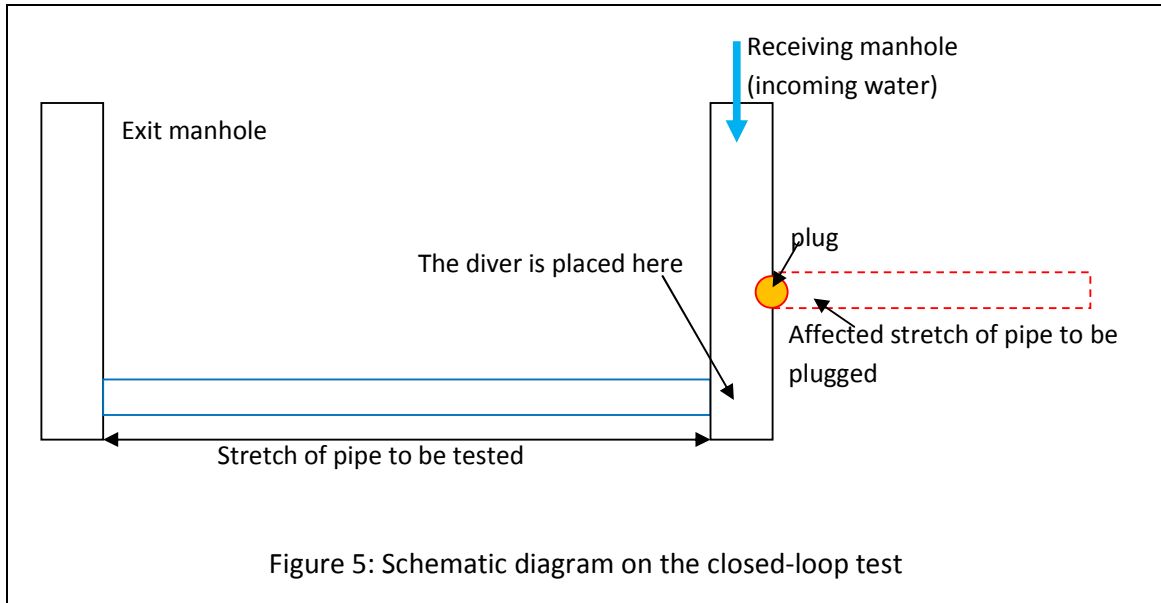
The required equipment for the test includes:

- 10m³ capacity Tanker;
- 6 Plugs (4 nos. of 0.25m diameter and 2 no. of 0.3m diameter); and
- Five divers (to be installed on one side of the *exit* manhole)

A short summary of the method statement (Figures 5 and 6):

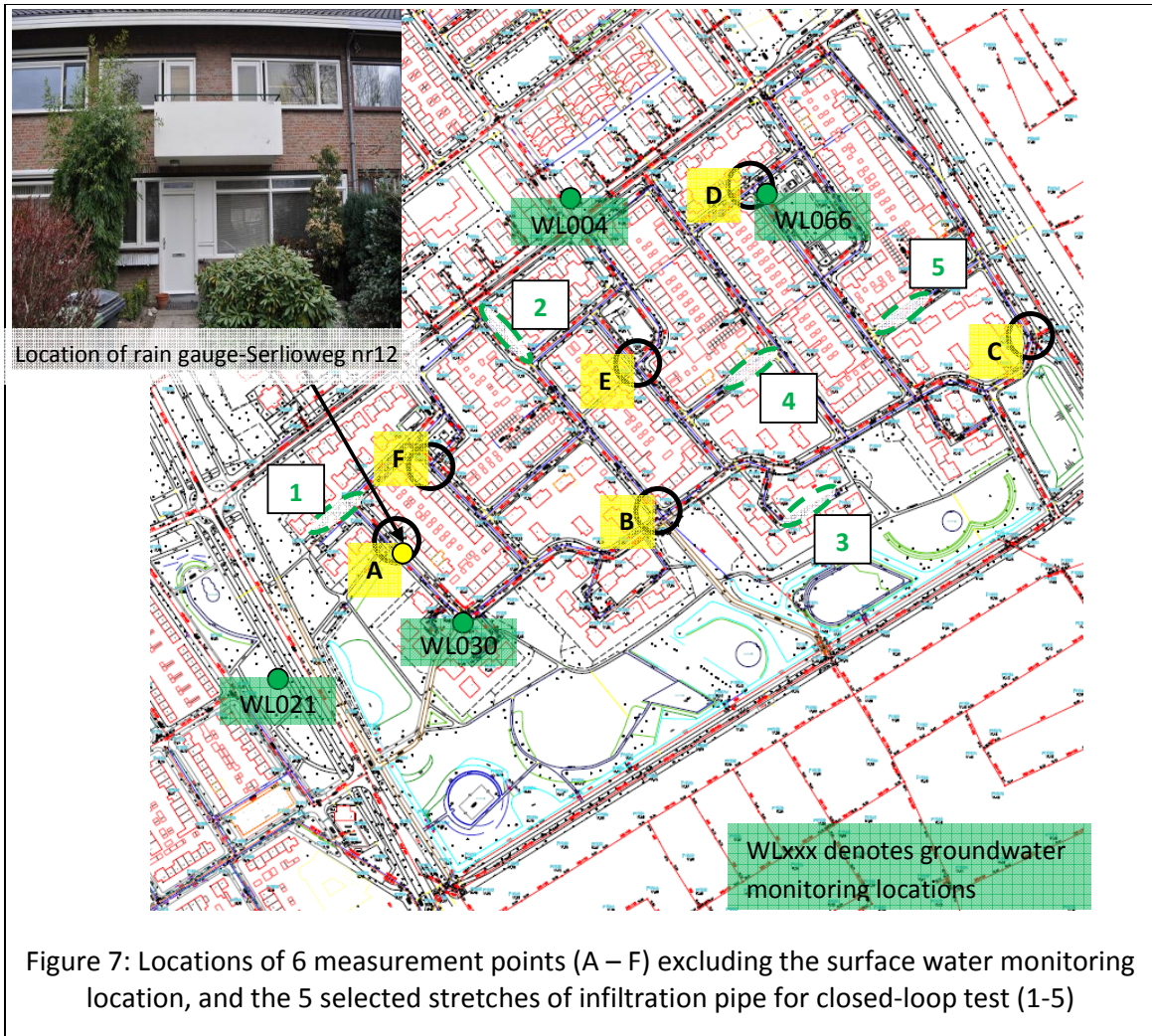
1. Measure the existing water level inside the manhole, and then proceed to plug the affected side of the pipe connections at the *receiving* manhole. The plug are pressurised to 3 bars atmospheric pressure to ensure that they stay water-tight throughout the 3-days test duration.
2. Pump water into the *receiving* manhole and place the diver
3. Monitor the water level raise at the *receiving* manhole to ensure that the entire stretch of pipe is filled to at least 0.5m above the pipe crown level

4. Take measurement on the starting water level with reference to the street level [m above NAP] since we have the manhole street level [m above NAP] from the drawings.
5. Retrieve the divers data and remove the plug for the affected stretch of pipe at the end of the test duration



Locations of periodic monitoring locations and closed-loop test

Figure 7 shows the locations of each individual periodic monitoring location, stretch of pipes designated for closed-loop test, groundwater monitoring points. Under our scheme, we have installed a total of 7 monitoring device at the periodic monitoring locations (A-F and Point 7) and tested 4 stretches of infiltration pipes (the pipe stretch at location 1 is not suitable for the closed-loop test as it was found to be covered with silt).



A (tipping bucket) rain gauge was also installed in the Prinsejagt catchment to collect rainfall data during the measurement period. For details on the specifications of the divers, rain gauge used and a short description of the infiltration drain installed in the measurement scheme, please refer to Appendix 3. Figure 7 shows the respective locations of the periodic monitoring (A-F), closed-loop test (1-5) and groundwater monitoring points (labelled with a prefix of WL).

Groundwater monitoring

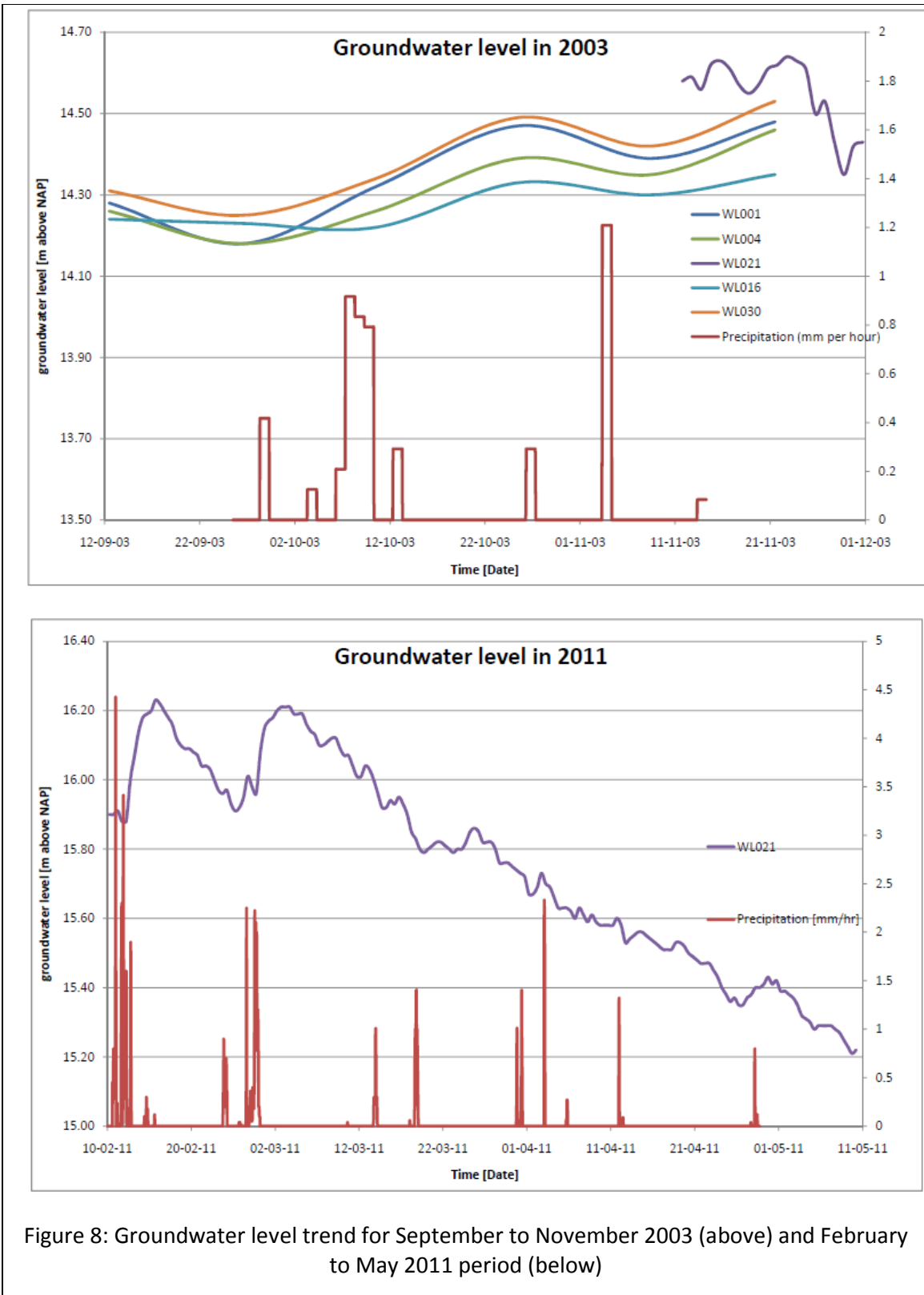


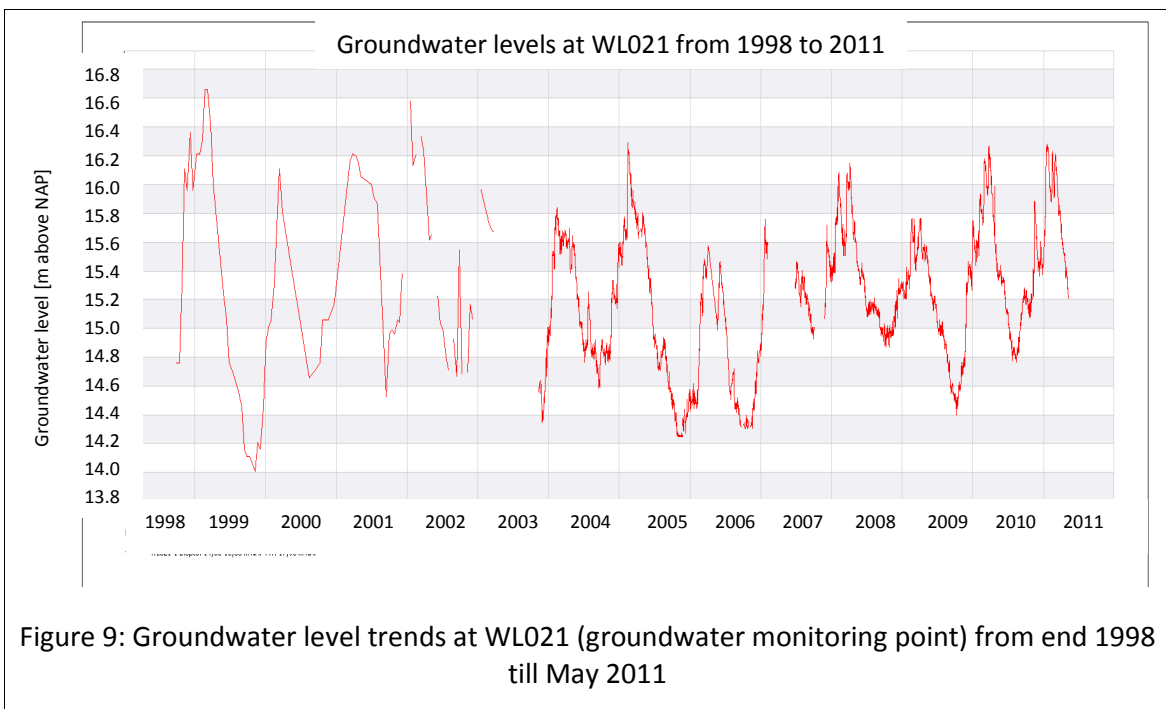
Figure 8: Groundwater level trend for September to November 2003 (above) and February to May 2011 period (below)

During the September – November 2003 monitoring period (Figure 8), the groundwater level measured had never exceeded NAP+14.70m. Thus it is consistently below the invert

levels of infiltration pipe in Prinsejagt. With the lowest pipe invert level in the Prinsejagt system at NAP+14.87m, the invert level of the infiltration system installed in Prinsejagt is always higher than the groundwater level during this period. As such, the infiltration process involved is under the unsaturated flow regime only.

During the early February to late March 2011 (Figure 8), we experienced high groundwater level where it is always higher than NAP+15.80m level. As such, some sections of the infiltration pipe system may be submerged or partially submerged in groundwater during our 2011 monitoring period. High groundwater level might affect the performance of the infiltration drain system to exfiltrate. In addition, even though the latest groundwater monitoring data we have for 2011 is until 10 May 2011, we are sure that the groundwater level will not exceed NAP+15.22m (as recorded on 10 May 2011) as the amount of evapotranspiration (from 10 – 20 May 2011) far exceeds the amount of rainfall (recharge). During 10 – 20 May 2011, the net precipitation is 6.59mm while the net potential evapotranspiration is 29.3mm.

Around 13 years of groundwater data (at WL021) is presented in the Figure 9 below. The groundwater level has a seasonal cyclic trend and the groundwater level fluctuation can be in the range of 2.2m (peak to trough), groundwater level generally tend to increase to its peak during end February period (end winter) before it starts to decline in mid spring and summer.



Moreover, previous studies have shown that Prinsejagt site has a loamy soil profile. All details on the evapotranspiration and rainfall data (obtained from KNMI website: <http://www.knmi.nl/klimatologie/uurgegevens/#no>), groundwater monitoring (obtained

from the Eindhoven municipality) and soil profile of Prinsejagt site can be found in Appendix 4.

We will discuss in details about groundwater effect on the performance of infiltration drain in the following chapters.

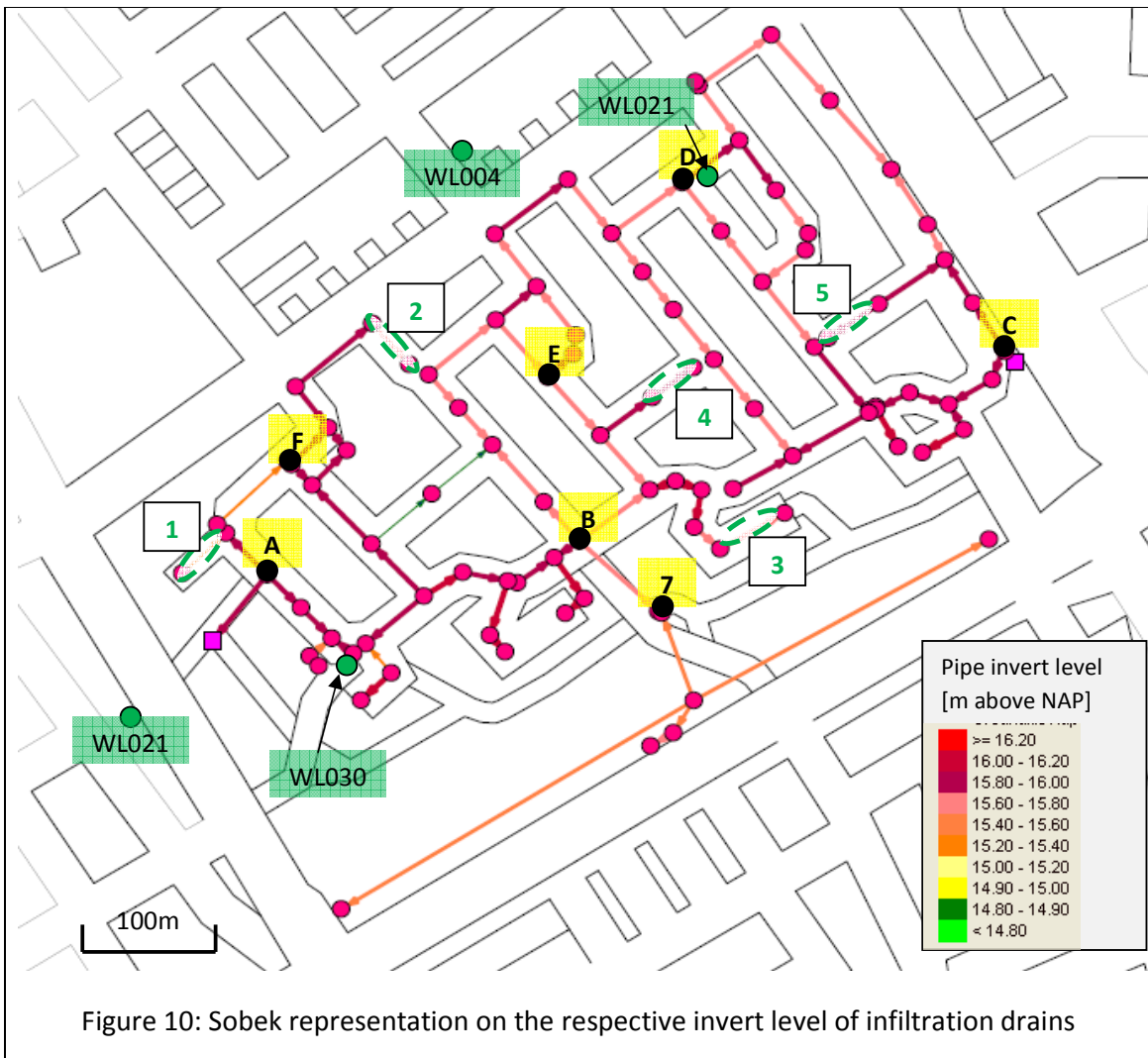
4 Qualitative Description on the Experimental Findings

4.1 Introduction

We will discuss on the experimental findings qualitatively in two parts. The first part is the periodic monitoring at locations A-F and Pt 7; and followed by the closed-loop test.

4.2 Overview of the infiltration drain system

The entire infiltration drain system is connected and thus it is important to have an overview of the system first. The diameter of infiltration pipes that were installed in Prinsejagt includes 250mm, 300mm, 400mm and 500mm. The pipe invert levels are plotted in Sobek (Figure 10) allow us to gain more insight on Prinsejagt infiltration system. Due to the differences in the invert levels of the infiltration pipe, we could see there are isolated sections within this system (catchment). These isolated sections may have an impact on the exfiltration rate depending mostly on the water level within the infiltration system and groundwater level. For a more detailed drawing indicating the 'lower-than-normal' invert levels of infiltration drain, please see Appendix 5.



Cumulative graph of the length of infiltration drain in Prinsejagt case study

Taking the pipe invert level as our reference, we have plotted a cumulative graph of the length of infiltration drain (Figure 11) to further aid in our understanding.

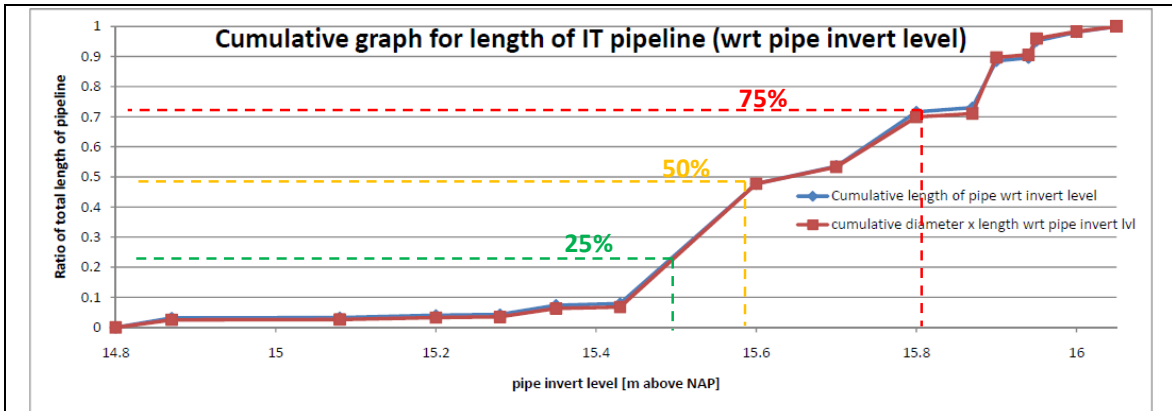


Figure 11: Graph on the ratio of the length of IT pipeline with respect to its invert level [m above NAP]

From the cumulative graph above, you will notice that ~75% of the infiltration drain network is below NAP+15.87m. So, when the groundwater level reaches NAP+15.87m, less than 25% of the infiltration drain within the network can function under the “unsaturated” soil condition. When part of the infiltration drain system is operating in near “saturated” soil condition, its exfiltration rate will be much slower than as compared to operating in “unsaturated” soil condition. Therefore, the groundwater level plays an important role when analyzing the exfiltration capabilities of the infiltration system. Depending on the design of the infiltration system, it can favourably or unfavourably influence the exfiltration rate of the infiltration drain network.

With this understanding, we will proceed to analyse qualitatively the water level trends observed during 2003 and 2011 monitoring periods at locations A-F and Pt 7; before we look at the closed-loop test results.

4.3 Water level trends

Water level trend observed at periodic monitoring Locations A – F in 2003

The plots of the water level trend for locations A to F are given in Figures 12 to 17 below.

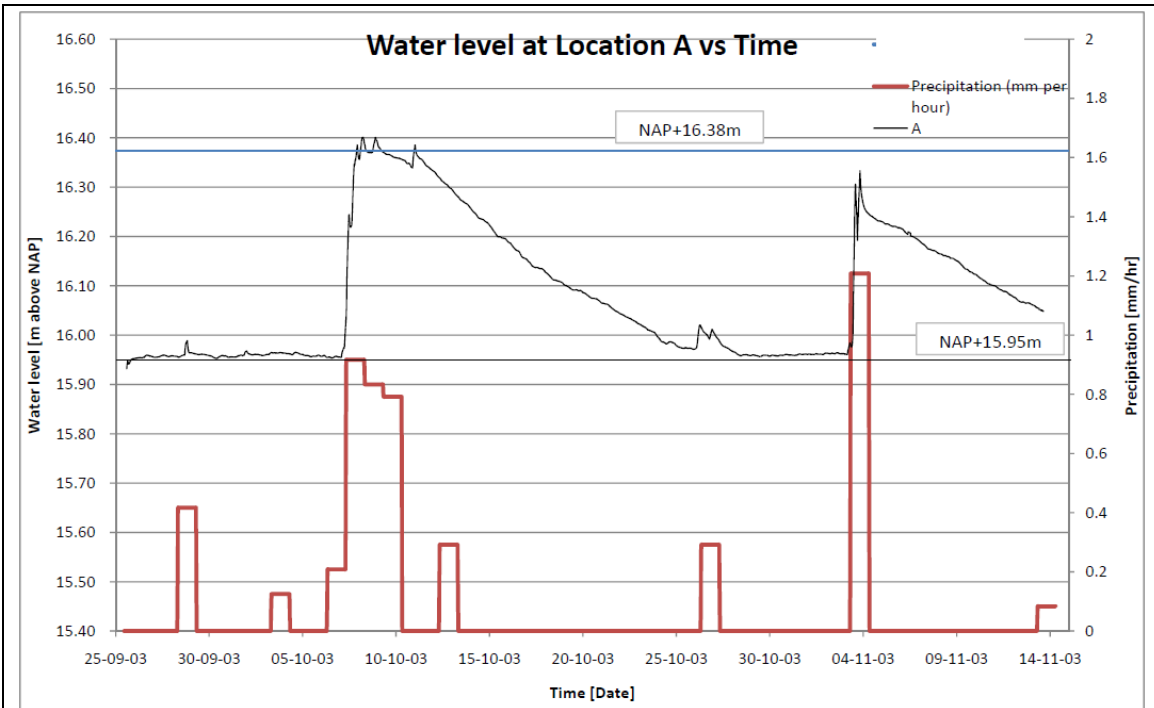


Figure 12 Water levels at monitoring location A including lowest invert level of connected infiltration pipes and overflow weir level, from 25 September to 13 November 2003

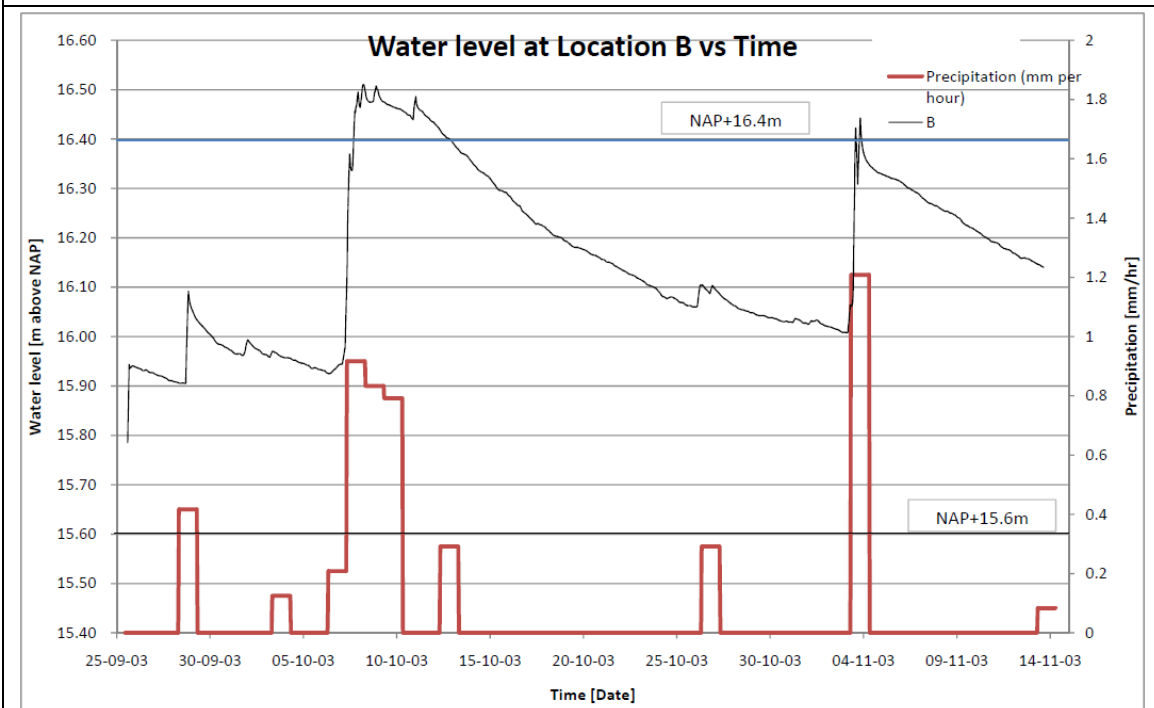


Figure 13: Water levels at monitoring location B including lowest invert level of connected infiltration pipes and overflow weir level, from 25 September to 13 November 2003

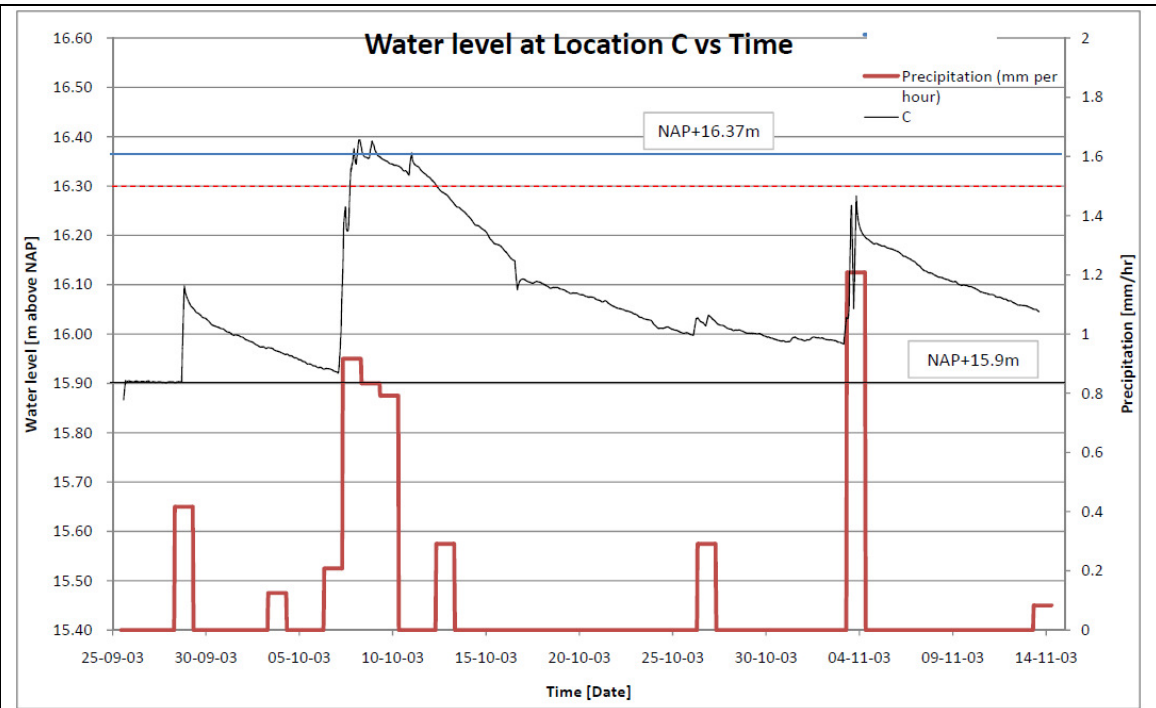


Figure 14: Water levels at monitoring location C including lowest invert level of connected infiltration pipes and overflow weir level, from 25 September to 13 November 2003

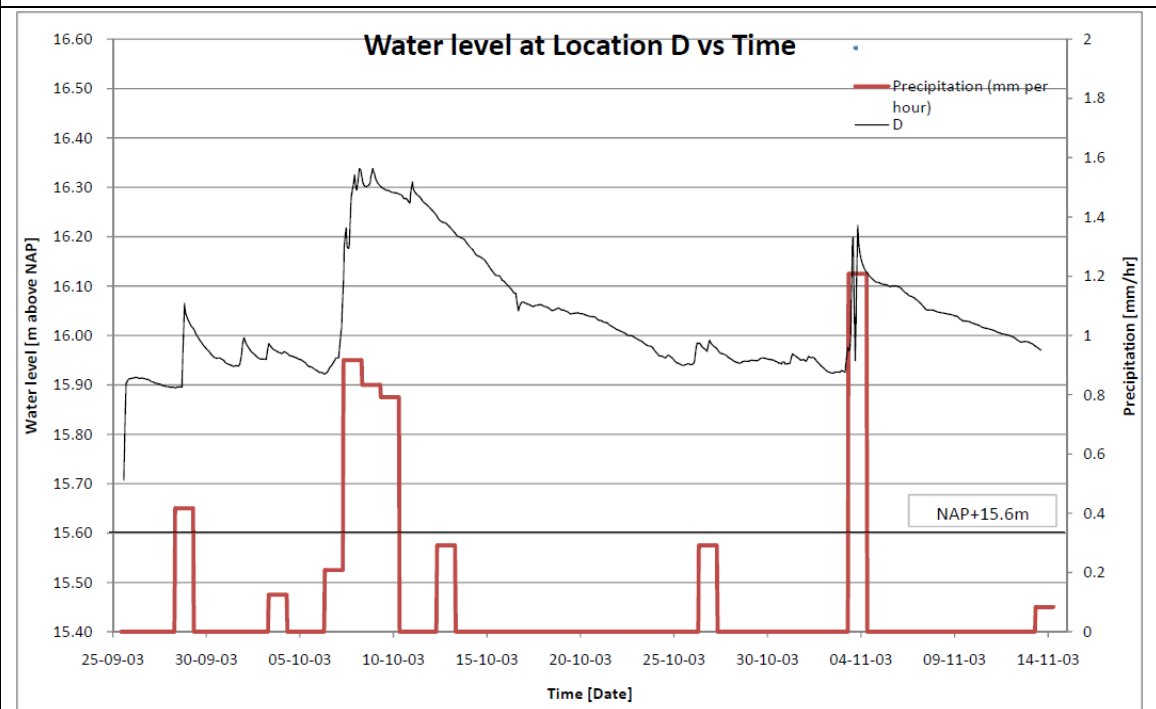


Figure 15: Water levels at monitoring location D including lowest invert level of connected infiltration pipes, from 25 September to 13 November 2003

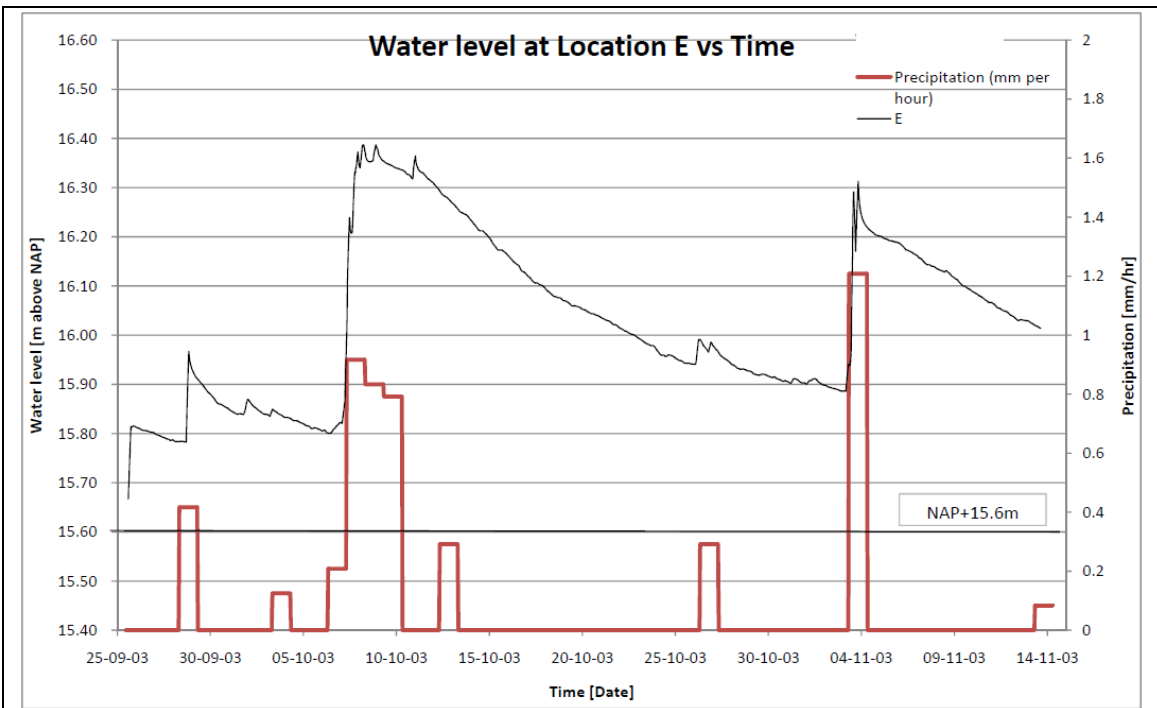


Figure 16: Water levels at monitoring location E including lowest invert level of connected infiltration pipes, from 25 September to 13 November 2003

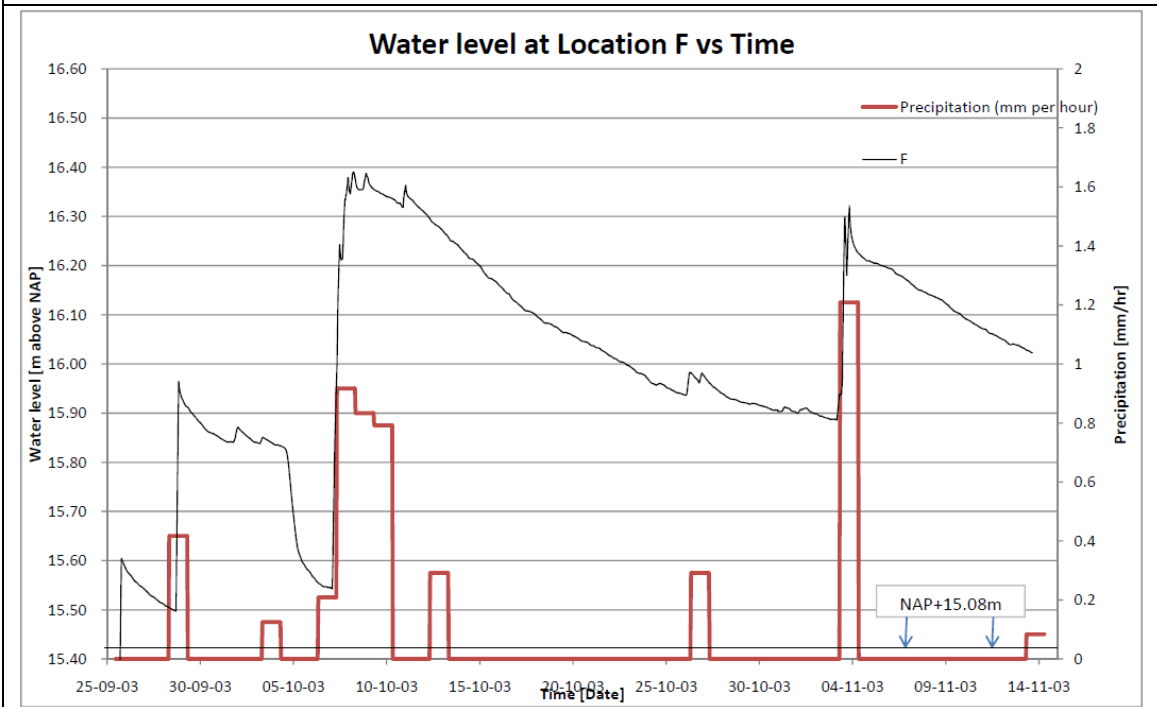


Figure 17: Water levels at monitoring location F including lowest invert level of connected infiltration pipes, from 25 September to 13 November 2003

It is assumed that the infiltration pipes were not affected by any clogging in 2003 since the infiltration system was relatively new then; As mentioned in our earlier Section 4.2 on the overview of the infiltration drain system (and in Figure 11), once the groundwater level drops lower than NAP+14.87m (lowest pipe invert level in the Prinsejagt infiltration drain system), the entire infiltration drain system can be mobilized to exfiltrate its collected water

out to the surrounding soil. During the monitoring period in 2003, the groundwater level had never exceeded NAP+14.70m (please refer to Figure 7 on “Groundwater level in 2003” for details). As such, the exfiltration process of the infiltration system is under the unsaturated flow regime only and with the system operating at its full capacity.

All the 2003 water level trends at the locations (A to F) displayed similar characteristics and order of magnitude. Without any groundwater influence to the infiltration drain system, the rate of water level drop at each location is very much dependent on the localised conditions (like soil permeability, the number and characteristics like diameter and length of pipe connections) at the respective manholes.

Water level trends observed at periodic monitoring Locations A – F and Point 7 in 2011

In this section, we will take a look at the experimental results observed in 10 February to 20 May 2011 for location A to F and Point 7 in more details. As the groundwater might play a role in influencing the performance of the infiltration pipe system, we have also included the groundwater level in our graphs of water level trend for each individual monitoring location.

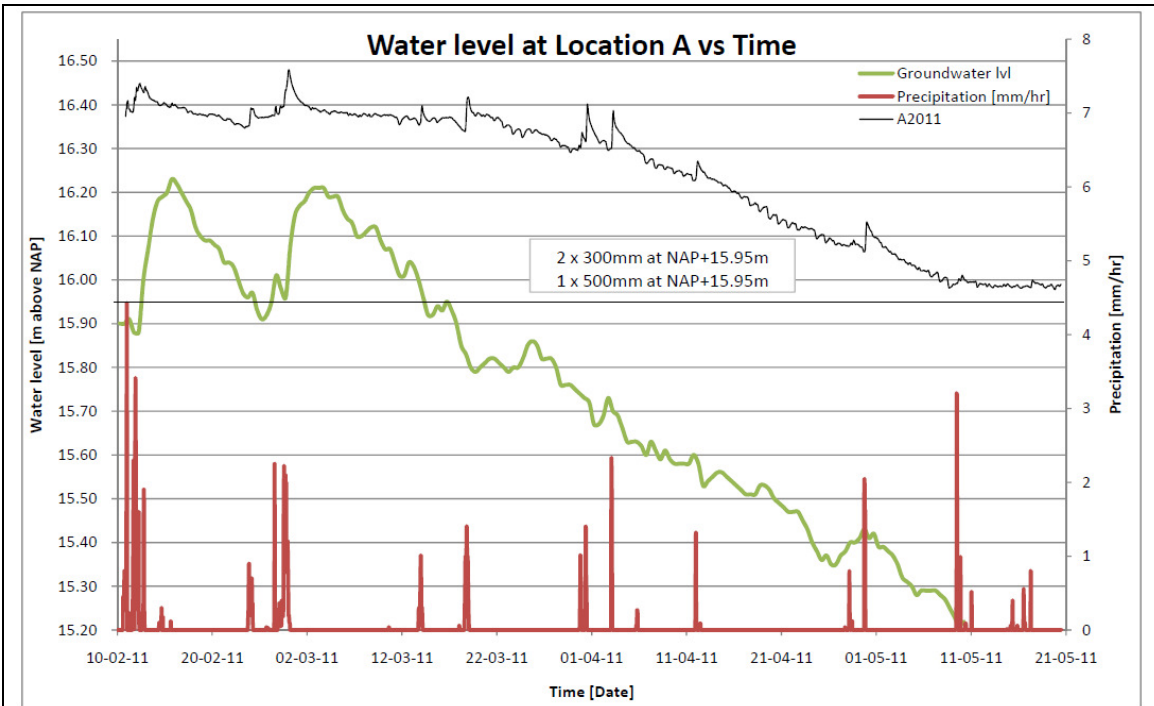


Figure 18: Water levels at monitoring location A including the groundwater level and invert levels of connected infiltration pipes from 10 February to 20 May 2011

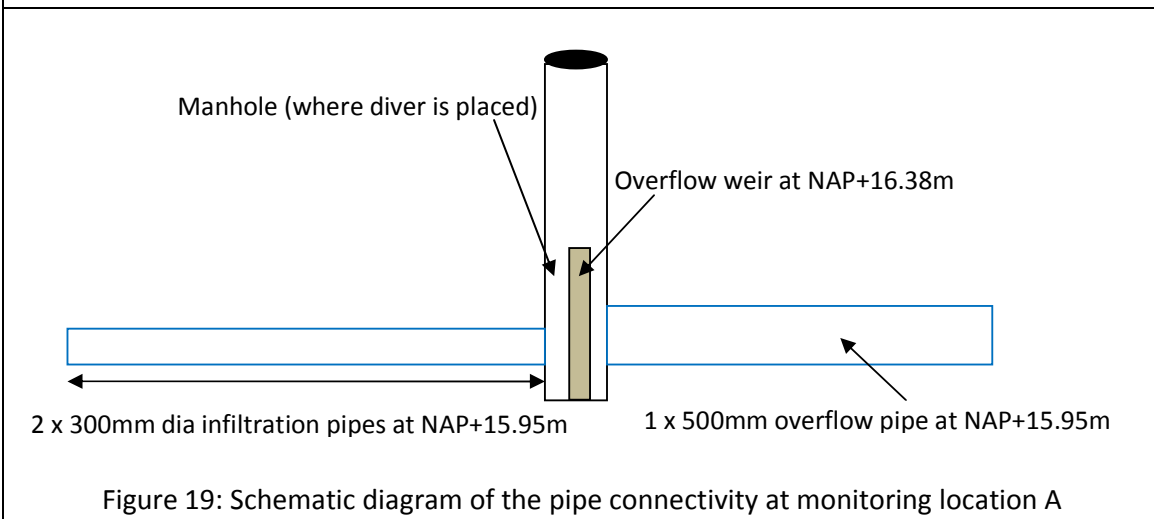


Figure 19: Schematic diagram of the pipe connectivity at monitoring location A

From monitoring period from 10 February till 17 March 2011, the exfiltration rate at monitoring location A remains stifled when the groundwater level stays above NAP+15.90m despite the groundwater level falls below the pipe invert level of its connected pipeline (of NAP+15.95m). As mentioned in Section 4.2, this phenomenon could be due to system behaviour experienced at monitoring location A; at NAP+15.95m level, less than 5% of the infiltration drain system is able to discharge the water collected through exfiltration

effectively. This explains why the water level measured in the manhole fluctuates around NAP+16.40m during this period. And whenever there is a heavy downpour, the only way the infiltration system can discharge its excess water is by spilling over its overflow weir (set at NAP+16.38m) to the nearby open surface water (buffer storage).

It is only after 17 March 2011 (~ 1800hrs) when the groundwater level starts to fall below NAP+15.90m that the infiltration drains system starts to exfiltrate its water collected within the system to the surrounding soil at a higher rate. When the groundwater level falls below NAP+15.85m, slightly more than 25% of the infiltration drain pipeline (refer to Figure 11) is 'activated' to exfiltrate its collected water into the surrounding soil. One may notice that when the groundwater level increases from NAP+15.80m to NAP+15.85m (on 25 March 2011, 0600hrs), the water level within the manhole also experiences a slight increase in water level even though there is no significant rainfall recorded around 25 March 2011 period (the nearest rainfall event were on 18 March and 31 March 2011). This is in line with our theory that the exfiltration rate increases substantially after the groundwater level drop below NAP+15.85m as more than 25% of infiltration drain pipeline can exfiltrate its collected water to the surrounding soil. This is very possible as the water collected within the infiltration pipe network are linked and shared, any difference in water level will cause the excess water to flow towards the location of lower water level thus achieving an equilibrium water level within the system gradually over time.

When the groundwater level drops below NAP+15.60m (on 9 April 2011, 0600hrs), more than 50% of the infiltration drain pipeline is 'activated' to exfiltrate its collected water into its surrounding soil. This will further lead to higher exfiltration rate for the system though the increase in exfiltration rate might not look very significant.

Next, theoretically the lowest water level that can be measured within the manhole would be the pipe invert level at NAP+15.95m. but this is not the case here, the water level stays at NAP+15.99m after prolonged dry period (10 – 20 May 2011). This could be due to clogging (by sediment) in the lowest portion of the infiltration drain thus hampering this remaining water from exfiltrating to the surrounding soil. In 2003, the lowest water level measured in 2003 and 2011 are NAP+15.95m and NAP+15.99m respectively. As such, it seems that there is an accumulation of sediment (~4cm) along this period of time (Year 2003 – 2011). Please see Figure 20 below.

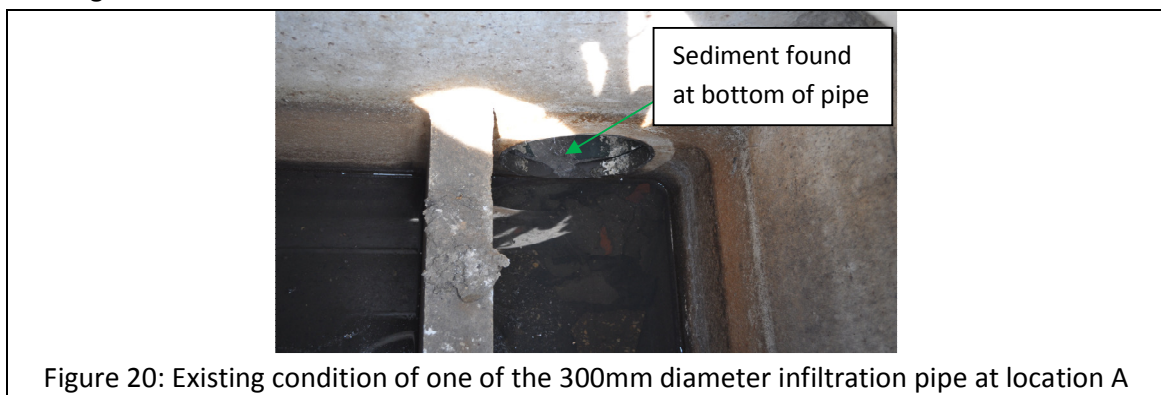


Figure 20: Existing condition of one of the 300mm diameter infiltration pipe at location A

One point to note here and for the subsequent monitoring locations in 2011 is the minor water level fluctuations at the end of the graph is due to atmospheric pressure difference in day & night, it may cause a pressure difference of 0.03m in this case.

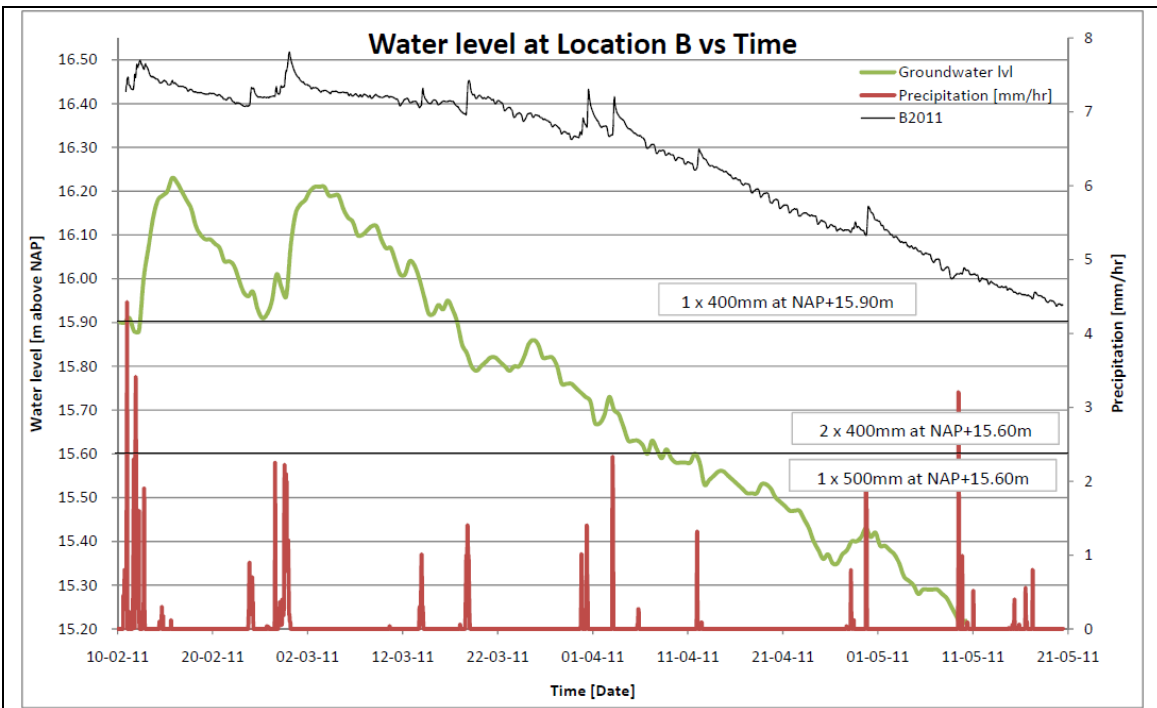


Figure 21: Water levels at monitoring location B including the groundwater level and invert levels of connected infiltration pipes from 10 February to 20 May 2011

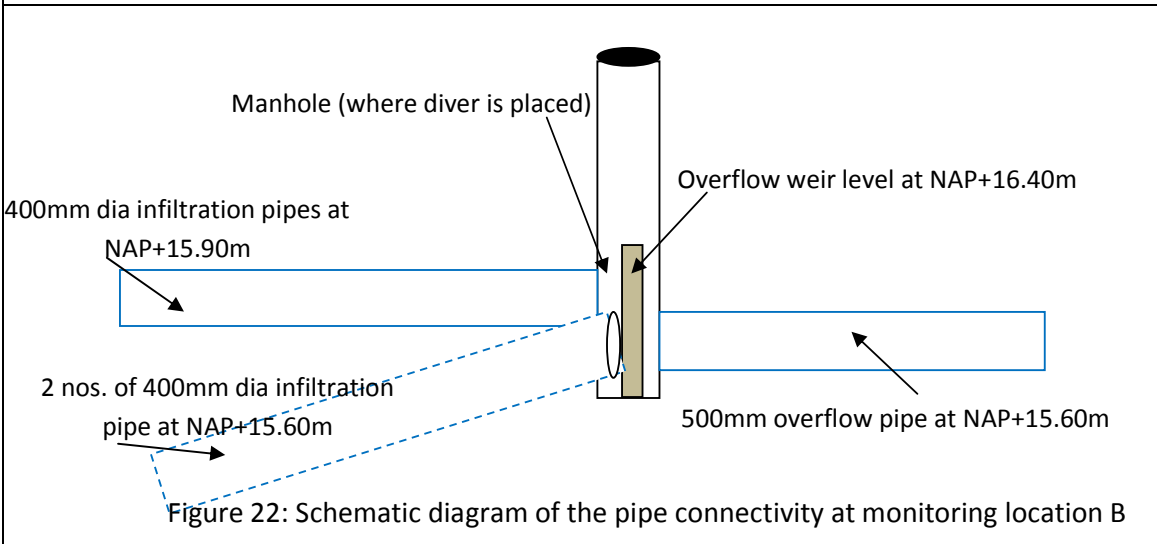
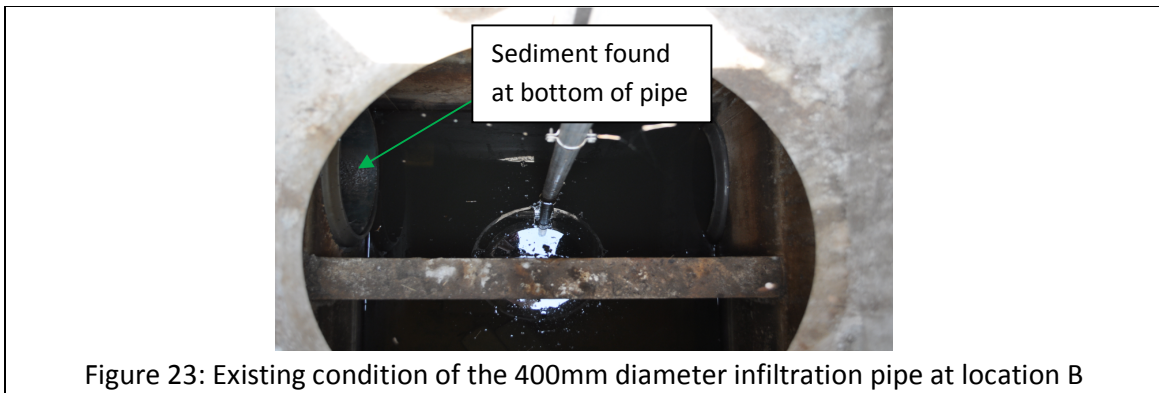


Figure 22: Schematic diagram of the pipe connectivity at monitoring location B

Similar to observations at monitoring location A, the exfiltration rate at monitoring location B was stifled whenever the groundwater level is above NAP+15.90m level for monitoring period between 10 February and 17 Mar 2011. As mentioned in Section 4.2, this could be due to system behaviour experienced at monitoring location B; at NAP+15.90m, around 10% of the infiltration pipelines can exfiltrate water to its surrounding soil. This limits the ability of the infiltration system to discharge water via exfiltration. Moreover, during this period, one would notice that the water level in the manhole remains around NAP+16.40m (this is also the overflow weir level). Thus, whenever there is heavy downpour, the only way for the infiltration system to discharge its excess water collected is by allowing its excess water to spill over its overflow weir (set at NAP+16.40m) to the nearby open surface water (buffer storage).

It is only after 17 March 2011 (~1800hrs) when the groundwater level starts to drop below the pipe invert level of NAP+15.90m that the infiltration drains system start to exfiltrate its water collected within the system to the surrounding soil at a higher rate. Whenever the groundwater level falls below NAP+15.85m, slightly more than 25% of the infiltration drain pipeline (Figure 11) is 'activated' to exfiltrate its collected water into the surrounding soil. Moreover, you may notice that when the groundwater level increases from NAP+15.80m to NAP+15.85m (on 25 March 2011, 0600hrs), the water level within the manhole also experiences a slight increase in water level though there is no significant rainfall recorded around 25 March 2011 period (the nearest rainfall event were on 18 March and 31 March 2011). This is in line with our observation the exfiltration rate increases substantially after the groundwater level drop below NAP+15.85m despite having the pipe invert levels of the remaining pipes (2 x 400mm diameter pipes located on NAP+15.60m) still below the groundwater level (in saturated zone). Since the water collected within the infiltration pipe network are linked and shared, if there is a slightly higher water level at a particular location, the water will flow and balances itself within the network of pipes gradually.

Though the increase in exfiltration rate might not look very significant, when the groundwater level drops below NAP+15.60m (on 9 April 2011, 0600hrs), more than 50% of the infiltration drain pipeline is 'activated' to exfiltrate its collected water into its surrounding soil. This will further accelerate the system's rate of exfiltration.



There is not much sediment found here (400mm diameter, pipe invert level at NAP+15.90m) as compared to location A. More sediment could be found on the pipes that were laid on lower level (ie at NAP+15.60m).

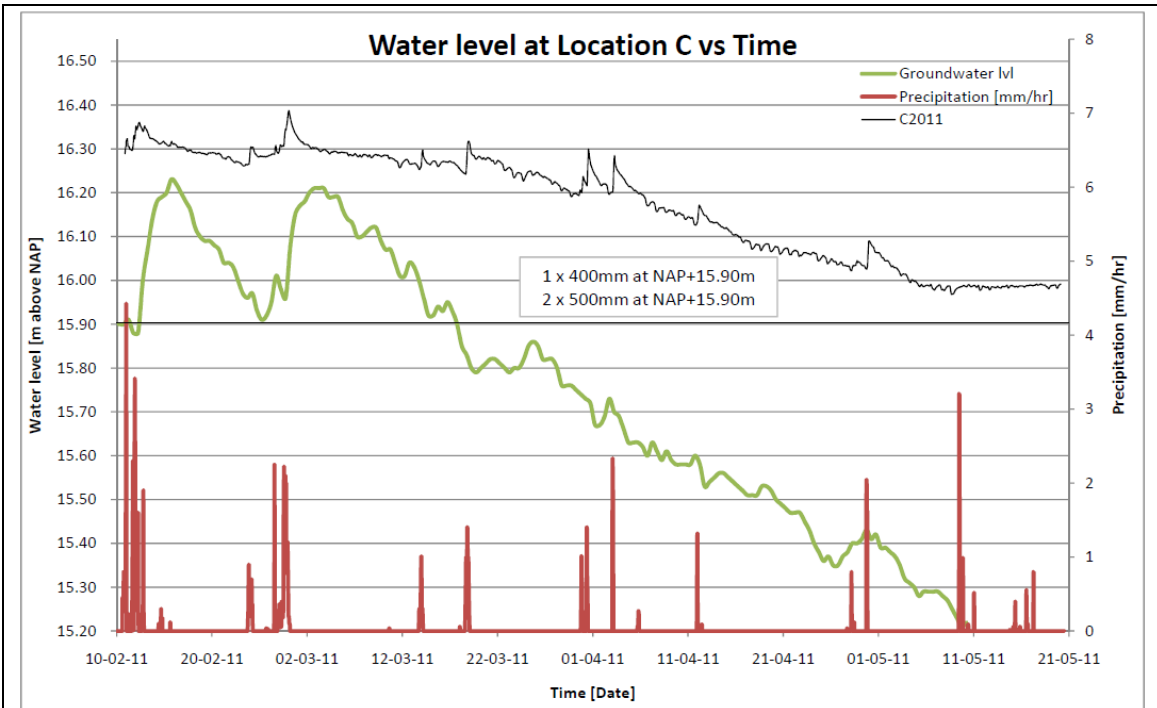


Figure 24: Water levels at monitoring location C including the groundwater level and invert levels of connected infiltration pipes from 10 February to 20 May 2011

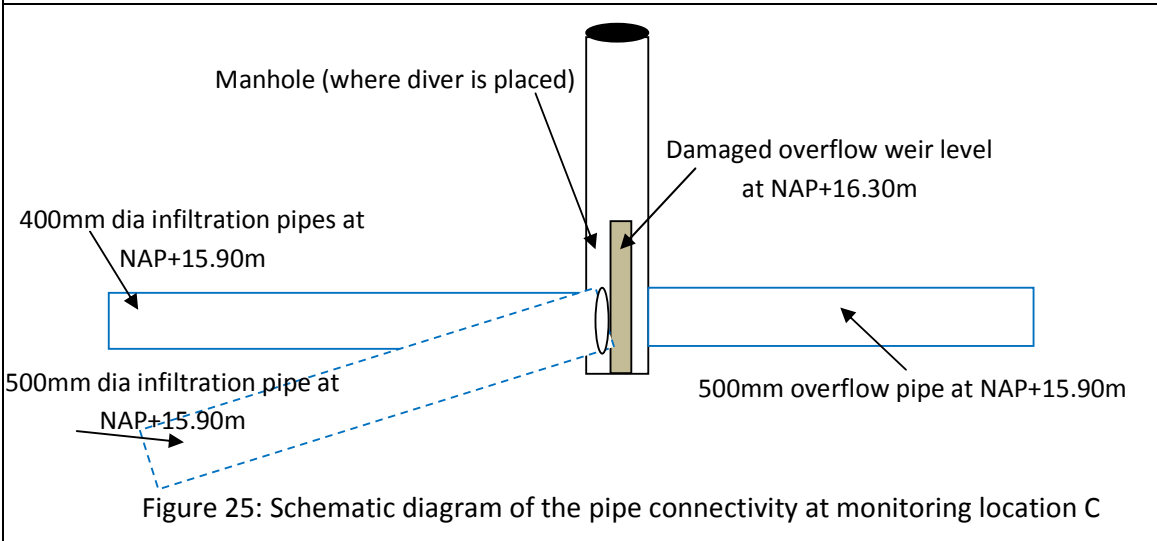


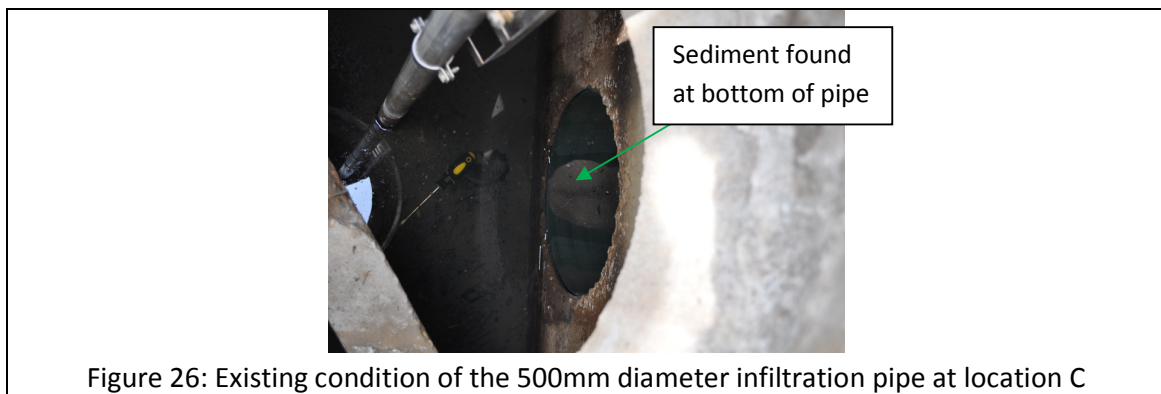
Figure 25: Schematic diagram of the pipe connectivity at monitoring location C

Similar to monitoring locations A & B, from monitoring period from 10 February till 17 March 2011, the exfiltration rate at monitoring location C remains stifled when the groundwater level stays above the highest pipe invert level (NAP+15.90m). It is very likely that the water level at monitoring location C is experiencing system behaviour too (as mentioned in Section 4.2). With 10% of the infiltration drain system exfiltrating at NAP+15.90m level (refer to Figure 11), the water level in the manhole remains around NAP+16.30m, this is because the overflow weir at monitoring location C is damaged thus its effective height has been reduced to NAP+16.30m instead of around NAP+16.40m at monitoring locations A and B. As such, whenever there is heavy downpour, the only option for the infiltration system to discharge its excess water collected is by discharging its excess water over its overflow weir to the nearby open surface water (buffer storage).

It is only after 17 March 2011 (~ 1800hrs) when the groundwater level starts to fall below the pipe invert level of NAP+15.90m that the infiltration drains system start to exfiltrate its water collected within the system to the surrounding soil at a higher rate. Whenever the groundwater level falls below NAP+15.85m, slightly more than 25% of the infiltration drain pipeline (within the system) is 'activated' to exfiltrate its collected water into the surrounding soil. One may notice that when the groundwater level increases from NAP+15.80m to NAP+15.85m (on 25 March 2011, 0600hrs), the water level within the manhole also experiences a slight increase in water level though there is no significant rainfall recorded around 25 March 2011 period (the nearest rainfall event were on 18 March and 31 March 2011). This is in line with our theory that the exfiltration rate increases substantially after the groundwater level drop below NAP+15.85m as more infiltration drain pipeline can exfiltrate its collected water. As the water collected within the infiltration pipe network is linked and shared, any difference in water level will cause the excess water to flow towards the locations of lower water level thus balancing itself gradually over time.

Similar with our observations at monitoring locations A and B, though the increase in exfiltration rate might not look very significant, when the groundwater level drops below NAP+15.60m (on 9 April 2011, 0600hrs), more than 50% of the infiltration drain pipeline is 'activated' to exfiltrate its collected water into its surrounding soil. This will further accelerate the system's rate of exfiltration.

Lastly, similarly to observations at Location A, theoretically the lowest water level that can be measured within the manhole would be the pipe invert level at NAP+15.90m, but this is not the case here, the water level stays at NAP+15.99m after prolonged dry period (10 – 20 May 2011). This could be due to clogging (by sediment) at the lowest portion of the infiltration drain thus hampering this remaining water from exfiltrating to the surrounding soil. In 2003, the lowest water level measured in 2003 and 2011 are NAP+15.98m and NAP+15.99m respectively. As such, it seems that there is little accumulation of sediment during this period of time (Year 2003 – 2011) at Location C. Please refer to Figure 26 below for the existing condition of the 500mm diameter infiltration pipe at location C.



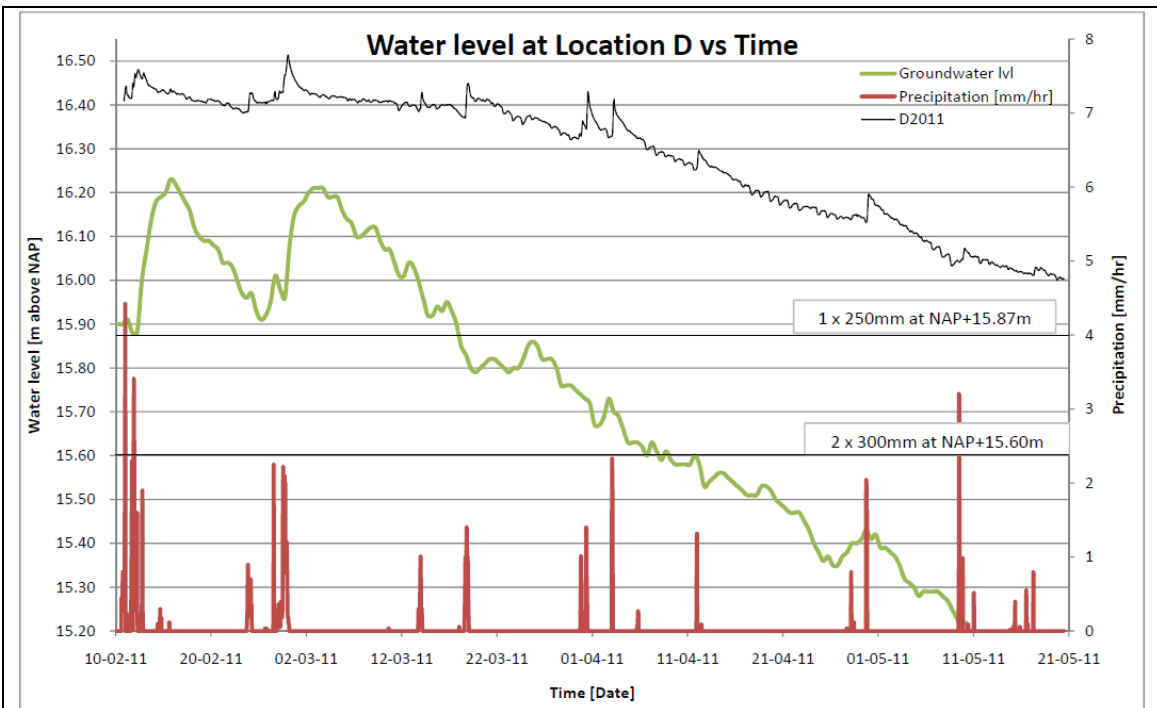


Figure 27: Water levels at monitoring location D including the groundwater level and invert levels of connected infiltration pipes from 10 February to 20 May 2011

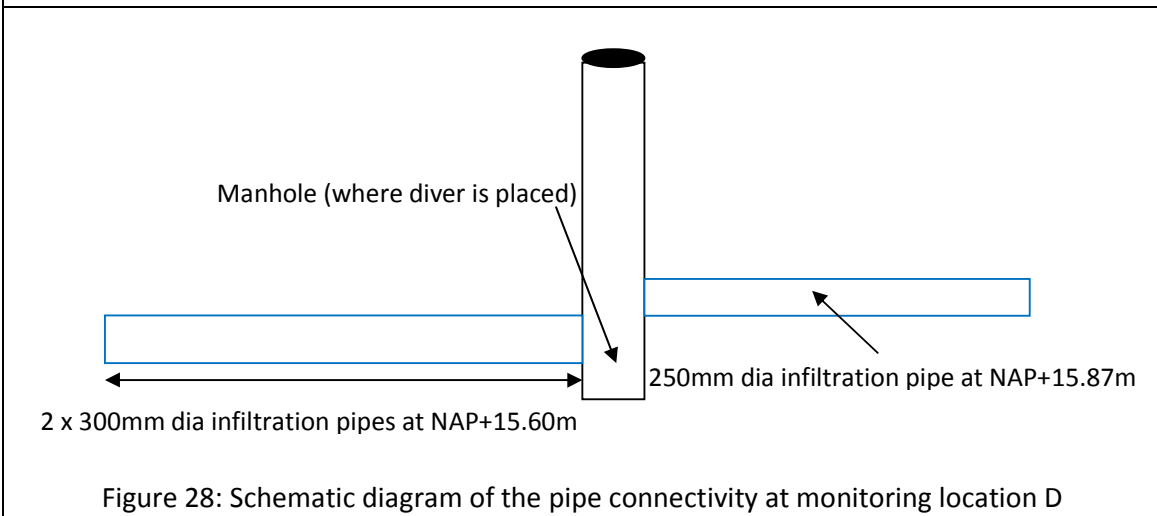


Figure 28: Schematic diagram of the pipe connectivity at monitoring location D

Throughout the monitoring period from 10 February till 17 March 2011, the exfiltration rate at monitoring location D remains stifled whenever the groundwater level stays above NAP+15.90m. This could be due to system behaviour experienced at monitoring location D (as mentioned in Section 4.2); at NAP+15.90m, less than 10% of the infiltration drain system is able to discharge the water collected through exfiltration effectively (refer to Figure 11). One would notice that the water level measured in the manhole fluctuates around NAP+16.40m during this period, and whenever there is a heavy downpour, the water collected here will be redistributed through the infiltration pipeline network to other locations. In this way, it maintains the water level at monitoring location D at around NAP+16.40m (at the system overflow level).

It is only after 17 March 2011 (~ 1800hrs) when the groundwater level starts to fall below NAP+15.90m that the infiltration drains system start to exfiltrate its water collected within the system to the surrounding soil at a higher rate. When the groundwater level falls below NAP+15.85m, slightly more than 25% of the infiltration drain pipeline (within the system) will start to exfiltrate its collected water into the surrounding soil. When the groundwater level increases from NAP+15.80m to NAP+15.85m (on 25 March 2011, 0600hrs), the water level within the manhole also experiences a slight increase in water level even though there is no significant rainfall recorded around 25 March 2011 period (the nearest rainfall event were on 18 March and 31 March 2011). This reinforces again our theory that the exfiltration rate increases substantially after the groundwater level drop below NAP+15.85m as more than 25% of infiltration drain pipeline can exfiltrate its collected water to the surrounding soil. This is very likely as the water collected within the infiltration pipe network are linked and shared, any difference in water level will led to excess water flowing towards the location of lower water level thus achieving an equilibrium water level within the system gradually over time.

More than 50% of the infiltration drain pipeline starts to exfiltrate its collected water into its surrounding soil when the groundwater level drops below NAP+15.60m (on 9 April 2011, 0600hrs). This lead to higher exfiltration rate for the system though the increase in exfiltration rate might not look very significant.



From Figure 29, we cannot see whether there are any sediment at the bottom of the 250mm diameter infiltration pipe since the water level is higher than the pipe invert level. Moreover this pipe is also not the lowest connecting pipe for the manhole. Nevertheless, we noticed that there are a lot of dead leaves in the water and along the sides of the manhole. If they are not removed regularly, they may end up clogging the infiltration drain as well.

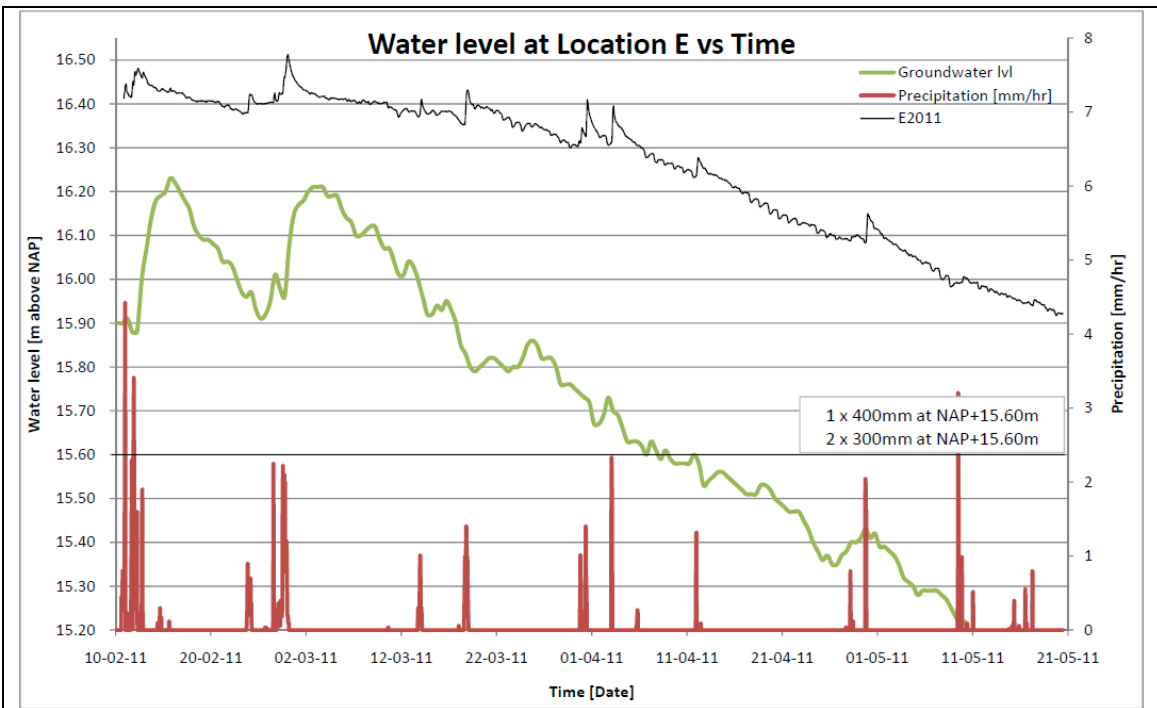


Figure 30: Water levels at monitoring location E including the groundwater level and invert levels of connected infiltration pipes from 10 February to 20 May 2011

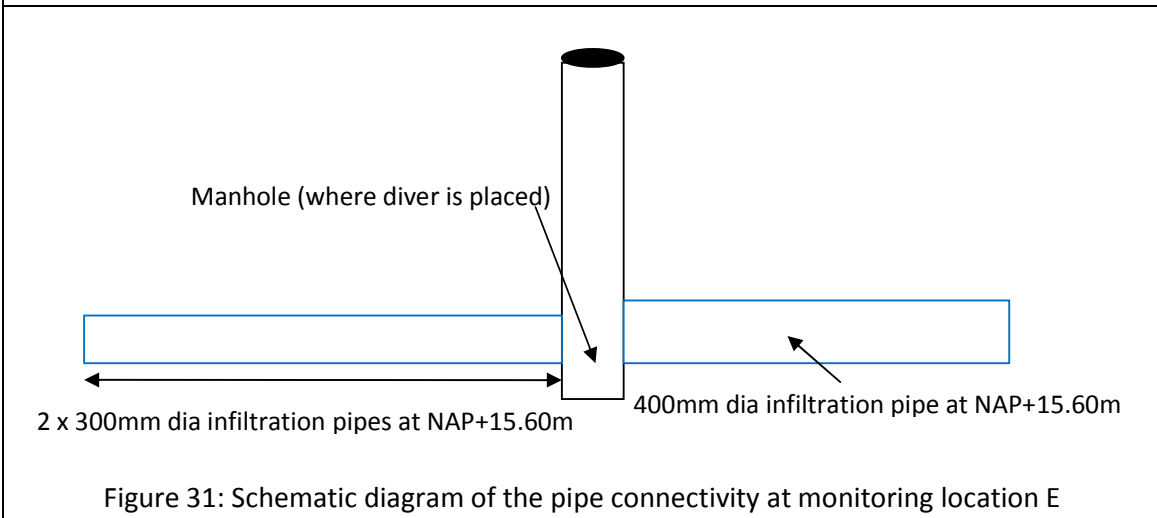


Figure 31: Schematic diagram of the pipe connectivity at monitoring location E

Similarly at monitoring location E, the exfiltration rate remains stifled when the groundwater level stays above NAP+15.90m during 10 February to 17 March 2011. As mentioned in Section 4.2, this phenomenon is most likely due to system behaviour experienced at monitoring location E; having less than 10% of the infiltration drain system discharging its water collected through exfiltration effectively at NAP+15.90m, the water level measured in the manhole fluctuates around NAP+16.40m. Whenever there is a heavy downpour, the water collected here will be redistributed through the rest of the infiltration pipeline network. This maintains the water level at monitoring location E around NAP+16.40m (at the system overflow level).

The groundwater level starts to fall below NAP+15.90m after 17 March 2011 (~ 1800hrs), this led to higher rate of exfiltration by the infiltration drains system. As the groundwater

level falls below NAP+15.85m, slightly more than 25% of the infiltration drain pipeline (within the system) will start to exfiltrate its collected water into the surrounding soil. When the groundwater level increases from NAP+15.80m to NAP+15.85m (on 25 March 2011, 0600hrs), the water level within the manhole also experiences a slight increase in water level even though there is no significant rainfall recorded around 25 March 2011 period (the nearest rainfall event were on 18 March and 31 March 2011). This further reinforces our theory that the exfiltration rate increases substantially after the groundwater level drop below NAP+15.85m when more than 25% of infiltration drain pipeline are able to exfiltrate its collected water to the surrounding soil. Water collected within the infiltration pipe network are linked and shared, any difference in water level will lead to excess water flowing towards the locations of lower water level thus achieving an equilibrium water level within the system gradually over time.

More than 50% of the infiltration drain pipeline starts to exfiltrate its collected water into its surrounding soil when the groundwater level drops below NAP+15.60m (on 9 April 2011, 0600hrs). This will lead to higher exfiltration rate for the system though the increase in exfiltration rate might not look very significant.



In Figure 32, we cannot see whether there is any sediment accumulated at the bottom of the 250mm diameter infiltration pipe since the water level is higher than the pipe invert level. Nevertheless, we noticed that there are also a lot of dead leaves in the water and along the sides of the manhole. If they are not cleared regularly, they may ended up clogging the infiltration drain and affect its performance as well.

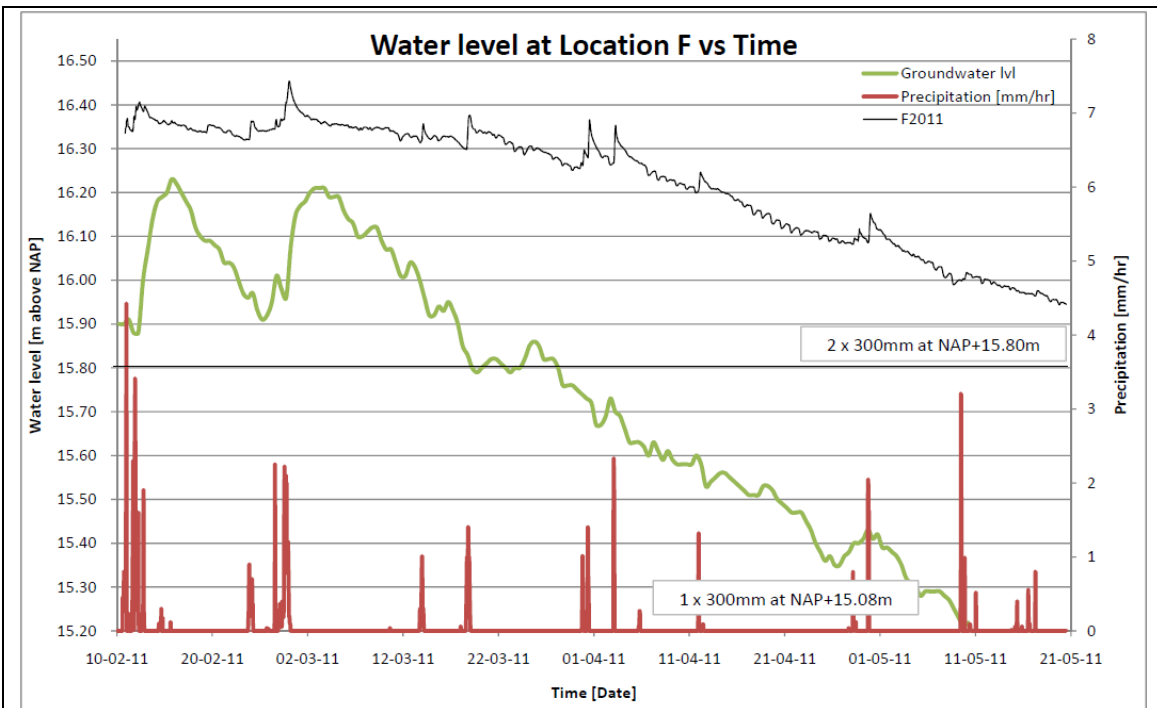


Figure 33: Water levels at monitoring location F including the groundwater level and invert levels of connected infiltration pipes from 10 February to 20 May 2011

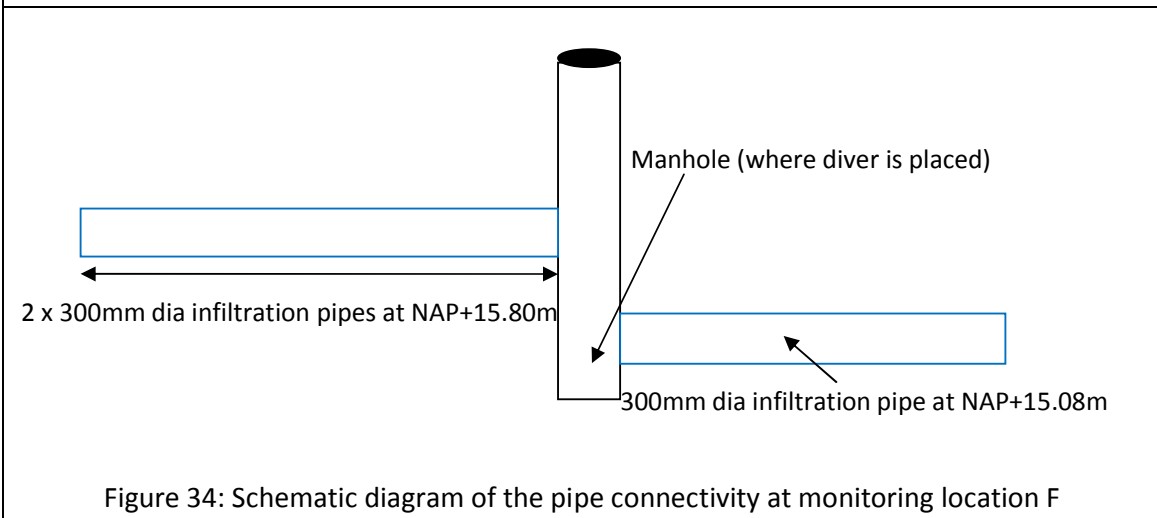
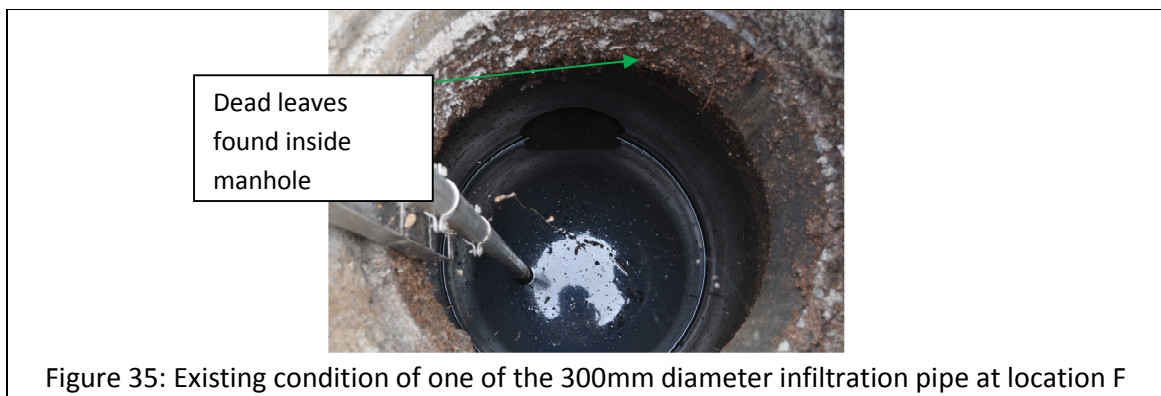


Figure 34: Schematic diagram of the pipe connectivity at monitoring location F

Similar to observations at monitoring locations D & E, the exfiltration rate at monitoring location F remains stifled when the groundwater level stays above NAP+15.90m during 10 February to 17 March 2011. Due to similar system behaviour experienced at monitoring location F, less than 10% of the infiltration drain system (refer to Figure 11) can discharge its water collected through exfiltration effectively at NAP+15.90m, as such, the water level measured in the manhole fluctuates around NAP+16.35m. Whenever there is a heavy downpour, the water collected here will be redistributed through the rest of the infiltration pipeline network. This maintains the water level at monitoring location F around NAP+16.35m (around the system overflow level).

As the groundwater level starts to fall below NAP+15.90m after 17 March 2011 (~ 1800hrs), a higher rate of exfiltration by the infiltration drains system could be achieved. Slightly more than 25% of the infiltration drain pipeline (within the system) will start to exfiltrate its collected water into the surrounding soil when the groundwater level falls below NAP+15.85m. However, when the groundwater level increases from NAP+15.80m to NAP+15.85m (on 25 March 2011, 0600hrs), we noticed a slight increase in water level within the manhole even though there is no significant rainfall recorded around 25 March 2011 period (the nearest rainfall event were on 18 March and 31 March 2011). This reinforces our theory that the exfiltration rate increases substantially after the groundwater level drop below NAP+15.85m when more than 25% of infiltration drain pipeline can exfiltrate effectively. Since water collected within the infiltration pipe network are linked and shared, any difference in water level will led to the excess water flowing towards the location of lower water level thus achieving an equilibrium water level within the system gradually over time.

More than 50% of the infiltration drain pipeline will starts to exfiltrate its collected water into its surrounding soil once the groundwater level drops below NAP+15.60m (on 9 April 2011, 0600hrs). This will lead to higher exfiltration rate by the system even though the increase in exfiltration rate might not look very significant.



Similar conditions of water within this manhole (as monitoring Locations D and E) are observed here. There are much dead leaves in the water and along the sides of the manhole. If they are not cleared regularly, they might clog up the infiltration drain and affect its performance. Please see Figure 35 above.

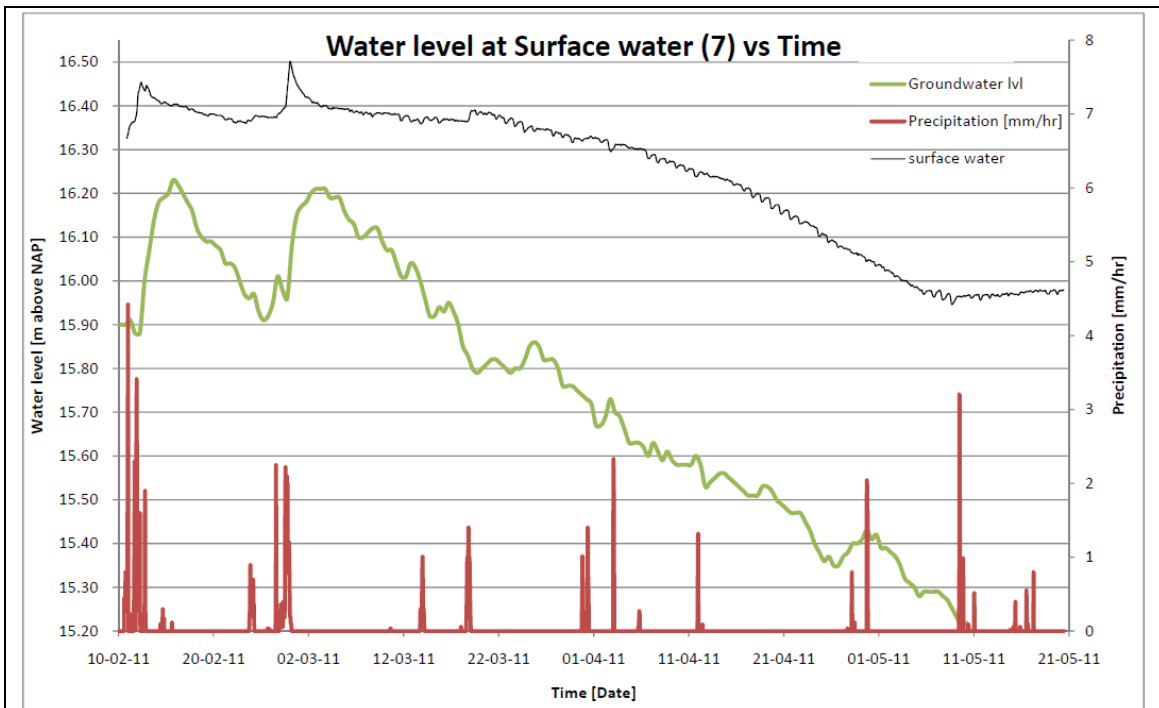


Figure 36: Water levels at monitoring location 7 (surface water near monitoring location B) including the groundwater level from 10 February to 20 May 2011

This is an additional monitoring location that was not installed in 2003. The monitoring location 7 is connected downstream of monitoring location B (after the overflow weir) connecting to the open surface water. Here, we observe water levels maintained above NAP+16.36m when the groundwater level stays above the NAP+15.9m level. Subsequently, when the groundwater level dropped below NAP+15.85m, the water level at monitoring location 7 declines as well. The surface water level is very much influenced by the groundwater level, the extent in which the surface water can exfiltrate to the groundwater will depend on the groundwater level. Notwithstanding that, losses through evapotranspiration processes will also help to lower the water level at location 7.

Towards the end of the monitoring period (10 – 20 May 2011), it is noticed that the water level at this location is almost dry (Figure 37). As such, there will be little influence from the surface water system on the infiltration pipe system during this period.

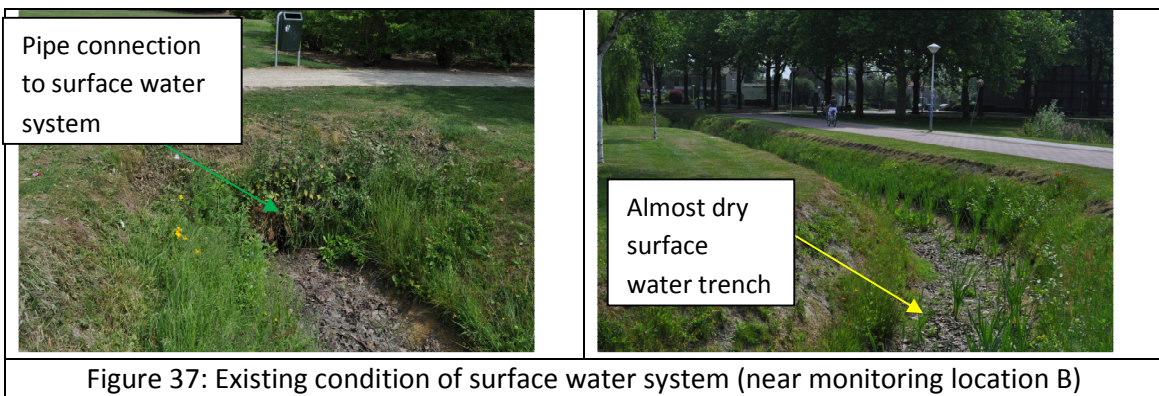


Figure 37: Existing condition of surface water system (near monitoring location B)

4.4 System behaviour at all monitoring locations in 2003 and 2011

Summary of 2003 and 2011 water level trends

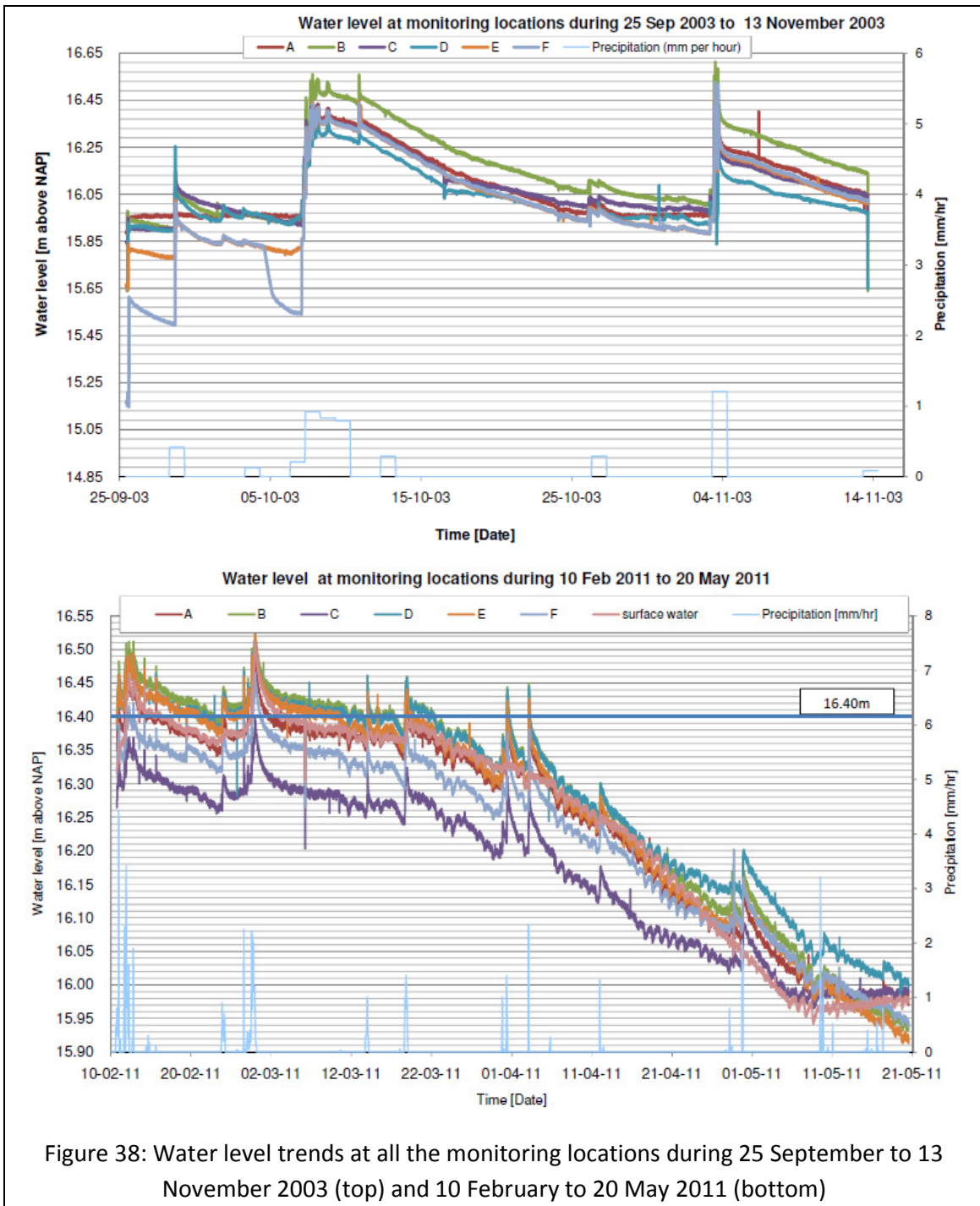


Figure 38: Water level trends at all the monitoring locations during 25 September to 13 November 2003 (top) and 10 February to 20 May 2011 (bottom)

From the 2003 and 2011 water level trends (Figure 38) for all the monitoring locations A – F (and Point 7), we could see that they all displayed similar water level trends and order of magnitude after each individual rain event. From our earlier analysis on the water level trends at each monitoring locations A – F (and Point 7), it is believed that the 2003 and 2011 water level trends had exhibited some form of system behaviour though each monitoring locations have their own variations in term of pipe connectivity (diameter and pipe invert level) and depth of manhole.

Relationship plots on the water level trends between locations A and B

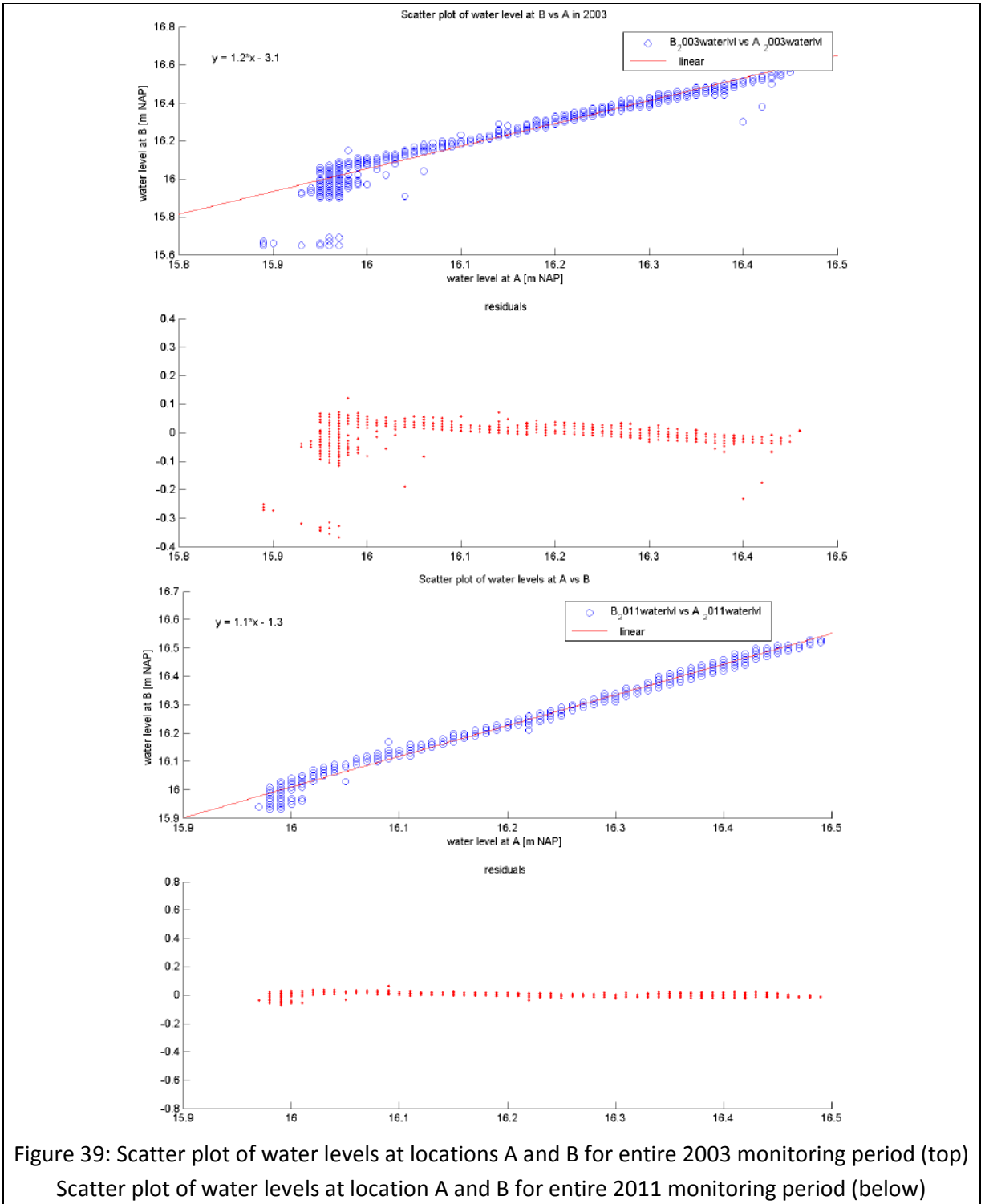


Figure 39: Scatter plot of water levels at locations A and B for entire 2003 monitoring period (top)
Scatter plot of water levels at location A and B for entire 2011 monitoring period (below)

Furthermore, during the entire monitoring period of 2003 and 2011 (ie 25 September to 13 November 2003 and 10 February to 20 May 2011), the relationship plots between Location A with the rest of the Locations (B-F) showed very good (1-1) linear relationship with minor deviation of the range:

- -0.10 to 0.10m (for 2003 data)
- -0.05 to 0.05m (for 2011 data)

This further reinforces on the system behaviour concept. As we could see from Figure 39 above, the error margin (residuals) would still be acceptable for general average rate of exfiltration purpose. For complete scatter plots of all other Locations in 2003 and 2011, please refer to Appendix 7.

4.5 Experimental results from the closed-loop test

We are unable to conduct the closed-loop test at location Point 1 as the manhole connecting to the infiltration pipe was covered with silt (Figure 40); under this condition, location Point 1 cannot provide the exfiltration performance that we expect for this stretch of pipe. Regular maintenance of the infiltration system should be carried out; the system is unable to perform its intended function once its pipe is completely covered with silt (like location Point 1).

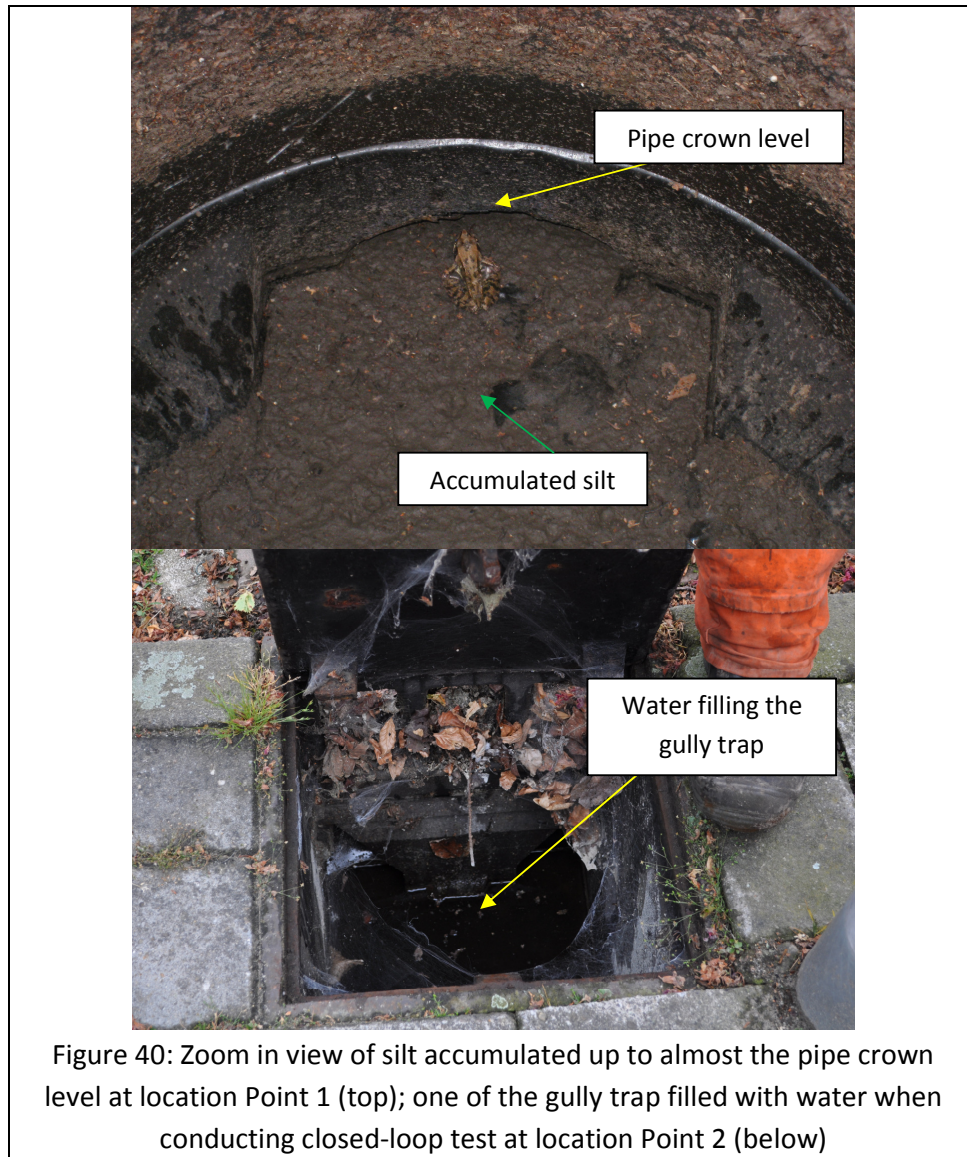


Figure 40: Zoom in view of silt accumulated up to almost the pipe crown level at location Point 1 (top); one of the gully trap filled with water when conducting closed-loop test at location Point 2 (below)

Atmospheric pressure data obtained from the baro diver installed at monitoring location E was used to account for the fluctuations in atmospheric pressure readings at for Location Points 2 – 5. Figures 41 and 42 below shows the water trends observed at the closed-loop test location Points 3 and 5. Please take note that the water level on the y-axis is water level above the respective pipe invert levels. Please refer to Appendix 8 for water trends of closed-loop test at location Points 2 and 4.

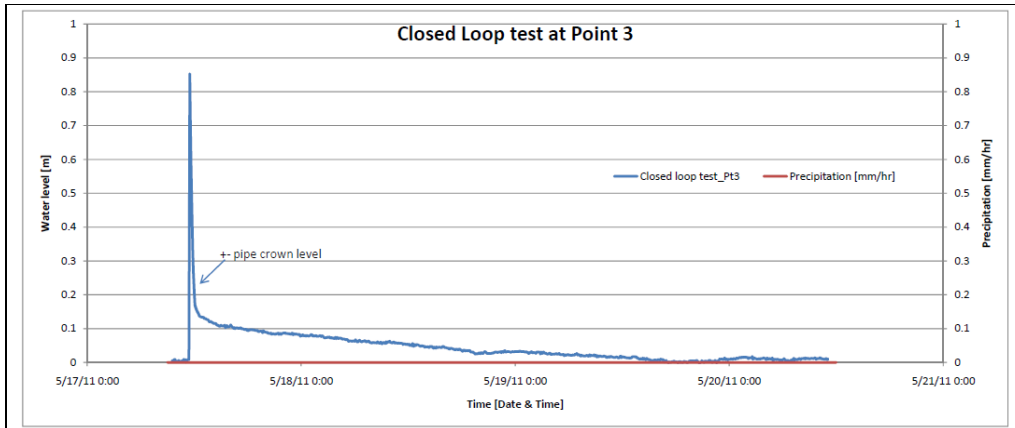


Figure 41: Water level trend at location Point 3

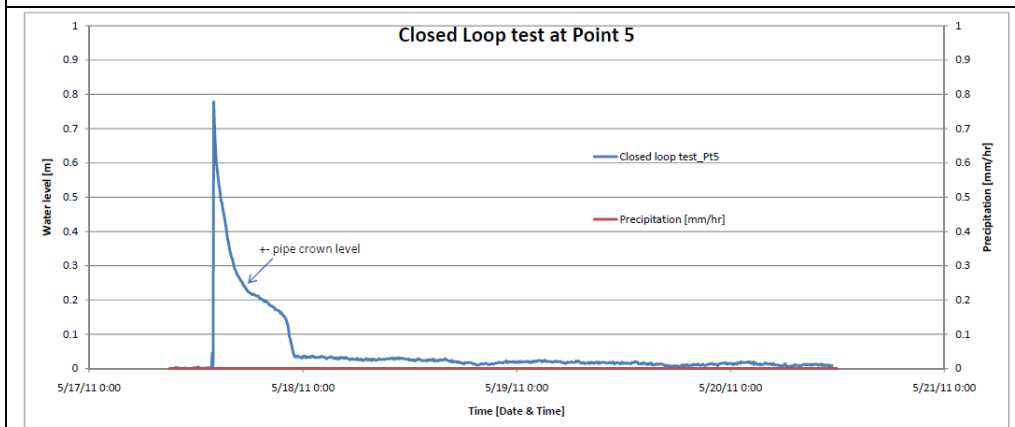
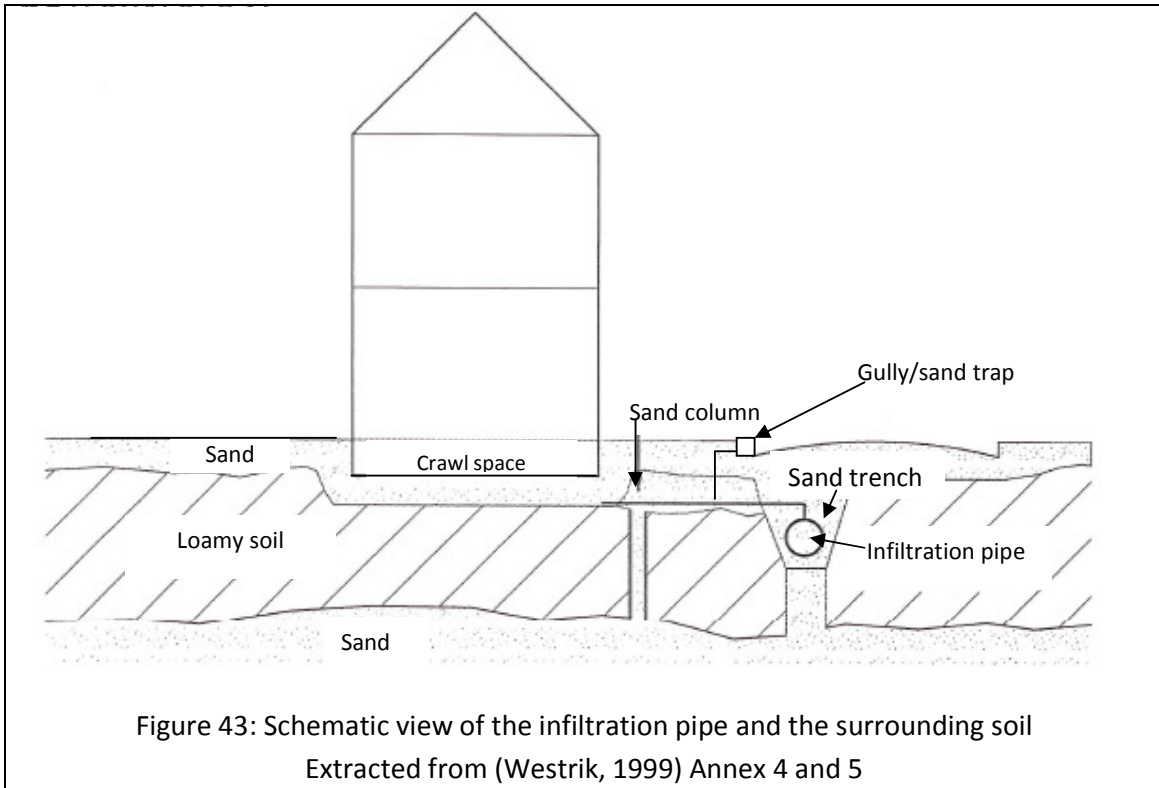


Figure 42: Water level trend at location Point 5

From the water level trend of all the four locations (Point 2 – 5), we noticed that the profile of water level decline is generally similar except for Point 5. First, the water level will drop rapidly from its initial water level to the pipe crown level. After the water level reaches the pipe crown level, the rate of water level drop will be reduced and this rate of water level drop will continued until it reaches the lowest recorded level.

In other words, there seems to have two flowrates or flow profiles for different water level within the manhole. Since there are multiple existing pipe connections to our infiltration pipe from the nearby houses (including sand and gully traps), the much higher exfiltration rate observed when the water level is higher than the pipe crown level could be attributed to water seepage to these connections and not totally discharged through the infiltration pipe. Figure 40 shows the water filled gully trap when we conducted the closed-loop test at location Point 2. Notwithstanding this, at low groundwater level, the surrounding soil/sand (sand column) is able to take in more water (exfiltrated from the infiltration pipe). The high exfiltration rate could also be due to water filling up the sand trench surrounding the infiltration pipe. Please see Figure 43 on the schematic diagram of the infiltration pipe and its surrounding soil.



There is some odd observations on the water level trends occurring at Location Point 5 (Figure 42). Its starting water trend is similar but at 17 May 2011, 2130hrs the water level starts to drop very rapidly to almost zero level. We believed that this is very likely caused by the sewer plug (which isolates the section of infiltration pipe at Location Point 5) losing its holding-pressure which in turn leads to the rapid leakage of water from Location Point 5 towards the other infiltration drains that it is connected to.

4.6 Additional analysis to study the characteristics of the infiltration system

Introduction and methodology

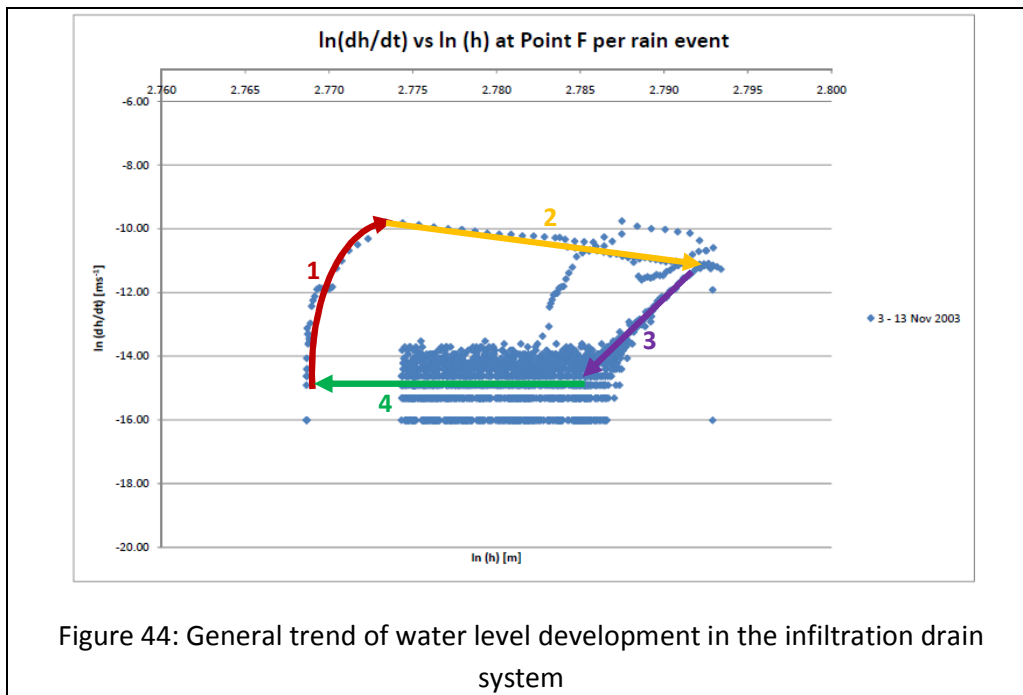
We are interested in knowing the processes involved in an infiltration drain system. From our observations, the water trends in 2003 and 2011 seem to follow an exponential profile of decrease. As such, we plotted $\ln(dh/dt)$ against $\ln(h)$ for each individual rain storms at each monitoring locations to determine their profile and explain its general characteristics.

Terminology

$dh = h_2 - h_1$ (change in water level)

$dt = 5 \times 60 \text{ secs} = 300 \text{ secs}$ (since our monitoring interval is 5 minutes)

Taking a micro view on the plots made for 2003 and 2011 data for each rainfall event recorded, the plots for all locations (A to F) showed similarities on the general profiles as to how the water level raises and fall.



From the water level trends observed in Figure 44, there seems to be four phases of water level development in the infiltration drain system every time after a rainstorm. They are:

- **1st phase:** increasing rate of water level raise (until peak)
- **2nd phase:** decreasing rate in the water level raise
 - 1st – 2nd phase is when the water level builds up until the maximum water level in the manhole (the raise in water level is caused by water inflow into the system from the catchment area of the manhole and its connected pipelines. Thus, during this phase, we will expect advection/transportation process to be predominant here)
- **3rd phase:** rate of change of water level (similar to exfiltration rate) will continue to drop at a linear rate (advection processes die out)

- **4th phase:** The rate of change of water level reaches a constant rate until the water level becomes lower than the lowest pipe invert level within the manhole system. Other than some slight differences, similar trends are also observed in 2011 data plots too.

Appendix 9 shows the $\ln (dh/dt)$ vs $\ln (h)$ plots at the monitoring locations (A-F) after a rain event (which occurred on 3 – 13 November 2003 and 29 April – 7 May 2011 periods).

5 Quantitative comparison of exfiltration rates in 2003 and 2011

5.1 Introduction

We adopted two approaches to compare or derive our exfiltration rates from the 2003 and 2011 data. These methods are:

1. Graphical method*

Once we have determined the average rate of water level drop at the monitoring locations (A-F), we can estimate the average volumetric exfiltration rate $[L^3/T]$ at each monitoring locations by multiplying their average rate of water level drop $[L/T]$ with the corresponding manhole cross-sectional area $[L^2]$. Thereafter, we can compare the exfiltration rates between 2003 and 2011. This process is repeated until all the exfiltration rates for the remaining monitoring locations have been obtained. A point to note here is we do not need to multiply the average rate of water level drop $[L/T]$ by the cross-sectional area of the manhole $[L^2]$ before we can proceed to compare the exfiltration rates (of 2003 and 2011 at the respective locations) since the cross-sectional area for this particular location (manhole) remains relatively constant. Therefore, we can simplify our comparison process by just looking at their respective average rate of water level drop $[L/T]$.

2. Curve-fitting method*

The curve-fitting approach requires us to utilise Matlab program to study and analyse which mathematical function is most appropriate in describing the water trends observed at each monitoring locations in 2003 and 2011. A series of mathematical function will be tested for its goodness-of-fit to the experimental data. Once a mathematical function (for $h(t)$) has been selected, further processing would be carried out in order to allow for direct comparison of 2003 and 2011 exfiltration rates at the respective monitoring locations. Similar to the graphical method above, we multiply the dh/dt expression $[L/T]$ for each respective monitoring location by their manhole cross-sectional area $[L^2]$ to obtain the volumetric exfiltration rate for comparing of results.

We will explain more in details these two approaches in the following sections.

****Note: Since no similar closed-loop test was carried out in 2003 previously, we will not be analysing the data obtained from closed-loop test using Graphical and Curve-fitting methods as we are unable to form any direct comparison of results between 2003 and 2011 data.***

5.2 Graphical method

Selection criteria and data processing

In order to have a fair comparison between the 2003 and 2011 data, the selected period of study that we select for 2011 should be under similar operating conditions. During September to November 2003 period, the infiltration drain system is operating at low groundwater levels (always lower than NAP+14.70m). While it is prefer to commence our monitoring in the month of September, we cannot afford to wait till then due to time constraints in our project. In addition, during our monitoring period (early February till mid May 2011), we have high groundwater level experienced in early February till end March 2011.

In order to ensure as little groundwater influence in our analysis on the exfiltration rates at the monitoring locations, we have selected our result analysis from end March onwards (till May 2011) when the groundwater level is below NAP+15.70m. This would, in our opinion, be the best possible combination to be used for our comparison of exfiltration rates in 2003 and 2011.

As there are many minor fluctuations in the water levels when we measure them at 5 minutes intervals, we used the moving average concept to smoothen the constant fluctuations (same weight has been put for all the data points used). The number of readings used for the moving average is arbitrary; the main objective is to reduce the fluctuations yet retaining the resolution of actual water level changes triggered by events. It is found that the number of readings used, ranging from 30 to 40, is sufficient for our purpose here. One should note that in employing the moving average method, there will be a time lag behind the latest data point, though this is the case here, it does not lead to any significant distortion to our data analysis here. While other techniques could also be employed to add extra weight to certain data points, this is not recommended here as the processes involved are still relatively unknown and there is no basis to do so. As such, we adopted a moving average that uses the previous 40 water level readings.

As illustrated earlier, we obtain the rate of water level drop [L/T] by measuring on the graph the gradient of the selected period of water trends measured in 2003 and 2011. We then compare these gradients for each respective location. Eg: the gradient obtained at Location A in 2003 (from 10 October – 2 November 2003) is compared against its 2011 (from 3 – 27 April 2011) gradient. Though the value of gradient [L/T] obtained here is the rate of water level drop at the manhole, it is directly related to the volumetric exfiltration rate [L^3/T] of the connected infiltration pipes.

We will illustrate the graphical method for monitoring Locations A, B and D. Appendix 6 contains the plots and explanation for the rest of the monitoring locations.

Graphical method at Location A for 2003 and 2011

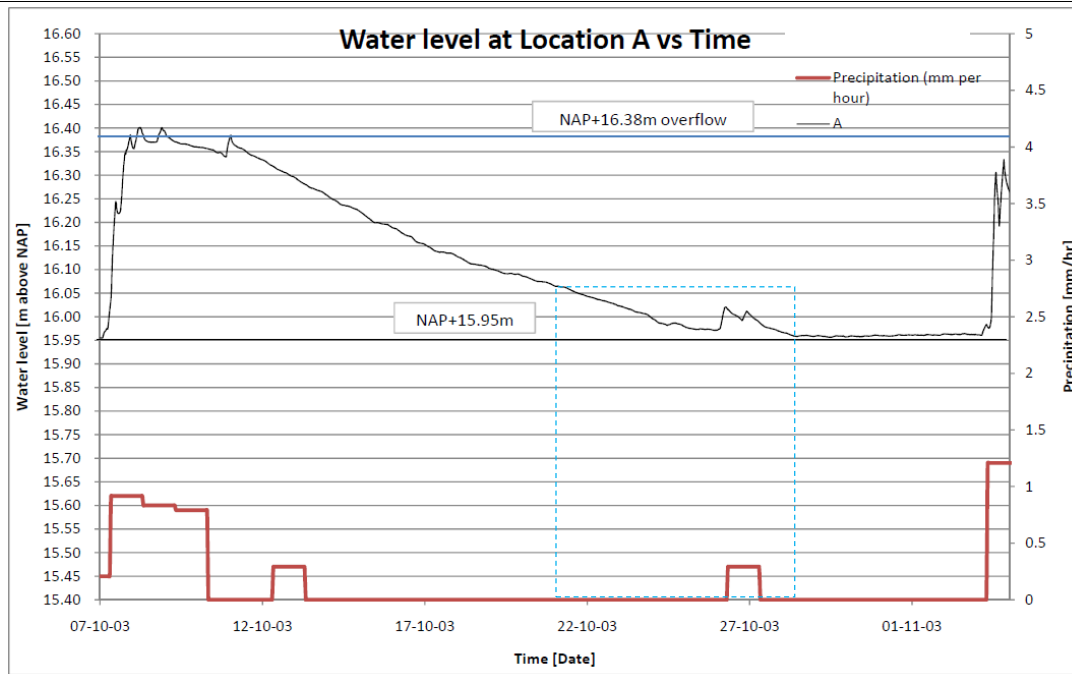


Figure 45: Graphical method used at Location A for 10 October – 2 November 2003 period

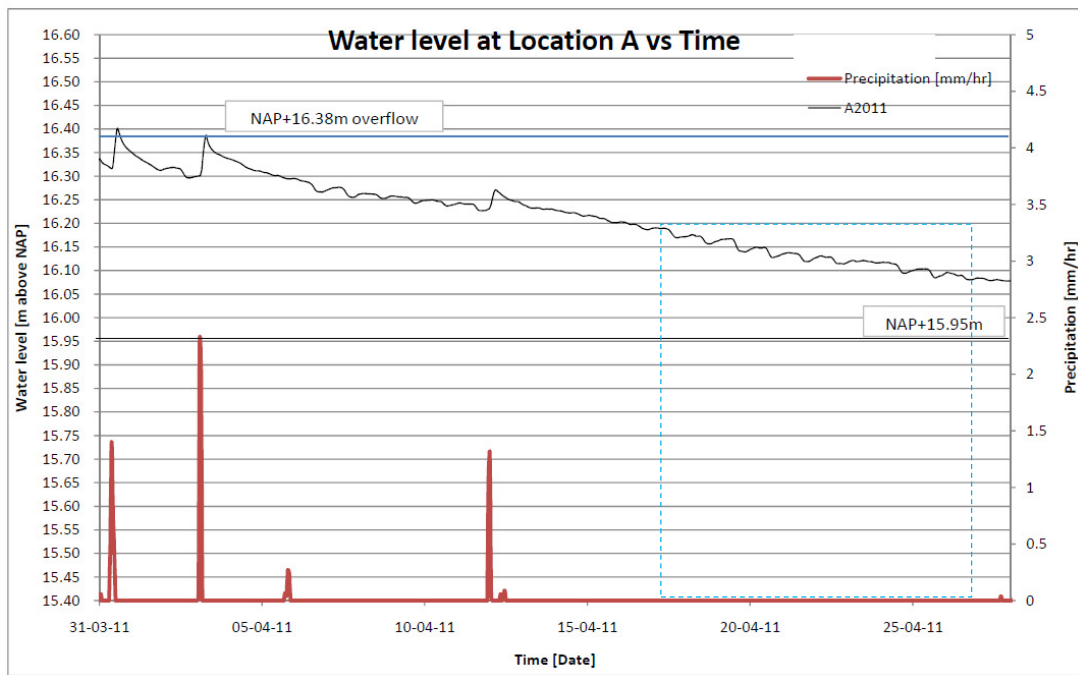


Figure 46: Graphical method used at Location A for 3 – 27 April 2011 period

From the Figure 45, during 21 – 28 Oct 2003 (7.1 days interval), the water level dropped from NAP+16.06m to NAP+15.96m. This leads to an average rate of water level drop of 0.014m/day. Factoring in the rain event on 27 Oct 2003, the actual time interval would be 5.3 days instead. This leads to 0.019m/day. The tail end section was not selected as the water level seems to be rising due to a rainfall event.

On Figure 46, we noticed during 17 – 27 Apr 2011(9.9 days interval), the water level dropped from NAP+16.18m – NAP+16.08m, leading to an average rate of water level drop of 0.010m/day.

Graphical method at Location B for 2003 and 2011

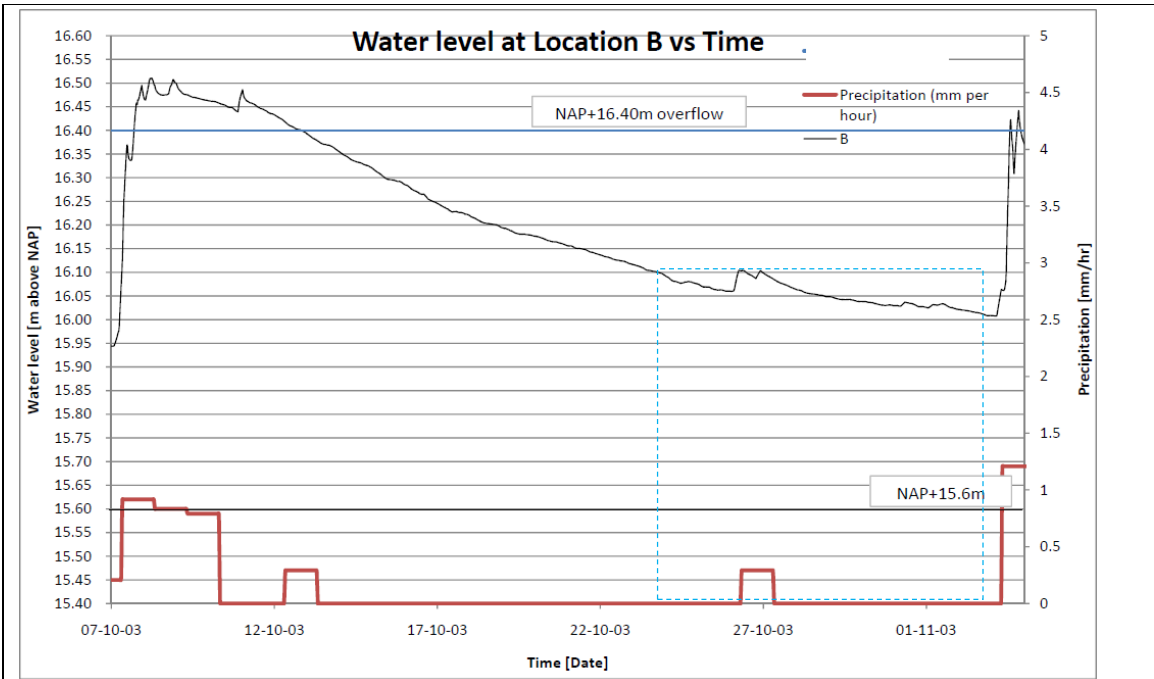


Figure 47: Graphical method used at Location B for 10 October – 2 November 2003 period

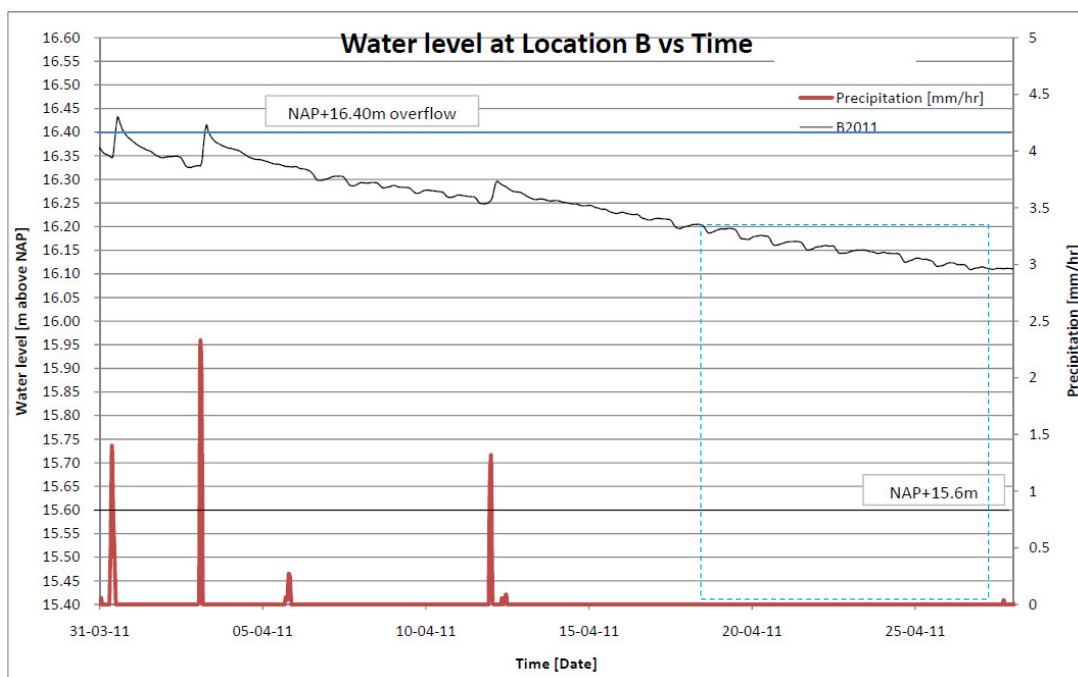


Figure 48: Graphical method used at Location B for 3 – 27 April 2011 period

From Figure 47, the water level dropped from NAP+16.11m to NAP+16.01m during 23 Oct – 2 Nov 2003 (10.6 days interval). This leads to an average rate of water level drop of 0.009m/day. Factoring in the rain event on 27 Oct 2003, the actual time interval would be 8.6 days instead. This leads to 0.012m/day.

We noticed on Figure 48 that during 17 – 27 Apr 2011(10 days interval), the water level dropped from NAP+16.21 – NAP+16.11m, leading to an average rate of water level drop of 0.010m/day.

Graphical method at Location D for 2003 and 2011

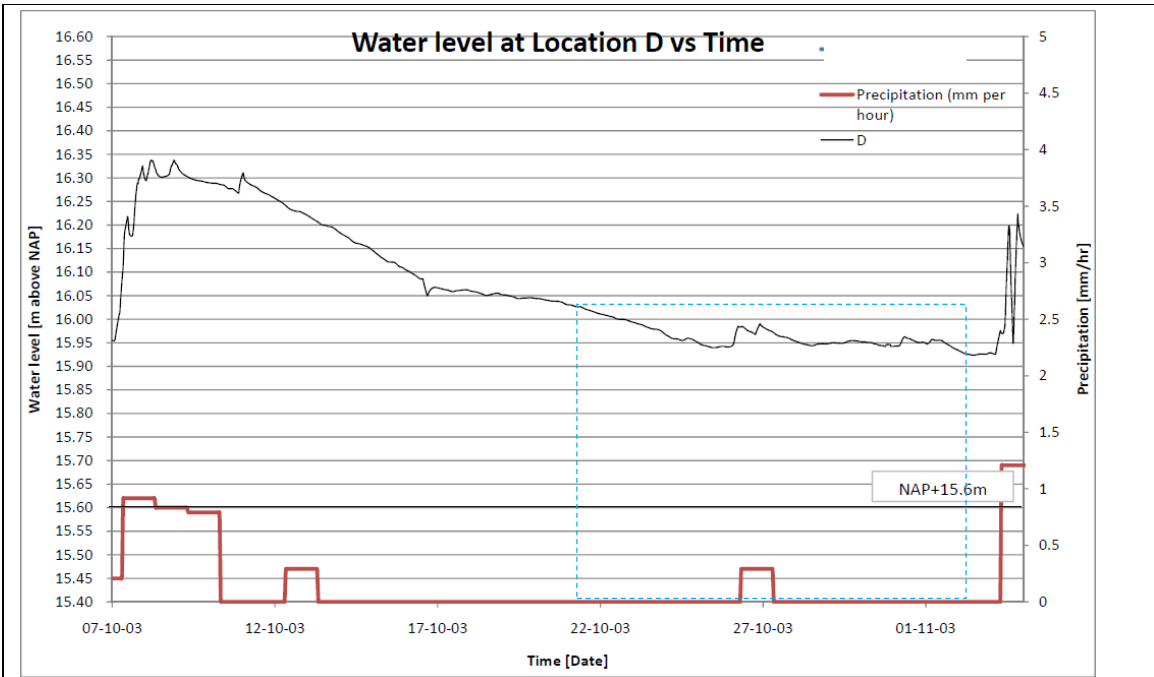


Figure 49: Graphical method used at Location D for 10 October – 2 November 2003 period

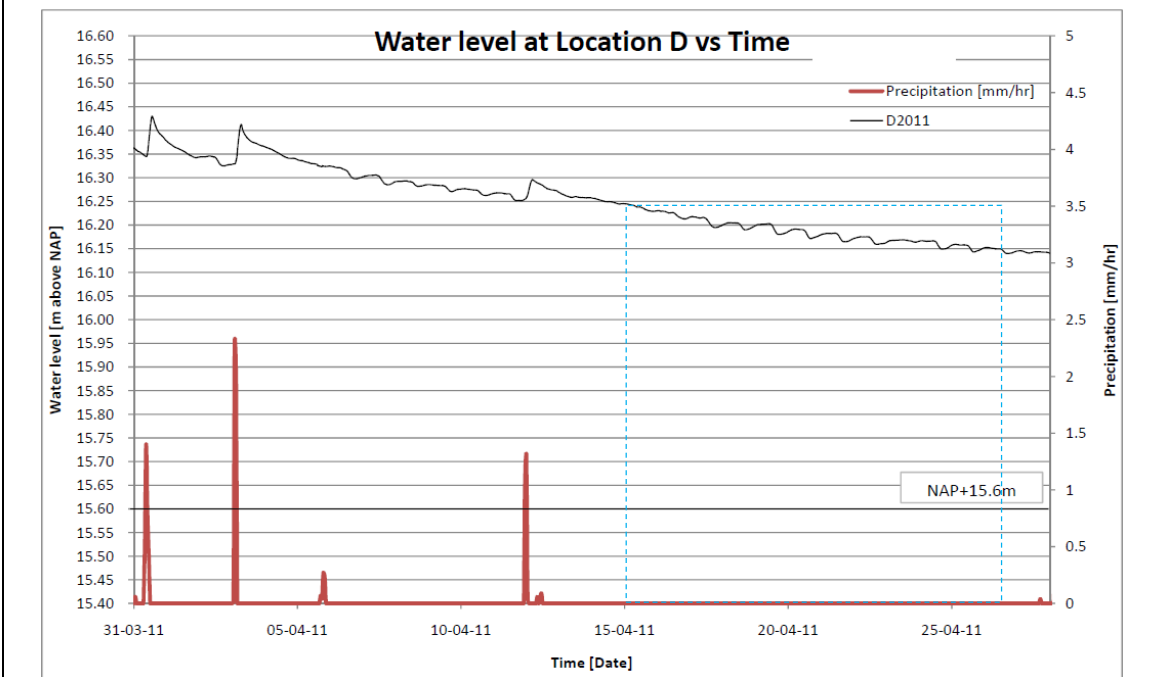


Figure 50: Graphical method used at Location D for 3 – 27 April 2011 period

On Figure 49 above, the water level dropped from NAP+16.03m to NAP+15.93m during 21 Oct – 2 Nov 2003 (12.1 days interval). This leads to an average rate of water level drop of 0.008m/day. Though there may be some interference here, after factoring in the rain event on 27 Oct 2003, the actual time interval would be 9.5 days instead. This leads to 0.011m/day.

On Figure 50, we noticed during 15 – 27 Apr 2011(11.8 days interval), the water level dropped from NAP+16.24m – NAP+16.14m, leading to an average rate of water level drop of 0.009m/day.

5.3 Analysis of average rate of water level drop using Graphical method

Table 2: Comparison of average rate of water drop between 2003 and 2011 data

Location	Average rate of water level drop [m/day]		
	2003	2011	% reduction
A	0.019 [^]	0.010	47.4 [^]
B	0.012	0.010	16.6
C	0.012	0.008	33.3
D	0.011 [*]	0.009	18.2 [*]
E	0.012	0.010	16.6
F	0.012	0.008	33.3

As our main objective of this investigation is on exfiltration effects with the Prinsejagt infiltration drain system, in order to remove/minimise the effects of advection (water flow within the pipes) in the system in our analysis, we need to allow for some time to let the system reach its equilibrium (a situation where most of the advection process had die out) thus leaving the primary driving potential in the infiltration drain as just exfiltration process when it is discharging its water to the surrounding soil.

Generally, a higher water level will mean more driving potential (hydrostatic pressure) for the infiltration drain to discharge water and recharge the groundwater level in the catchment.

In order to factor in (as much as possible) the effect of groundwater level into our analysis, the section of water level selected (for average rate of water level drop analysis) is from the low level upwards (0.1m). On the whole, the average percentage reduction is in the range of 16.6 – 47.4%[^] after factoring in the effects of the rain event occurring on 27 Oct 2003 for 2003 data. Please refer to Table 2 above for details.

Due to differences in the soil profile (permeability) and pipe invert level, it is expected that the average rate of water level drop will differ slightly from location to location. While the average rate of water level drop in 2003 is slightly more varied (between 0.011^{*} to 0.019[^]), the average rates observed in 2011 is within the range of 0.008 to 0.010m/day.

[^] Did not select the tail-end section as the water level seems to be raising slightly, thus the exfiltration rate tabulated here seems higher than the rest (at other locations).

^{*}Suspect there might be some interference during this duration (notice some minor humps that might be caused by localized rainfall, thus leading a lower exfiltration rate)

The exfiltration rate values above have already factored in the delay caused by the 27 Oct 2003 rain event, all the values were rounded up to the nearest millimeters.

5.4 Curve-fitting method

Selection criteria and data processing

A section of the infiltration profile is selected for analysis; this duration was selected because during this period the infiltration system does not experience any rainfall from 11 – 25 Oct 2003 (14 days). During this dry period, the water collected in the infiltration system can be discharged out to its surrounding through the infiltration pipes (assuming no major loss at the manholes and negligible advection process).

For 2011 data, as the groundwater level started to fall below NAP+15.90m after 17 March 2011 (~ 1800hrs), this allows a higher rate of exfiltration by the infiltration drains system than when there is high groundwater level (of NAP+15.90m). This phenomenon (of system effect) was mentioned in the earlier section 4.4. Since the 2003 measurements were taken during low groundwater level (of less than NAP+14.70m), we try to adopt similar selection criteria for our analysis in 2011 data. As such, the periods selected are all after 17 March 2011 and each period is between two major rainfall events recorded. They are:

- 18 to 30 March 2011 (~13 days)
- 3 to 11 April 2011 (~9 days)
- 11 to 22 April 2011 (~12 days)
- 22 to 27 April 2011 (~6 days)
- 29 April to 7 May 2011 (~8 days)

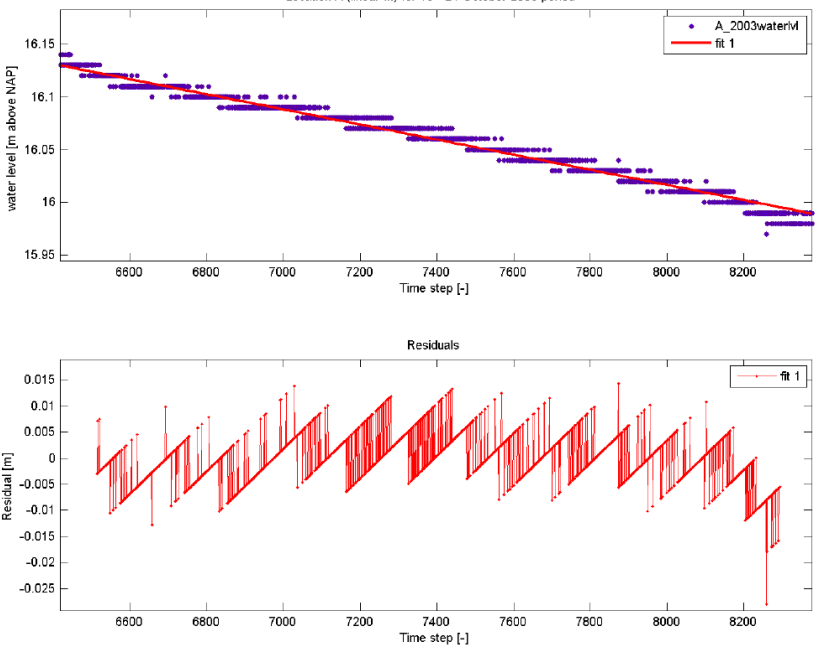
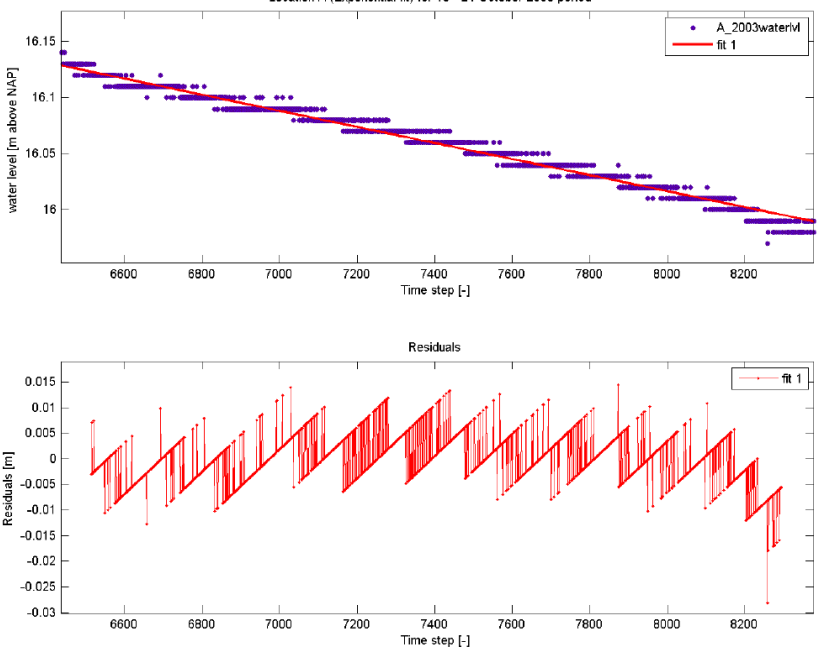
Using Matlab's curve-fitting function, we analyze the change in water level ($h(t)$) for these durations by attempting to curve-fit the water level trend to a few mathematical functions. The three mathematical functions were shortlisted for this purpose and they are: **linear**, **exponential** and **power** functions. The exponential and power mathematical functions are chosen for their ability to describe the water level trend observed from our experimental results whereas linear mathematical function is chosen for its simplicity. The goodness-of-fit (MATLAB, 2011) is subsequently assessed by the following criteria:

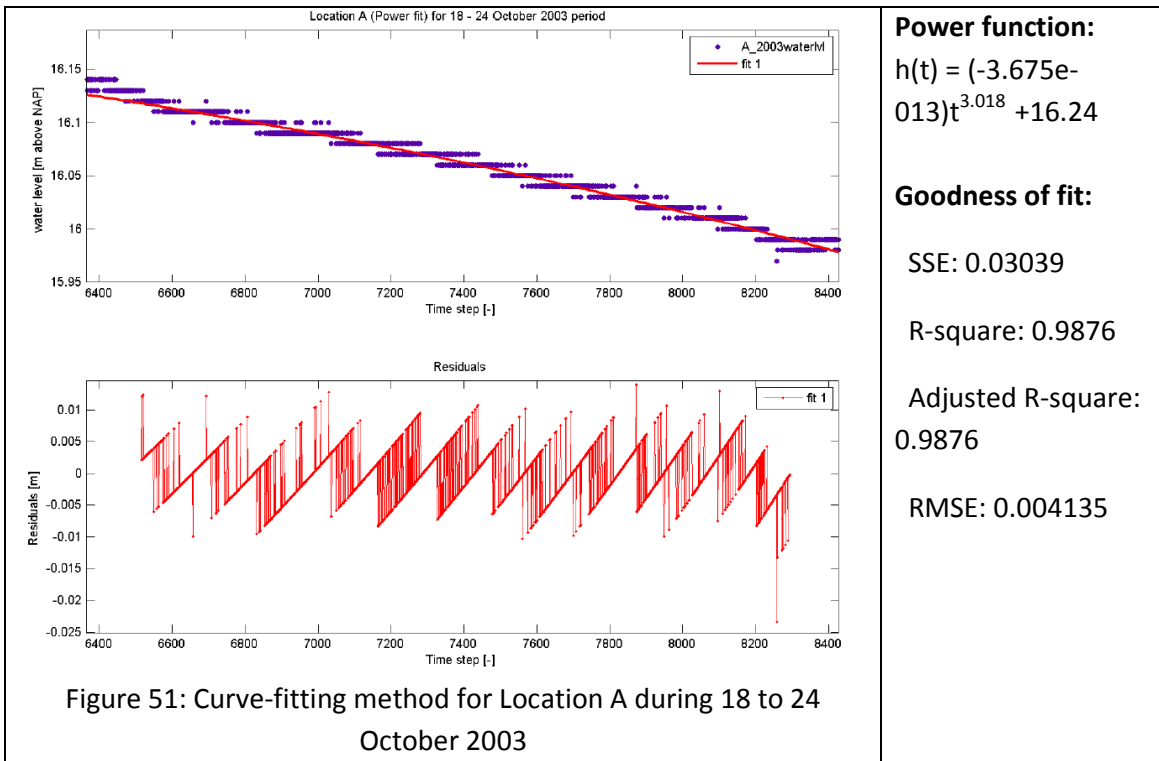
- sum of squares due to error, SSE
- R-square
- Adjusted R-square
- Root Mean Squared Error, RMSE

Through this assessment criteria and its residual plots, we are able assess which mathematical function would be sufficient to describe the observed phenomenon for the infiltration system. Since all the locations (A-F) exhibit system behaviour in their water level profile (as mentioned in section 4.4), we shall only focus on Location A in our selection for the mathematical function that is sufficient to describe the observed phenomenon within the infiltration system. Detailed explanation on each individual goodness-of-fit criterion can be found in Appendix 10.

On the x-axis and y-axis are the timestep [-] (each time step is equivalent to 5 minutes interval) and water level [m above NAP] respectively. We have carried out numerous plots of curve-fitting in which one of the set will be illustrated here to demonstrate our case. The curve-fitting results will be summarised in Table 3 later in this section. Please refer to Appendix 11 for details on the remaining plots.

Curve-fitting method using 3 mathematical functions for Location A during 18 to 24 October 2003

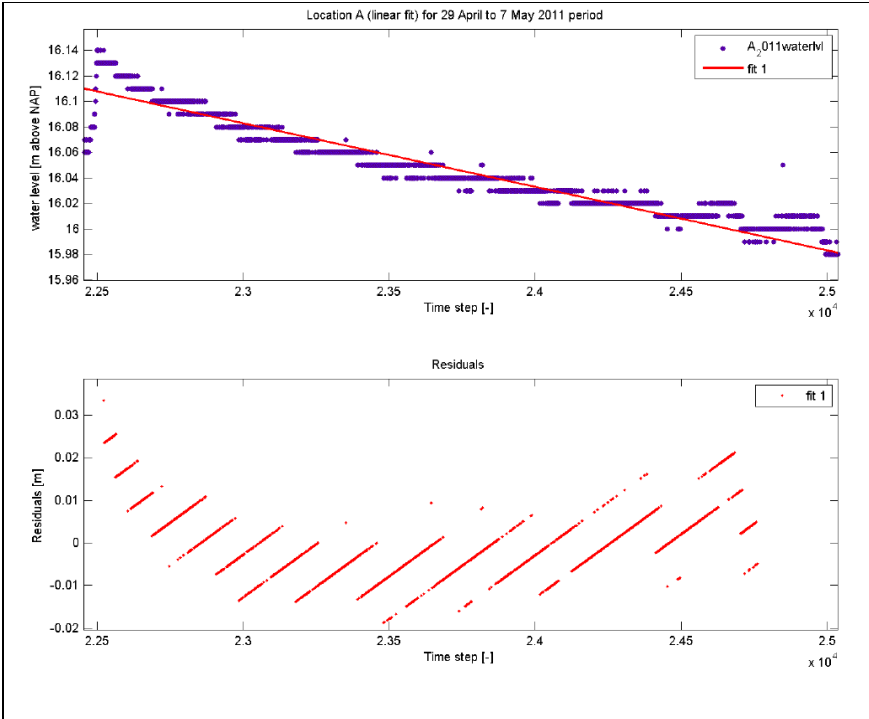
 <p>Location A (linear fit) for 18 - 24 October 2003 period</p> <p>water level [m above NAP]</p> <p>Time step [-]</p> <p>Residuals</p> <p>Residual [m]</p> <p>Time step [-]</p>	<p>Linear function:</p> $h(t) = (-7.166e-005)t + 16.59$ <p>Goodness of fit:</p> <p>SSE: 0.04032</p> <p>R-square: 0.9836</p> <p>Adjusted R-square: 0.9836</p> <p>RMSE: 0.004762</p>
 <p>Location A (Exponential fit) for 18 - 24 October 2003 period</p> <p>water level [m above NAP]</p> <p>Time step [-]</p> <p>Residuals</p> <p>Residual [m]</p> <p>Time step [-]</p>	<p>Exponential function:</p> $h(t) = 16.6 \exp^{-4.461e-6 t}$ <p>Goodness of fit:</p> <p>SSE: 0.04064</p> <p>R-square: 0.9834</p> <p>Adjusted R-square: 0.9834</p> <p>RMSE: 0.004781</p>



From Figure 51, the three functions fit the water level trend rather well, in particular their Root Mean Squared Error are around 0.004m (less than 0.01m). This demonstrates very good capabilities, by these selected mathematical functions, in describing the experimental water level trends for this particular event from 18 to 24 October 2003.

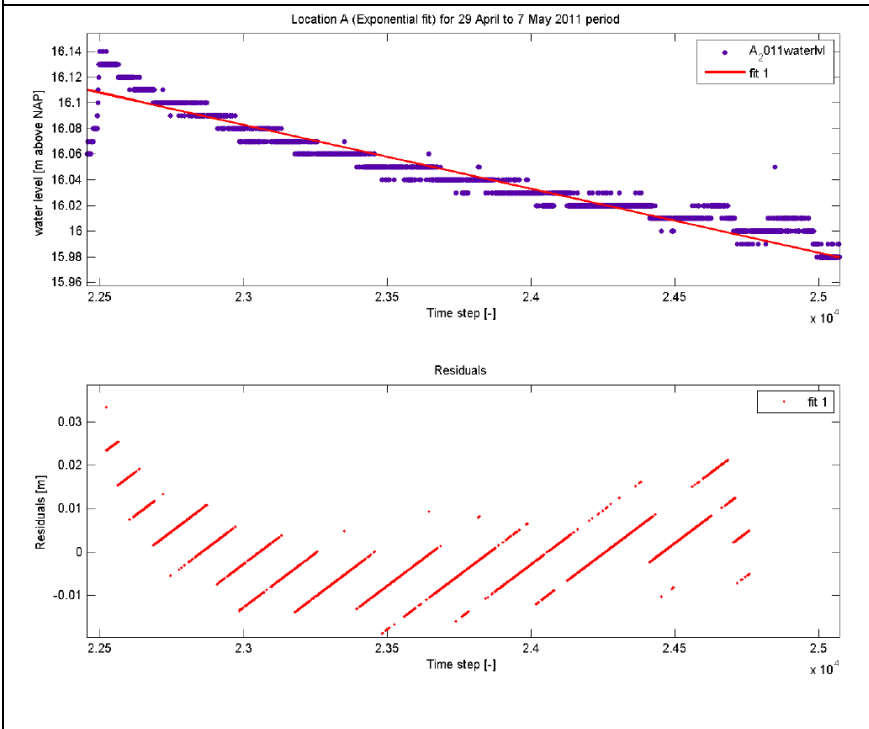
The saw-like trends observed in the residuals plots here is caused by the constant minor fluctuation of water level as the water levels were recorded in very short time interval (of 5 minutes), therefore it is very sensitive to any fast fluctuations to water level (including random water ripple/minor disturbances within the manhole).

Curve-fitting method using 3 mathematical functions for Location A during 29 April to 7 May 2011



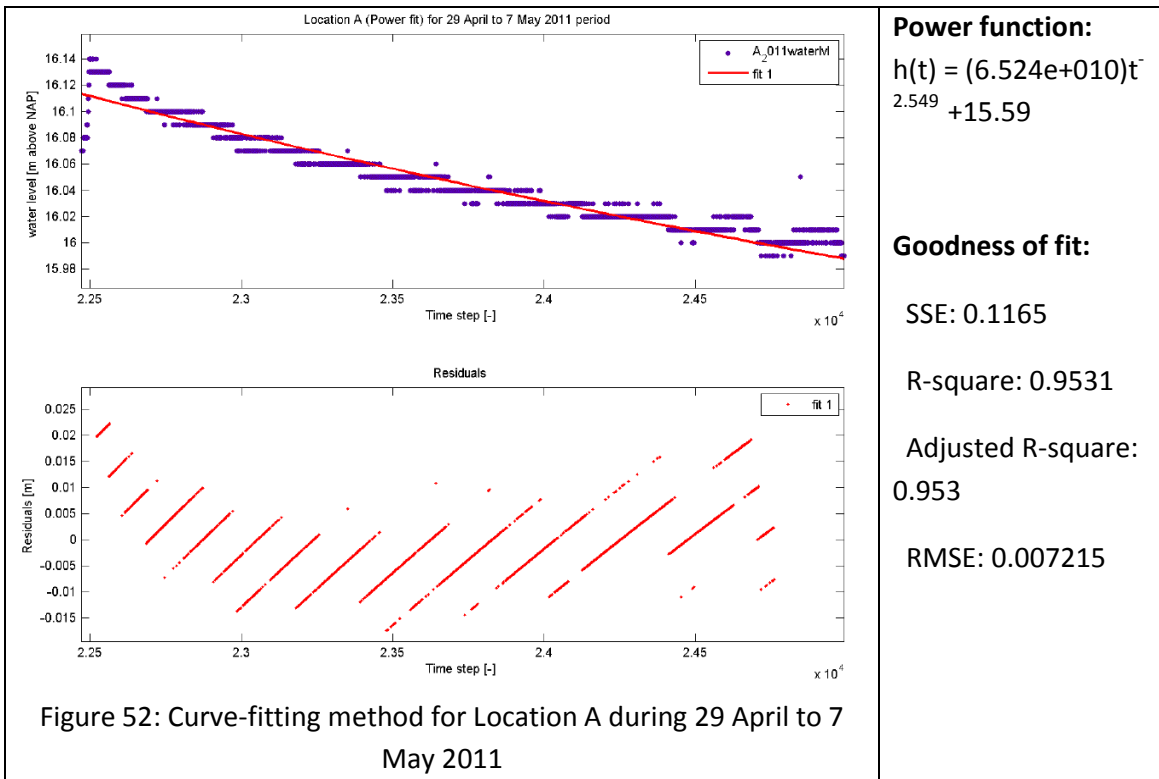
Linear function:
 $h(t) = (-4.985e-005)t + 17.23$

Goodness of fit:
 SSE: 0.1533
 R-square: 0.9383
 Adjusted R-square: 0.9382
 RMSE: 0.008274



Exponential function:
 $h(t) = 17.27 \exp^{-3.107e-6 t}$

Goodness of fit:
 SSE: 0.1525
 R-square: 0.9386
 Adjusted R-square: 0.9386
 RMSE: 0.008252



Similarly for the 29 April to 7 May 2011 event (Figure 52), all the three mathematical functions are able to describe the water level trend well here. All of the functions achieve less than 0.01m of Root Mean Squared Error.

As mentioned earlier, the diagonal lines as observed in the residuals plots due to constant minor fluctuation of water level as our water levels monitoring is done in very short time interval (of 5 minutes). Therefore, it can pick up any fast fluctuations to water level (including random water ripple/minor disturbances within the manhole).

5.5 Selection of mathematical function to be used for curve-fitting analysis

Methodology

One of the three mathematical functions will be selected to be used for subsequent curve-fitting analysis for the remaining monitoring locations.

In order to decide which function is most apt in describing the water level trends ($h(t)$), we have included two additional assessment criteria. Firstly, we check whether the RMSE (between measured and mathematical function) is within our acceptable tolerance error of 0.01m (an accuracy of 0.01m is sufficient in describing the water levels within water sewer or gravity pipeline). Next, we look at the ease of use for the particular mathematical function and its suitability in describing the processes involved in an infiltration drain system. Table 3 below shows the summary of our findings and the ranking for the three mathematical functions.

Table 3: Assessment of mathematical functions for various events occurring at Location A

Event	Function used	$h(t)$ equation	RMSE [m]	Within acceptable tolerance of error?	Preferred function in rank ()
11 to 18 October 2003	Power	$h(t) = (20.2)t^{-0.05194} + 3.32$	0.0043	Yes <0.01m	Don't have physical meaning, best RMSE (3)
	Exponential	$h(t) = 16.91\exp^{(-7.363e-6 t)}$	0.0050	Yes <0.01m	Has physical meaning, RMSE acceptable (2)
	Linear	$h(t) = (-0.0001194)t + 16.89$	0.0050	Yes <0.01m	Simple to use, RMSE acceptable (1)
18 to 24 October 2003	Power	$h(t) = (-3.675e-013)t^{3.018} + 16.24$	0.0041	Yes <0.01m	Don't have physical meaning, best RMSE (3)
	Exponential	$h(t) = 16.6\exp^{(-4.461e-6 t)}$	0.0047	Yes <0.01m	Has physical meaning, RMSE acceptable (2)
	Linear	$h(t) = (-7.166e-005)t + 16.59$	0.0047	Yes <0.01m	Simple to use, RMSE acceptable (1)
18 to 30 March 2011	Power	$h(t) = (-2.493e-007)t^{1.458} + 16.57$	0.0074	Yes <0.01m	Don't have physical meaning, best RMSE (3)
	Exponential	$h(t) = 16.67\exp^{(-1.641e-6 t)}$	0.0074	Yes <0.01m	Has physical meaning, RMSE acceptable (2)
	Linear	$h(t) = (-2.682e-005)t + 16.67$	0.0074	Yes <0.01m	Simple to use, RMSE acceptable (1)
3 to 11 April 2011	Power	$h(t) = (6.204e+010)t^{2.698} + 16$	0.0094	Yes <0.01m	Don't have physical meaning, best RMSE (3)
	Exponential	$h(t) = 17.05\exp^{(-2.881e-6 t)}$	0.0113	Yes ~0.01m	Has physical meaning, RMSE acceptable (2)
	Linear	$h(t) = (-4.688e-005)t$	0.0114	Yes	Simple to use, RMSE

		+ 17.03		~0.01m	acceptable (1)
11 to 22 April 2011	Power	$h(t) = (1.404e+005)t^{1.24} + 15.48$	0.0065	Yes <0.01m	Don't have physical meaning, best RMSE (3)
	Exponential	$h(t) = 17.08 \exp^{(-2.863e-6 t)}$	0.0068	Yes <0.01m	Has physical meaning, RMSE acceptable (2)
	Linear	$h(t) = (-4.633e-005)t + 17.06$	0.0068	Yes <0.01m	Simple to use, RMSE acceptable (1)
22 to 27 April 2011	Power	$h(t) = (3.941e+010)t^{2.589} + 15.85$	0.0062	Yes <0.01m	Don't have physical meaning, best RMSE (3)
	Exponential	$h(t) = 16.76 \exp^{(-1.886e-6 t)}$	0.0063	Yes <0.01m	Has physical meaning, RMSE acceptable (2)
	Linear	$h(t) = (-3.269e-005)t + 16.79$	0.0061	Yes <0.01m	Simple to use, RMSE acceptable (1)
29 April to 7 May 2011	Power	$h(t) = (6.524e+010)t^{2.549} + 15.59$	0.0072	Yes <0.01m	Don't have physical meaning, best RMSE (3)
	Exponential	$h(t) = 17.27 \exp^{(-3.107e-6 t)}$	0.0082	Yes <0.01m	Has physical meaning, RMSE acceptable (2)
	Linear	$h(t) = (-4.985e-005)t + 17.23$	0.0082	Yes <0.01m	Simple to use, RMSE acceptable (1)

Based on Table 3, the three functions are very comparable to each other although the **power** function is slightly more accurate (lower RMSE) than **linear** and **exponential** functions. Since **linear** function is simple to understand and yet sufficiently accurate to describe the water trends, we prefer to adopt the **linear** function as our primary yardstick for curve-fitting the water trends for the remaining Locations (B-F and Point 7).

Moreover, as explained earlier in Section 4.4, we can see from the 2003 and 2011 water level plot for all Locations (A-F) in Figure 38 that they all displayed similar trends and the order of magnitude after each individual rain event. Furthermore, for the entire monitoring period in 2003 and 2011, the relationship plots between monitoring Location A and the rest of the Locations (B-F) showed very good (1-1) linear relationship with minor deviation in the range of +/-0.1m (for 2003 data) and +/-0.05m (for 2011 data). Please refer to Appendix 7 for more details.

In view of the above, instead of comparing the events with the three mathematical functions (**linear**, **exponential** and **power**), we shall simplify this curve-fitting process to just applying the **linear** function only. This would help to avoid any unnecessary repetition in our analysis. Therefore, in our subsequent sections of curve-fitting analysis for monitoring Locations B-F and Point 7, we will only use the **linear** function for our curve-fitting analysis.

Curve-fitting results using linear mathematical function for Locations B - F

There are 7 curve-fitting plots for each monitoring location, 2 plots for 2003 data and the remaining 5 plots for 2011 data. All the individual plots for the remaining locations (B-F and

Point 7) were analysed using *linear* function and the plots can be found in Appendix 12. Using the linear function, we are able to achieve less than 0.01m of Root Mean Squared Error for all the selected events in 2003 and 2011 at all monitoring locations (except for the “3-11 April 2011” scenario, where the Root Mean Square Error is about 0.011m). This magnitude of RMSE (0.011m) is still acceptable for our purpose.

5.6 Analysis of average rate of water level drop using Curve-fitting method

Methodology

Since our main interest is to compare the difference in exfiltration rate of each particular monitoring locations, we can simplify the comparison process by just looking at the *dh/dt* expression since dh/dt expression is equivalent to the slope of a linear equation ($y = mx + c$). As such, we compare results obtained in 2003 with 2011 by using the value of their respective slopes derived from our curve-fitting exercise. We analysed the value of slope [L/T] at each individual monitoring locations.

Comparison of exfiltration rates without taking into account the groundwater level effect

Firstly, we attempt to compare the difference in exfiltration rates without taking into consideration the groundwater effect (as mentioned in Section 4.3 under *Water level trends*). To facilitate our comparison, we group the 2003 and 2011 slopes into upper, lower and average ranges. We then use the highest value of slope in 2003 (among the two 2003 events) to compare it against the highest value of slope observed in 2011 (among the five 2011 events); and similarly for the lowest rate by comparing the lowest values of each respective year. Lastly, we take the average values of slopes obtained in 2003 and compare them with the average value of slopes in 2011. The results of our curve-fitting analysis are as summarised in Table 4 below.

Table 4: Percentage reduction of exfiltration rates at the respective monitoring locations

Monitoring location	Percentage difference in exfiltration rates <i>Results(2011 – 2003)/Results 2003</i>
Location A	Upper range: -58.2%, Lower range: -62.5%
	Average difference: 57.6% reduction
Location B	Upper range: -57.3%, Lower range: -59.1%
	Average difference: 57.4% reduction
Location C	Upper range: -64.6%, Lower range: -55%
	Average difference: 60.8% reduction
Location D	Upper range: -55.2%, Lower range: -64.6%

	Average difference: 60.8% reduction
Location E	Upper range: -57.1%, Lower range: -58%
	Average difference: 57.2% reduction
Location F	Upper range: -59.5%, Lower range: -72.9%
	Average difference: 62.1% reduction
Location Pt 7 (surface water)	Not applicable as this location was not monitored in 2003.

By making comparison between 2003 and 2011 results on the highest, lowest and average rates of water level drop [L/T], we can draw conclusion on the range of percentage reduction in exfiltration rates [L^3/T] (as the cross-sectional area at each respective monitoring location remains the same).

Our results have shown that there is an average of ~60% reduction in exfiltration rates between 2003 and 2011 which is rather substantial. This method of comparison enables us to find out on the extreme percentage reduction in the exfiltration rates (between 2003 and 2011).

Comparison of exfiltration rates after taking into account the groundwater level

Secondly, we factor in the influence of groundwater level on the respective exfiltration rates. In order to do so, we will only compare the results of 18 – 24 October 2003 against 29 April – 7 May 2011 (this is when groundwater level is lowest during our 2011 monitoring period). The results are as shown in Table 5 below.

Table 5: Percentage reduction of exfiltration rates at the respective monitoring locations after factoring the influence of groundwater level

Monitoring location	2003 slope [L/T]	2011 slope [L/T]	Percentage drop $\frac{Results(2011 - 2003)}{Results 2003}$
Location A	-7.166e-5	-4.985e-5	30%
Location B	-7.054e-5	-5.197e-5	26%
Location C	-4.784e-5	-4.646e-5	3%
Location D	-5.748e-5	-5.515e-5	4%
Location E	-6.93e-5	-5.336e-5	23%
Location F	-7.176e-5	-5.006e-5	30%

In this case, the range of percentage drop in exfiltration rate is between 3 to 30%. This result is more reasonable as the groundwater level will affect the system exfiltration performance and therefore the exfiltration results at respective monitoring locations. A summary of the equations of exfiltration rates derived from curve-fitting method can be found in Appendix 13.

6 Excel simulation using the derived differential equation (dh/dt)

6.1 Introduction

A differential equation that seeks to explain the physical processes involved in an infiltration pipe will be derived. This dh/dt expression will subsequently be used to simulate the experimental water trend results for the closed-loop test first before attempting to simulate the water trends for Location A (for 2003 and 2011 data). We simulate the closed-loop test first because the closed-loop test was conducted in a controlled environment and therefore easier for us to check and fault-find our differential equation (dh/dt). The goodness-of-fit between the simulated and experimental data is assessed by the value of Root Mean Square Error (RMSE). Further details on how the analysis of simulation results is being carried will be explained in following sections.

Further explanation on Excel simulation method

Using the derived differential equation (dh/dt), we simulate the water level trends for 4 closed-loop test locations first before proceeding to simulate a section of water level trends observed in both 2003 and 2011 for monitoring location A. As mentioned earlier, we adopted this approach because the closed-loop test was conducted in a controlled environment and therefore easier for us to check, fault-find and verify our differential equation.

Since the Prinsejagt infiltration drain system exhibits system behaviour, thus we believe that having the simulated results for monitoring location A alone would be sufficient for us to have a brief idea on the exfiltration process occurring in the infiltration drain system.

The obtained results on the percentage reduction in exfiltration rates will subsequently be compiled and compared.

6.2 Derivation of differential equation

The differential equations for closed-loop test and at the monitoring location A will be derived in this section.

6.2.1 Formulation of differential equation for closed-loop test

There are two water level scenarios in which the infiltration drain may be subjected to, one of which is when the water level is higher than the pipe crown level and the other is when the water level is lower than the pipe crown level. As such, we will be deriving the differential equations for these two scenarios.

6.2.1.1 Situation when water level is equal or lower than the pipe crown level:

- Drainage q [L^2/T] (2D discharge)
- Width water surface W [L]
- Water depth h [L]
- Radius drain r [L]
- Angle θ [rad]

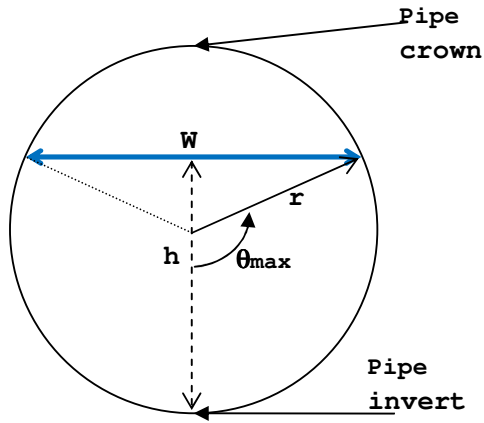


Figure 53: Symbols used and their definitions for differential equation

Both q and W are functions of h and by conservation of mass:

$$\frac{dh}{dt} = q(h)/W(h)$$

Assuming the following scenarios,

- $\theta = 0$ when the pipe is dry;
- $\theta = 0.5\pi$ radian when the pipe is half filled; and
- $\theta = \pi$ radian when the pipe is full

We arrive at the following relation for $W(h)$:

$$W(h) = 2(r - h) \tan \left(\arccos \left(\frac{r - h}{r} \right) \right) \quad [\text{Eq. 6.1}]$$

Using the conductivity of the soil, K [L/T], and the assumption that flow is directly proportional to the water pressure (ie flow=0 at surface, driving force is highest at bottom at h). We derive the $q(h)$ equation for circular pipe exfiltration flow.

$$q(h) = 2 \int_0^{\theta_{\max}} K \cdot \frac{(h - z(\theta))}{\text{longitudinal length of pipe}} \cdot r \cdot d\theta \quad \text{where } z(\theta) = r(1 - \cos \theta)$$

For 2D scenario, we take the longitudinal length of pipe as 1 (for unit length)

$$= 2 \int_0^{\theta_{\max}} K \cdot (h - r(1 - \cos \theta)) \cdot r \cdot d\theta \quad [\text{Eq. 6.2}]$$

$$= 2 \cdot K \cdot r \int_0^{\theta_{\max}} (h - r(1 - \cos \theta)) d\theta = 2 \cdot K \cdot r [h\theta - r\theta + r \cdot \sin \theta]_0^{\theta_{\max}}$$

$$= 2 \cdot K \cdot r \{ [h\theta_{\max} - r\theta_{\max} + r \cdot \sin \theta_{\max}] - [0] \}$$

$$= 2 \cdot K \cdot r \cdot \theta_{\max} [h - r] + 2Kr^2 \sin \theta_{\max}$$

Since $\theta_{\max} = \arccos \frac{r-h}{r}$, we have

$$q(h) = 2.K.r.\left\{[h-r]\arccos\left(\frac{r-h}{r}\right) + r\sin\left(\arccos\left(\frac{r-h}{r}\right)\right)\right\}$$

where $\left\{[h-r]\arccos\left(\frac{r-h}{r}\right) + r\sin\left(\arccos\left(\frac{r-h}{r}\right)\right)\right\}$ term is dimensionless as it is divided by the unit length of pipe

Substituting both equations of W(h) and q(h) into dh/dt

$$\frac{dh}{dt} = \frac{-2.K.r.\left\{[h-r]\arccos\left(\frac{r-h}{r}\right) + r\sin\left(\arccos\left(\frac{r-h}{r}\right)\right)\right\}}{2(r-h)\tan\left(\arccos\left(\frac{r-h}{r}\right)\right)} \quad [\text{Eq. 6.3}]$$

6.2.1.2 Situation when water level is higher than the pipe crown level

When the water level in the manhole is higher than the pipe crown level, the wetted perimeter of the infiltration pipe is equal to the circumference of the infiltration pipe (therefore it is a scenario where W(h) remains constant). As such, the equation of q(h) when water level is greater than the pipe crown would be when $\theta = \pi$ radian. We then obtain q(h) by integrating the expression [Eq. 6.2] from values of $\theta = 0$ to π radian.

$$\begin{aligned} q(h) &= 2.K.r \int_0^\pi \frac{(h-r(1-\cos\theta))}{1} d\theta = 2.K.r[h\theta - r\theta + r.\sin\theta]_0^\pi \\ &= 2.K.r\{[h\pi - r\pi + r.\sin\pi] - [0]\} \\ &= 2\pi K.r.[h-r] \end{aligned} \quad [\text{Eq. 6.4}]$$

where $[h-r]$ term is dimensionless as it is divided by unit length of pipe

Due to the nature of the differential equations above, we used the Runge-Kuta 4 scheme to solve it.

6.2.2 Formulation of differential equation for monitoring Location A

To derive the differential equation for monitoring Location A, we used a similar two-step approach where there are two scenarios:

1. When water level is greater than the pipe crown level; and
2. When water level is equal or below the pipe crown level

Depending on the water level at the specific time, the relevant differential equation will be applied.

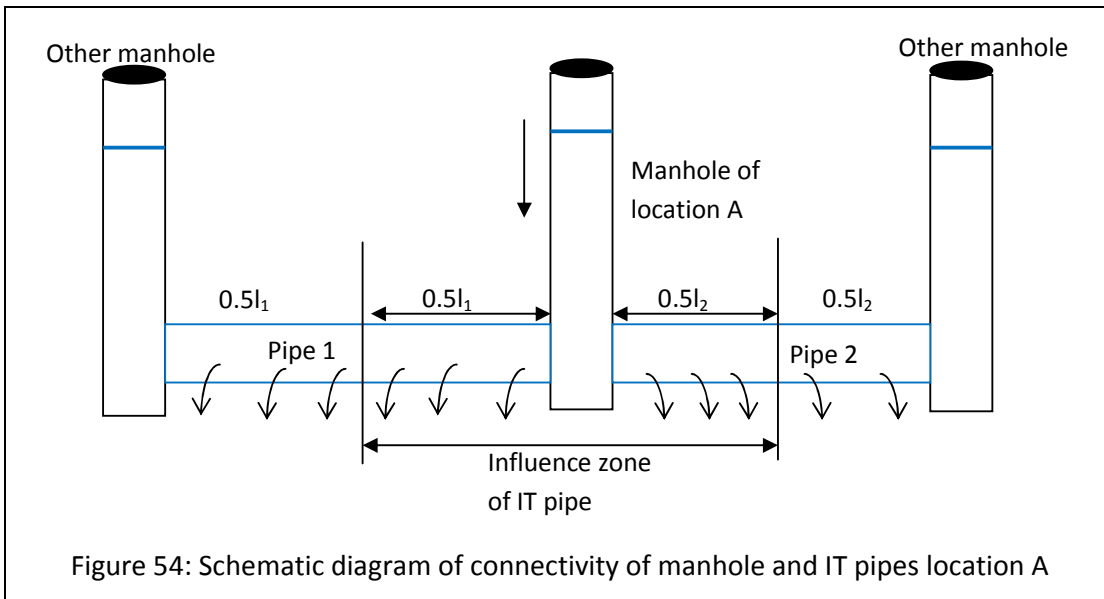
6.2.2.1 Situation at location A:

- $W(h)$ does not change when water level is greater than the pipe crown
- Number of infiltration drains connected to manhole is 2
- Cross-sectional area of manhole is rectangular
- Assuming the effective influence zone of infiltration drains (that we are analysing) as half of its respective length from the other connecting manholes

Data used:

- Length of IT pipe 1 used = $42/2 = 21\text{m}$
- Length of IT pipe 2 used = $34/2 = 17\text{m}$
- Radius of IT pipe 1 and 2 = 0.15m
- Cross sectional area of manhole = 0.5m^2

Therefore, the total flowrate out for 1 pipe is equivalent to $q(h) [L^2/T] \times \text{length of the IT pipe } [L]$.



6.2.2.2 Situation when water level is equal or lower than the pipe crown level:

Once the water level is equal to or below the pipe crown level, we need to apply the concept of volumetric discharge of infiltration pipes divided by the area of manhole to obtain the differential equation (dh/dt).

$$\begin{aligned} \frac{dh_{manhole}}{dt} &= \sum_1^{no.of\ connected\ pipes} \frac{Q_i(h)}{Area\ of\ manhole} \\ &= \sum_1^{no.of\ connected\ pipes} \frac{-K \cdot r_i \cdot l_i \left\{ [h - r_i] \arccos\left(\frac{r_i - h}{r_i}\right) + r_i \sin\left(\arccos\left(\frac{r_i - h}{r_i}\right)\right) \right\}}{Area\ of\ manhole} \end{aligned}$$

Since both connecting pipes have similar length and radius dimensions for location A, we can directly apply Eq. 6.3 to obtain the water level profile over time once the water level is equal or below the pipe crown level.

6.2.2.3 Situation when water level is higher than the pipe crown level:

From Figure 54, you could see that dh/dt of the water level in manhole (until the pipe crown level) can be expressed as:

$$\frac{dh_{manhole}}{dt} = \sum_1^{no.of\ connected\ pipes} \frac{-2\pi K \cdot r_{pipe,i} \cdot [h - r_{pipe,i}] \cdot 0.5l_i}{Area\ of\ manhole}$$

Similarly, we applied Runge Kuta 4 method to solve the differential equations.

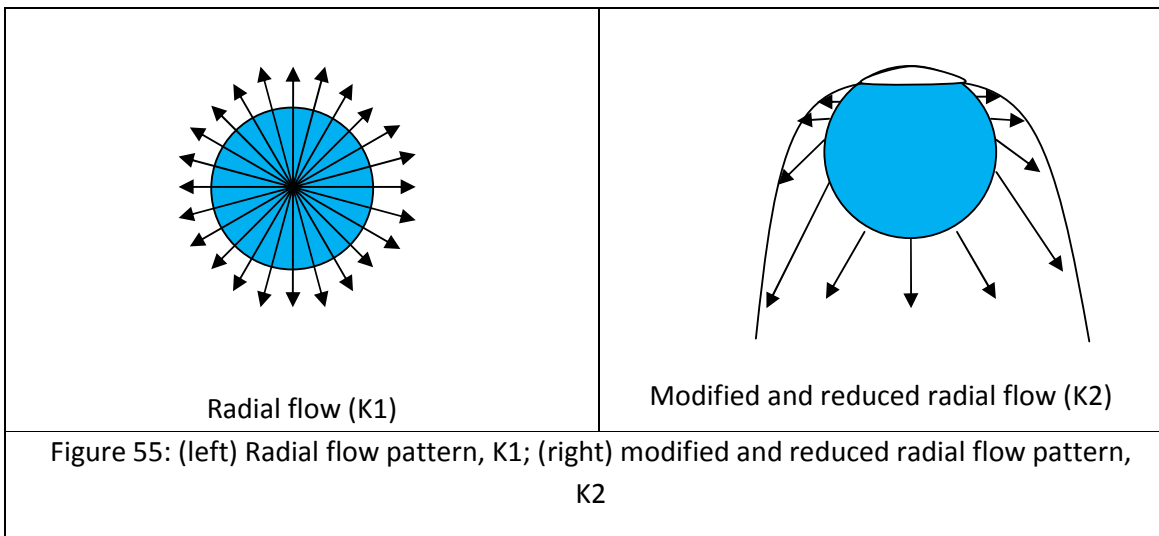
6.3 Simulation of closed-loop test results

6.3.1 Introduction and concept

We selected highest water level observed at the respective test locations as our initial water level and starting time. Next, we used the same time-step as the divers monitoring interval (5 minutes). With the excel spreadsheet is set up, we simulate the drop in water level for the same number of timesteps (duration) taken in our measured readings (for each respective locations).

We used $K [L/T]$ as our tool to fine-tune our simulation model to best-fit the experimental results. K values that give the lowest RMSE (between our simulated results and actual readings) are then selected for our analysis. In order to avoid any unnecessary confusion, this K -value is not the soil conductivity although it is closely linked to it. To allow us in differentiating which flow regime (above pipe crown or below pipe crown), we denote $K1$ as flow regime when water level is above pipe crown level while $K2$ is used for flow regime when water level is equal or below pipe crown level. For our simulation, data on the radius and length of infiltration pipe are required as input for the differential equation (dh/dt).

When the groundwater level is much lower than the pipe invert level, $K1$ would describe a radial-type of exfiltration flow while $K2$ will mean a modified and reduced radial-type of exfiltration flow as shown in Figure 55. When the hydrostatic pressure is high, the exfiltration flow pattern will be more likely to be more radial-like due to higher driving force (water height). Whereas once the water level reaches around the pipe crown level, the hydrostatic pressure is not high enough to sustain this radial flow pattern, this led to a drop in K value (we use $K2$ to denote this new K value)



The respective K -values [m/day] will be analysed in more details in the subsequent section as it is an indicator of the exfiltration rate of the individual infiltration pipe

6.3.2 Simulation results for closed-loop test

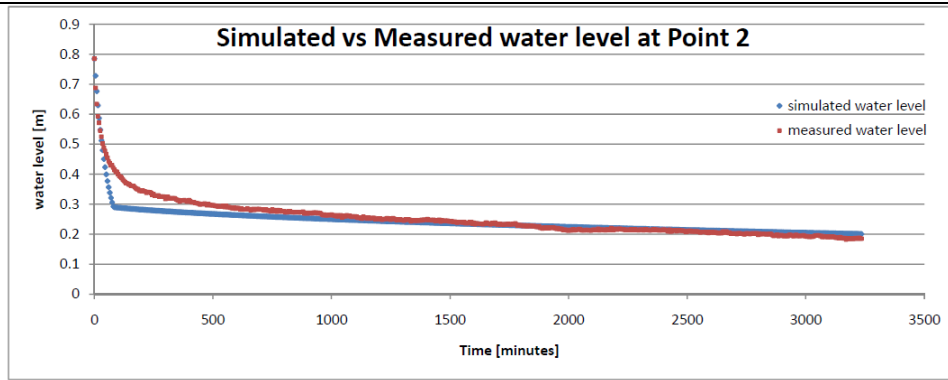


Figure 56: Plot of simulated and measured water levels at location Point 2

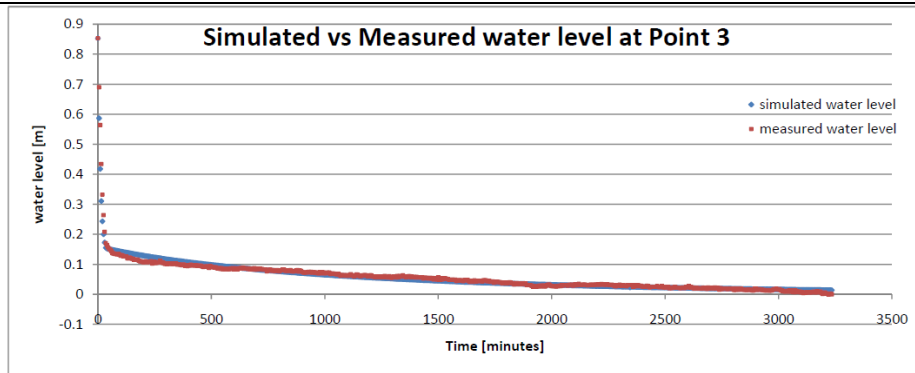


Figure 57: Plot of simulated and measured water levels at location Point 3

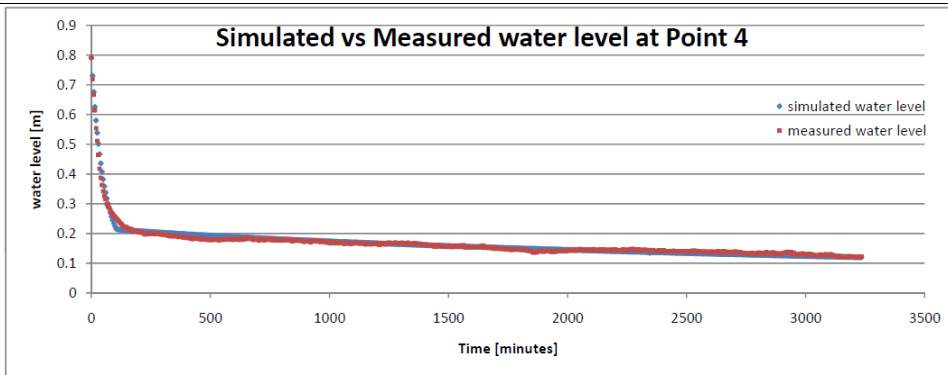


Figure 58: Plot of simulated and measured water levels at location Point 4

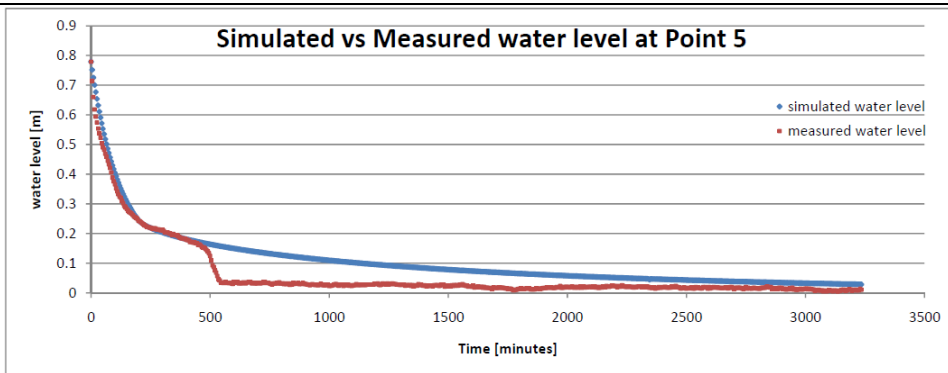


Figure 59: Plot of simulated and measured water levels at location Point 5

Our simulated water levels fit the measured water levels relatively well for all the four locations (Figures 56 to 59), the range of RMSE achieved is between 0.008 – 0.025m, and this is quite remarkable considering the simple differential equation used for this purpose. It is normal to expect the K1 value to be larger than K2 value; this is due to large driving force from higher water level.

The K1, K2 and RMSE values for the respective locations are given in the Table 6 below.

Table 6: K1, K2 and RMSE values obtained for closed-loop tests

Location	K1 [m/day]	K2[m/day]	RMSE [m]
Point 2	0.0087	0.0041	0.025
Point 3	0.05	0.05	0.015
Point 4	0.012	0.009	0.008
Point 5	0.0053	0.026*	0.008*

** the values of K2 and RMSE at Point 5 should be used with caution as the number of data points available for comparison is much lower before the water level plunged to almost zero level.*

Next, we shall proceed to simulate the measured water level trend for monitoring location A.

6.3.3 Simulation results for monitoring location A

Introduction

We are aware that there is little or negligible groundwater influence on the infiltration drain system during 2003 monitoring period as the groundwater is lower than the lowest pipe invert level in the system then. However, during our 2011 monitoring period, we experienced high groundwater level in the early phase of our measurement period before the groundwater level starts to drop to lower than NAP+15.43m level in late April period. In order to investigate this effect, we will be looking into how groundwater level influence the performance of Prinsejagt infiltration drain system in 2011 first before comparing our 2011 data with the results of 2003 data.

6.3.3.1 Effect of groundwater level on the K values at location A in 2011

Introduction

A similar approach as the closed-loop test is applied here. We used K [L/T] as our tool to fine-tune our simulation model to best-fit the experimental results. K values that give the lowest RMSE (between our simulated results and actual readings) are then selected for our analysis.

However, we would like to factor in our understanding (Section 4.4) that the entire infiltration drain system in Prinsejagt is connected and behaves like a system, therefore knowing the respective K (K1 or K2) values for different groundwater levels will give us a better understanding on the exfiltration capabilities of this system and how the groundwater level would influence or limit the performance of the infiltration drain system as a whole, in terms of the system exfiltration rate [m^3/day].

As such, we analysed the effect of different groundwater levels (from high to relatively low) in the exfiltration rates of the system during our monitoring period in 2011. The respective K-values [m/day] will be analysed in more details as it is an indicator of the exfiltration rate of the infiltration drain system.

The 2011 water level trends that were simulated include:

- 18 – 29 March 2011 (when groundwater level greater than NAP+15.94m)
- 3 – 10 April 2011 (when groundwater level around NAP+15.70m)
- 12 – 26 April 2011 (when groundwater level around NAP+15.53m)
- 29 April – 7 May 2011 (when groundwater level below NAP+15.43m)

Our simulation results are shown in the Figures 60 to 63.

Simulation results at Location A for different groundwater levels in 2011

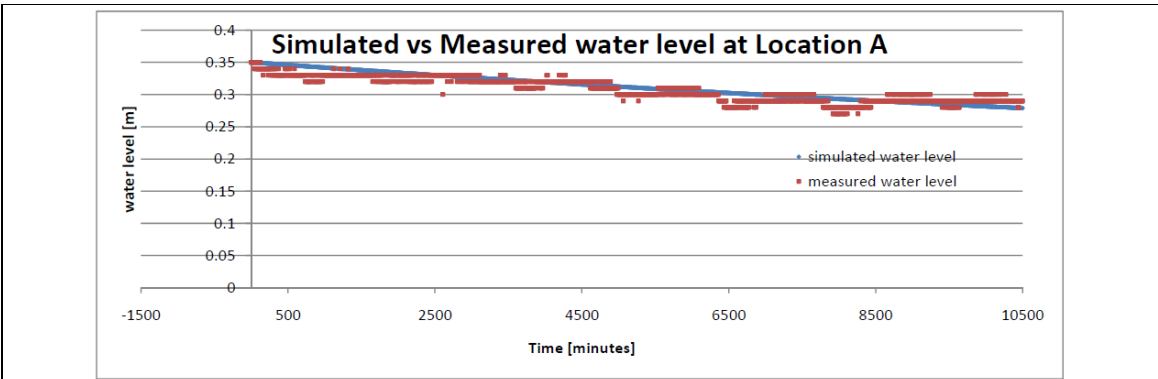


Figure 60: Plot of simulated and measured water levels at location A (18 – 29 March 2011)

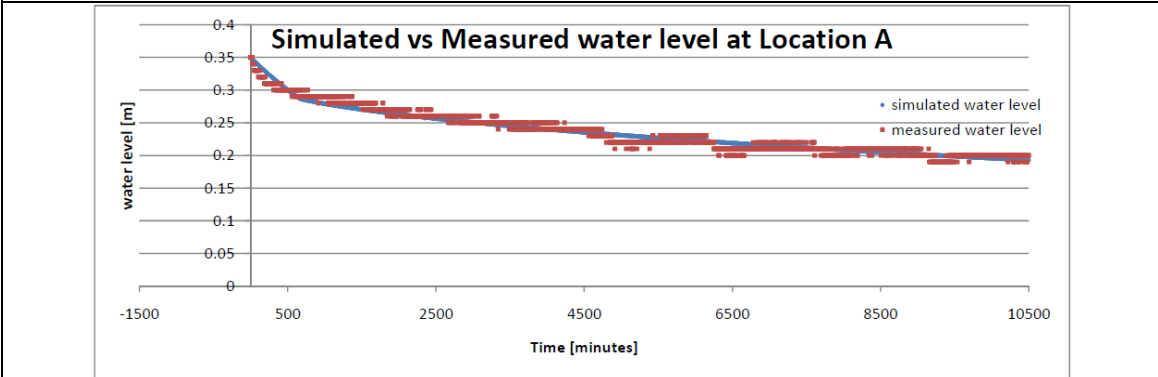


Figure 61: Plot of simulated and measured water levels at location A (3 – 10 April 2011)

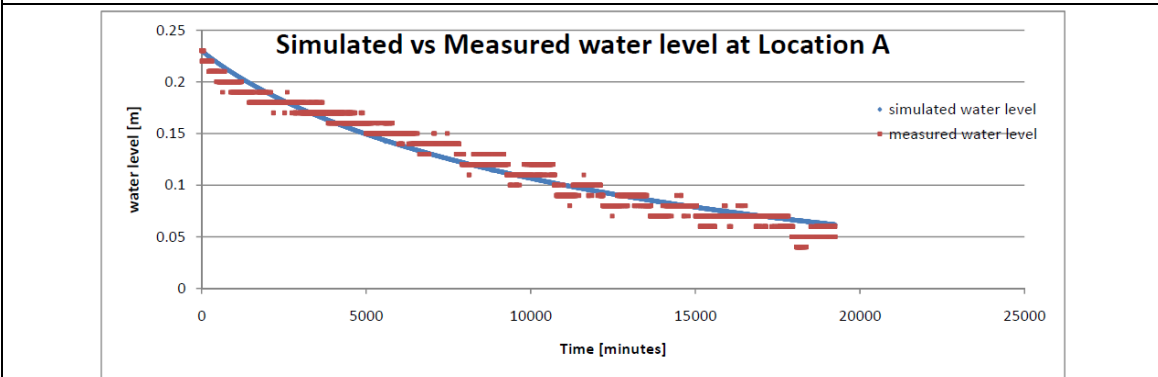


Figure 62: Plot of simulated and measured water levels at location A (12 – 26 April 2011)

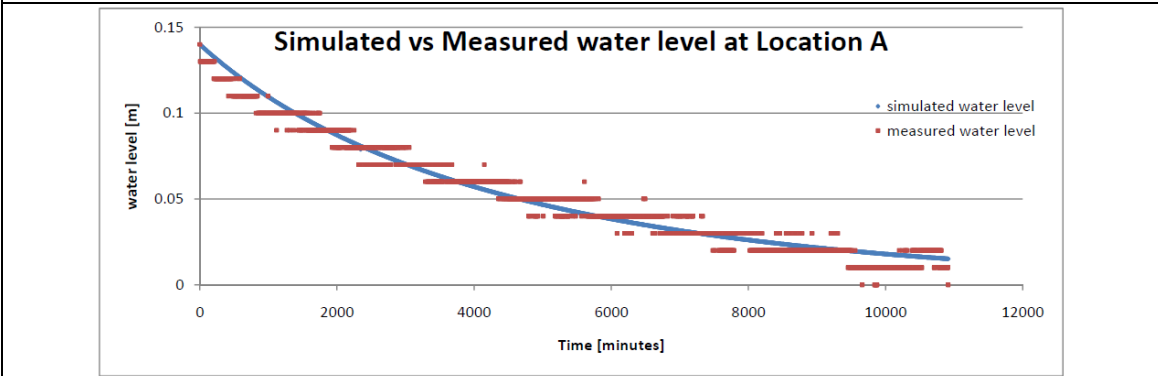


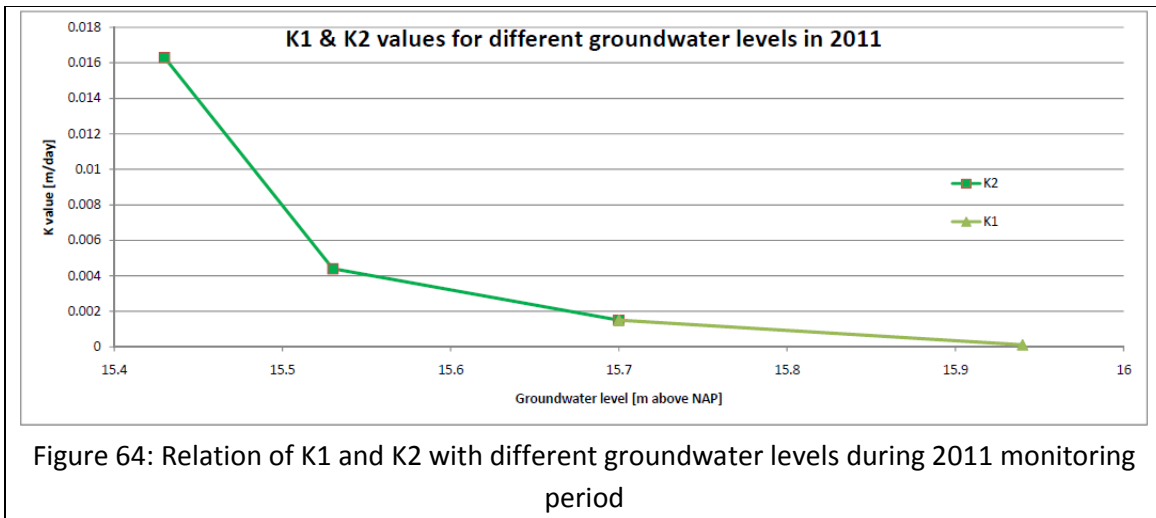
Figure 63: Plot of simulated and measured water levels at location A (29 April – 7 May 2011)

The selected periods, their respective groundwater level and corresponding percentage of network affected are summarised in the Table 7 below:

Table 7: Summary of K1 and K2 values for various groundwater level at location A

Period	Starting groundwater level [m above NAP]	Percentage of network affected by groundwater	K1 [m/day]	K2 [m/day]	RMSE [m]
18 – 29 March 2011	>15.94	90%	0.00011	-	0.0088
3 – 10 April 2011	~15.70	54%	0.0013	0.0015	0.0068
12 – 26 April 2011	~15.53	30%	-	0.0044	0.0094
29 April – 7 May 2011	<15.43	10%	-	0.0163	0.0056

We are able to demonstrate a good fit between our simulated results and the measured readings (Please see the Figures 60 to 63 and their respective RMSE values. Our model can describe the water trend with less than 0.01m of RMSE value; this close fit could be attributed to the slow variation of water levels experienced in the system.



In order to obtain the respective system K values in 2011, we plot the values of K [m/day] against the groundwater level [m above NAP]. At higher groundwater level, the ability of the infiltration system to exfiltrate its water out to the surrounding soil will be reduced and Figure 64 above shows the relationship of K1 and K2 values with the respective groundwater level observed during our monitoring period (Feb – May 2011). This information would be especially useful for water planner to estimate the system exfiltration rates during different seasons that have different groundwater level trend.

Effect of different K values (due to different groundwater levels) on the system exfiltration rate

K values are determined for each corresponding groundwater level (Table 7). To obtain the system exfiltration rate [m^3/day] for different groundwater conditions (Figure 65), we used the available wetted perimeter ($\pi \times pipe\ diameter \times "available\ length"$) and its corresponding K value. The "available length" is defined as the section of pipe that has its pipe invert level higher than the existing groundwater level. In other words, we assumed that when the groundwater level is equal or higher than the pipe invert level, this section of pipe is not 'available' for exfiltration. With the system exfiltration rate curve (similar concept to how we derive Figure 11), we can determine the instantaneous system exfiltration rate [m^3/day] for any starting water level within the infiltration drain system.

For instance, when the water level within the system is above NAP+16.05m and the groundwater level is below NAP+15.43m (ie $K_2=0.0163m/day$), the instantaneous system exfiltration rate is $53.1m^3/day$. Assuming the groundwater level remains below NAP+15.43m, the instantaneous system exfiltration rate will follow the trendline (labelled $K_2=0.0163$) as the water level drops within the infiltration drain system.

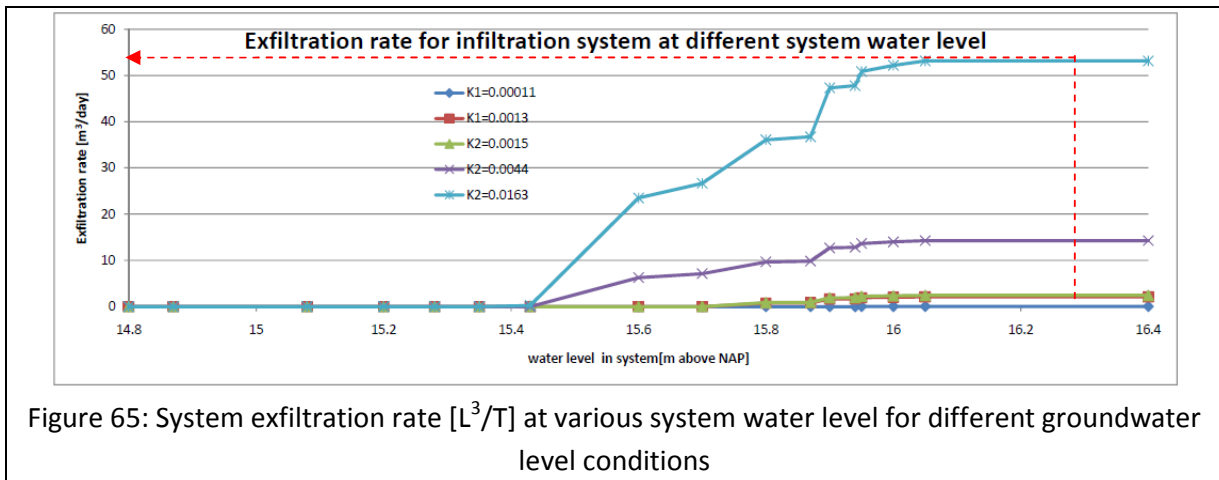
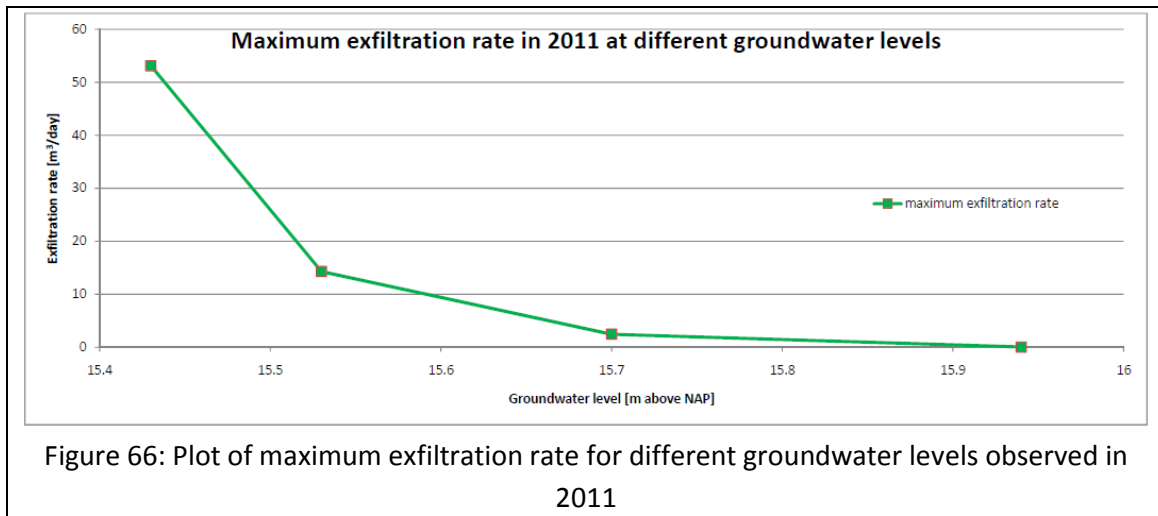


Figure 65: System exfiltration rate [L^3/T] at various system water level for different groundwater level conditions

Next, during period of high groundwater level at NAP+15.70m or higher (before 3 April 2011), we observed from the system exfiltration curve (for $K_1=0.00011$, 0.0013 and $K_2=0.0015$) that the exfiltration rate [m^3/hr] for the entire Prinsejagt catchment is almost negligible (having a maximum exfiltration rate of $2.4m^3/day$ at system water level greater than NAP+16.05m). If the infiltration drain system is unable to recharge itself (by exfiltrating sufficient volume of water) in time for the next rainstorm event, it will tend to overflow its excess water to the surface water (through its overflow connections, set at NAP+16.40m).

When the groundwater level is below NAP+15.43m, the infiltration system is able to exfiltrate at a maximum rate of $53.1m^3/day$ for system water levels higher than NAP+16.05m. This is a huge difference in exfiltration rate would mean that the infiltration system is able to recharge itself in a much shorter time and be ready for the next rainstorm event.

In Figure 66, we see the maximum system exfiltration rate for each groundwater level measured in 2011, the system exfiltration rate $[L^3/T]$ decreases exponentially as the groundwater level increases. This is also in line with our explanation of effect of groundwater level in Section 4.3.



6.3.3.2 Comparison of K-values at Location A for 2003 and 2011

Similar sections of the water levels trend for 2003 and 2011 are used for our simulation and the values of K [m/day] that gives the best-fit on the experimental data are compared to determine whether there is any significant drop in the exfiltration rate (Figures 67 and 68). We have chosen “15 to 21 October 2003” water trend data to be compared with “29 April to 7 May 2011” data because they have the closest groundwater level.

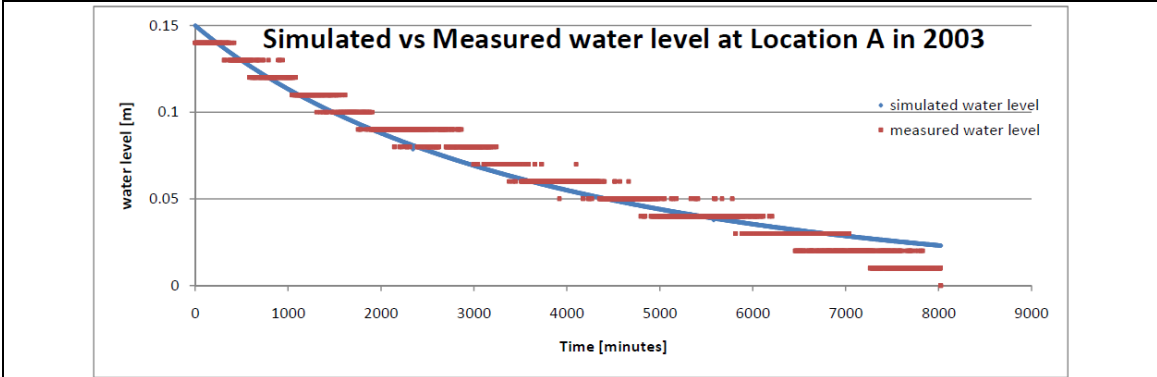


Figure 67: Plot of simulated and measured water levels at location A (15 – 21 October 2003)

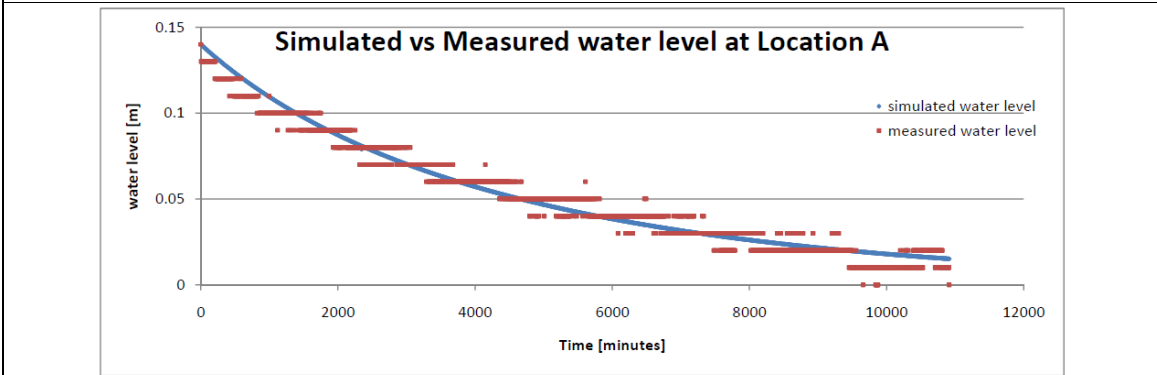


Figure 68: Plot of simulated and measured water levels at location A (29 April – 7 May 2011)

Table 8: Comparison table of K2 values obtained from simulation for 2003 and 2011 data

Period	Starting groundwater level [m above NAP]	Percentage of network affected by groundwater	K2 [m/day]	RMSE [m]
15 – 21 October 2003	<14.70	0%	0.018	0.0072
29 April – 7 May 2011	<15.43	10%	0.0163	0.0056

From Table 8, we notice that there is a 9.4% drop in the K-value since 2003.

6.3.3.3 Comparison of system exfiltration rate using Location A for 2003 and 2011

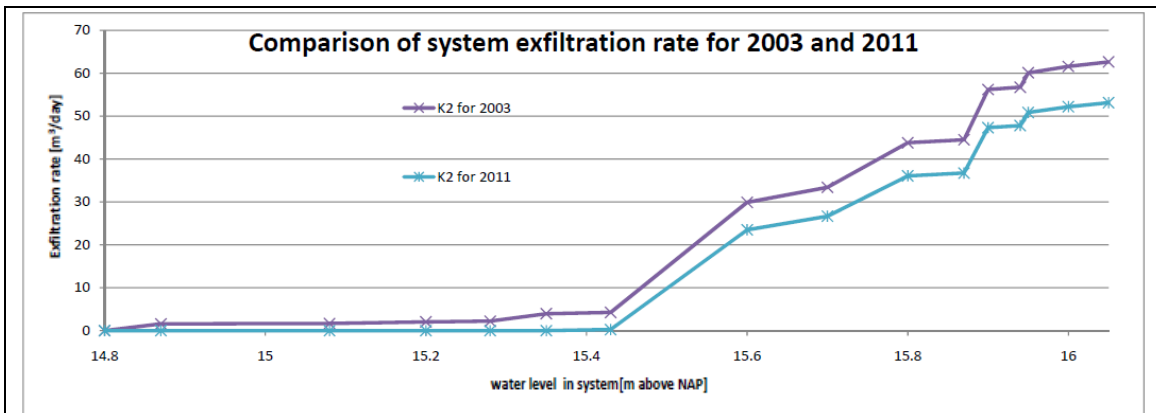


Figure 69: Difference in the system exfiltration rate [m³/hr] between 2003 and 2011 for the respective water levels in the infiltration system

Since the groundwater is always lower than the lowest pipe invert level in 2003, we used the 29 April to 7 May 2011 data for our comparison with the 2003 data. This is the closest comparison we could establish between 2003 and 2011 system volumetric exfiltration rates, based on our available data.

Similar profiles of system exfiltration rate are observed for 2003 and 2011 in Figure 69. In 2011, the groundwater level is around NAP+15.43m so you will notice that there is negligible amount of water exfiltrated when the system water level is equal or less than the groundwater level. On the other hand, the entire system can be utilised to exfiltrate its collected water in 2003.

Moreover, once the system water level is above NAP+15.60m, we noticed a significant jump in the system volumetric exfiltration rate to 30m³/day (2003) and 23.5m³/day (2011). This is due to a huge proportion of the infiltration pipe is laid at NAP+15.60m. We also found that the percentage difference in volumetric exfiltration rate between the two trends (2003 and 2011) is approximately 15% after the system water level reaches above NAP+15.90m. The maximum exfiltration rates for 2003 and 2011 are 62.6m³/day and 53.1m³/day respectively.

A decrease in exfiltration capacity will lead to longer retention time and possible more incidents of overflow as the system is unable to discharge its collected water to surrounding soil fast enough before the next rainstorm event.

6.3.3.4 Summary of K values obtained for closed-loop test and system (at location A)

Results from the similar flow regime (for water level below the pipe crown level) at our monitoring location A are compared with the closed-loop test results.

Table 9: Comparison of K values of closed-loop test and location A (system)

Type of measurement	Location	K2[m/day]	RMSE [m]
Regular monitoring	System (location A)	0.0163	0.0056
Closed-loop test	Point 2	0.0041	0.025
	Point 3	0.05	0.015
	Point 4	0.009	0.008
	Point 5	0.026*	0.008*

**The values of K2 and RMSE at Point 5 should be used with caution as the number of data points available for comparison are much lower before the water level plunged to almost zero level.*

Table 9 showed that the K2 value of infiltration system is around 0.0163m/day while K2 values from the individual closed-loop tests conducted, exhibits a larger variation, from 0.0039 to 0.05m/day. The relatively larger difference in the K and RMSE values of the individual section of infiltration pipe could be attributed to differences in localised soil profiles, localised groundwater level and degree of clogging at the respective pipe sections. Whereas at monitoring location A, there is more buffering and averaging effect due to its connectivity to the rest of the infiltration system (helps to reduce the RMSE).

7 Analysis of results

7.1 Introduction

The respective values of the average rate of water level drop [L/T] obtained from the 3 approaches (graphical, curve fitting and simulation) are compiled for our analysis. We used the results of monitoring Location A for this purpose.

- Graphical method (refer to Table 2)
- For curve-fitting method, the average rate of water level drop at location A can be found in Appendix 13. One thing to note is that the value of slope at location A is similar with the rest of the monitoring locations (B-F) between range of $(-8.9 \times 10^{-5}$ to -9.8×10^{-5} m per 5-minutes interval). Similarly, in 2011, the average rate of water level drop at location A is of same order of magnitude as the rest of the monitoring locations which falls in the range of $(-3.51 \times 10^{-5}$ to -4.14×10^{-5} m per 5-minute interval). To allow direct comparison of results between the two other approaches (namely Graphical and Simulation), we need to convert the units of the slope [m per 5 minutes] to [m/day] by multiplying the value of slope by a factor of 288.
- For Excel simulation method, K2 values in Table 8 are used

7.2 Comparison and analysis of results for the three approaches

We noticed there are some differences in the percentage reduction of average rate of water level drop when we use different approaches. This is normal as each approach would have their own differences.

Table 10: Comparison on the values of average rate of water level drop obtained from the three approaches

Type of approach	Selected period	Average rate of water level drop [m/day]	Percentage reduction [%]
Graphical method	2003	0.0190	~47
	2011	0.0100	
Curve-fitting method	2003	0.0206	~30
	2011	0.0143	
Excel simulation	2003	0.0180	~10
	2011	0.0163	

From Table 10, there is a 47% reduction in the average rate of water level drop at location A when we used the graphical method. Since this method is the most primitive method, we will be more prone to making mistakes in our estimations, but it is fast and does not require much data processing.

Both the curve-fitting and excel simulation methods yield similar results in their values (of the average rate of water level drop) however, the percentage reduction tabulated for curve-fitting is 30% as compared to excel simulation's 10%. Looking at the difference in percentage reduction difference for curve-fitting and excel simulation, it is caused by the

low baseline value (in 2003) that leads to a very sensitive percentage reduction in our calculations. Any small changes in the 2011 value will be magnified, therefore, leading to very sensitive percentage reduction outcome.

If there is not much time, one should go for the Graphical method for a rough estimation on the percentage reduction in the exfiltration rate. To achieve more accuracy in determining the percentage reduction in exfiltration rate, the curve-fitting method would be a better choice as it is much faster than the Excel simulation method since there is no fine-tuning procedure involved for the curve-fitting method. All we need for curve-fitting procedure is the experimental data and the proposed mathematical function.

7.3 Forecast of the system exfiltration rate trend

Introduction

Before we can forecast the trend of exfiltration rate for the system, we need to derive the function that describes the rate of decrease in the exfiltration rate through time. Over time, the infiltration system gets clogged by physical (especially sediment), chemical and biological processes. Suspended solids found in the urban stormwater may exfiltrate through the infiltration pipes but eventually get trapped at the nearest soil layer causing the system exfiltration rate to decrease.

In addition, we have confirmed with Eindhoven Municipal that no maintenance have been carried out for the infiltration pipes in Prinsejagt from 2003 to 2011, except for some regular cleaning at gully, sand trap and the pipe connection at the houses.

Projected K-value in future

Using a simple approach (Bergman, 2010), we assumed that the thickness of the clogging layer increases linearly with time and the K value for the overall system can be represented by the following 'clogging' model:

$$K_{new}(t) = \frac{1}{\frac{1}{K_{initial}} + c \cdot t} \quad \text{Eq. 7.1}$$

where $K_{initial}$ and K_{new} are the values of K [m/day] during the start and end of the monitoring period respectively.

c is a constant term which depends on the soil layer thickness, the growth rate of the clogging layer and the hydraulic conductivity of the clogging layer. Taking a conservative figure for K-values from Table 8 (the Excel simulation method) for 2003 and 2011, we can obtain the value of c by equating the clogging equation with the values of $K_{initial}=K_{2003}=0.018\text{m/day}$ and $K_{new}=K_{2011}=0.0163\text{m/day}$, and $t=7 \text{ years}=2555\text{days}$. By assuming a linear relationship in the rate of clogging, we are able to forecast a conservative reduction in the system exfiltration rate over time.

Eq. 7.1 is then to predict the performance of the system for 50 year useful lifespan of the infiltration system. Figure 70 shows the predicted progression of K value over the 50 years period. The rate of decrease in the exfiltration rate is the highest during the first few years of operation, this is reasonable as the most probable incident of clogging would occur at near the bottom arc of the circular pipe and the chance of clogging occurring on the pipe crown is much lesser.

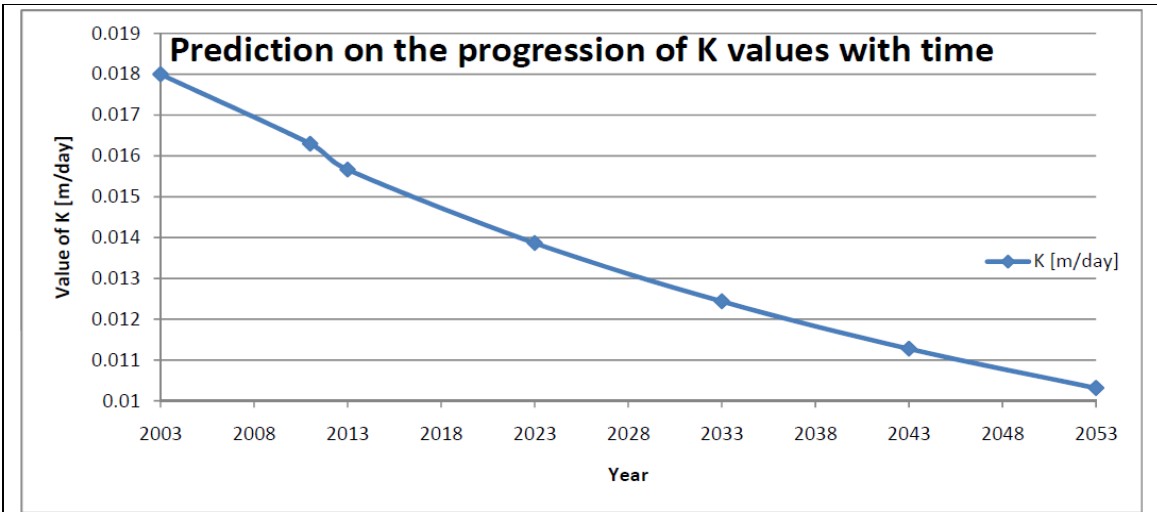


Figure 70: Prediction of the progress of K values over time using the 'clogging' model

Projected system exfiltration rates in future

A comparison graph of the system exfiltration rate for 2003, 2011 and the predicted 2021 is shown in Figure 71. It is predicted that in Year 2021, the maximum exfiltration rate will drop to 49.7m³/day, this is a 20% drop in performance from the initial 62.2m³/day.

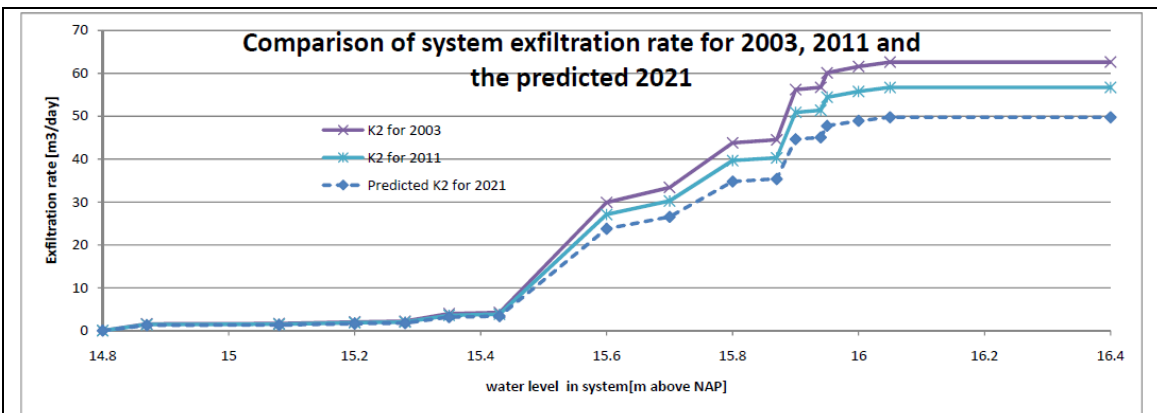


Figure 71: System exfiltration rate in 2003, 2011 and predicted system exfiltration rate for 2021

Although these figures are rather simple and rough estimates, the effect of clogging will have a severe impact on the ability of the infiltration system to perform its intended

purpose. Through this approach, the system planner can more effectively plan and execute their maintenance schedule for the infiltration system. A timely maintenance schedule to restore the system back to its (near) new original performance is essential.

8 Conclusion

8.1 Answers to our Primary research objective

The main objective of the research was to determine the percentage reduction in exfiltration rate at the measurement site as compared to initial readings derived from previous research (Boogaard, 2006)

To achieve this, a research approach was set up which involves the monitoring of water levels at the same locations of the infiltration drain system in Prinsejagt (carried out the previous monitoring scheme in 2003) and to carry out infiltration drain model simulations. Additional closed-loop tests were conducted to determine the exfiltration properties of the four stretches of infiltration pipes. Our research approach consisted of two main components: qualitative and quantitative descriptions. They will be discussed in detail for the subsequent section.

8.1.1 Qualitative description

Before we look into the percentage reduction in exfiltration rate at the Prinsejagt infiltration drain system, it is important that we understand and appreciate the water trend phenomenon observed from our measurement data in 2003 and 2011.

We used the experimental data of 2003 and 2011 and observations from our site visits to analyse qualitatively and explain the phenomenon observed at the 6 monitoring locations (A-F) within the Prinsejagt infiltration system.

The water level trends at the respective monitoring locations were found to be very similar to each other, this system behaviour and linear relationship among the respective monitoring locations (within the Prinsejagt infiltration drain system) has been explained in details under Section 4.4. Moreover, it was found that the groundwater level plays a significant role in influencing the performance of the infiltration drain system in 2011 as well. At groundwater level of NAP+15.85m or above, less than 25% of the infiltration drain system can start to exfiltrate its water (refer to Figure 11); this groundwater interference reduces tremendously the system exfiltration rate [L^3/T].

Therefore, the system behaviour (of the infiltration drains) coupled with the influence of groundwater level determine the overall performance of the infiltration drain system at Prinsejagt. Please refer to Sections 4.2 to 4.4 for a full description and analysis of the system behaviour and groundwater effects at the respective monitoring locations.

8.1.2 Quantitative description

With a better understanding of the physical phenomenon, we proceed to analyse the experimental data quantitatively. This involves carrying out our analysis using the following approaches:

1. Graphical
2. Curve-fitting
3. Simulation (in Excel)

Graphical method

Graphical method is used to give us a rough estimation on the percentage reduction in the average exfiltration rate between the 2003 and 2011 data at the respective monitoring locations (A-F). On the whole, we found that the percentage reduction of average exfiltration rate is in the range of 16.6 – 47.4%. Table 2 in Section 5.3 illustrates the respective percentage reduction in exfiltration rates at all the monitoring locations.

Curve-fitting method

In Curve-fitting method, we used Matlab program to study and analyse which mathematical function is suitable in describing the water level trends at the monitoring locations. We verified that a linear function can adequately describe the water level trends to an accuracy of 0.01m Root Mean Square Error (RMSE) for all monitoring locations. This small RMSE value is more than sufficient for our research purpose as we can easily observed a “virtual” cyclic water level fluctuation caused by the daily difference in atmospheric pressure of ~0.03m (for day and night). After factoring in the influence of groundwater level in our curve-fitting analysis, we noticed the range of percentage drop in exfiltration rate is between 3 to 30% for all the monitoring locations (refer to Table 5) between 2003 and 2011 experimental data. For more details, please refer to Table 5 under Section 5.6.

Simulation method

An infiltration drain model was conceptualised for simulation of the water level trends observed for four closed-loop tests first and before attempting to simulate water levels trends at monitoring location A for different groundwater levels during four rain events. To execute the simulation, the derived differential equations are solved and approximated using Runge Kutta 4 method on an Excel spreadsheet. We compared the simulation results to the experimental data using RMSE method to assess the goodness-of-fit. The model was calibrated (by adjusting the K-value) in the differential equations for the closed-loop tests and monitoring location A.

The effects of groundwater level on the K-values of location A are explained in Section 6.3.3.1 and illustrated with Figure 64. Using the simulation approach, we observed a 9.4% drop in exfiltration rate for location A from 2003 to 2011. There is a higher variance in K-values of the four closed-loop tests which is between 0.0039 to 0.05m/day. The larger difference in the K values of the individual section of infiltration pipe could be attributed to differences in localised soil profiles, localised groundwater level and degree of clogging at the respective pipe sections. Whereas at monitoring location A, there is more buffering and averaging effect due to its connectivity to the rest of the infiltration system (Section. 4.4), this helps to reduce the RMSE.

Furthermore, we used the K-values obtained from the simulation at monitoring location A (at low groundwater level of NAP+15.43m in 2011) and 2003 value to forecast the future system exfiltration rate performance.

8.2 Answers to our Secondary research objectives

Our secondary research objectives are:

1. How can we describe the processes involved in the performance of an infiltration drain system?
2. How do the infiltration drains develop after 10 years of usage? Do they clog every year?
3. How can we forecast the performance of the infiltration drain for its useful lifespan and perhaps introduce a maintenance plan to restore its performance?

In order to shed more insight to these secondary research questions, an additional experiment (closed-loop test) has been carried out. The objective of the closed-loop test is to find out the exfiltration rate of the selected stretch of infiltration drain only. Before conducting the test, we have to plug the other sections of infiltration drains that are also connected to the selected manhole. This experiment is different from our periodic monitoring done at Locations A to F, as we conduct the test in a relatively controlled environment by eliminating the possibility of water flowing toward the other infiltration drains when we fill the manhole with water to at least 0.5m above the pipe crown level. For more details, you may wish to refer to Section 3.3.

How can we describe the processes involved in the performance of an infiltration drain system?

We will describe the processes involved in the performance of an infiltration drain system in two levels. One is at the individual pipe level and while the other is the system (at the respective monitoring locations) level.

At individual pipe level, the exfiltration rate is predominately hydrostatic pressure-driven. When the water level is above the pipe crown level, the exfiltration flow pattern is similar to a radial flow due to the high driving force (water height). When the water level is below the pipe crown level (as shown in Figure 55) as the hydrostatic pressure is not high enough to sustain this radial flow pattern, a modified and reduced radial-type of exfiltration flow pattern is expected.

Next, at system level (Section 4.6, Figure 44), we observe four phases of water level trends after a rainstorm event. They are:

- 1st phase: increasing rate of water level raise (until peak)
- 2nd phase: decreasing rate in the water level raise
 - 1st – 2nd phase is when the water level builds up until the maximum water level in the manhole (the raise in water level is due to water inflow into the system from the catchment area of the manhole and its connected pipelines. Thus, during this phase, we will expect advection/transportation process to be predominant here)
- 3rd phase: rate of change of water level (similar to exfiltration rate) will continue to drop at a linear rate (advection processes die out)

- 4th phase: The rate of change of water level reaches a constant rate until the water level becomes lower than the lowest pipe invert level within the manhole system.

Essentially, the processes involved for both individual pipe and system levels are very similar. However, it is much easier to visualise the processes for an individual pipe as the advection-portion of the process is eliminated/minimised when we conduct the closed-loop test (by plugging out the rest of the infiltration pipes).

How do the infiltration drains develop after 10 years of usage? Do they clog every year?

The infiltration drain system can get clogged by physical (especially sediment), chemical (iron oxide) and biological processes. Suspended solids found in the urban stormwater may exfiltrate through the infiltration pipes but eventually get trapped at the nearest soil layer causing the system exfiltration rate to decrease. We found sediment and a substantial amount of dead leaves in infiltration pipe and manhole when the system water level is low (please see Figures 20, 23, 26, 29, 32 and 35). These are just the physical site observations, we are unable to assess and confirm whether the infiltration drain system is clogged chemically or biologically. Routine cleaning or maintenance of sand/gully traps connected to the infiltration drain system might not be sufficient to keep the sediment and dead leaves from entering the system. Therefore, it is strongly recommended that the preventive maintenance programme to include the cleaning of the manhole and infiltration pipes to remove the sediment as well.

In Section 7.3, we introduced a simple “clogging” model to estimate the rate of deterioration in the system exfiltration rates, should no maintenance is done. It uses the K-values obtained from the infiltration drain model simulation to forecast in the future system exfiltration rate. It is believed that by Year 2021, the maximum exfiltration will drop to 49.7m³/day. This is a 20% drop in performance as compared to the initial 62.2m³/day (Figure 71) in 2003.

How can we forecast the performance of the infiltration drain for its useful lifespan and perhaps introduce a maintenance plan to restore its performance?

Assuming a scenario when the groundwater level is lower than NAP+15.43m, we used the “clogging” model (Section 7.3) to predict the maximum system exfiltration rates [L³/T] after incorporating the system physical dimensions (its wetted perimeter). The peak exfiltration flowrate is expected to drop to 50m³/day by Year 2020. So, we need to carry out maintenance of the infiltration system before Year 2020, if the water system planners expect a minimum peak exfiltration rate of 50m³/day (Figure 73).

This projection is done for the useful lifespan of 50 years for infiltration pipes; this forecast allows the water system planners to design their preventive maintenance programme. Though this is a simple projection, it is sufficient to form a preliminary structure to the planning process and help us gain more insight to the clogging issue inside the infiltration drain system.

9 Recommendations and Discussion

Arising from our site observations and experimental findings, we propose the following recommendations and issues for discussion. The aim is to contribute to a better understanding on our research topic, help to improve the approach of research and bring about new insight to our research area (of infiltration drain system). They are categorised into 3 broad categories, namely improvement to existing research, proposed new areas of research and proposed improvements for the Prinsejagt measurement site.

9.1 Improvement to existing research

Approach in determining the percentage reduction in exfiltration rates

From the three approaches used in determining the percentage of reduction in exfiltration rates for Prinsejagt infiltration drain system, the curve-fitting method can achieve relatively fast and accurate results. If one seeks to get a quick insight of the exfiltration rates from the water trends, we would recommend him to use the curve-fitting method.

9.2 Proposed new areas of research

Further investigation on designed rainstorm

Based on the forecast of clogging rate, further investigation can be done to ascertain and predict the effectiveness of infiltration drains with respect to its designed rainstorm, yearly average rainstorm and extreme rainstorm events and the parameters used to quantify performance of IT drains can be:

- Effectiveness in reducing the surface runoff for:
 - designed rainstorm; and
 - average and extreme rainstorm
- Turnover time for the system (for designed rainstorm)
- Detention or storage capabilities
- Peak discharge reduction

This would enable us and the water system planners in their decision-making process of maintenance or replacement and in seeking alternatives remedial actions.

Seasonal Effect

While our 2011 monitoring period coincided with the high groundwater period, in temperate countries, like the Netherlands, there are variations in seasonal conditions throughout the entire year that we can study for the infiltration drain system. Each season will exert a different scenario and influence on the infiltration drain system. Some factors that may influence the processes and performance of the infiltration drain system include drought or wet periods, snow or rain conditions and different groundwater level. As such, it is recommended that the investigation be continued for at least a year so as to take into account the entire year's seasonal effects. In addition, suitable groundwater and surface

water monitoring locations could be installed nearby of the existing monitoring locations to facilitate more accuracy in the results analysis.

Sobek program

There is on-going work at Deltares to create an infiltration drain module in Sobek (Deltares). We believe that the results from our investigation (both experimental and simulation results) can be used as a resource point, and certainly hope that the investigation results will contribute towards the building of the infiltration drain module and eventually the whole Low Impact Development (green roofs, swales, porous pavement and infiltration drains) suite.

Different locations that have different land use, hydrology, soil type, climate conditions and the rainfall patterns will require different combinations of Low Impact Development (LID). As such, some combinations of LIDs will appear to be more effective than others. Perhaps, efforts could be put in to find out some optimal combination of LIDs for flood prevention (or other objectives decided by the stakeholders and decision-makers).

Research for infiltration drains installed in different environment

Further research could be conducted for different types of infiltration system installed and put into use (for example, 5 years and above) in different soil conditions (like vertical infiltration drain in loamy soils or horizontal infiltration drain in sandy soils). The intention is to determine any relation of soil type or installation type to the rate of clogging. With this knowledge, better infiltration drain system could be designed and maintained more cost-effectively.

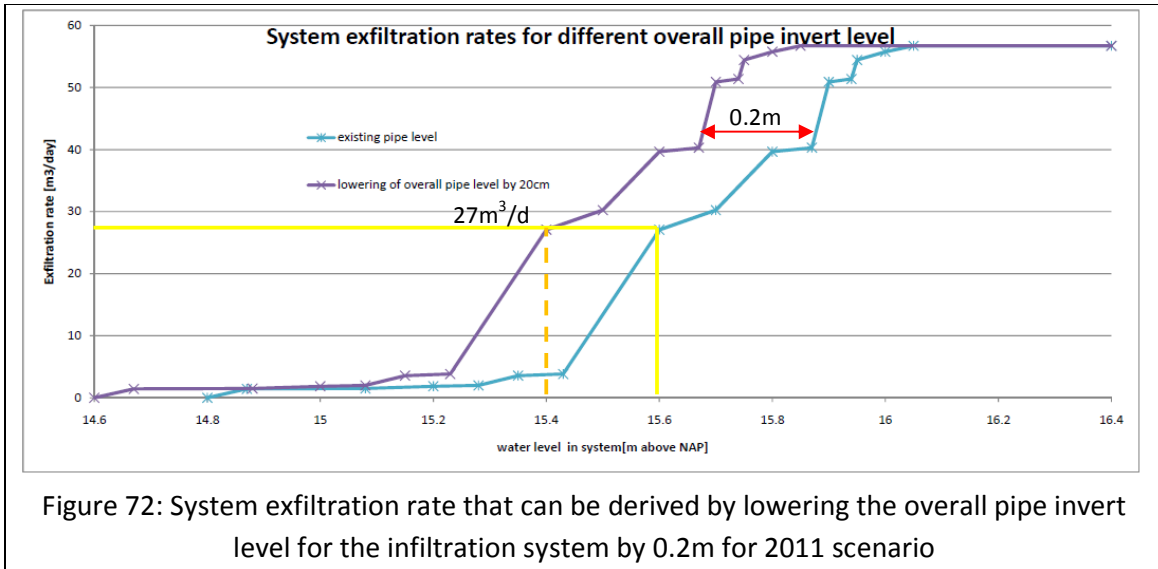
9.3 Proposed improvement measures for the Prinsejagt measurement site

Lowering the pipe invert levels of the entire infiltration drain system

In retaining the overall dimensions of the infiltration pipe and lowering the respective pipe invert levels, it will help to increase the system curve that can be activated for exfiltration, thereby bolstering the overall system efficiency. Figure 72 illustrates that by lowering the pipe invert level by 0.2m, we can maintain the system exfiltration rate at its maximum ($56.7\text{m}^3/\text{day}$) until the system water level drops to NAP+15.85m. At existing pipe invert levels, this maximum exfiltration rate can only be maintained till the system water level drops to NAP+16.05m. This would mean water can be exfiltrated within a shorter interval of time thus enhancing the overall infiltration drain system performance.

On the other hand, the effectiveness of this proposal would be limited during high groundwater level period. If we managed to lower the overall pipe invert level for the infiltration system, from Figure 9 in Section 3.3, we could see that every year almost half of the time the groundwater level will be higher than NAP+15.4m. This would mean that around 48% of the total infiltration drain system is unable to exfiltrate water during this high groundwater level period (of NAP+15.4m). Despite this unfavourable situation of high groundwater level, the infiltration drain system can almost start to exfiltrate at $27\text{m}^3/\text{day}$ once the groundwater level drops below NAP+15.4m as compared to the existing

exfiltration rate of $4\text{m}^3/\text{day}$. This will definitely help the infiltration drain system to discharge/recharge water into the groundwater.



Although this proposal (of lowering the overall pipe invert level) is quite attractive, it is very costly to replace the entire pipe system and the other existing underground infrastructure (like especially the sewer system) will also be affected, therefore this proposal should only be considered during the design stage of the infiltration drain system or when the infiltration drain system is due for replacement at its end of useful lifespan.

Regular maintenance of the infiltration drain system

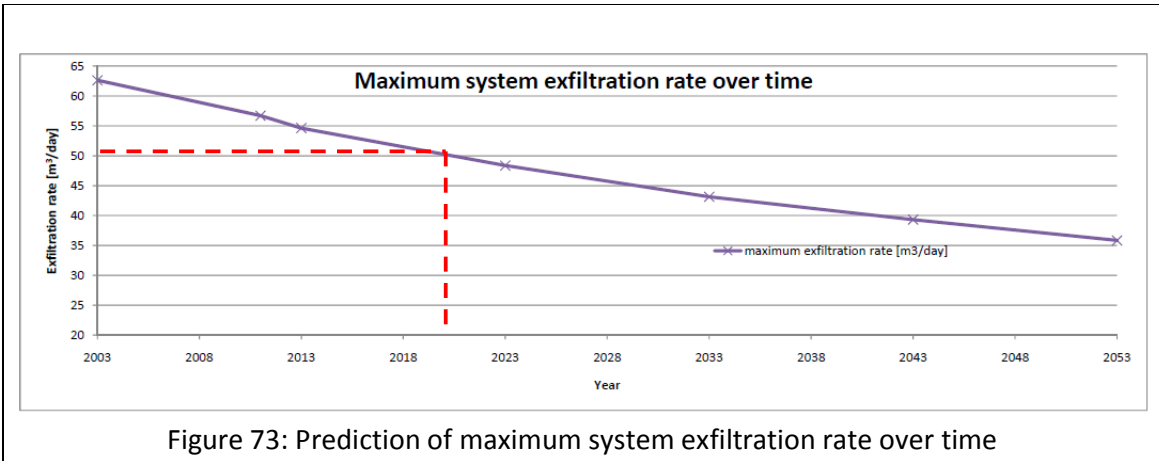
As mentioned in (Woods-Ballard, 2007), effective sediment management and maintenance is vital to ensure the long-term effectiveness of infiltration drain system. Monitoring the “health” of the infiltration drain system (using the system K-values) is one option.

(1) Infiltration system

The drop in efficiency of the infiltration system is predicted using the “clogging” model (Section 7.3). Suppose the Eindhoven Municipality expects the infiltration drain system is be able to deliver at least $50\text{m}^3/\text{day}$ of peak exfiltration flowrate, maintenance of the infiltration system will need to be carried out before Year 2020 (Figure 73).

It is recommended that once the maintenance works is done (e.g. using pressure-jet), monitoring on the infiltration drain system performance should commence so as to determine its effectiveness in increasing the overall permeability.

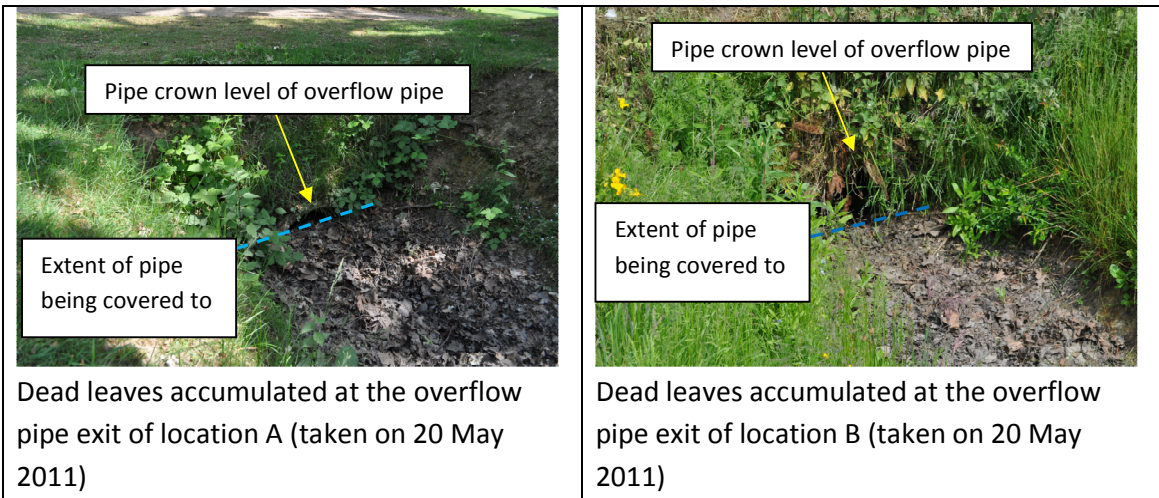
Should normal preventive maintenance fail to restore the system exfiltration rates to its initial K-value of $0.018\text{m}/\text{day}$, laboratory analysis on the soil surrounding the infiltration pipe could be carried out to determine its permeability and what type of the compounds that are clogging it. This would enable the water planners to decide the course of action and whether the infiltration drain system can meet its designed function/s.



In order to reduce the cost of maintenance, we recommend the scope of maintenance to be focused at pipe invert levels equal or more than NAP+15.60m to reduce cost and time needed for maintenance. In addition, the maintenance activities should be carried out before winter period when the high groundwater level coincides with high rainfall.

(2) Overflow connections

To regularly clear the dead leaves accumulated at the exit pipe of the overflow weir (for monitoring locations A, B and C). Firstly, this is to allow a clear passage for water overflowing from the infiltration system towards the surface water system (located at the green zone area). As the bottom level of the surface water system rises, its storage capacity will be reduced. Clearing the accumulated dead leaves regularly will help to maintain the storage capacity of the surface water system at a satisfactory level.



Use of tanker to draw out water within the infiltration drain

In case of emergencies, tanker could be deployed to withdraw water out of the infiltration drain system at the system low points. During winter season where there is high groundwater level, the exfiltration rates are especially low ($0.04\text{m}^3/\text{day}$). Level sensor with telemetry could be installed at the location A, B and C to monitor the water levels and activate the tankering service when necessary. Alternatively, a water pump could be installed. The pump can start pumping water to the nearby sewer connection when the system water level exceeded a threshold level (to be determined by the Municipal authorities).

During high groundwater period (groundwater level exceeds NAP+15.94m), the entire infiltration drain system can only exfiltrate $\sim 0.3\text{m}^3$ in 7 days whereas a tanker is able to withdraw 10m^3 of water in less than half a day. However, one has to be cautioned not to withdraw the water level lower than the groundwater level as groundwater can infiltrate into the infiltration drain system. This will be counter-productive.

Water quality monitoring

While it was approved during the design stage (in 1999) that the water (from the infiltration drain system) can be allowed to be exfiltrated into the groundwater system, it is still recommended to monitor the water quality within the infiltration drain system regularly, through grab samples, as the situation of vehicular loading might have change over time. This would help to prevent any unintended pollution of groundwater resources which requires expensive and lengthy remediation (Adler, 2009). It was noticed that at some monitoring locations there are some animal waste materials present in the manholes.

Literature List

- ADLER, R. W. 2009. *Legal Framework for the Urban Water Environment*, Springer Science.
- ANNETTE SEMADENI-DAVIES, C. H., GILBERT SVENSSON AND LARS-GÖRAN GUSTAFSSON 2008. The impacts of climate change and urbanisation on drainage in Helsingborg, Sweden: Suburban stormwater. *Journal of Hydrology*, 350, 114-125.
- BERGMAN, M., HEDEGAARD, M.R., PETERSEN, M.F., BINNING, P., MARK, O. AND MIKKELSEN, P.S. 2010. Evaluation of two stormwater infiltration trenches in central Copenhagen after 15 years of operation. *NOVATECH 2010, Proceedings of the 7th International Conference on Sustainable Techniques and Strategies in Urban Water Management*, 1-10.
- BOOGAARD, F. C., DIJCK B.V., AND KRONENBURG, W 2006. Monitoring IT-riolering Prinsejagt 3 Meetjaar 2004 for Gemeente Eindhoven. Tauw B.V.
- DECHESNE, M., BARRAUD, S. AND BARDIN, J-P 2004. Indicators for hydraulic and pollution retention assessment of stormwater infiltration basins. *Journal of Environmental Management*, 71, 371-380.
- DECHESNE, M., BARRAUD, S. AND BARDIN, J-P 2005. Experimental assessment of stormwater infiltration basin evolution. *Journal of Environmental Engineering*, 131(7), 1090-1098.
- DELTARES. *SOBEK suite* [Online]. [Accessed 5 May 2011].
- ENDO, J., FUJIWARA, H., TAMOTO, N. AND SAKAKIBARA, T. 2009. Deterioration of rainwater infiltration facilities with time. *Proceedings of the 8th International Conference on URBAN DRAINAGE MODELLING*.
- LINDSEY, G., ROBERTS, L. AND PAGE W. 1992. Inspection and maintenance of infiltration facilities. *Journal of Soil and Water Conservation*, 47 (6), 481-486.
- MATLAB 2011. MATLAB 7 Data Analysis.
- REVITT, M., ELLIS, B. AND SCHOLES, L. 2003. Report 5.1 Review of the Use of stormwater BMPs in Europe. *Project under EU RTD 5th Framework Programme*. Middlesex University.
- SIRIWARDENE, N. R., DELETIC, A. AND FLETCHER, T.D. 2007. Clogging of stormwater gravel infiltration systems and filters: Insights from a laboratory study. *Water Research*, 41, 1433-1440.
- UN 2010. World Urbanization Prospects, the 2009 Revision: Highlights.
- VAN DE VEN, F. H. M. 2010. Watermanagement in Urban Areas. Delft.
- WARNAARS, E., LARSEN, A.V., JACOBSEN, P AND MIKKELSEN, P.S. 1999. Hydrologic behaviour of stormwater infiltration trenches in a central urban area during 2 ¾ years of operation. *Water Science and Technology*, 39, 217-224.
- WESTRIK, K. G. A. G., G.D. 1999. Advies Waterproblematiek Prinsejagt 3 Gemeente Eindhoven. Tauw BV.
- WOODS-BALLARD, B. K., R; MARTIN, P; JEFFERIES, C; BRAY, R; SHAFFER, P 2007. CIRIA 2007.

Appendix 1 Verification of water levels at the monitoring locations during site visits

Date	Approximate time	Monitoring locations	Water level measured during site visit [m above NAP]	Water level registered by divers [m above NAP]	Difference [m] <i>Site reading – divers reading</i>
19 Feb 2011	0945hrs	A	16.34	16.37	-0.03
	1015hrs	B	16.34	16.43	-0.09
	1125hrs	C	16.32	16.29	0.03
	1055hrs	D	16.33	16.40	-0.07
	1040hrs	E	16.35	16.41	-0.05
	1000hrs	F	16.21	16.34	-0.13
	1030hrs	Pt 7	16.32	16.38	-0.06
10 Mar 2011	1055hrs	A	16.33	16.38	-0.05
	1110hrs	B	16.34	16.42	-0.08
	1130hrs	C	16.30	16.29	0.01
	1210hrs	D	16.32	16.39	-0.07
	1200hrs	E	16.35	16.40	-0.05
	1150hrs	F	16.21	16.35	-0.14
	1145hrs	Pt 7	16.28	16.38	0
28 Apr 2011	1110hrs	A	16.04	16.08	-0.04
	1150hrs	B	16.05	16.11	-0.06
	1455hrs	C	16.05	16.03	0.02
	1530hrs	D	16.07	16.15	-0.08
	1600hrs	E	16.05	16.10	-0.05
	1650hrs	F	15.91	16.08	-0.17
	1225hrs	Pt 7	16.00	16.07	-0.07
20 May 2011	1125hrs	A	15.96	15.99	-0.03
	1100hrs	B	15.86	15.94	-0.08
	1055hrs	C	15.89	15.99	-0.10
	1150hrs	D	15.91	16.00	-0.09
	1145hrs	E	15.87	15.92	-0.05
	1155hrs	F	15.78	15.95	-0.17
	1105hrs	Pt 7	15.93	15.98	-0.05

Measurement points

	Location	Description	Manhole no.	Indicated on map
P1	Serlioweg no. 12	With overflow facilities	E1125U	A
P2	Isidorusweg, intersecting Fontanalaan st.	With overflow facilities	F1100U	B
P3	Vanvitelliweg, near hse unit 3	With overflow facilities	F1050U	C
P4	Roosenburgstraat, intersecting Van Heukelomstraat st.	Within the system	F10543	D
P5	Neumannlaan, near hse unit 17	Within the system	F10515	E
P6	Madernolaan, intersecting Serlioweg st.	Within the system	E11251	F
P7	Isidorusweg (downstream of the overflow weir)	Surface water level	-	Near B

Total: 7 divers + 1 baro-diver (placed inside P5)

Appendix 2 The locations and details of the selected stretch of infiltration pipes for closed-loop test are indicated in map below.



Locations of the 5 pipe sections selected for the closed-loop test

Section name (location)	Length of pipe	Diameter	Volume required to fill pipe	Volume of Manhole	Total volume	Diameter & no. of Plugs reqd
E11253-E1126I (1)	42.54m	0.25m	2.1m ³	1.2m ³	3.3m ³	2x0.3m
F10505-F10507 (2)	39.679m	0.3m	2.81m ³	0.5m ³	3.31m ³	1x0.25m
F11043-F11045 (3)	52.206m	0.25m	2.563m ³	0.6m ³	3.163m ³	1x0.25m
F10519-F10521 (4)	36.249m	0.25m	1.8m ³	0.5m ³	2.3m ³	1x0.25m
F10575-F10577 (5)	43.472m	0.25m	2.14m ³	0.5m ³	2.64m ³	1x0.25m

Technology Sheet



Mini-Diver Datalogger

Compact design, reliable results



Mini-Diver datalogger shown with Pocket-Diver software

Applications:

- Monitoring projects
- Groundwater monitoring network automation

The Mini-Diver features:

- 3 year warranty
- Long-term and frequent measurements
- Temperature corrected measurement
- Reliable and accurate measurement of data
- Non-volatile memory
- Compact size
- Hermetically sealed in stainless steel housing
- Maintenance free

Overview

Groundwater professionals depend on the accuracy, resolution and reliability of the Mini-Diver* datalogger for effective monitoring of groundwater conditions. You get the renowned Diver quality in a low cost solution!

Mini-Diver Datalogger

The Mini-Diver* provides reliable automatic measurement and registration of groundwater level and temperature data. Measuring 22 mm in diameter and 90 mm in length, it is a suitable choice for virtually any monitoring well. Based on proven, innovative technology, the Mini-Diver has an impressive internal memory capable of storing 24,000 measurements per parameter. This is essentially one measurement every ten minutes for six months. For each measurement, the Mini-Diver simultaneously registers groundwater level, groundwater temperature, date and time.

Mini-Diver: Specifications

Type	DI 501	DI 502	DI 505	DI 510	DI 500 (Baro)
Range	10 m H2O	20 m H2O	50 m H2O	100 m H2O	1.5 m H2O
accuracy	0.5 cm H2O	1 cm H2O	2.5 cm H2O	5 cm H2O	0.5 m H2O
resolution	0.2 cm H2O	0.4 cm H2O	1 cm H2O	2 cm H2O	0.1 cm H2O

*Within temperature compensated range ©Schlumberger *Mark of Schlumberger

For additional information, contact:

Van Essen Instruments
 A Schlumberger Company
 PO Box 553 2600 AN
 Delft, The Netherlands
 Tel: +31 (0)15 275 50 00
 Fax: +31 (0)15 275 50 55
 Email: sws-diver@slb.com

July 2006

General specifications of divers used in the measurement scheme – mini diver

Baro-Diver, Mini-Diver, Micro-Diver and Cera-Diver

The Diver types meet the following general specifications:



<i>Diameter</i>	Ø22 mm
<i>Length</i>	90 mm incl. suspension eye
<i>Weight</i>	approx 70 grams
<i>Protection class</i>	IP68, 10 years continuously submerged in water at 100 m
<i>Storage/</i>	-20 °C to 80 °C (affects battery life)
<i>Transport temperature</i>	
<i>Operating temperature</i>	0 °C to 50 °C
<i>Material</i>	
– <i>Casing</i>	316L stainless steel (active substance no. 1.4404)
– <i>Pressure sensor</i>	Alumina (Al ₂ O ₃)
– <i>Suspension eye/ nose cone</i>	Nylon PA6 glass fibre reinforced 30%
– <i>O-rings</i>	Viton®
<i>Communication</i>	Optically separated
<i>Memory capacity</i>	24,000 measurements
<i>Memory</i>	Non-volatile memory. A measurement consists of date/time/level/temperature
<i>Sample interval</i>	0.5 sec to 99 hours
<i>Sampling options</i>	
– <i>Fixed interval</i>	Yes
– <i>Event-based</i>	No
– <i>Pump test</i>	No
<i>(to be configured by user)</i>	
– <i>Averaging</i>	No
<i>Battery life*</i>	10 years, depending on use
– <i>Theoretical capacity</i>	5 million measurements 2000× memory readouts 2000× programming
<i>Clock accuracy</i>	Better than ± 1 minute per year at 25 °C Better than ± 5 minutes per year within the calibrated temperature range
<i>CE marking</i>	EMC in accordance with the 89/336/EEC directive Basic EN 61000-4-2 standard
– <i>Emissions</i>	EN 55022 (1998) + A1 (2000) + A2 (2003), Class B
– <i>Immunity</i>	EN 55024 (1998) + A1 (2000) + A2 (2003)
– <i>Certificate number</i>	06C00301CRT01

Detailed specifications of mini-diver (length 90mm) extracted from page 11 & 12 of user manual

Technical specifications

General:

Sample rate*	0.5 sec. to 99 hrs
Memory	24,000 measurements (non-volatile)
Housing material	stainless steel (AISI 316L)
Pressure sensor material	ceramic
Temperature range	-20° to 80°C
- accuracy	± 0.1°C
- resolution	0.01°C
- compensation range	-10°C to 40°C
Battery life	8-10 years (depending on use)
Dimensions	Ø22 mm x 125 mm
Weight	160 grams



Pressure:

Type	DI 240	DI 241	DI 242
Calibrated range	5 m water column	10 m water column	20 m water column
Usable range	4 m water column	9 m water column	19 m water column
- accuracy**	± 0.1% FS	± 0.1% FS	± 0.1% FS
- resolution	0.1 cm	0.2 cm	0.4 cm

Type	DI 243	DI 245	DI 250 (BaroDiver)
Calibrated range	30 m water column	100 m water column	1.5 m water column (approx. 150 mbar)
Usable range	29 m water column	99 m water column	n/a
-accuracy**	± 0.1% FS	± 0.1% FS	± 0.3% FS
- resolution	0.6 cm	2 cm	0.1 cm

Detailed specifications of the diver (length 125mm)



Onset Rain Gauge (photo extracted from <http://www.onsetcomp.com/products/data-loggers/rg3>)

Model: Onset Model no. RG2M,

Serial no.: 20993

Serial no. of HOBO datalogger:
90-H07-RG2-M #20993

Rain Gauge	
Maximum Rainfall Rate	127 cm (5 in.) per hour
Calibration Accuracy	±1.0% (up to 1 in./hour for the RG3 or 20 mm/hour for the RG3-M)
Resolution	0.01 in. (RG3) or 0.2 mm (RG3-M)
Calibration	Requires annual calibration: can be field calibrated or returned to the factory for re-calibration
Operating Temperature Range	0° to +50°C (+32° to +122°F)
Storage Temperature Range	-20° to +70°C (-4° to +158°F)
Environmental Rating	Weatherproof
Housing	15.24cm (6-in.) aluminum bucket
Tipping Bucket Mechanism	Stainless steel shaft and bearings
Dimensions	25.72 cm height x 15.24 cm diameter (10.125 x 6 in.); 15.39 cm (6.06 in.) receiving orifice
Weight	1.2 Kg (2.5 lbs)
Part Numbers	RG3 (0.01 in. per tip) RG3-M (0.2 mm per tip)
CE	The CE Marking identifies this product as complying with all relevant directives in the European Union (EU).

Specifications of the Onset rain gauge - extracted from Page 2 of *Data-logger rain gauge users' manual*

Logger	
Time stamp Resolution	1.0 second
Time accuracy	± 1 minute per month at 25°C (77°F), see Plot B.
Operating range	-20° to 70°C (-4° to 158°F)
Environmental rating (for logger used outside of rain gauge)	Tested to NEMA 6 and IP67; suitable for deployment outdoors
NIST traceable certification	Available for temperature only at additional charge; temperature range -20° to 70°C (-4° to 158°F)
Battery	CR-2032 3V lithium battery; 1 year typical use
Memory	64K bytes – 16K to 23K when recording events only; 25K to 30K data points when recording events and temperature; see <i>Data storage</i> on page 7.
Materials	Polypropylene case; stainless steel screws; Buna-N o-ring; PVC cable insulation
CE	The CE Marking identifies this product as complying with all relevant directives in the European Union (EU).

Specifications of the data-logger – extracted from page 3 of *Data-logger rain gauge users' manual*

A short description of the infiltration drain installed – *Azura IT pipe*



Azura infiltration drain pipes



Internal view of the IT pipe (with open slots to allow for water to flow in/out)
photo extracted from Wavin product brochure (<http://nl.wavin.com/nl/Brochures.html>)

The IT pipe is manufactured by Wavin B.V. Netherlands. These (green) pipes contain regular slots along the whole length of pipe to allow for water to flow in or out. Though its interior is smooth, it has a ribbed exterior that is wrapped with geotextile to prevent sediment/particles from entering it while allowing water to flow through it.

Appendix 4 Daily precipitation and potential evapotranspiration plot (10 – 20 May 2011), details on groundwater monitoring locations and general soil profile at Prinsejagt monitoring site

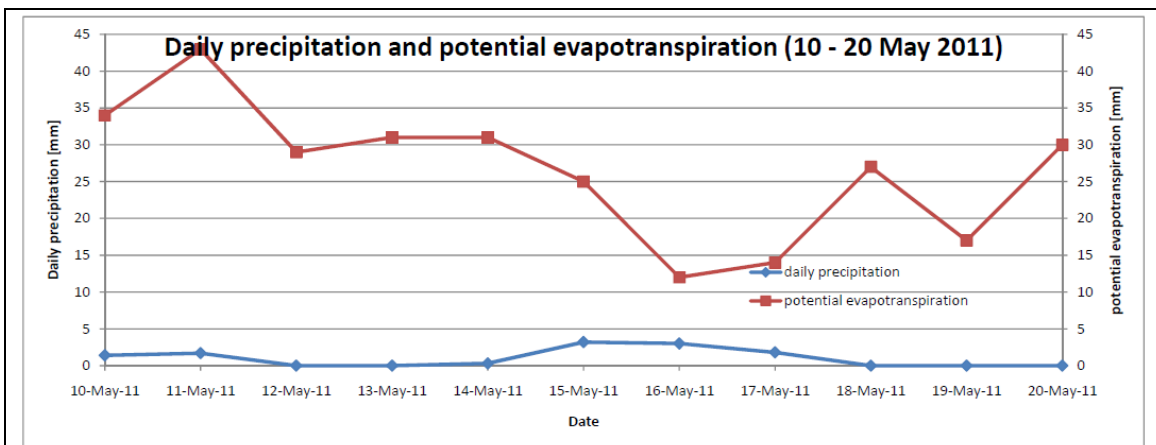
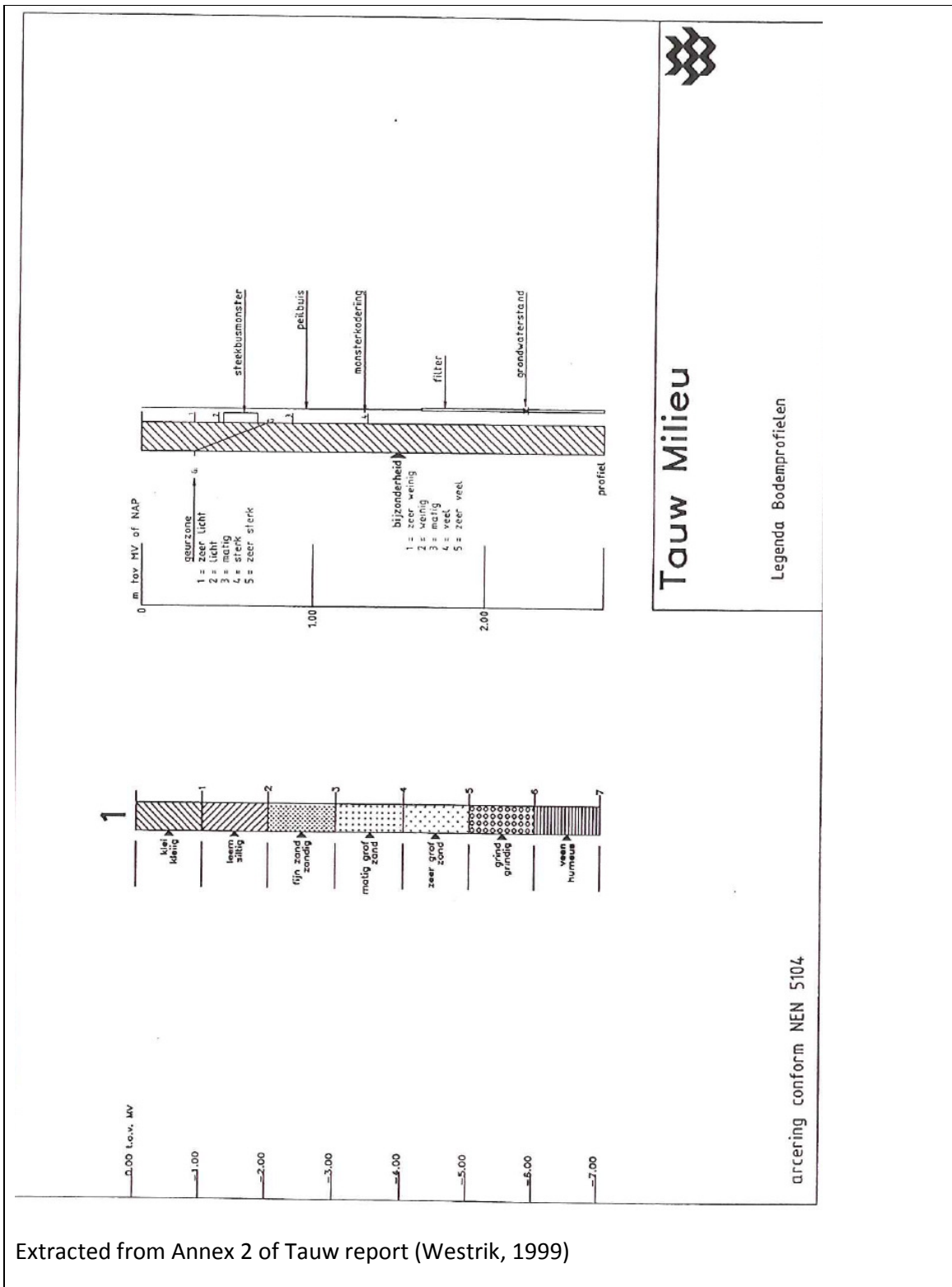


Figure: Rainfall vs evapotranspiration graph (during 10 – 17 May 2011)
 data extracted from KNMI - <http://www.knmi.nl/klimatologie/daggegevens/download.html>

Details on groundwater monitoring locations

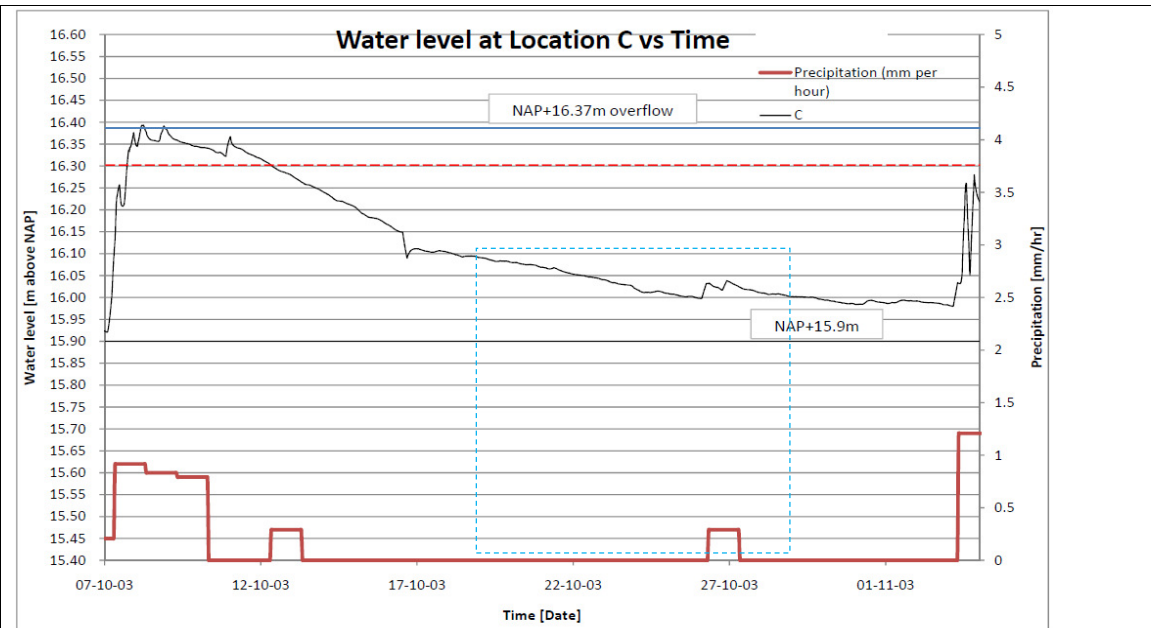
Locations	Level [m above NAP]	Frequency of monitoring (duration of data available)
WL004	12.14 – 11.14m	Fortnightly till 25 May 2009 (stopped monitoring)
WL021	14.36 – 13.36m	12 hourly until present
WL030	13.57 – 12.57m	Fortnightly till 11 Mar 2004 (stopped monitoring)
WL066-1	9.92 – 8.92m	Fortnightly; data available till 9 Nov 2010
WL066-2	-8.56 – -9.56m	- ditto -
WL066-3	-40.78 – -41.78m	- ditto -

General soil profile at Prinsejagt monitoring site

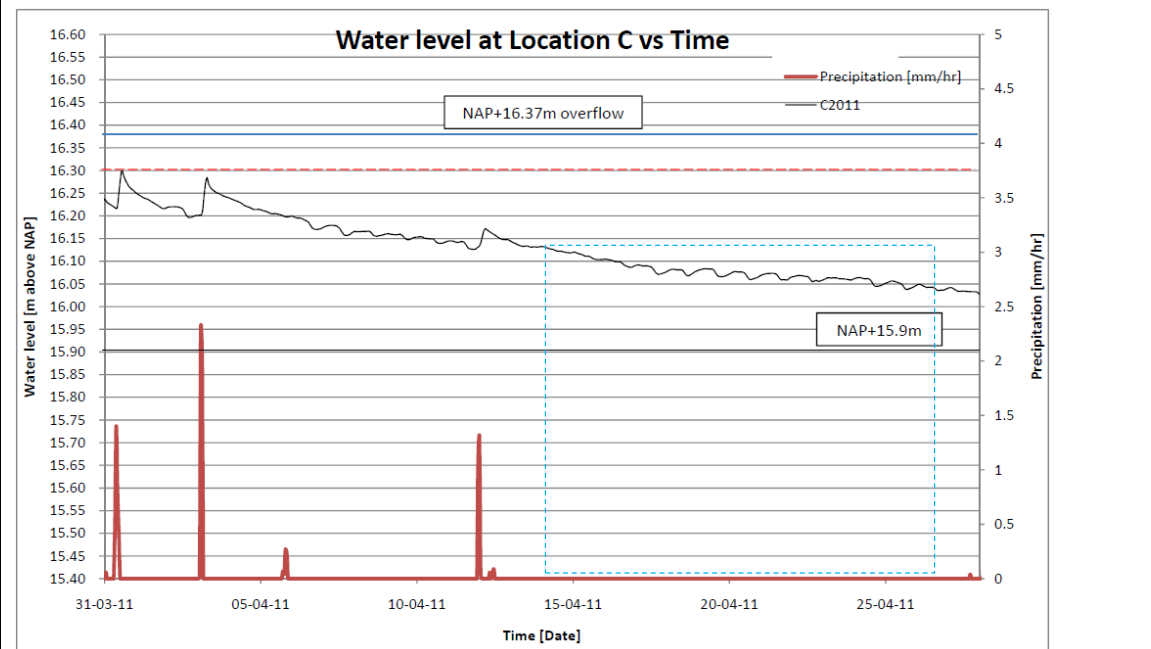


Extracted from Annex 2 of Tauw report (Westrik, 1999)

Appendix 6 Graphical method for location C, E & F



Graphical method used at Location C for 10 October – 2 November 2003 period

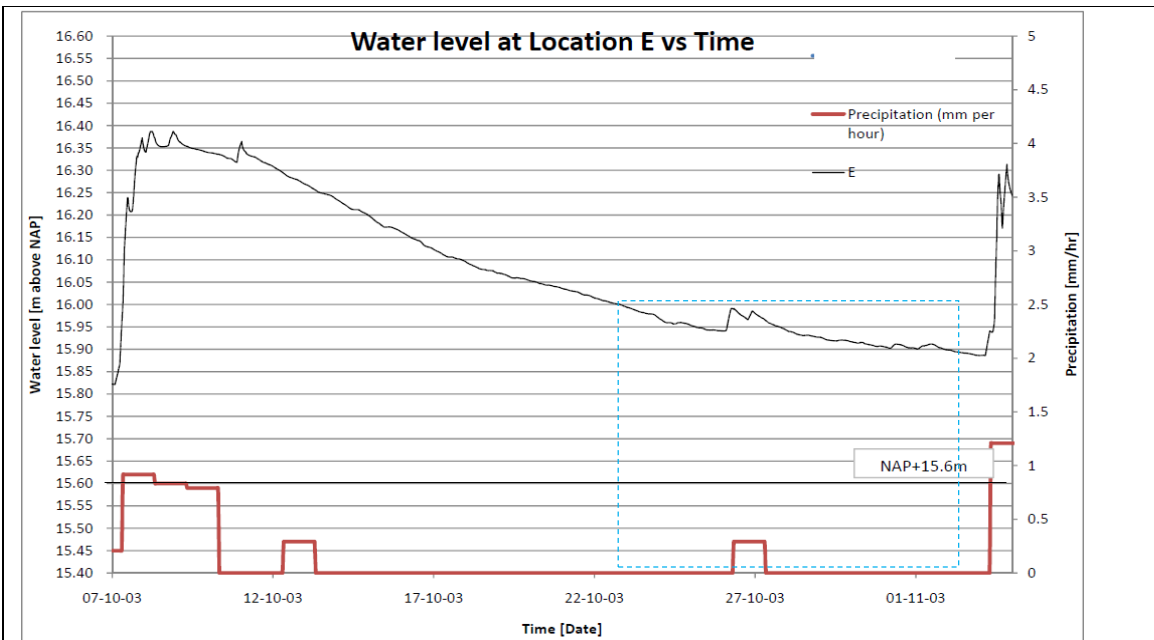


Graphical method used at Location C for 3 – 27 April 2011 period

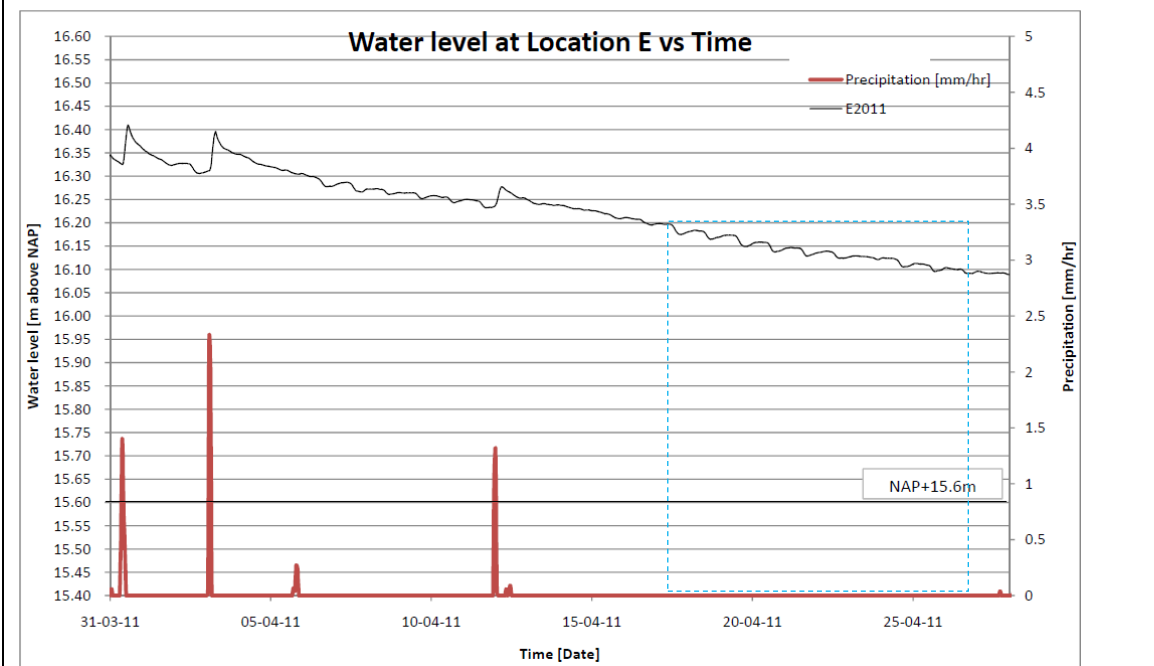
Graphical method at Location C

During 19 – 30 Oct 2003 (12.1 days interval), the water level dropped from NAP+16.09m to NAP+15.99m. This leads to an average rate of water level drop of 0.008m/day. Factoring in the rain event on 27 Oct 2003, the actual time interval would be 8.2 days instead. This leads to 0.012m/day.

We noticed during 14 – 27 Apr 2011(13.3 days interval), the water level dropped from NAP+16.13m – NAP+16.03m, leading to an average rate of water level drop of 0.008m/day.



Graphical method used at Location E for 10 October – 2 November 2003 period

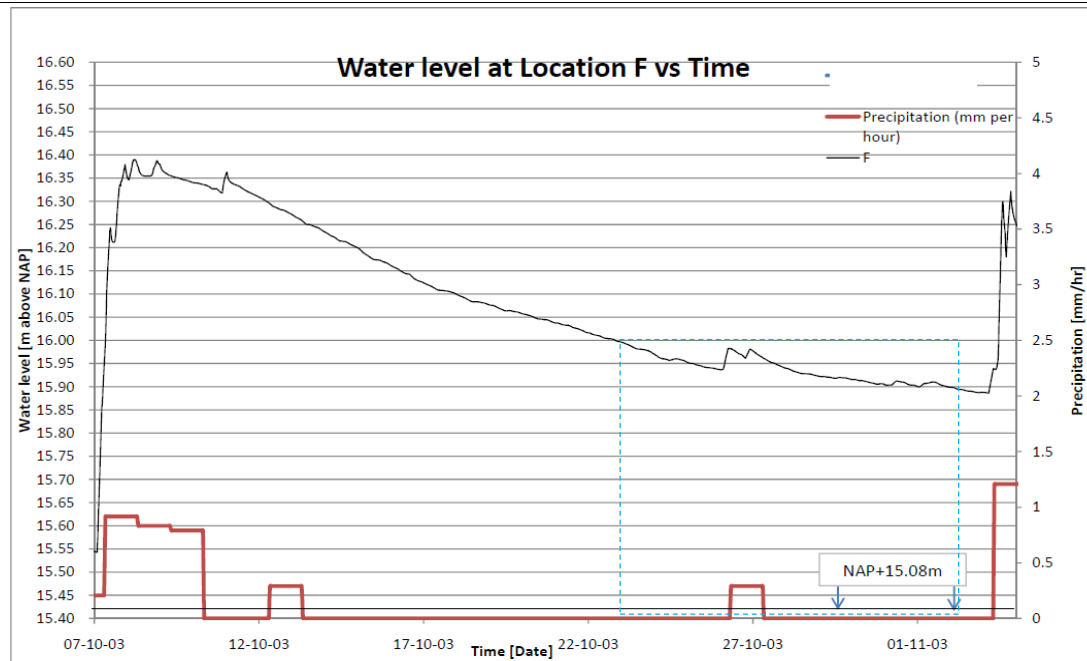


Graphical method used at Location E for 3 – 27 April 2011 period

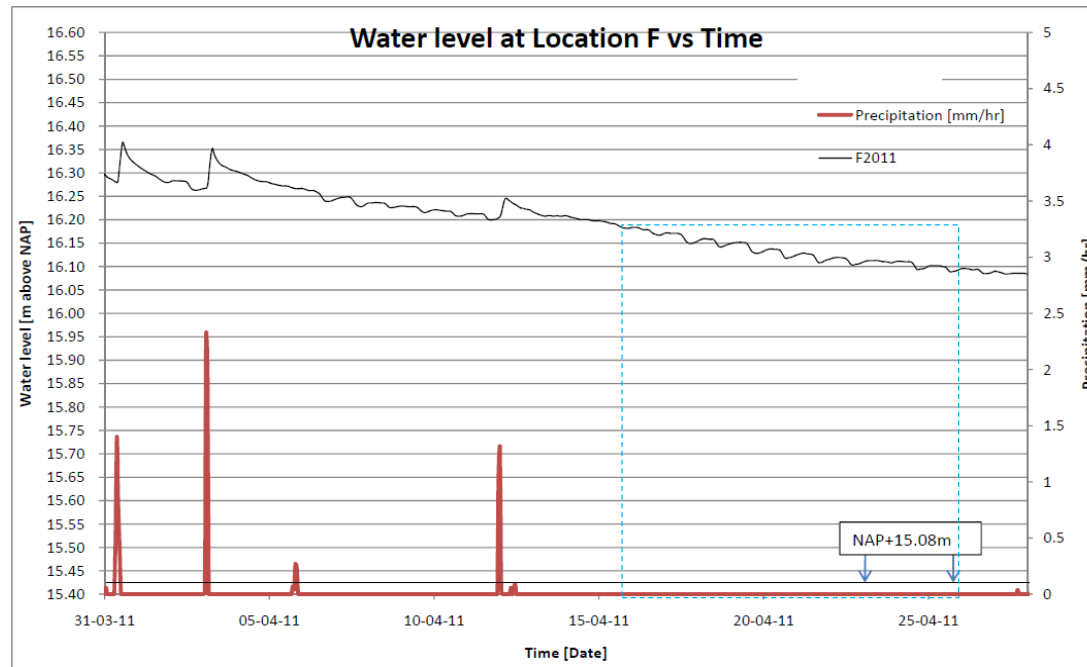
Graphical method at Location E

During 23 Oct – 2 Nov 2003 (10.6 days interval), the water level dropped from NAP+15.99m to NAP+15.89m. This leads to an average rate of water level drop of 0.009m/day. Factoring in the rain event on 27 Oct 2003, the actual time interval would be 8.7 days instead. This leads to 0.012m/day.

We noticed during 17 – 27 Apr 2011 (10.4 days interval), the water level dropped from NAP+16.20m – NAP+16.10m, leading to an average rate of water level drop of 0.010m/day.



Graphical method used at Location F for 10 October – 2 November 2003 period



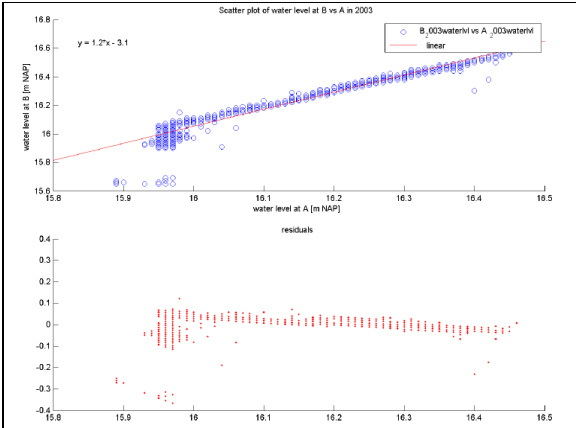
Graphical method used at Location F for 3 – 27 April 2011 period

Graphical method at Location F

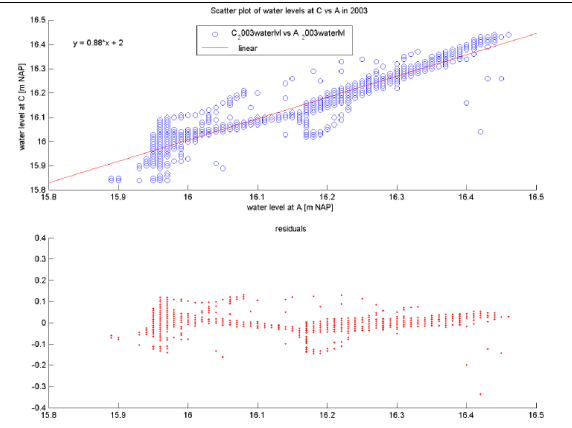
During 23 Oct – 2 Nov 2003 (10.6days), the water level dropped from NAP+15.99m to NAP+15.89m. This leads to an average rate of water level drop of 0.009m/day. Factoring in the rain event on 27 Oct 2003, the actual time interval would be 8.6 days instead. This leads to 0.012m/day.

We noticed during 15 – 27 Apr 2011(12.2 days interval), the water level dropped from NAP+16.18m – NAP+16.08m, leading to an average rate of water level drop of 0.008m/day.

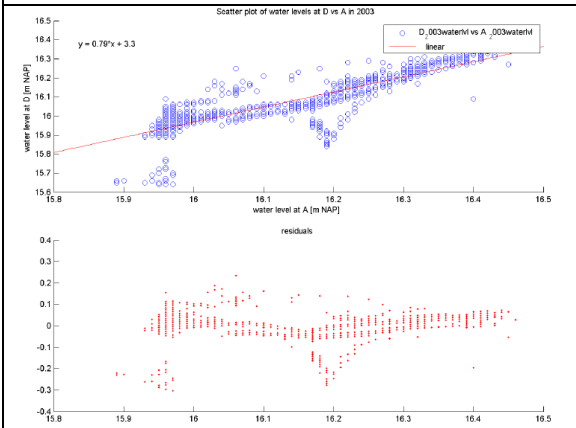
Appendix 7 Scatter plots between all monitoring locations for monitoring period in 2003 and 2011



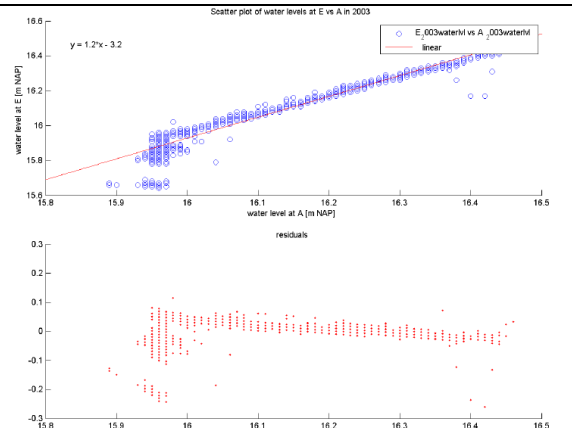
Plot of water levels at Location B vs Location A in 2003



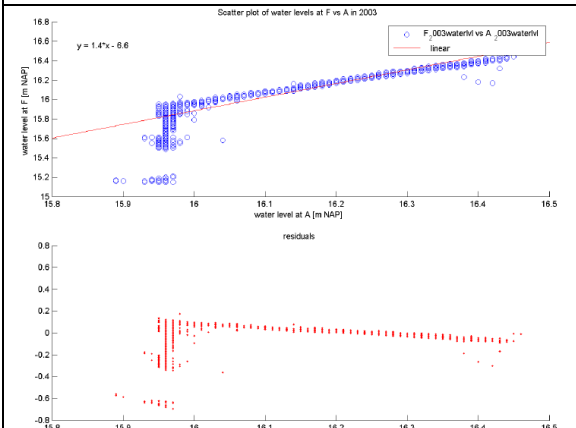
Plot of water levels at Location C vs Location A in 2003



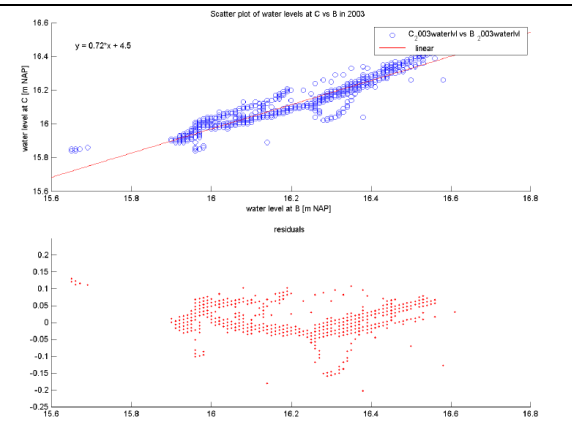
Plot of water levels at Location D vs Location A in 2003



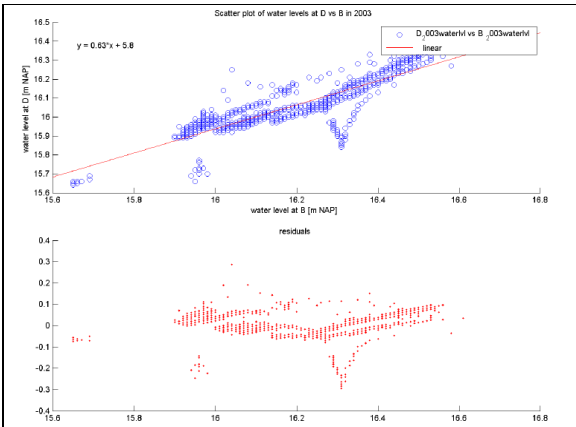
Plot of water levels at Location E vs Location A in 2003



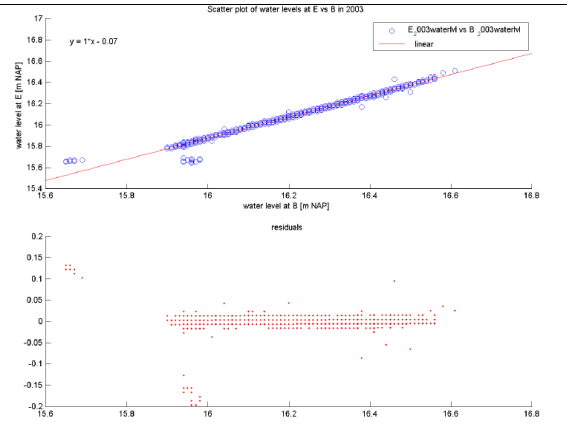
Plot of water levels at Location F vs Location A in 2003



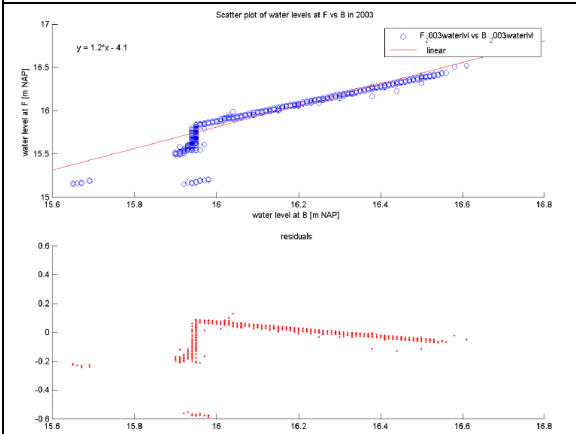
Plot of water levels at Location C vs Location B in 2003



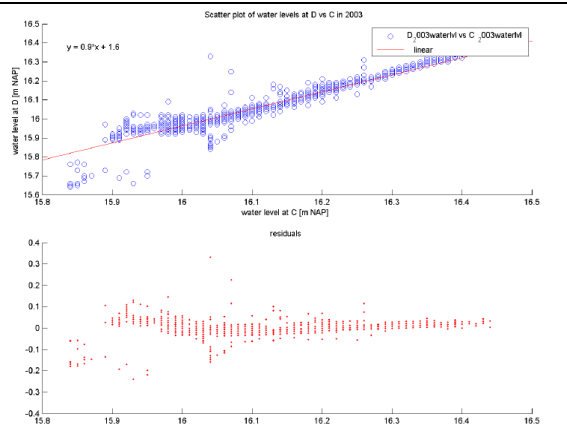
Plot of water levels at Location D vs Location B in 2003



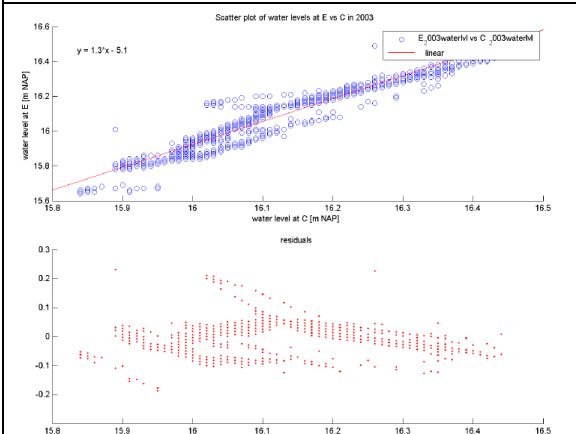
Plot of water levels at Location E vs Location B in 2003



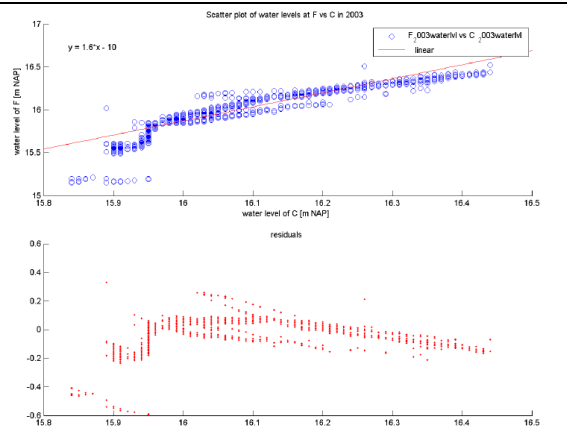
Plot of water levels at Location F vs Location B in 2003



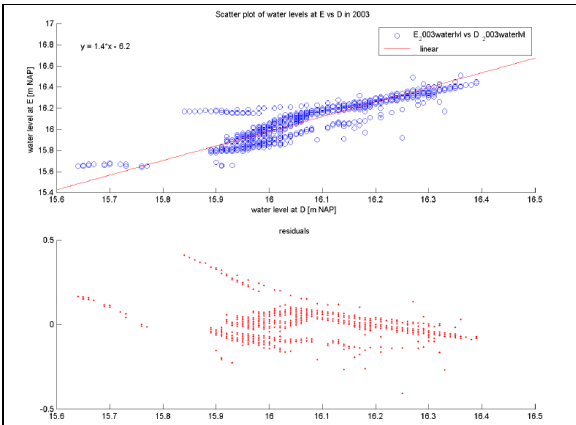
Plot of water levels at Location D vs Location C in 2003



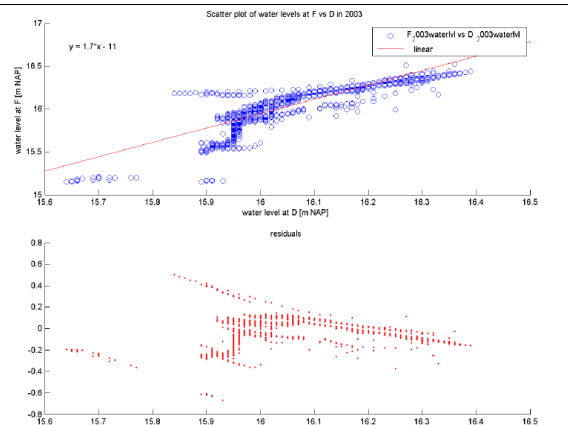
Plot of water levels at Location E vs Location C in 2003



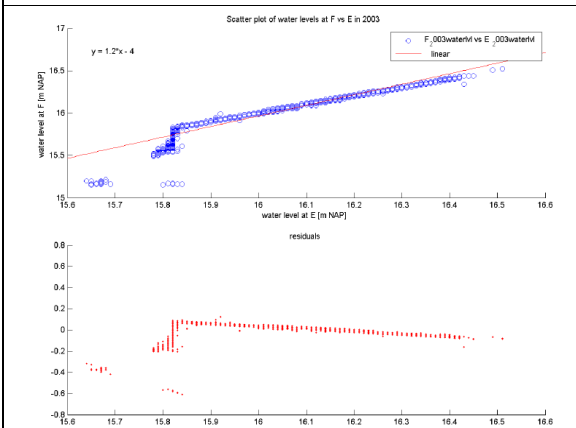
Plot of water levels at Location F vs Location C in 2003



Plot of water levels at Location E vs Location D in 2003

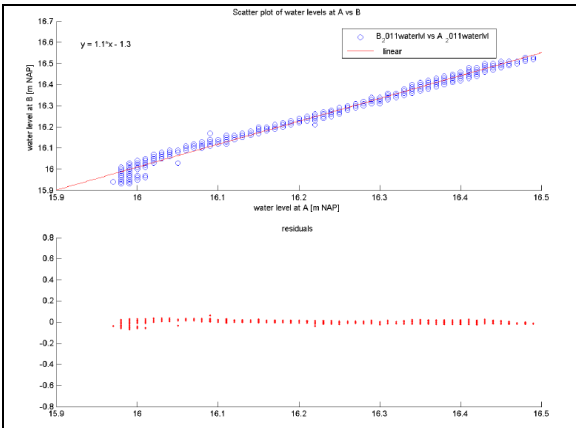


Plot of water levels at Location F vs Location D in 2003

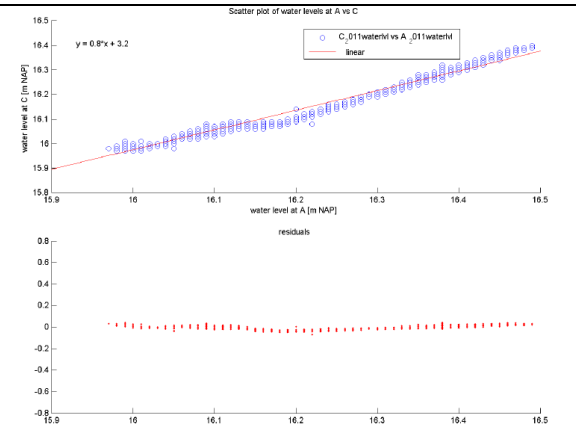


Plot of water levels at Location F vs Location E in 2003

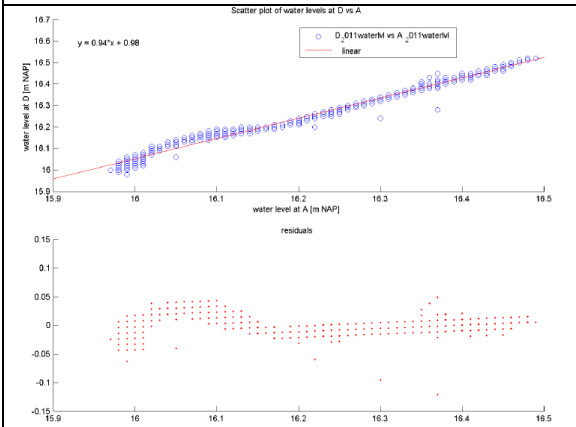
Scatter plots between all monitoring locations (A-F and Point 7) for monitoring period in 2011



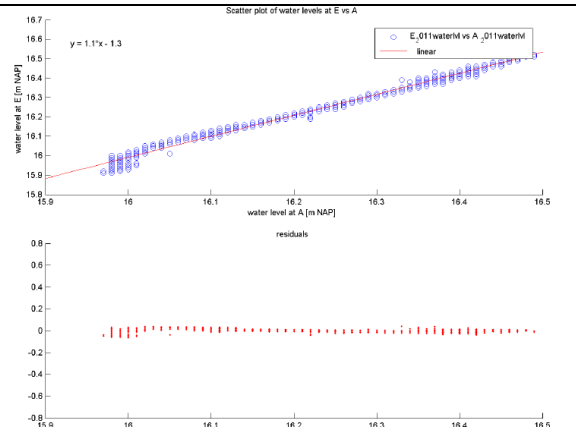
Plot of water levels at Location B vs Location A



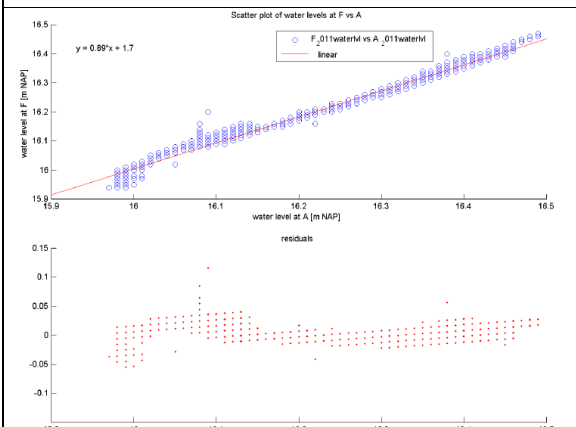
Plot of water levels at Location C vs Location A



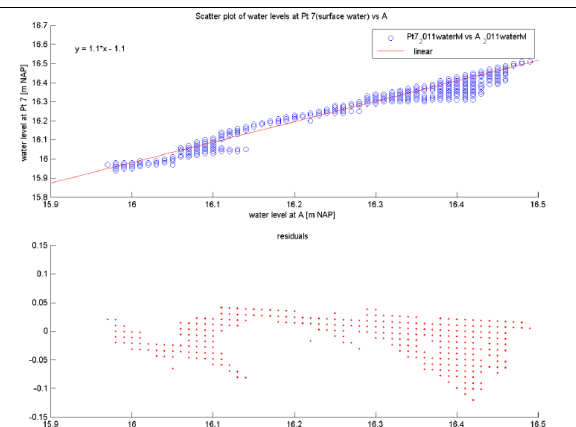
Plot of water levels at Location D vs Location A



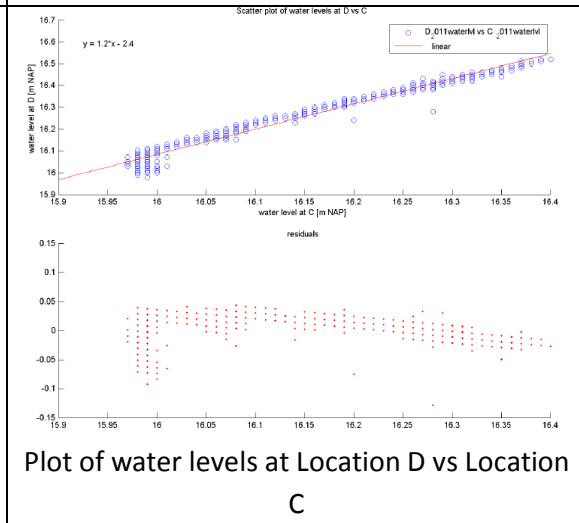
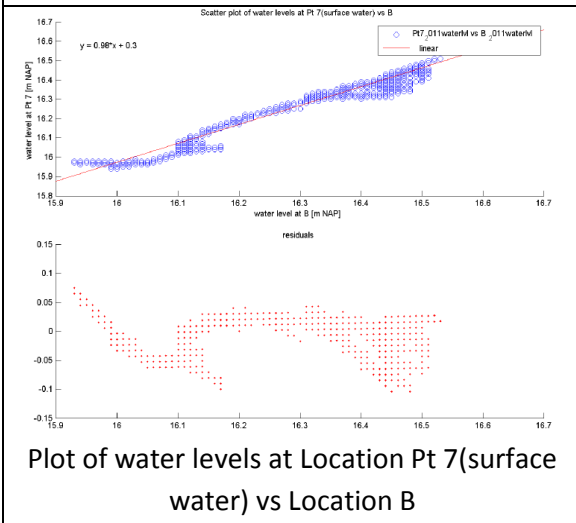
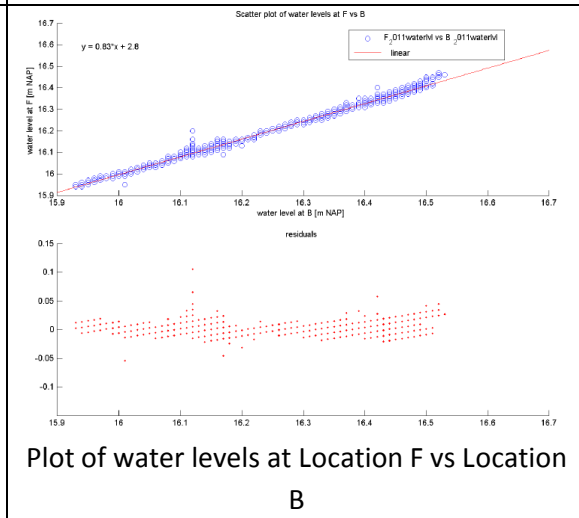
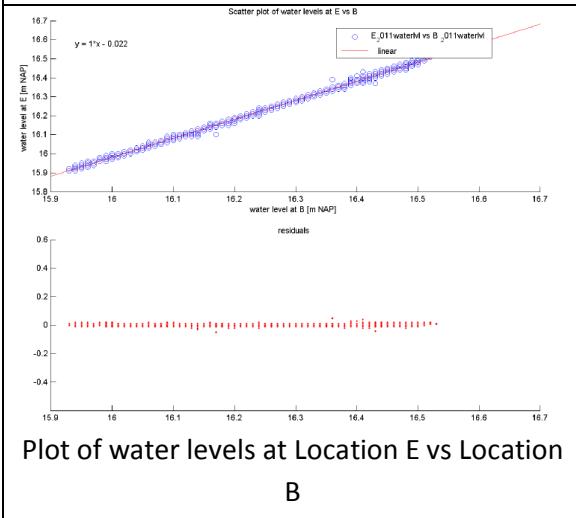
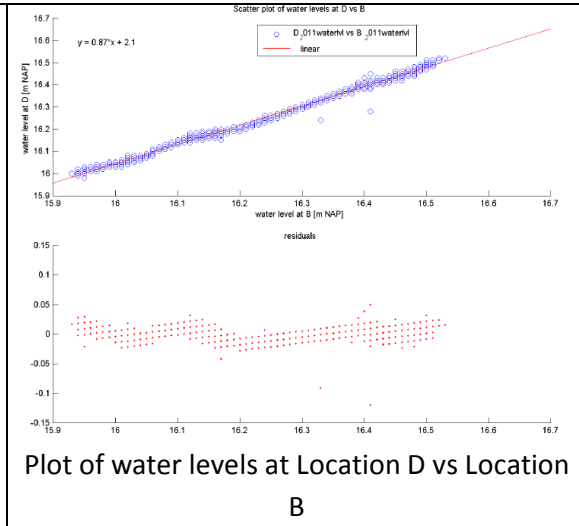
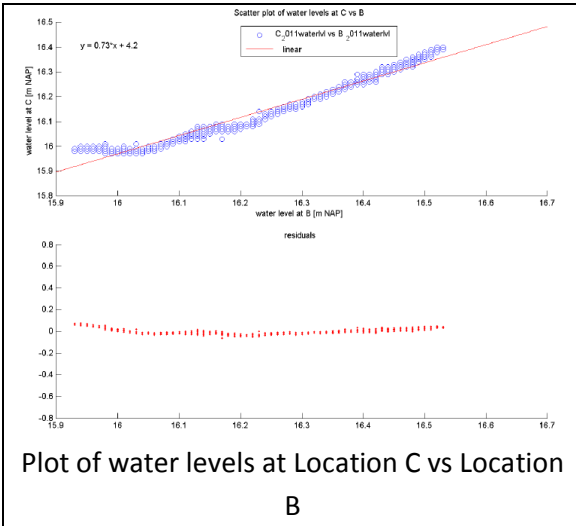
Plot of water levels at Location E vs Location A

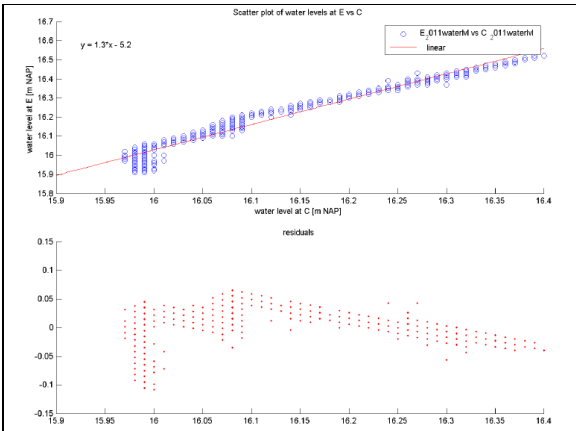


Plot of water levels at Location F vs Location A

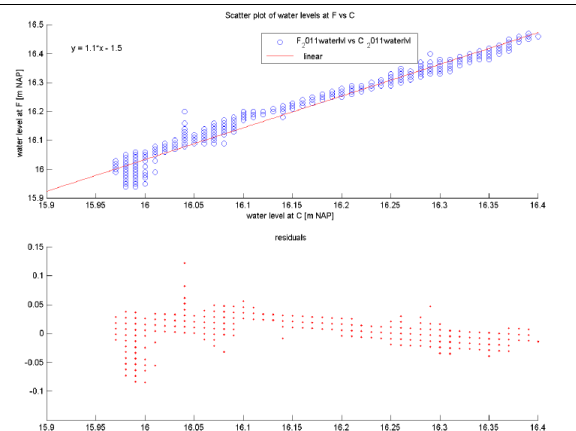


Plot of water levels at Location Pt 7 (surface water) vs Location A

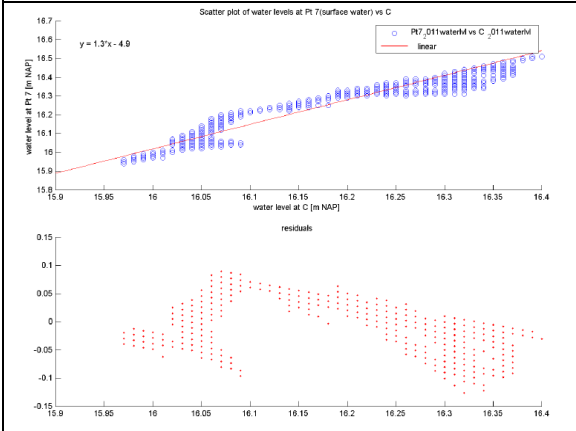




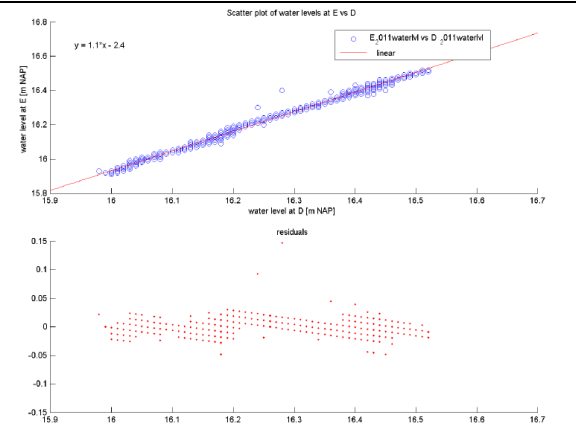
Plot of water levels at Location E vs Location C



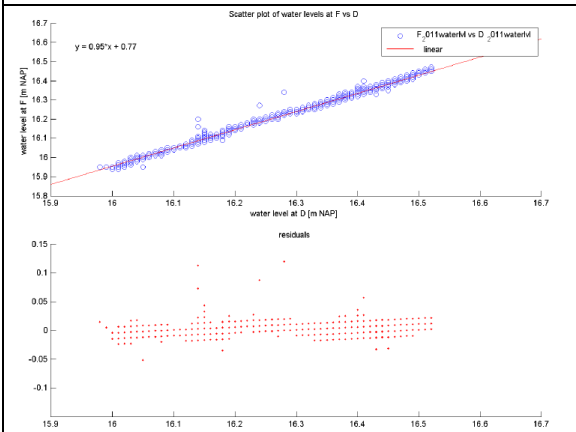
Plot of water levels at Location F vs Location C



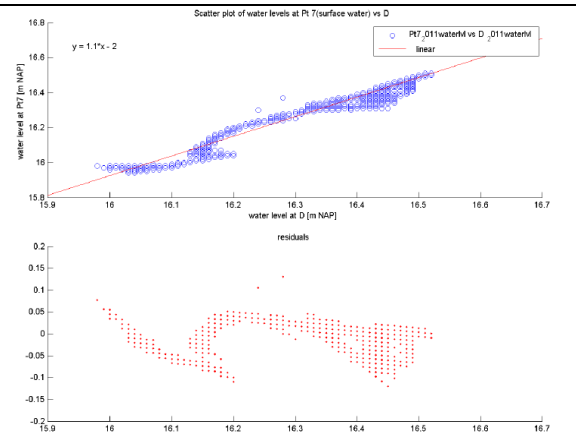
Plot of water levels at Location Pt 7(surface water) vs Location C



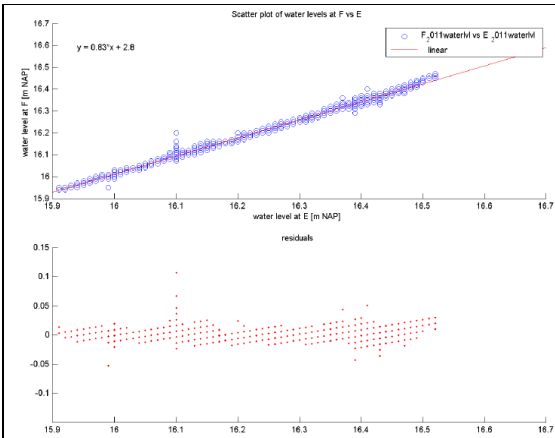
Plot of water levels at Location E vs Location D



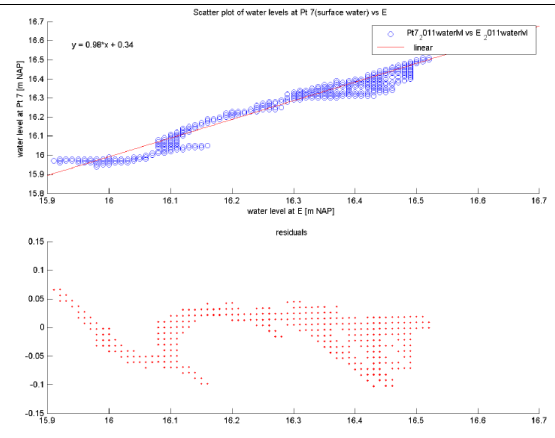
Plot of water levels at Location F vs Location D



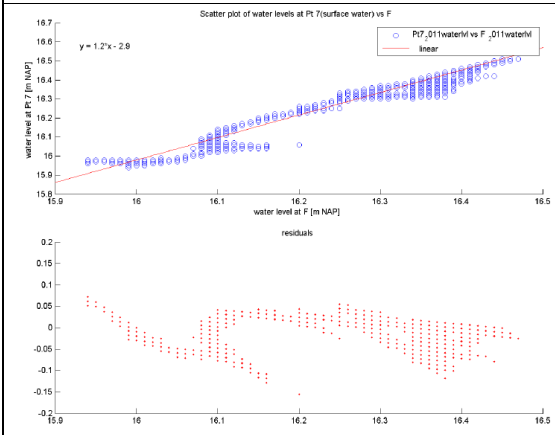
Plot of water levels at Location Pt 7(surface water) vs Location D



Plot of water levels at Location F vs Location E

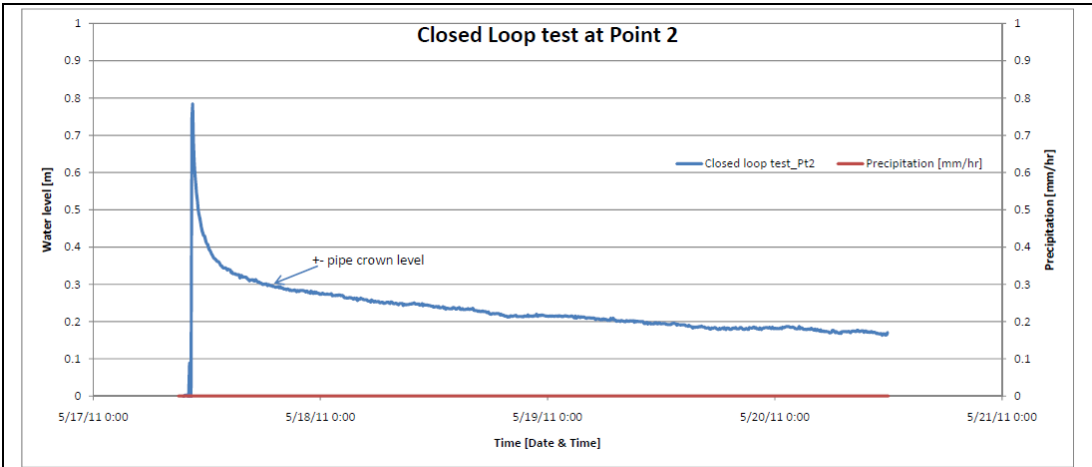


Plot of water levels at Location Pt 7(surface water) vs Location E

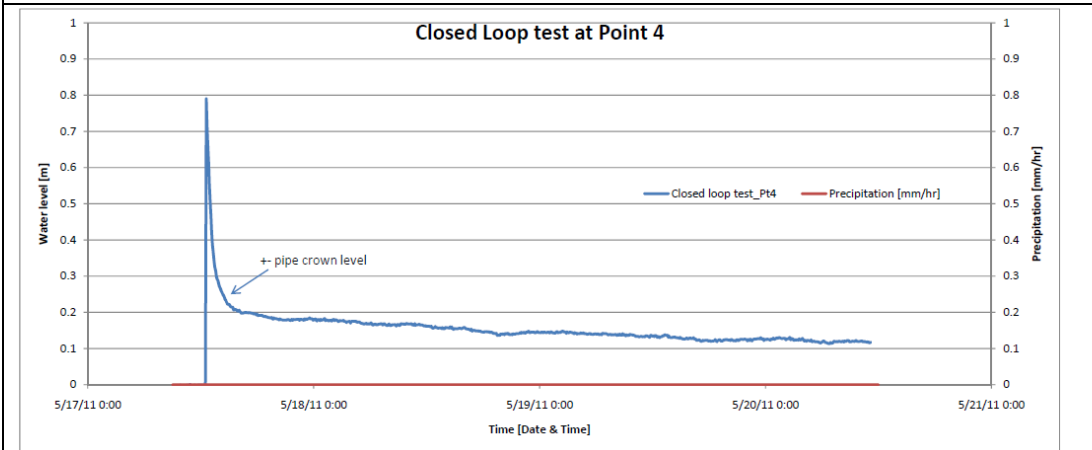


Plot of water levels at Location Pt 7(surface water) vs Location F

Appendix 8 Water trends of closed-loop test at locations: Point 2 and Point 4

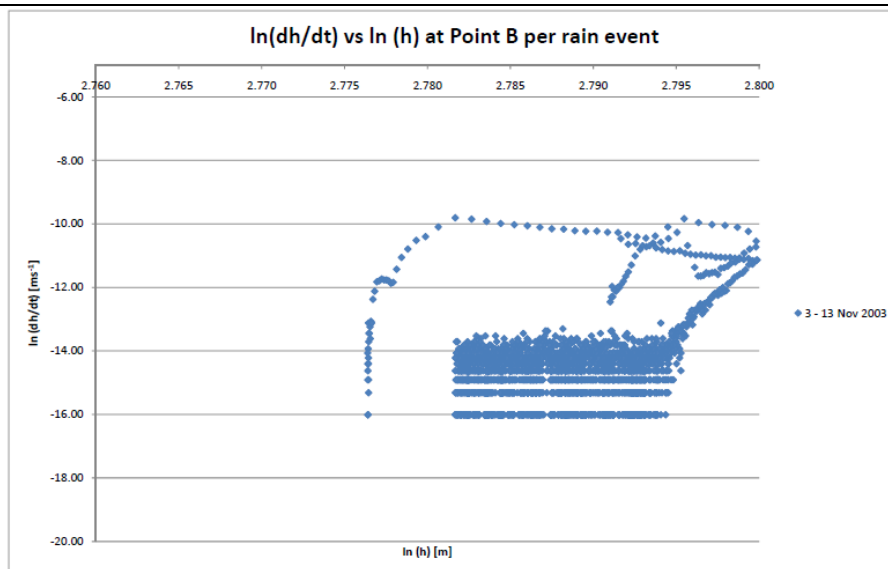
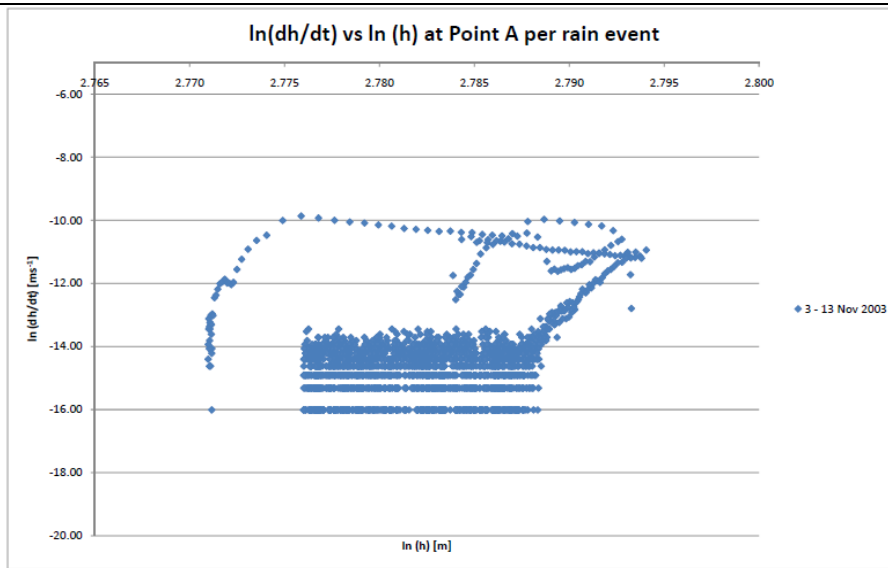


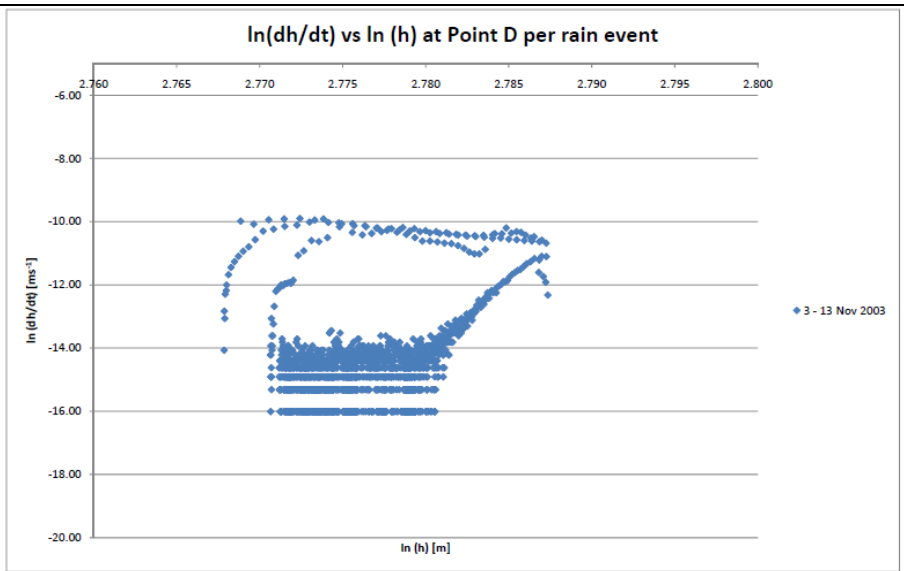
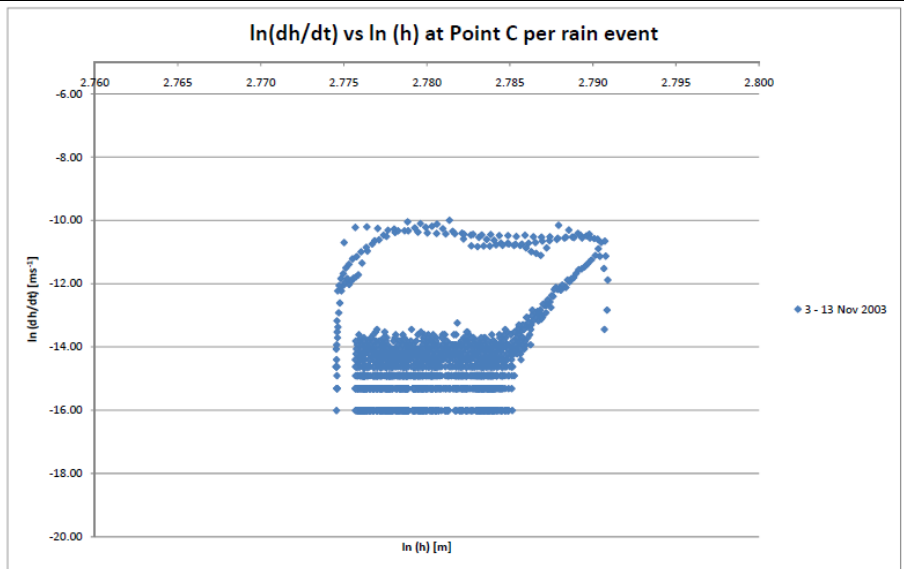
Water level trend at Point 2 for closed-loop test

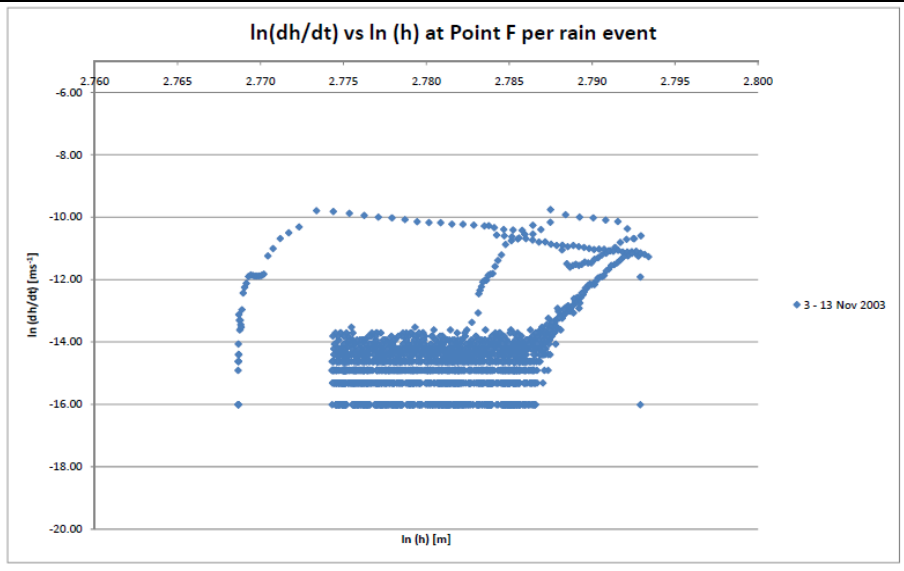
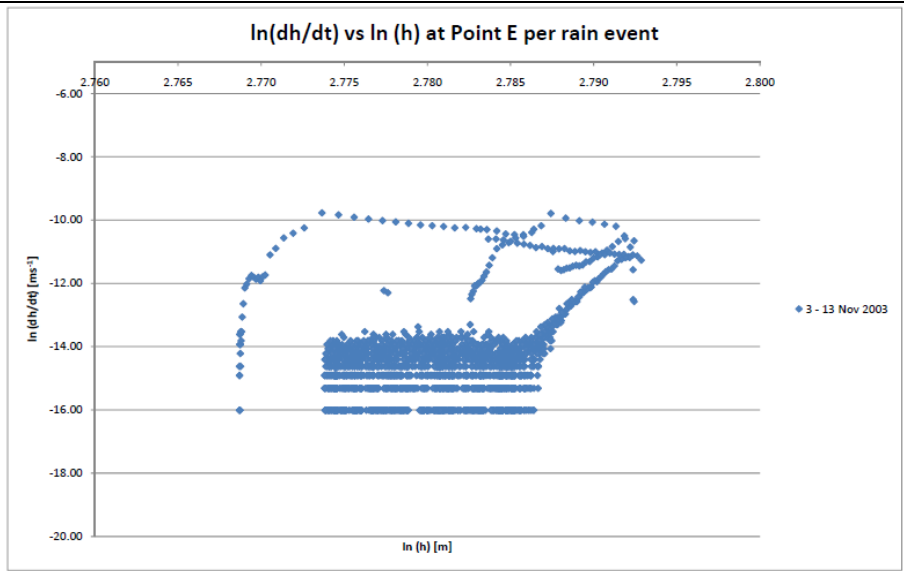


Water level trend at Point 4 for closed-loop test

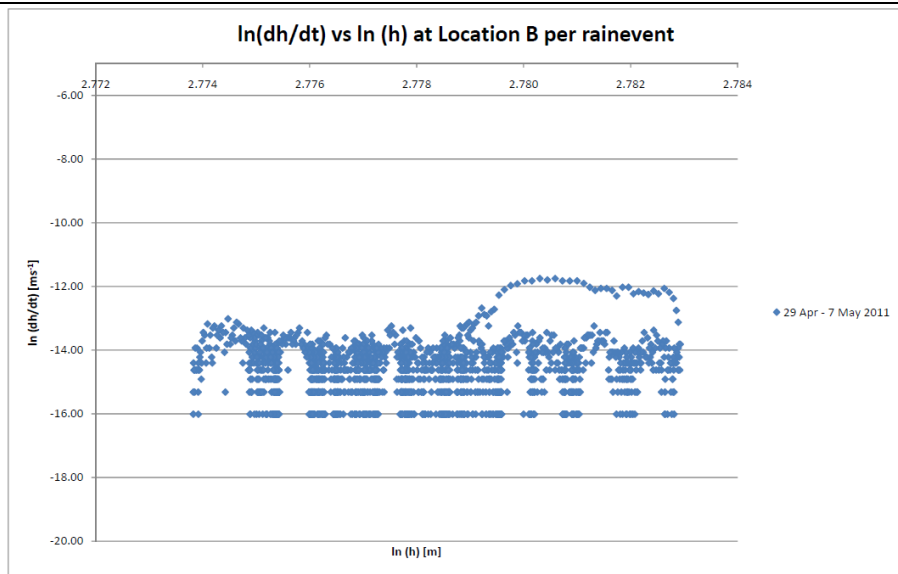
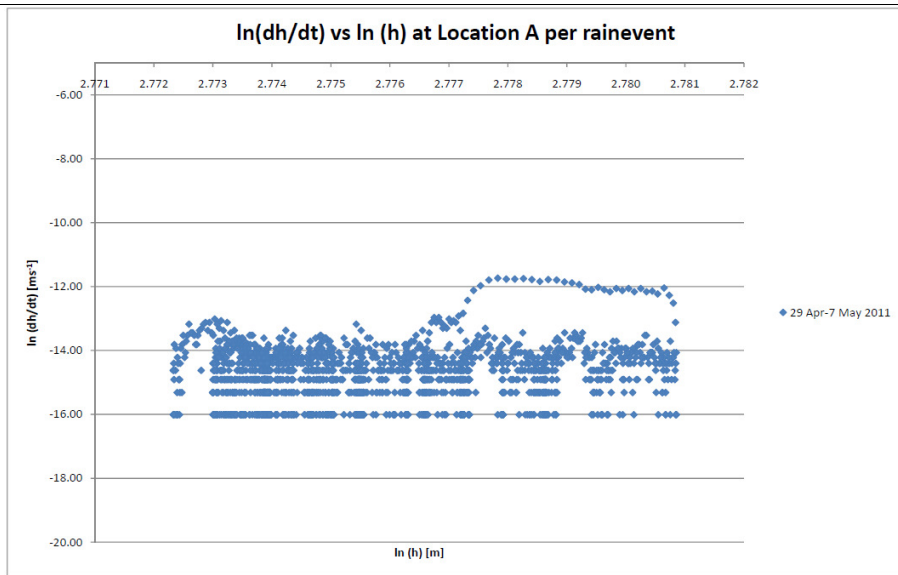
Appendix 9 In (dh/dt) vs ln (h) plots for 3 to 13 November 2003 for Locations A - F

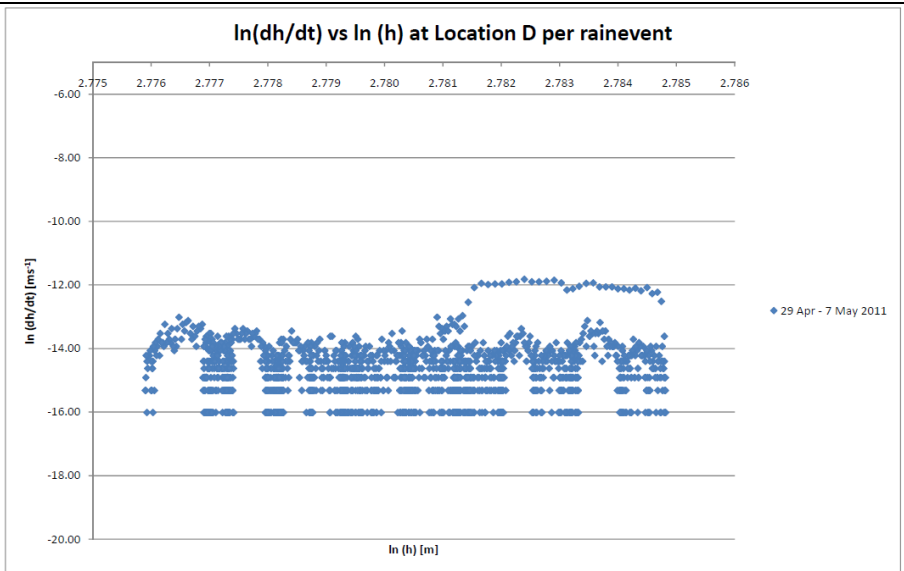
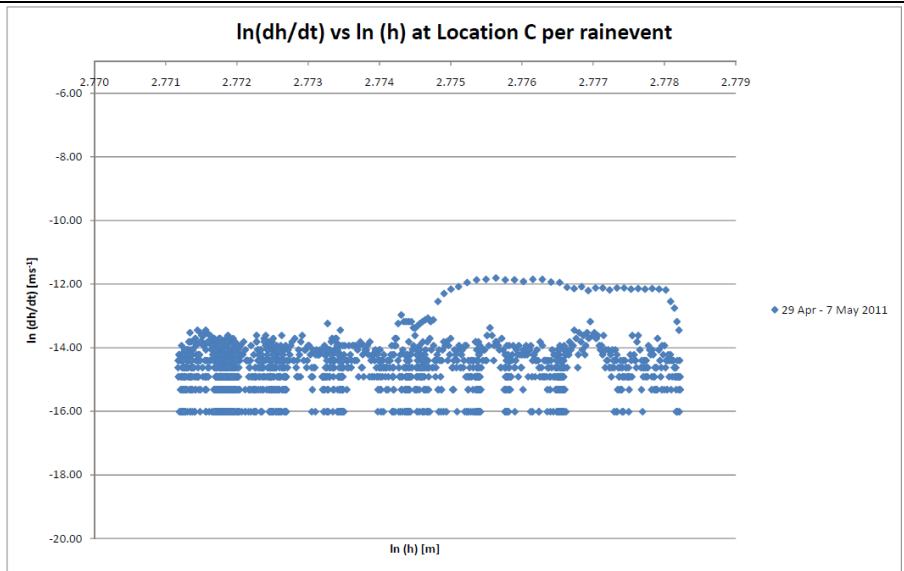


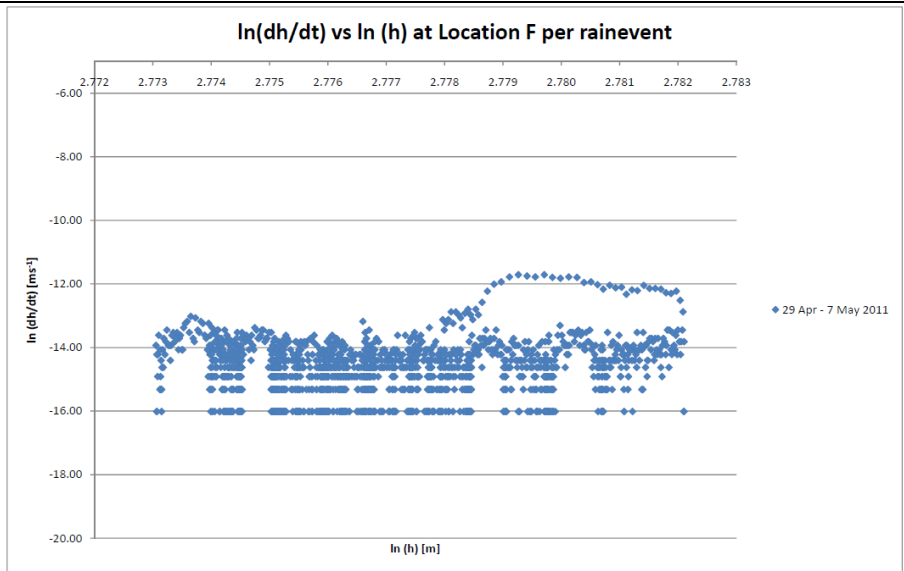
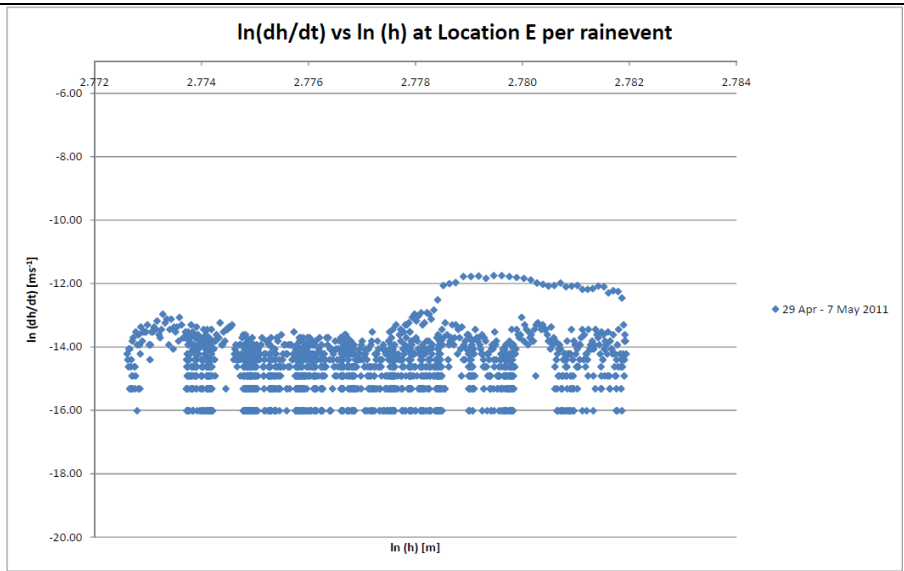




In (dh/dt) vs In (h) for 29 April to 7 May 2011 for Locations A - F







Appendix 10 Definitions on the statistics used to determine the goodness-of-fit:

(Extracted from Matlab help explanation)

The sum of squares due to error (SSE)

This statistics measures the total deviation of the response values from the fit to the actual experimental value measured. It is also referred to as the summed square of residuals.

$$SSE = \sum_{i=1}^n w_i (y_i - \hat{y}_i)^2$$

A value that is closer to zero will indicate that the proposed fit has a smaller random error component and the proposed fit is better in its prediction.

R-square

The R-square statistics describes how successful the proposed fit is in interpreting the variation of the data. It is also the square of the correlation between the experimental values and the predicted response values and called the square of the multiple correlation coefficient and the coefficient of multiple determination.

R-square is the ratio of the sum of squares of the regression (SSR) and the total sum of squares (SST). SSR is defined as:

$$SSR = \sum_{i=1}^n w_i (\hat{y}_i - \bar{y})^2$$

SST (also the sum of squares about the mean) is defined as:

$$SST = \sum_{i=1}^n w_i (y_i - \bar{y})^2$$

Since $SST = SSR + SSE$. R-square can take the following form.

$$\text{R-square} = \frac{SSR}{SST} = 1 - \frac{SSE}{SST}$$

The value of R-square is between 0 and 1. Values nearer to 1 will mean that a greater proportion of variance is accounted for by the proposed fit/model. Take for instance, a value of 0.9 means that the proposed fit can account for 90% of the total variation in the data about the average.

Adjusted R-square

This statistics uses the R-square statistics and adjusts it according to the residual degrees of freedom. The residual degrees of freedom is defined as the number of response values n minus the number of fitted coefficient m estimated from the response values.

$$V = n - m$$

V denotes the number of independent pieces of information involving the n data points that are required to calculate the sum of squares. If the parameters are bounded and one or more of the estimates are at their bounds, those estimates are regarded as fixed. With more parameters, would mean more degrees of freedom.

The adjusted R-square statistic is generally the best indicator of the fit quality when you compare two models that are nested (ie a series of models each of which adds additional coefficients to the previous model).

$$\text{adjusted R-square} = 1 - \frac{SSE(n-1)}{SST(v)}$$

The value of adjusted R-square statistic is always less than or equal to 1. A value that is nearer to 1 will imply a better fit. Negative value occur when the proposed fit contain terms that do not help to predict the response.

Root mean squared error (RMSE)

The Root Mean Squared Error, RMSE is an estimate of the standard deviation of the random component in the data.

$$RMSE = s = \sqrt{MSE}$$

Where MSE is the mean square error or the residual mean square

$$MSE = \frac{SSE}{v}$$

A value closer to zero will indicate a better fit and better prediction capabilities.

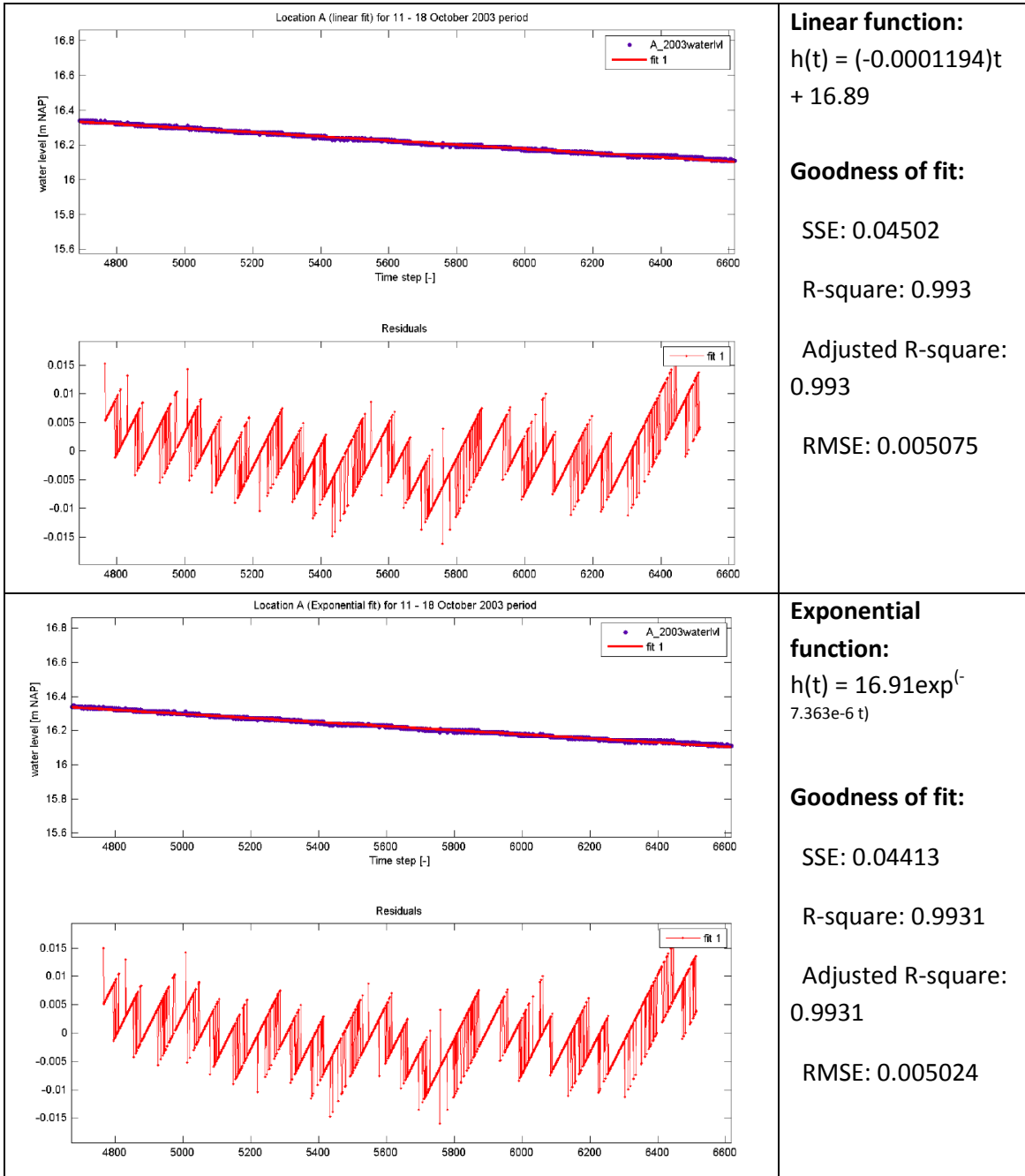
Confidence and Prediction bound

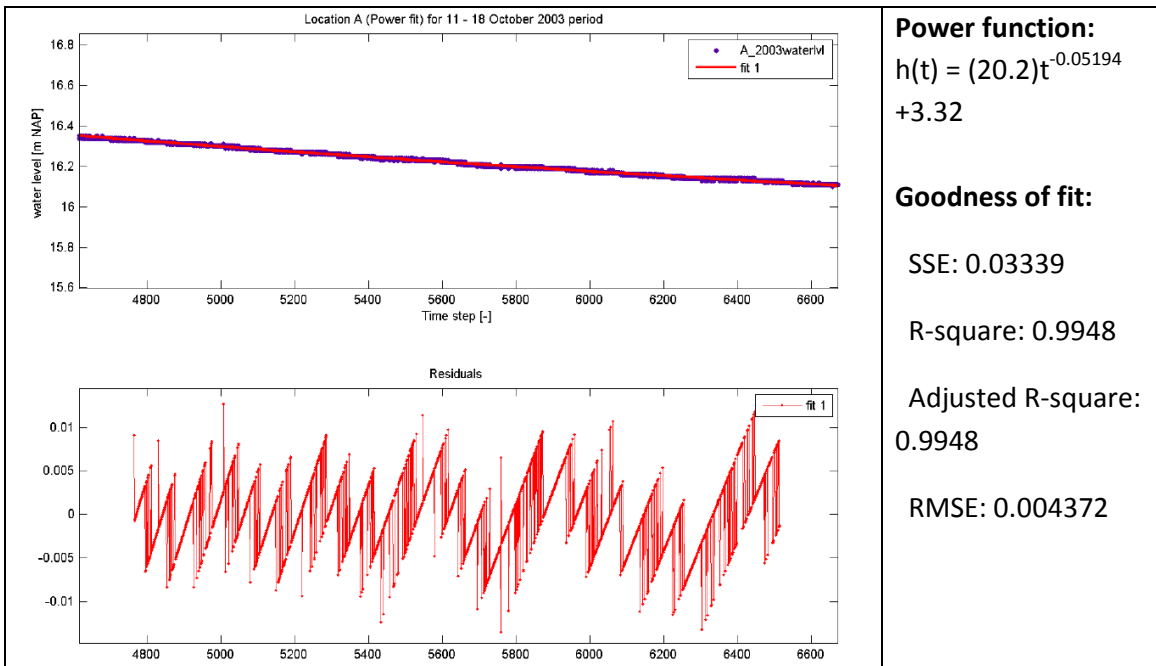
Confidence bound defines the lower and upper values of the associated interval while *prediction bound* defines the width of the interval where it gives an indication on how uncertain the predicted model is using the fitted coefficients. For example, a very wide

interval for the fitted coefficients can indicate that you should gather more data when fitting before you can draw a conclusion on the coefficients obtained. With the default confidence level is set at 95% here, this would imply that there is a 5% chance that the proposed model/fit is incorrect in predicting the new observation. In other words, this interval gives us 95% chance that the new observation will be bounded within the lower and upper prediction bounds.

Appendix 11 For remaining curve-fitting of rain events using 3 different mathematical functions for Location A

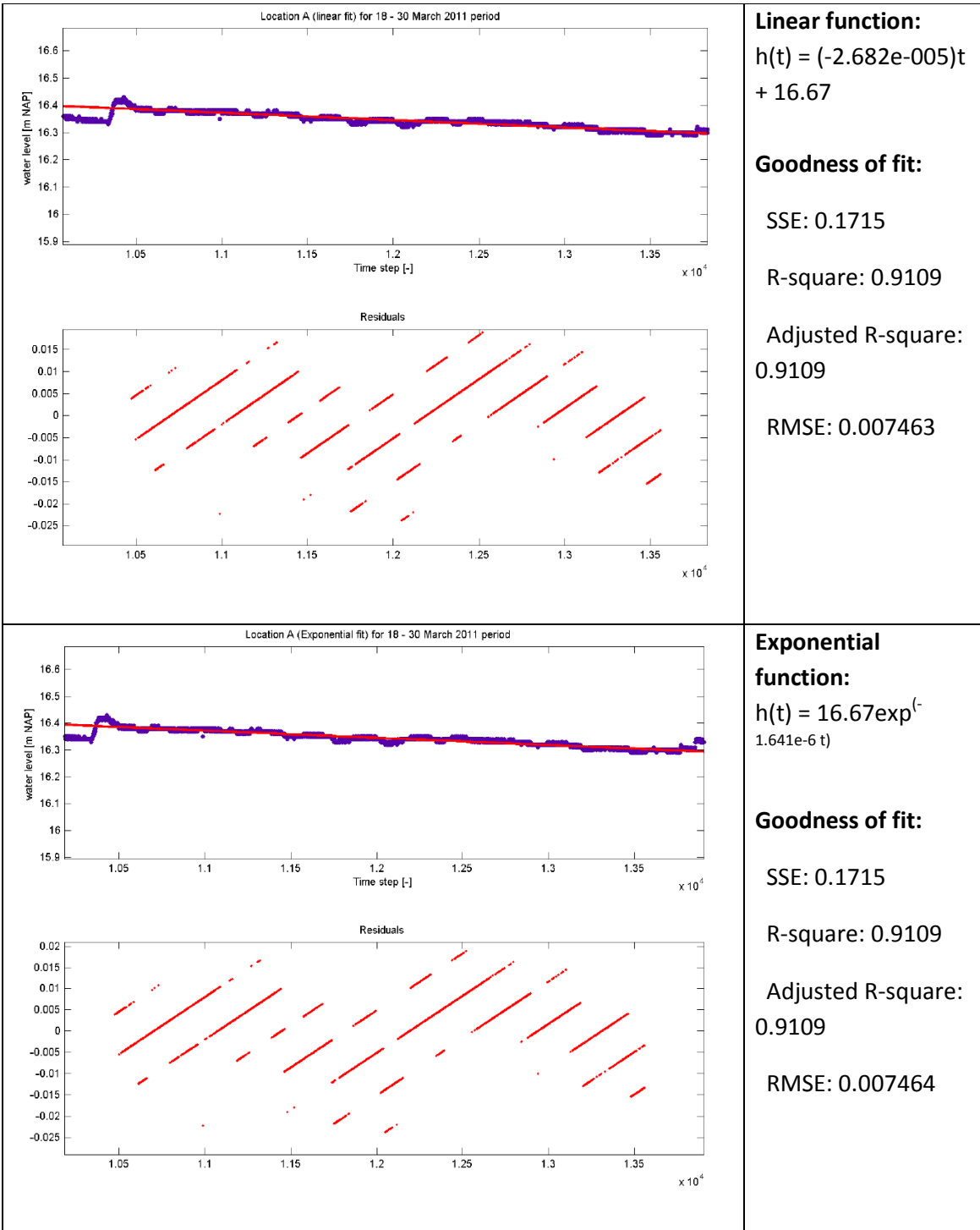
For Location A, during 11 to 18 October 2003

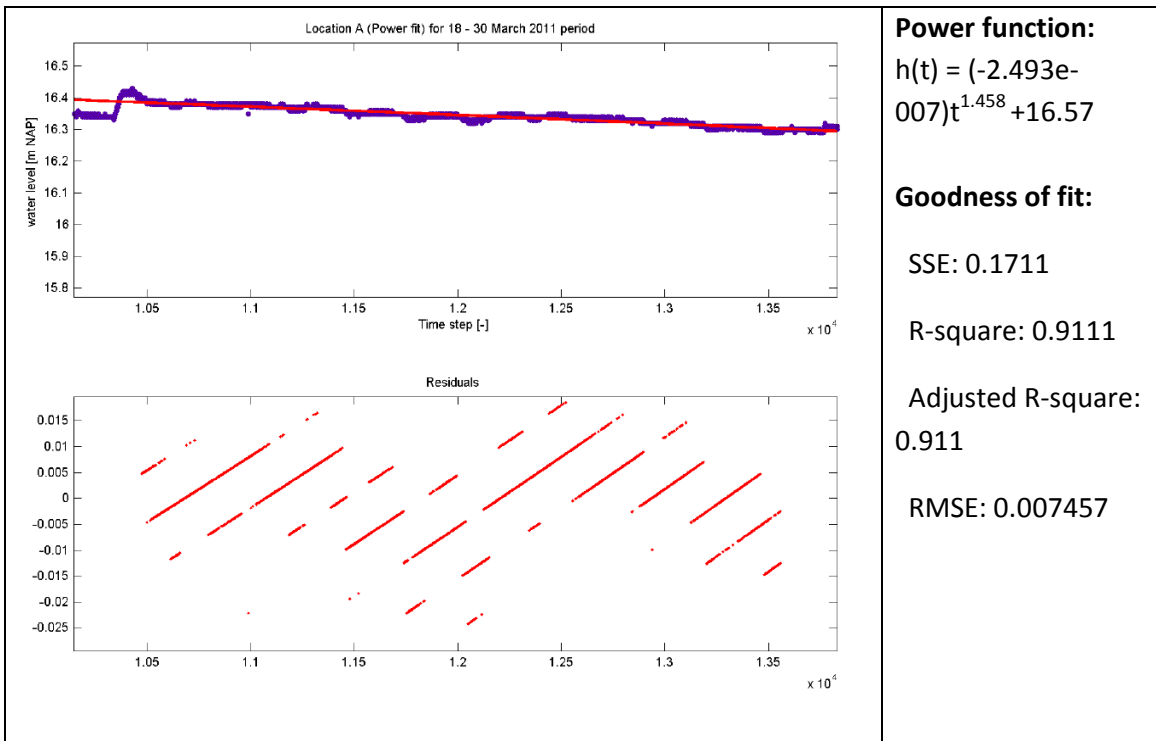




The three functions fit the water level trend well, in particular the Root Mean Squared Error are all way below 0.01m. This indicates the three functions have very good prediction capabilities for this particular event on 11 to 18 October 2003.

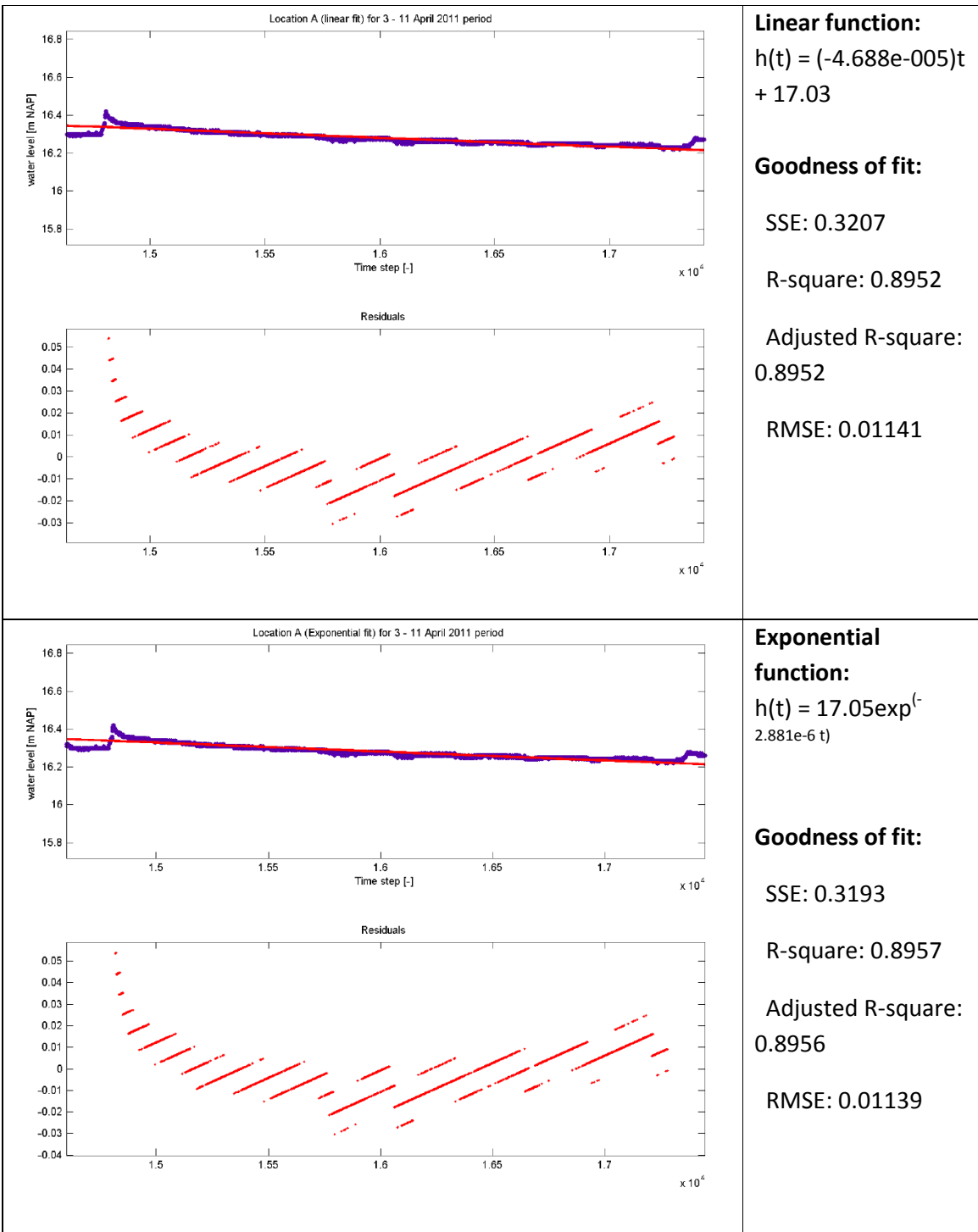
For Location A, during 18 to 30 March 2011

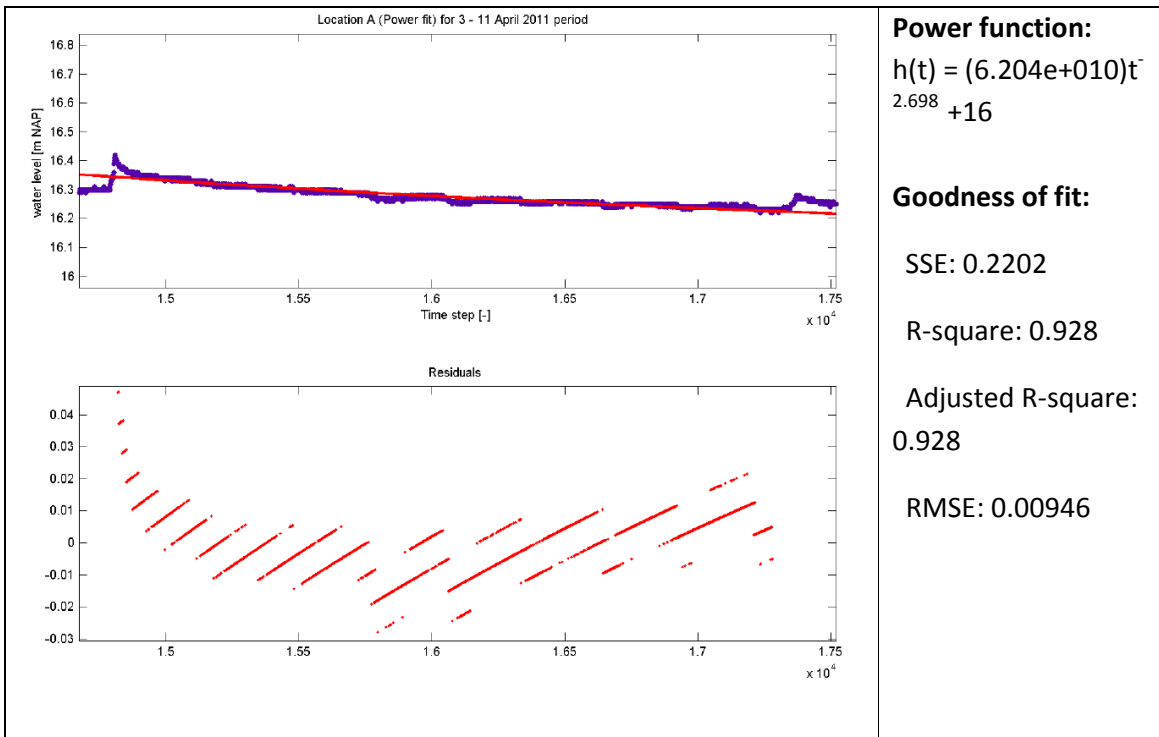




The three functions fit the water level trend well, in particular the Root Mean Squared Error are all below 0.01m. This indicates the three functions have very good prediction capabilities for this particular event (18 to 30 March 2011).

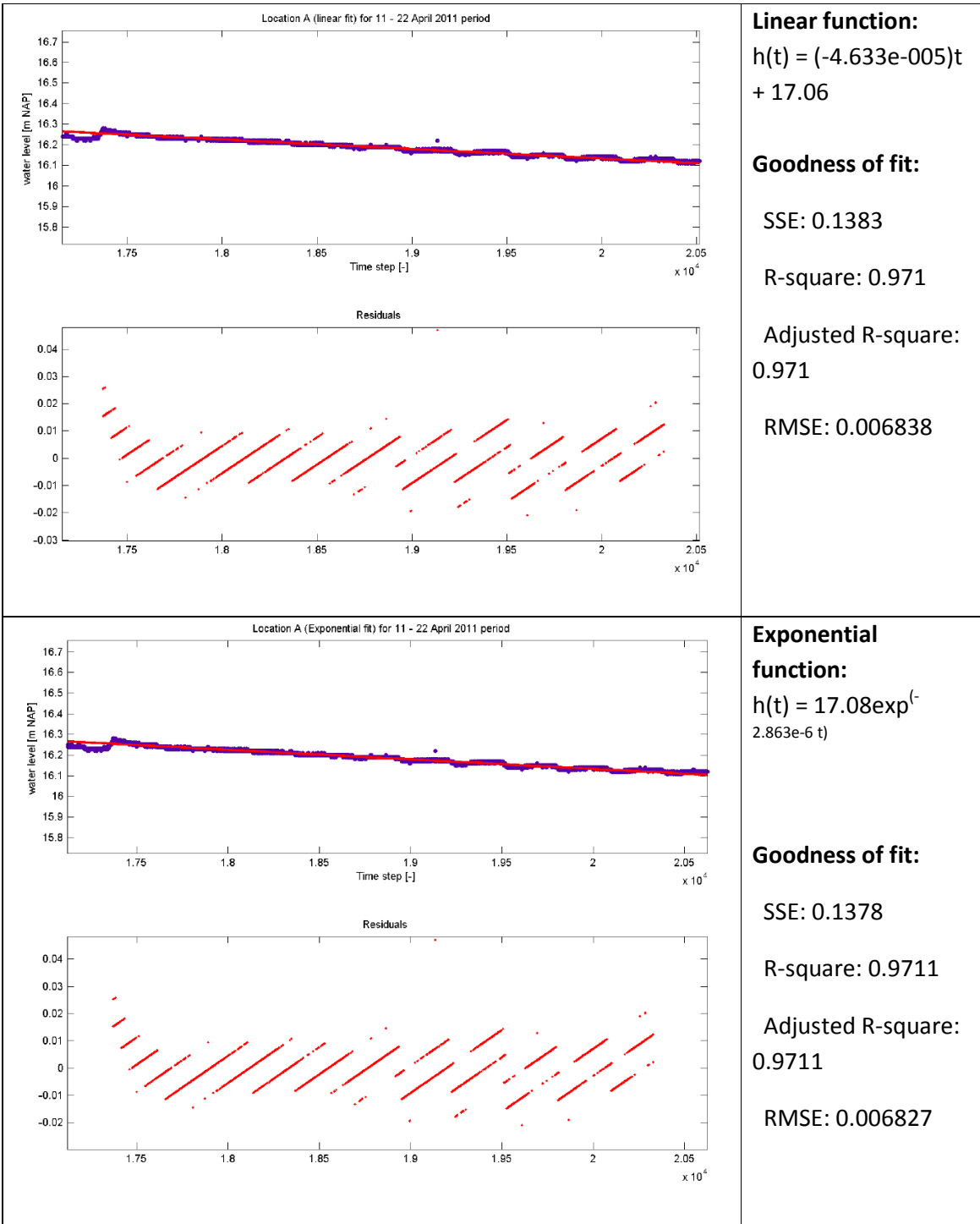
For Location A, during 3 to 11 April 2011

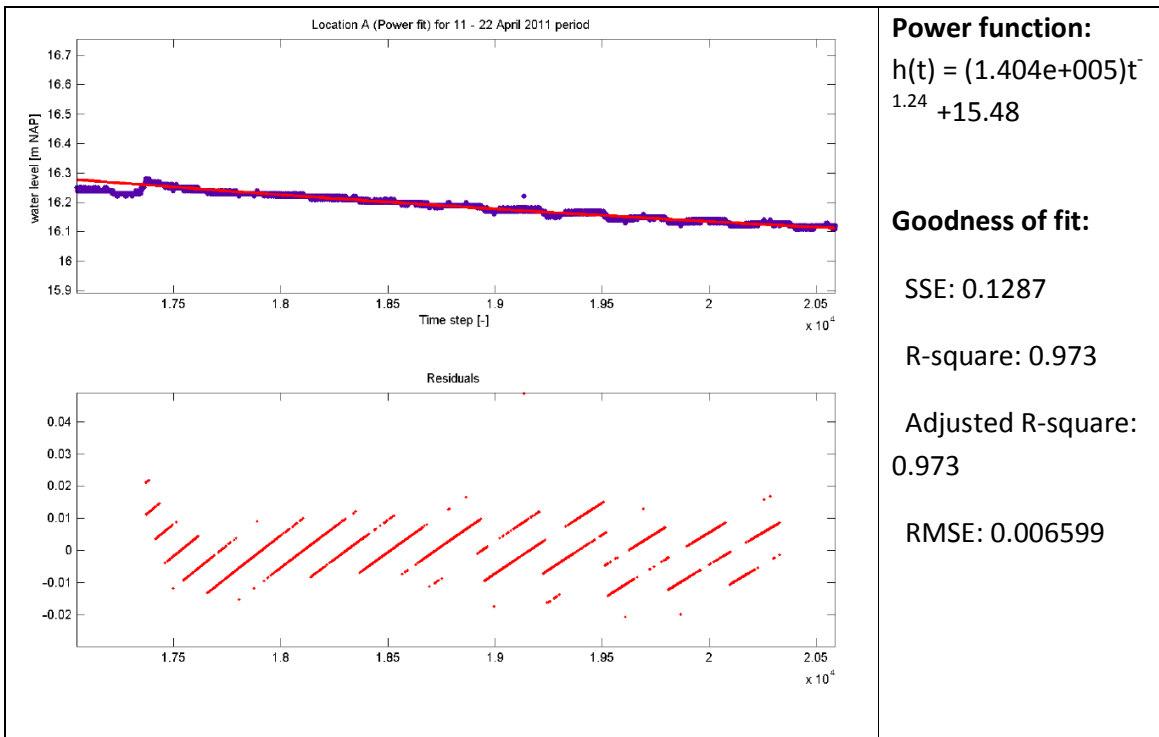




Similarly, the three functions is able to fit the water level trend well, in particular the Root Mean Squared Error are around 0.01m. This shows very good prediction capabilities by these functions, for this particular event (3 to 11 April 2011).

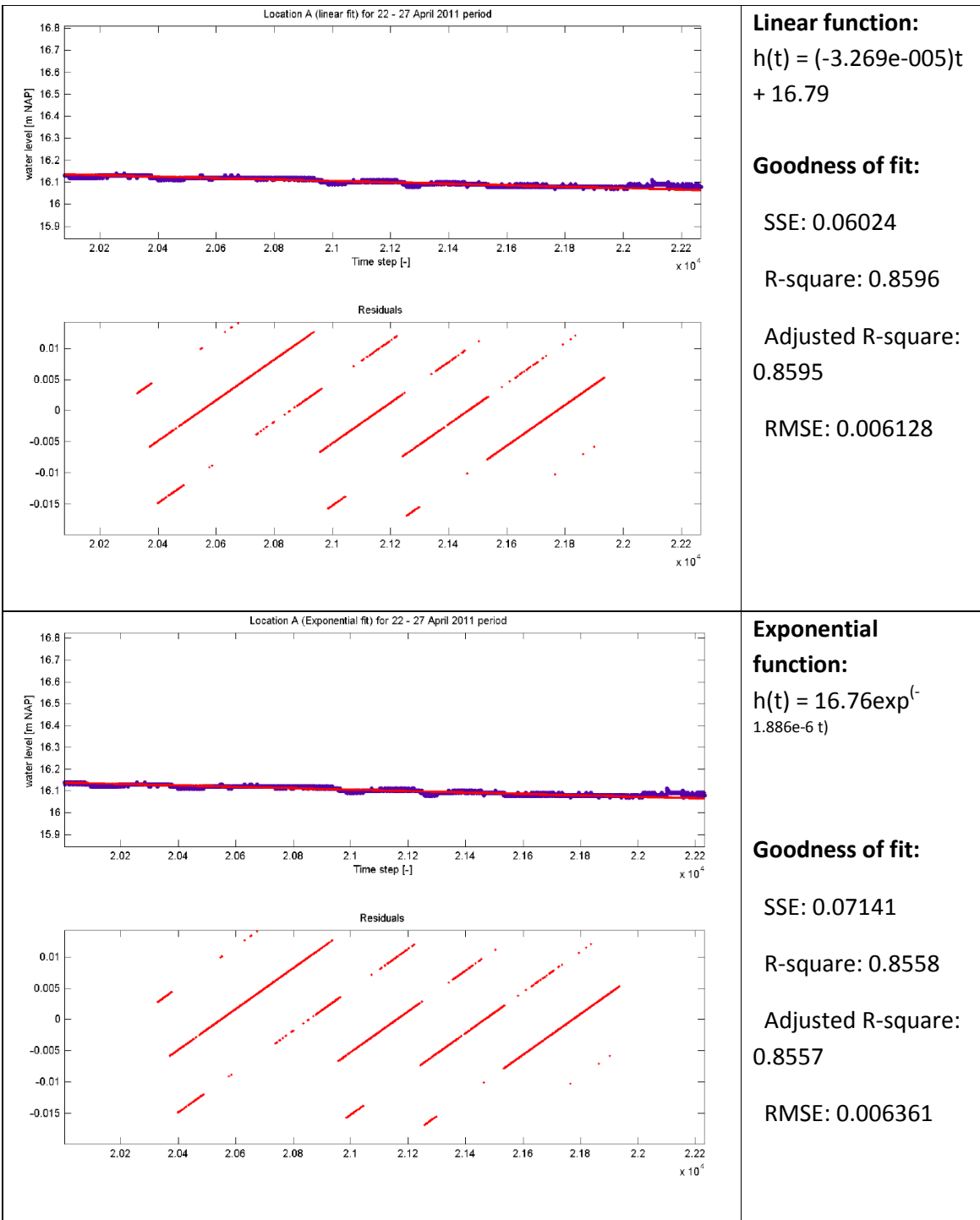
For Location A, during 11 to 22 April 2011

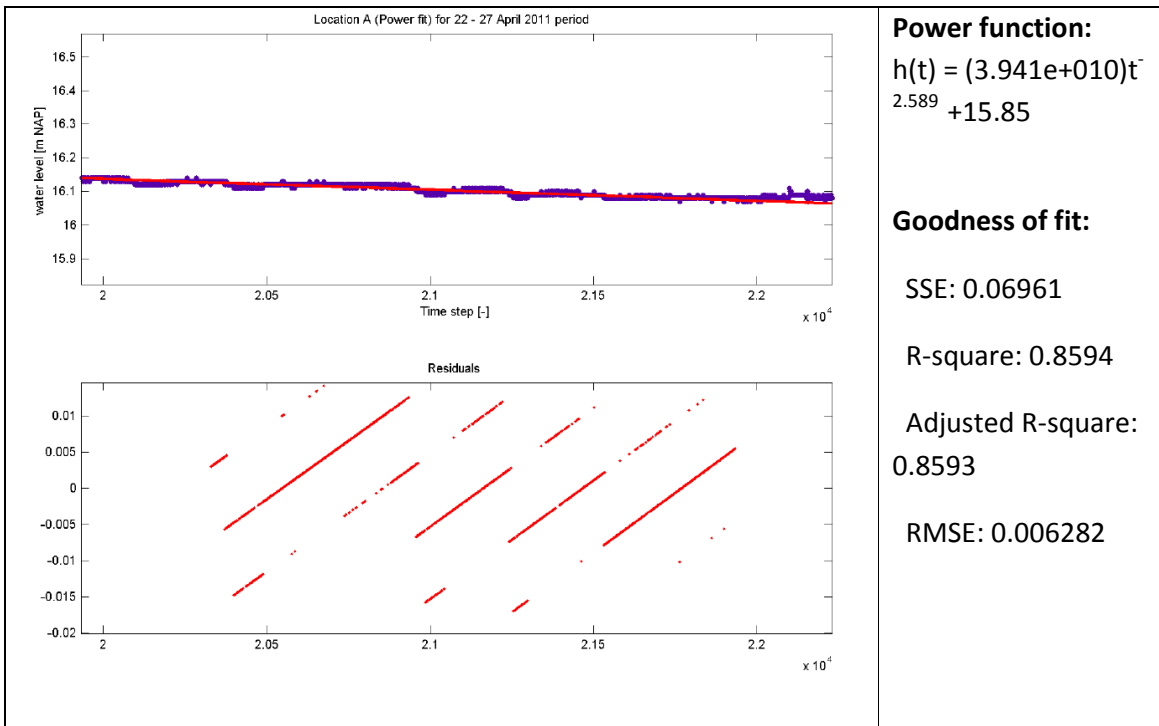




We could see, in the 11 to 22 April 2011 event, that the three functions are able to fit the water level trend well too. The Root Mean Squared Error are less than 0.01m, this demonstrates very good prediction capabilities by these functions.

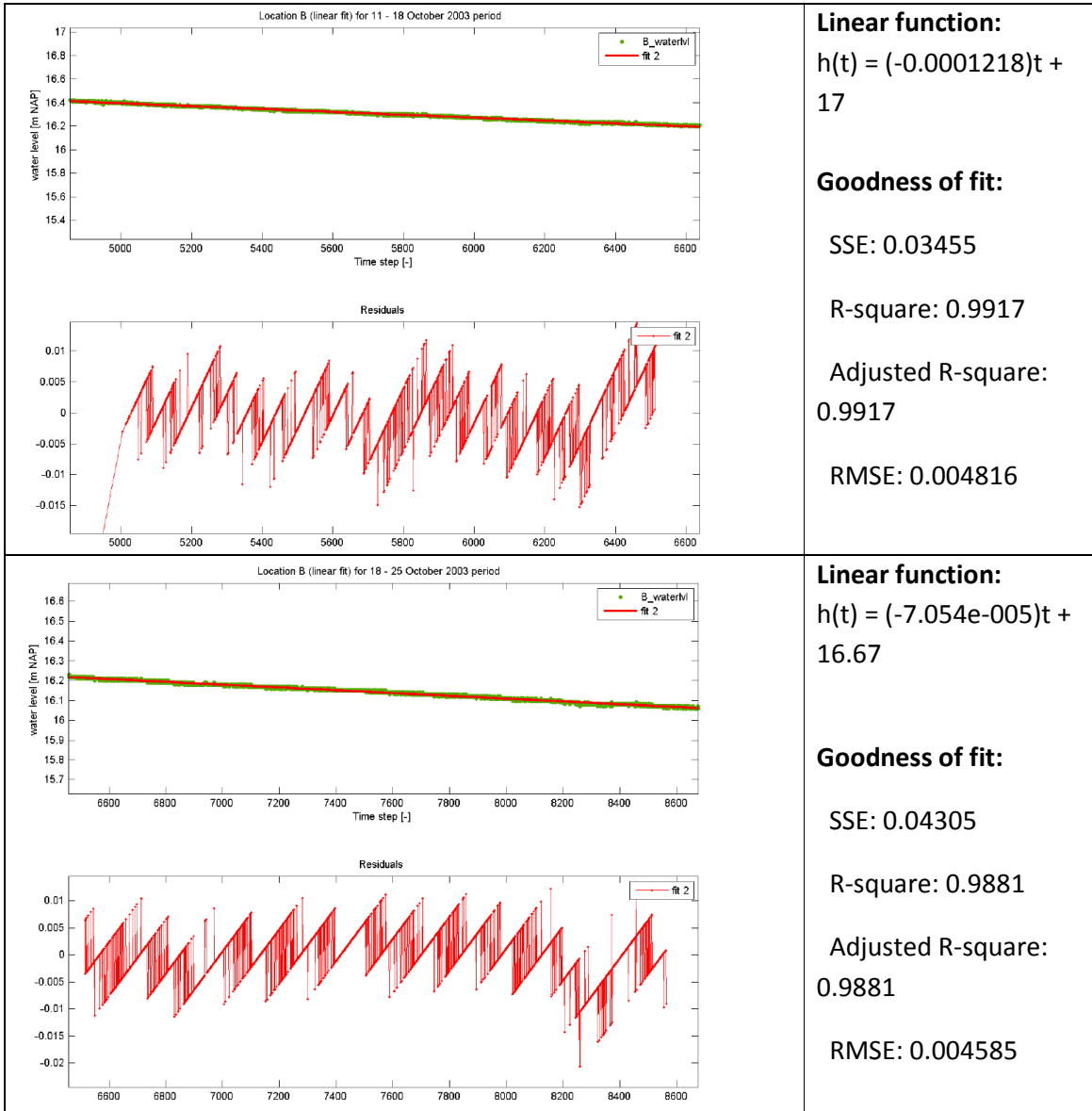
For Location A, during 22 to 27 April 2011

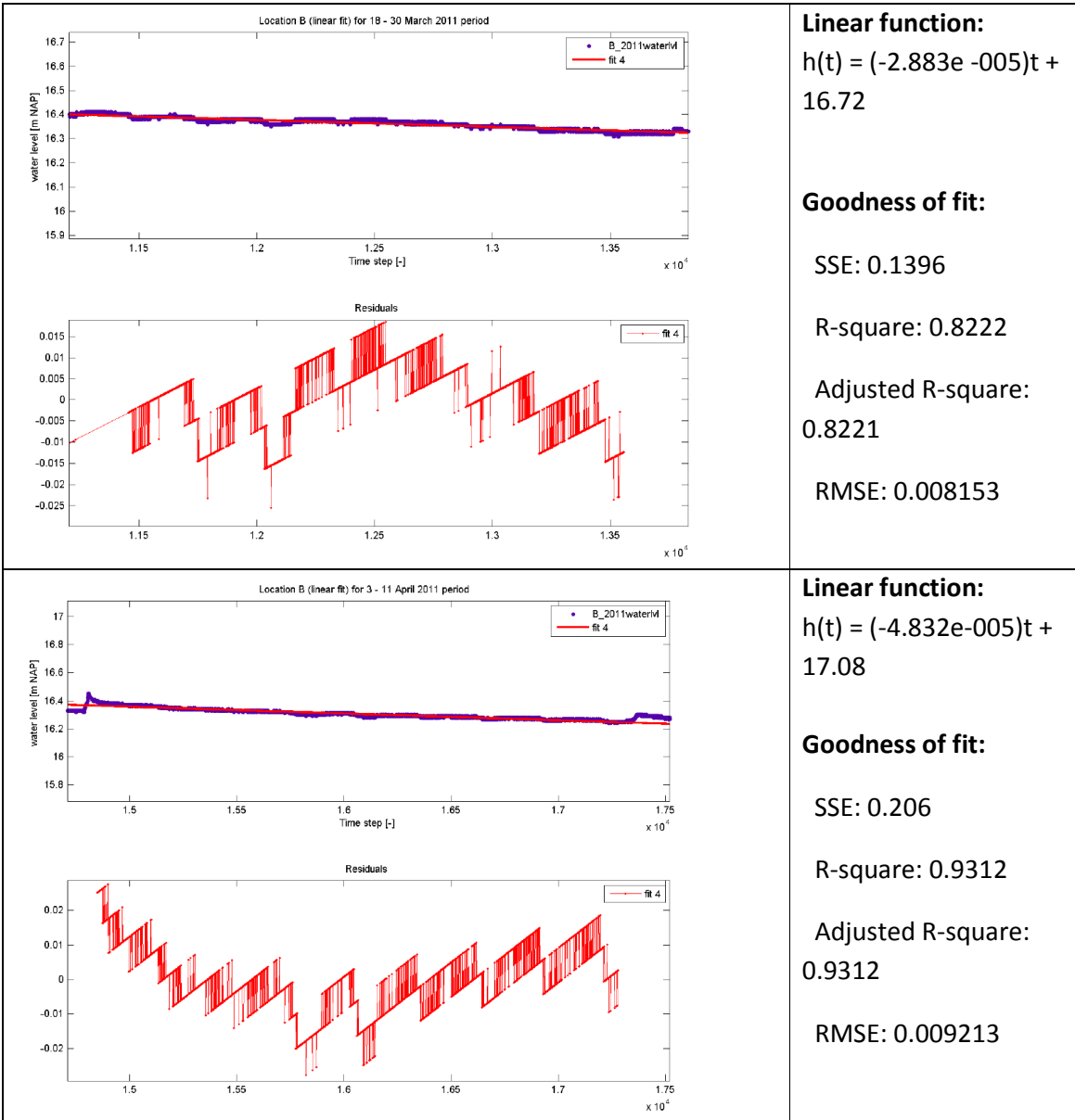


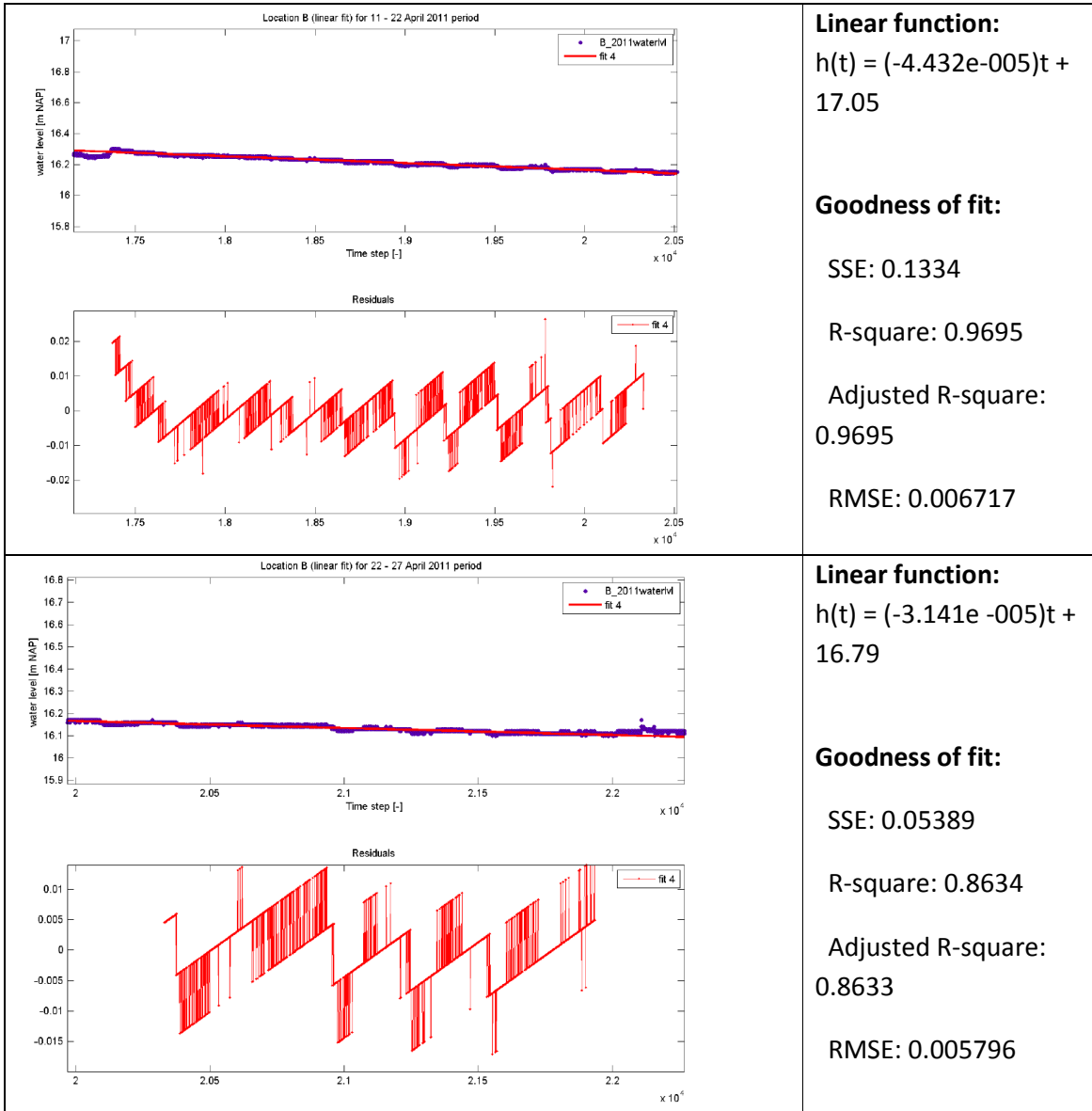


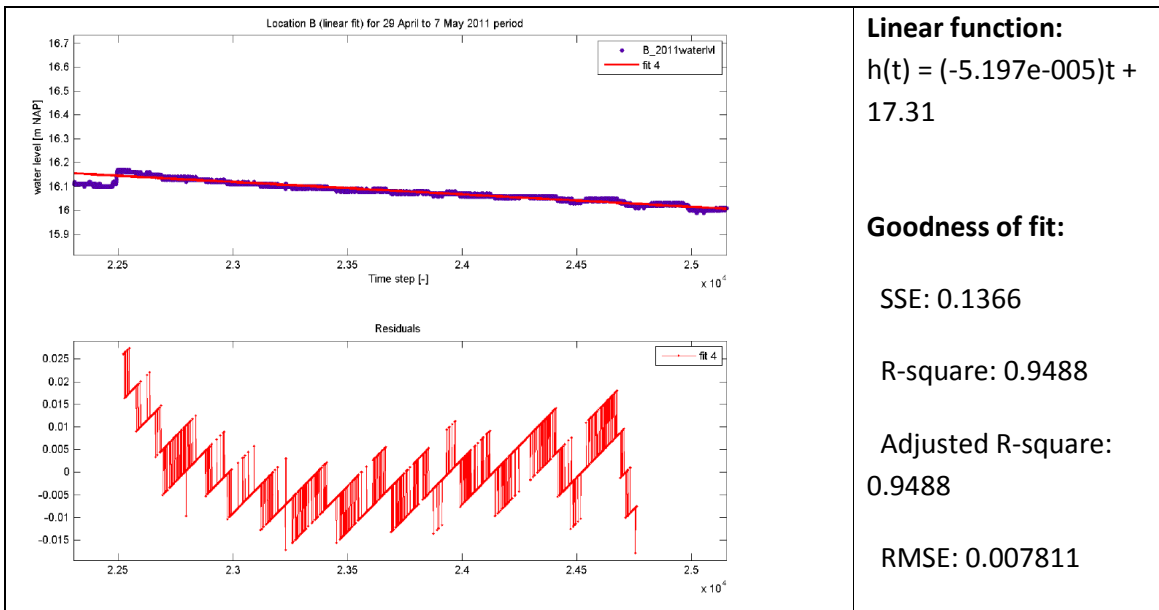
Similar to the previous curve-fitting examples, we observe that the three functions is able to fit the water level trend well during the 22 to 27 April 2011 event. All the Root Mean Squared Error are less than 0.01m, this further demonstrates the good prediction capabilities by these functions.

Appendix 12 Curve-fitting using linear function at Locations B, C, D, E, F and Pt7



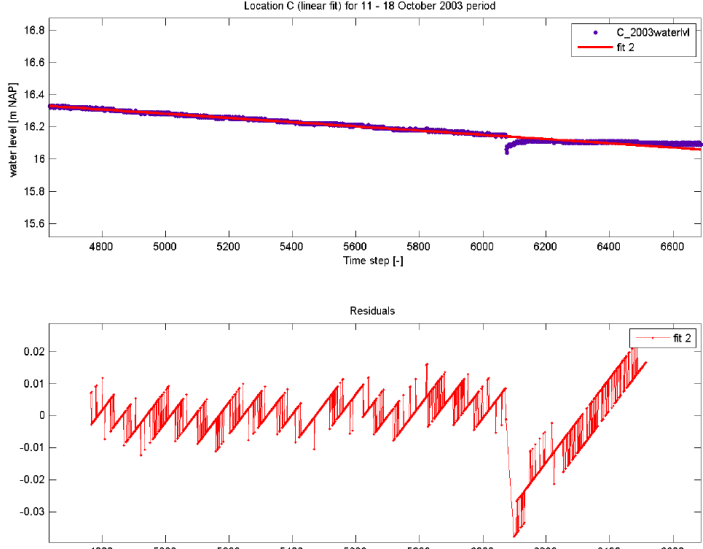
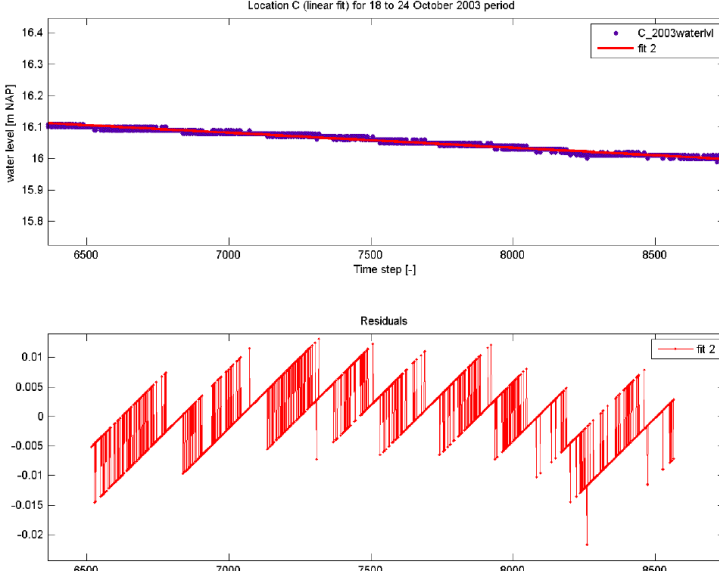


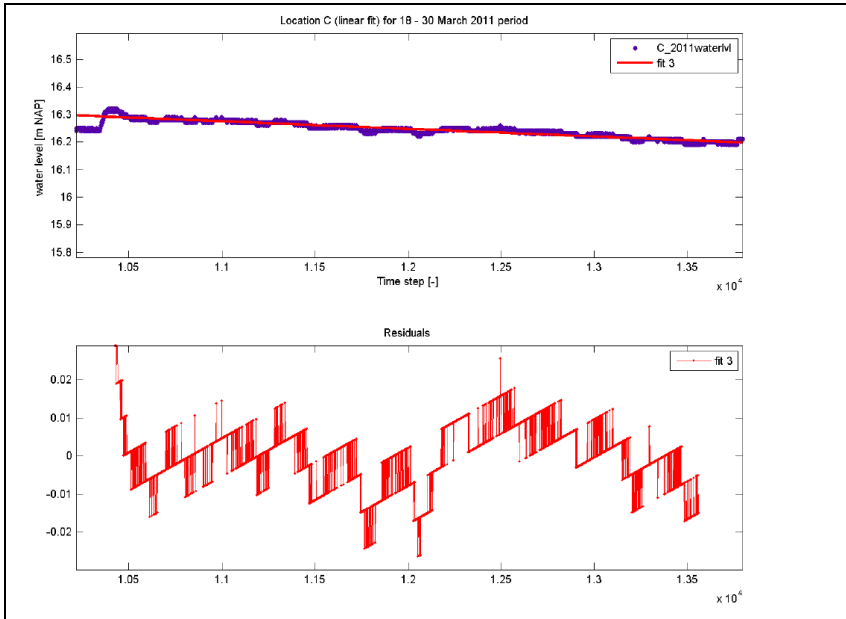




The linear function is capable of fitting the water trend observed at Location B in 2003 and 2011. All of them have less than 0.01m of Root Mean Squared Error and therefore within acceptable error tolerance limit for our analysis.

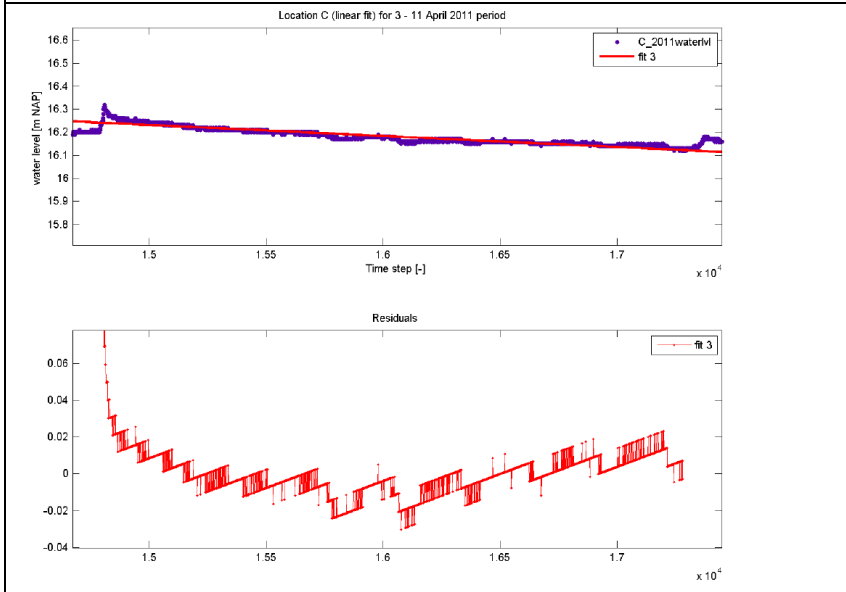
Curve-fitting using linear function at Location C

	<p>Linear function: $h(t) = (-0.0001312)t + 16.94$</p> <p>Goodness of fit:</p> <p>SSE: 0.121</p> <p>R-square: 0.9843</p> <p>Adjusted R-square: 0.9843</p> <p>RMSE: 0.008384</p>
	<p>Linear function: $h(t) = (-4.784e-005)t + 16.42$</p> <p>Goodness of fit:</p> <p>SSE: 0.05952</p> <p>R-square: 0.965</p> <p>Adjusted R-square: 0.965</p> <p>RMSE: 0.005391</p>



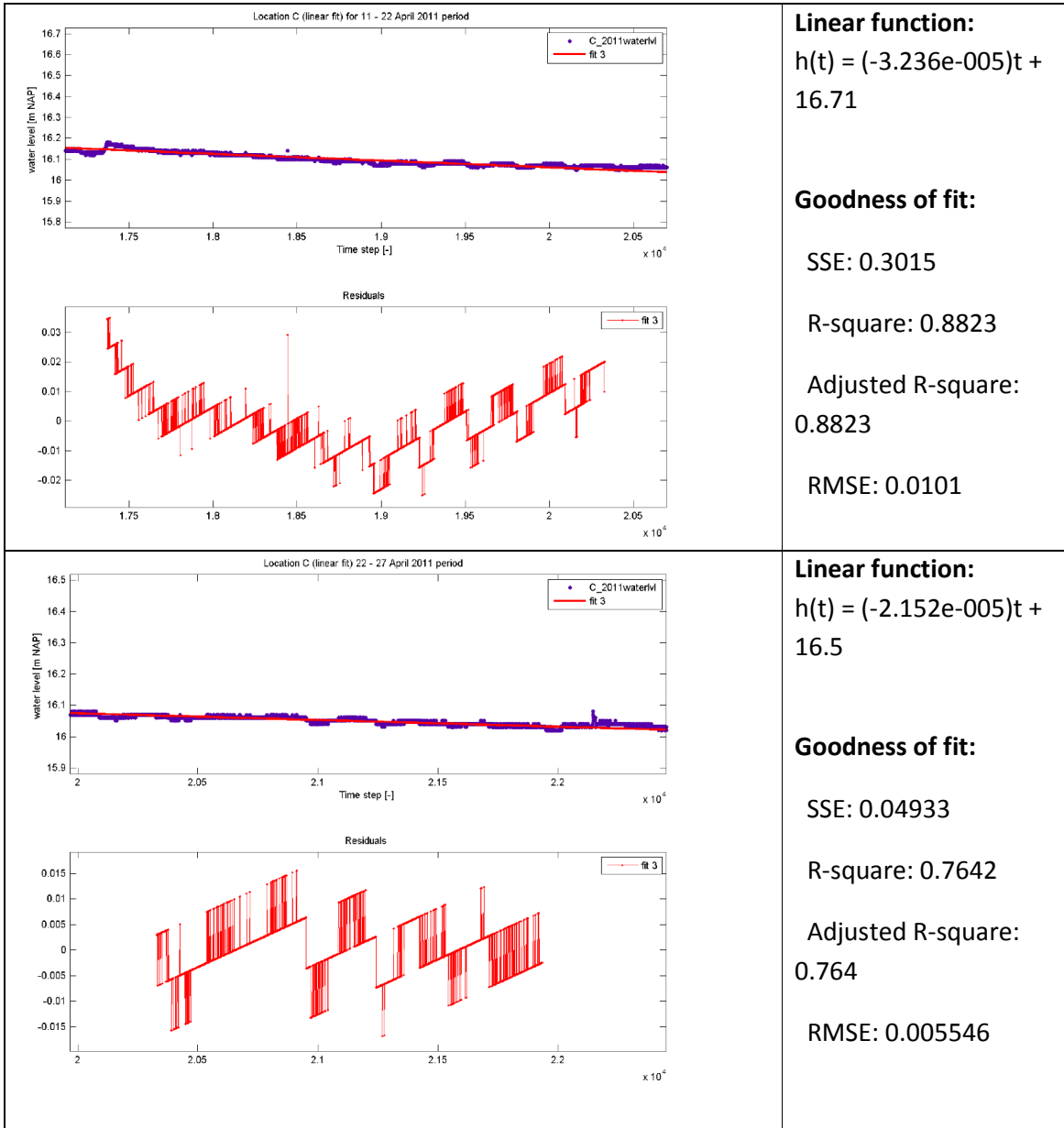
Linear function:
 $h(t) = (-2.749e-005)t + 16.58$

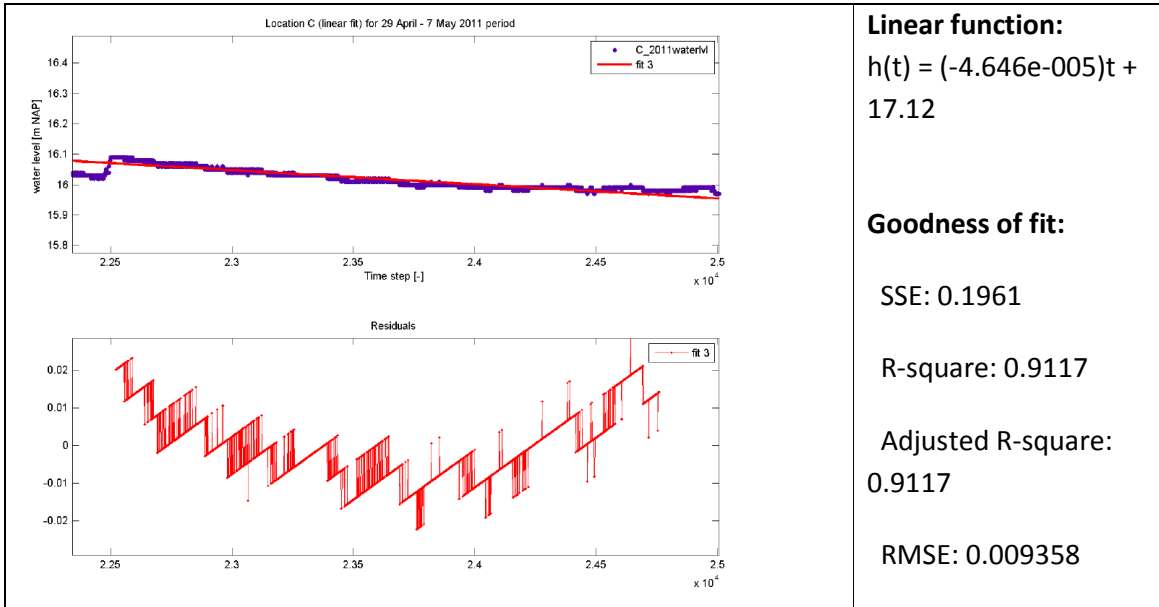
Goodness of fit:
 SSE: 0.2143
 R-square: 0.9004
 Adjusted R-square: 0.9004
 RMSE: 0.008272



Linear function:
 $h(t) = (-4.767e-005)t + 16.95$

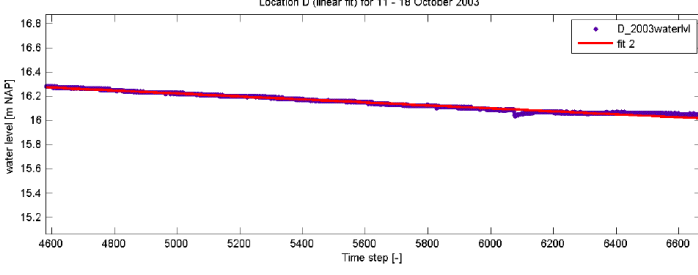
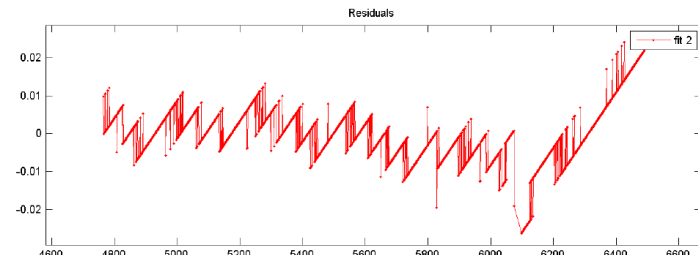
Goodness of fit:
 SSE: 0.3248
 R-square: 0.8983
 Adjusted R-square: 0.8982
 RMSE: 0.01146

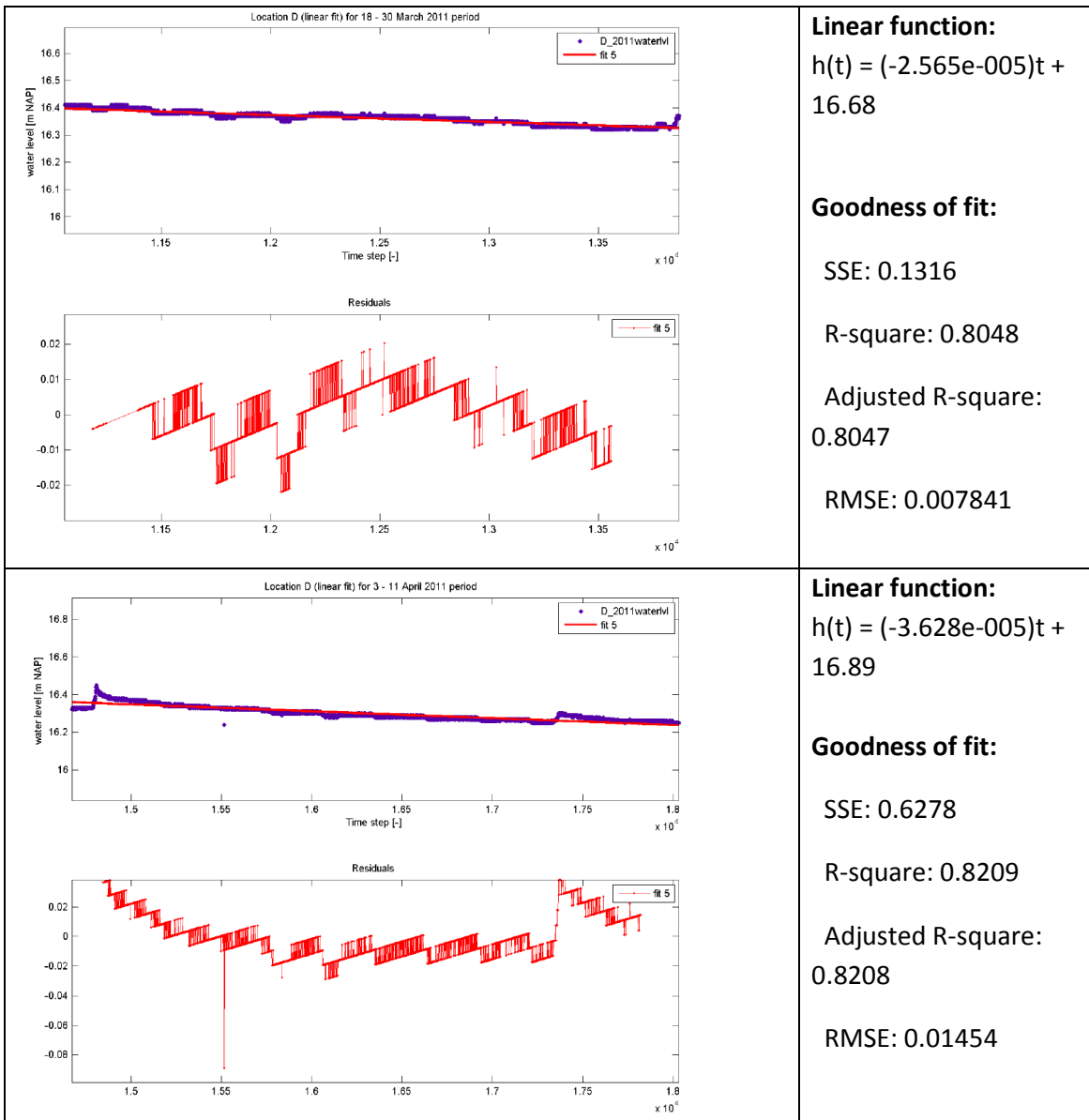


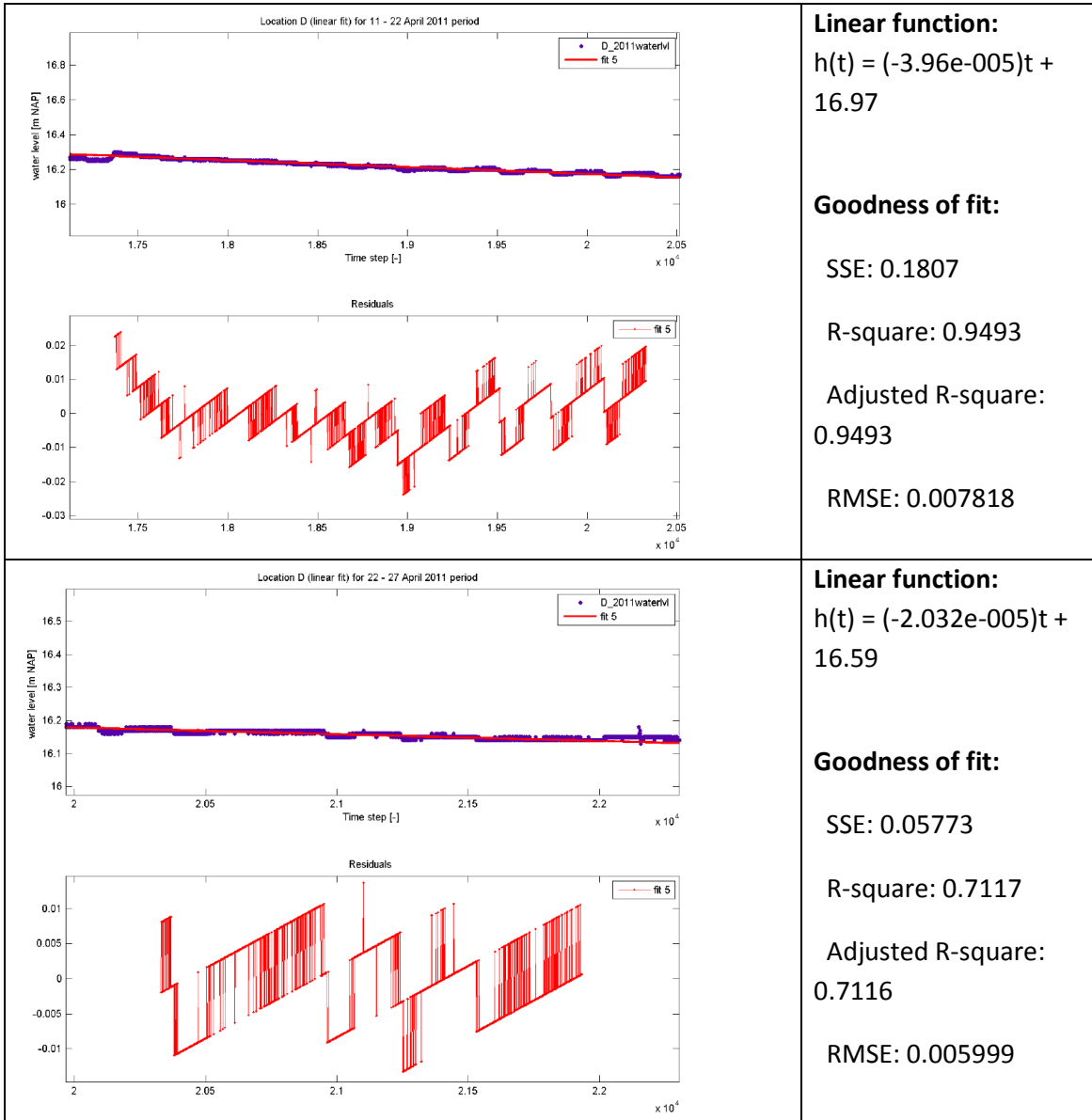


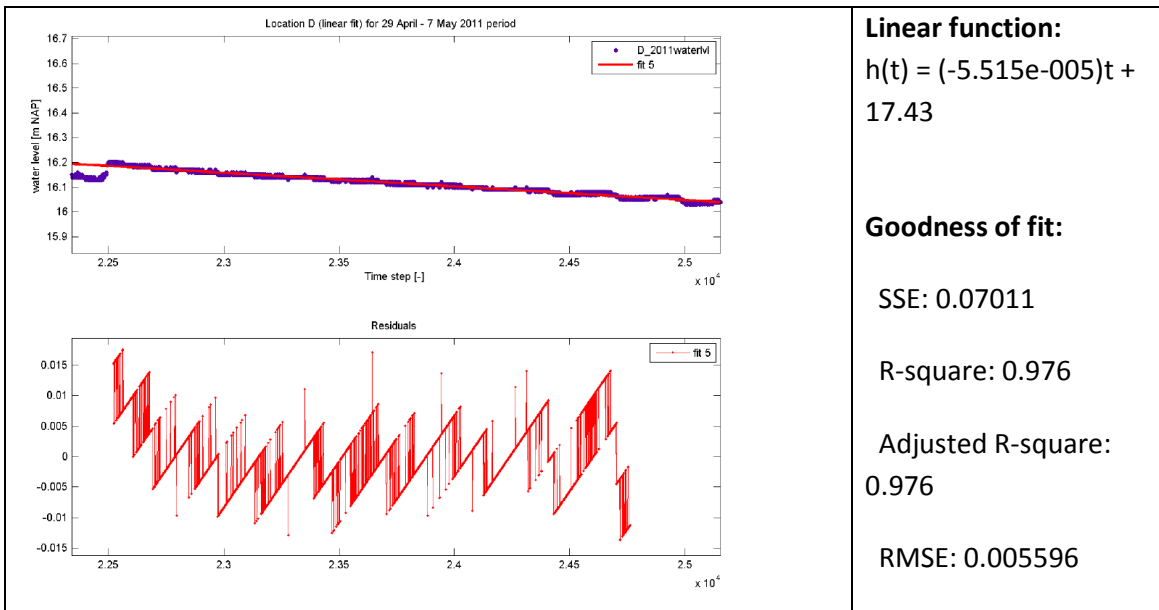
Using the linear function, we are able to achieve close to 0.01m of Root Mean Squared Error for our curve-fitting of the water trend observed at Location C in 2003 and 2011.

Curve-fitting using linear function at Location D

 <p>Location D (linear fit) for 11 - 18 October 2003</p>	<p>Linear function: $h(t) = (-0.000123)t + 16.84$</p> <p>Goodness of fit:</p> <p>SSE: 0.1045</p> <p>R-square: 0.9846</p> <p>Adjusted R-square: 0.9846</p> <p>RMSE: 0.007791</p>
 <p>Residuals</p>	<p>Linear function: $h(t) = (-5.748e-005)t + 16.45$</p> <p>Goodness of fit:</p> <p>SSE: 0.1198</p> <p>R-square: 0.9519</p> <p>Adjusted R-square: 0.9519</p> <p>RMSE: 0.00765</p>

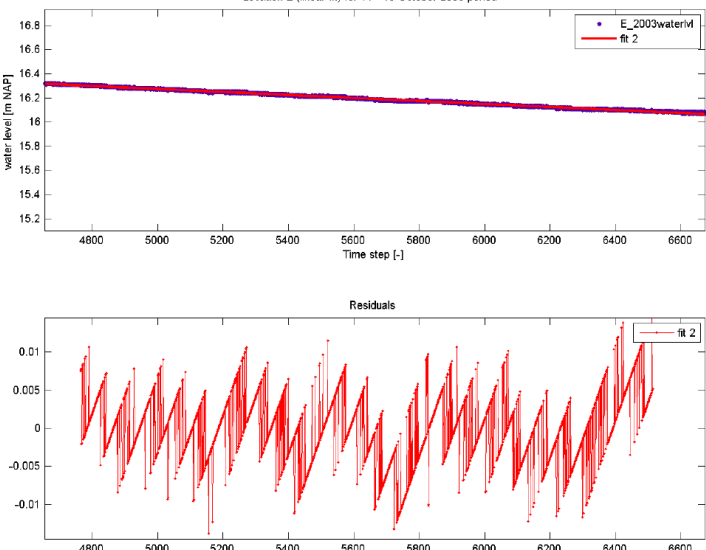
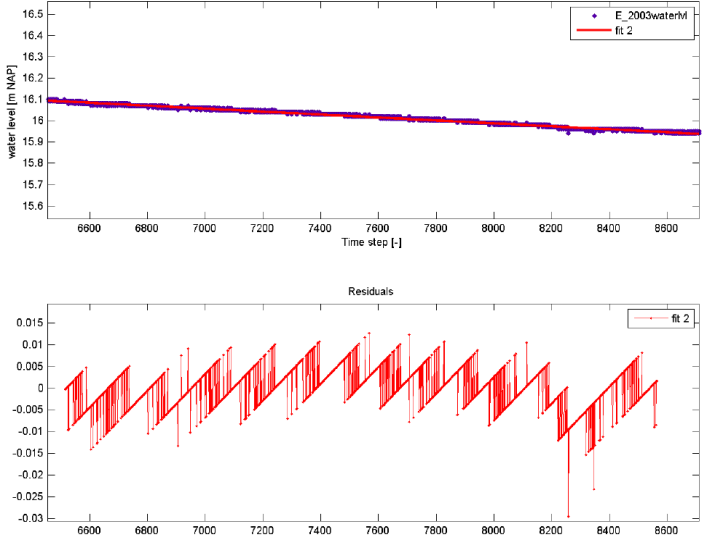


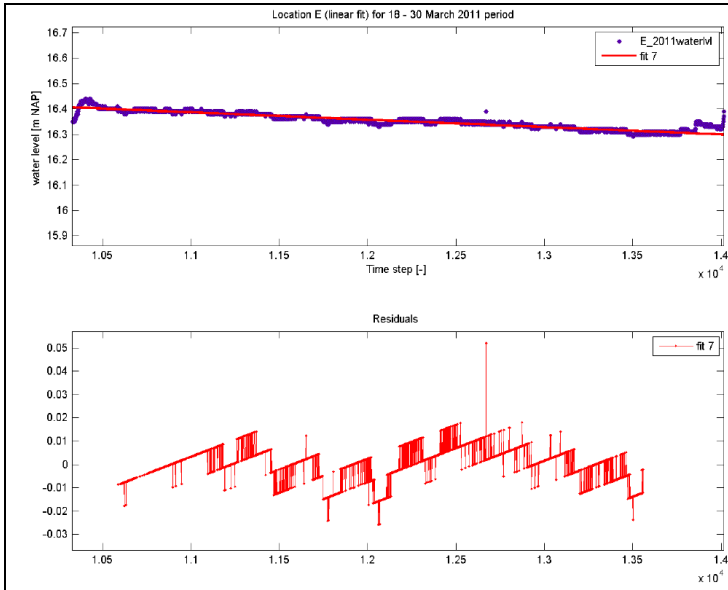




Using the linear function, we are able to achieve less than 0.01m of Root Mean Squared Error (except for one, the 3 – 11 April 2011 plot with RMSE of 0.014m) for our curve-fitting of the water trend observed at Location D in 2003 and 2011.

Curve-fitting using linear function at Location E

 <p>Location E (linear fit) for 11 - 18 October 2003 period</p> <p>water level [m NAP]</p> <p>Time step [-]</p> <p>Residuals</p>	<p>Linear function:</p> $h(t) = (-0.0001244)t + 16.9$ <p>Goodness of fit:</p> <p>SSE: 0.03863</p> <p>R-square: 0.9944</p> <p>Adjusted R-square: 0.9944</p> <p>RMSE: 0.004701</p>
 <p>Location E (linear fit) for 18 - 24 October 2003 period</p> <p>water level [m NAP]</p> <p>Time step [-]</p> <p>Residuals</p>	<p>Linear function:</p> $h(t) = (-6.93e-005)t + 16.54$ <p>Goodness of fit:</p> <p>SSE: 0.04304</p> <p>R-square: 0.9877</p> <p>Adjusted R-square: 0.9877</p> <p>RMSE: 0.004585</p>



Linear function:

$$h(t) = (-2.914e-005)t + 16.71$$

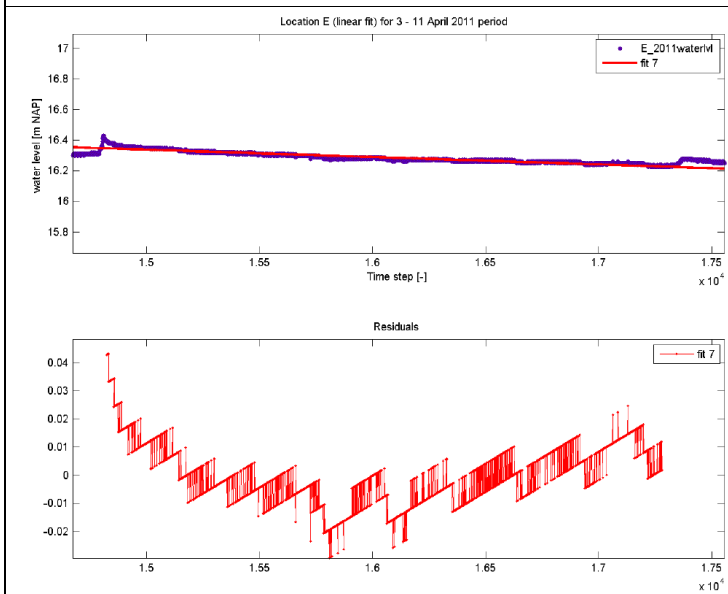
Goodness of fit:

SSE: 0.1592

R-square: 0.9127

Adjusted R-square:
0.9127

RMSE: 0.007481



Linear function:

$$h(t) = (-4.845e-005)t + 17.07$$

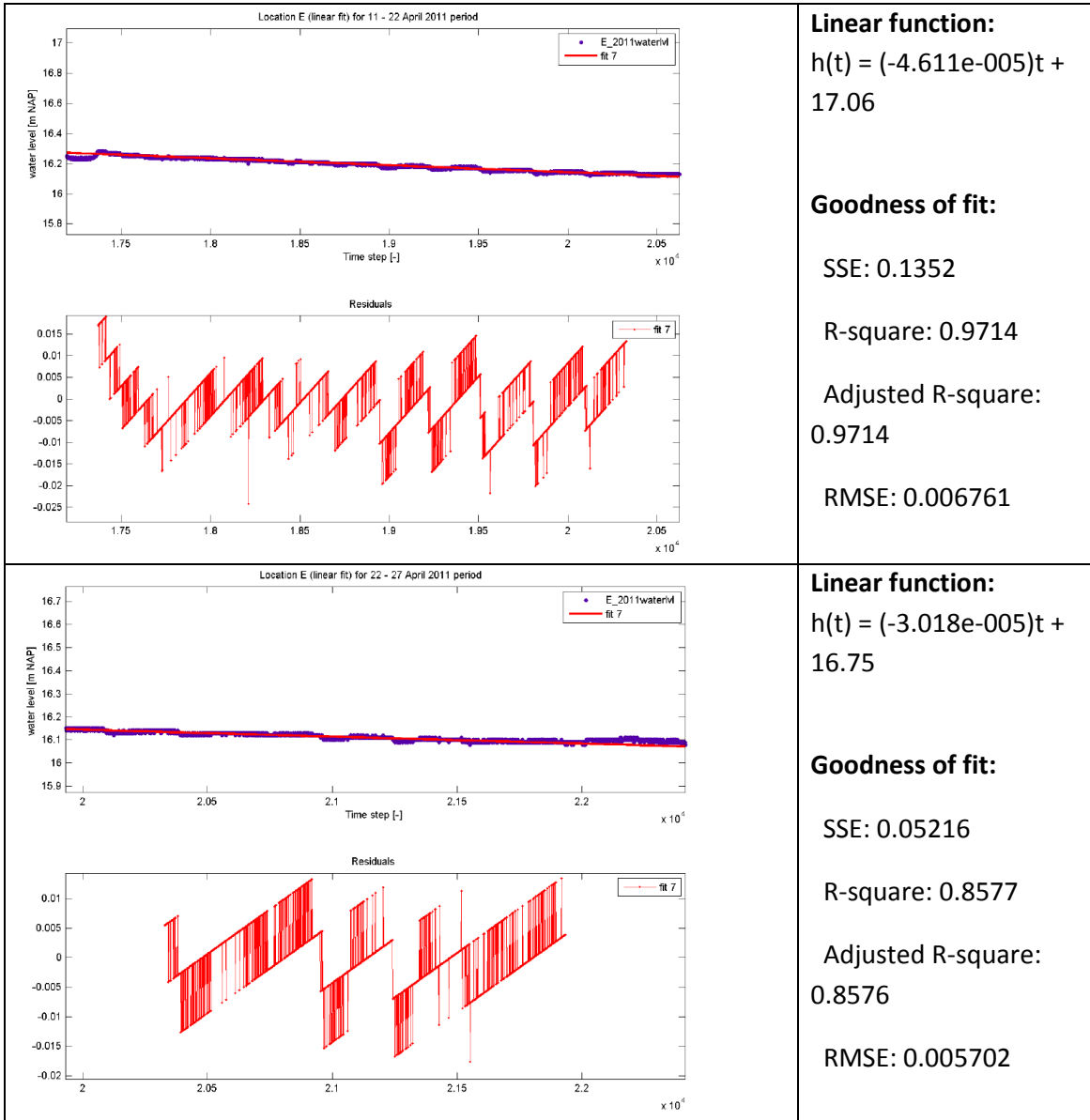
Goodness of fit:

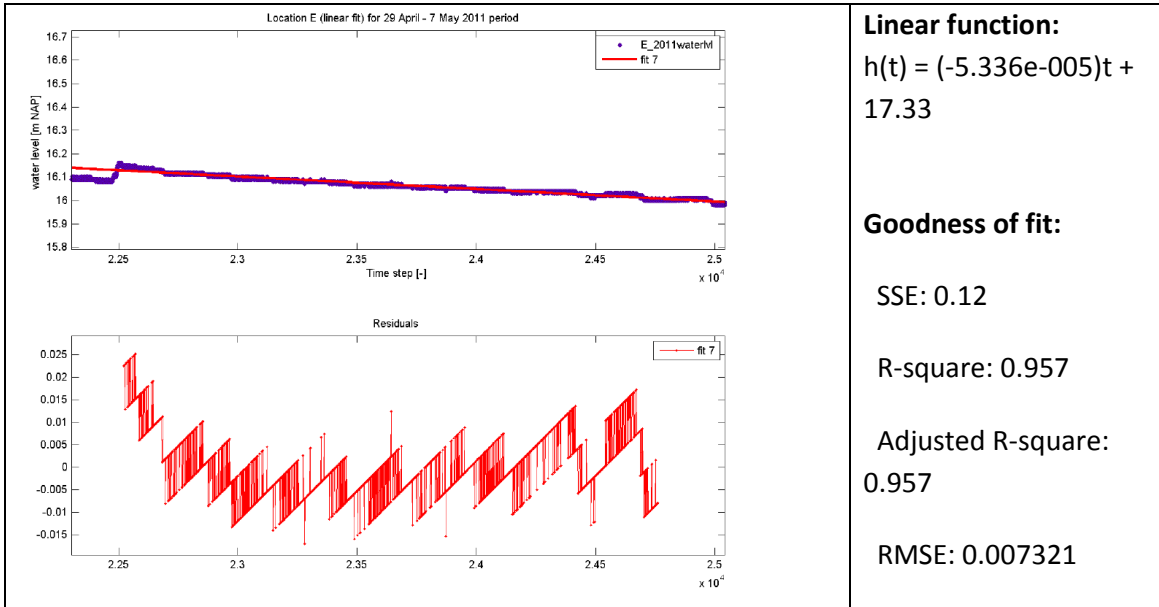
SSE: 0.2815

R-square: 0.9118

Adjusted R-square:
0.9117

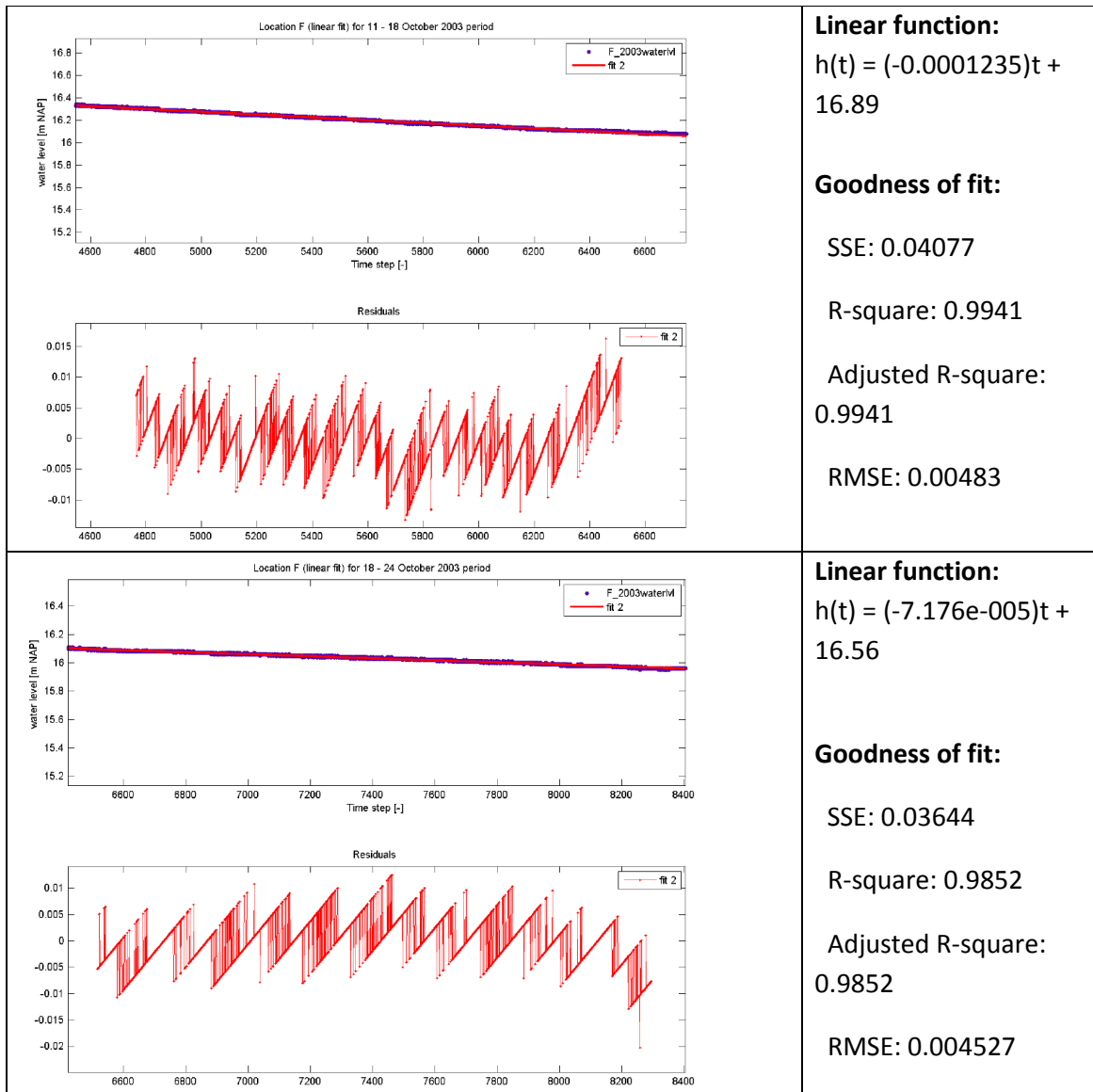
RMSE: 0.0107

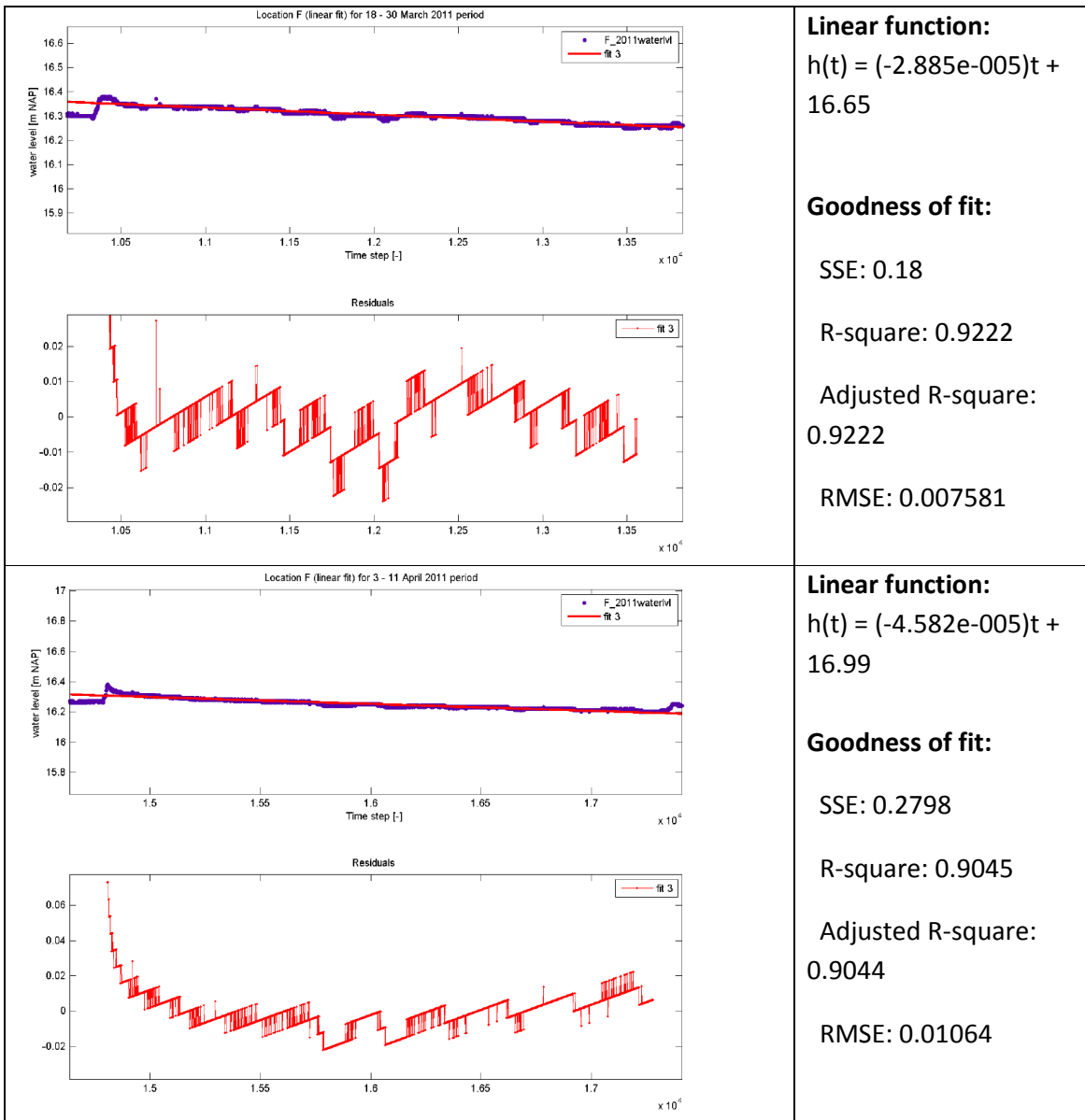


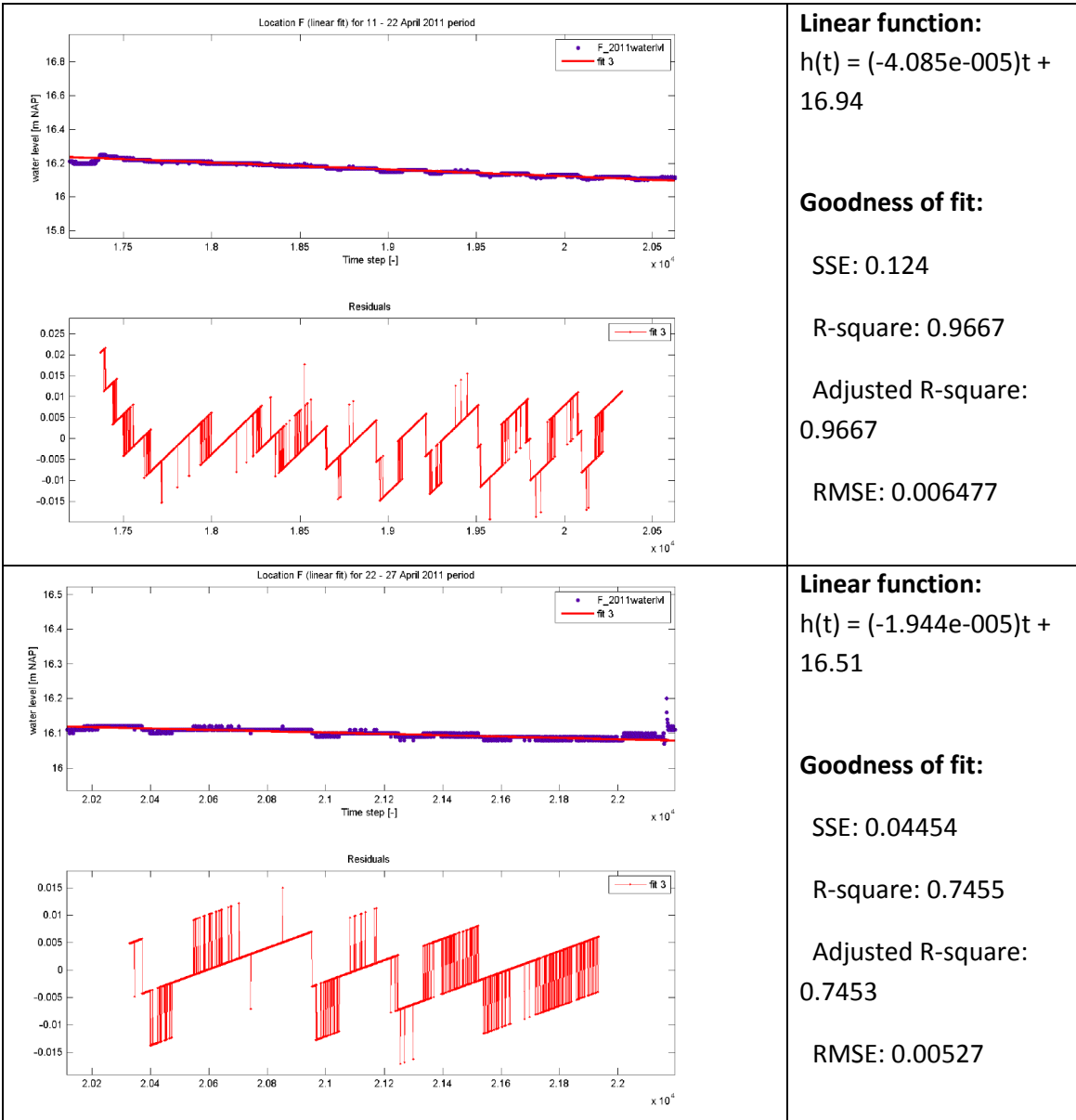


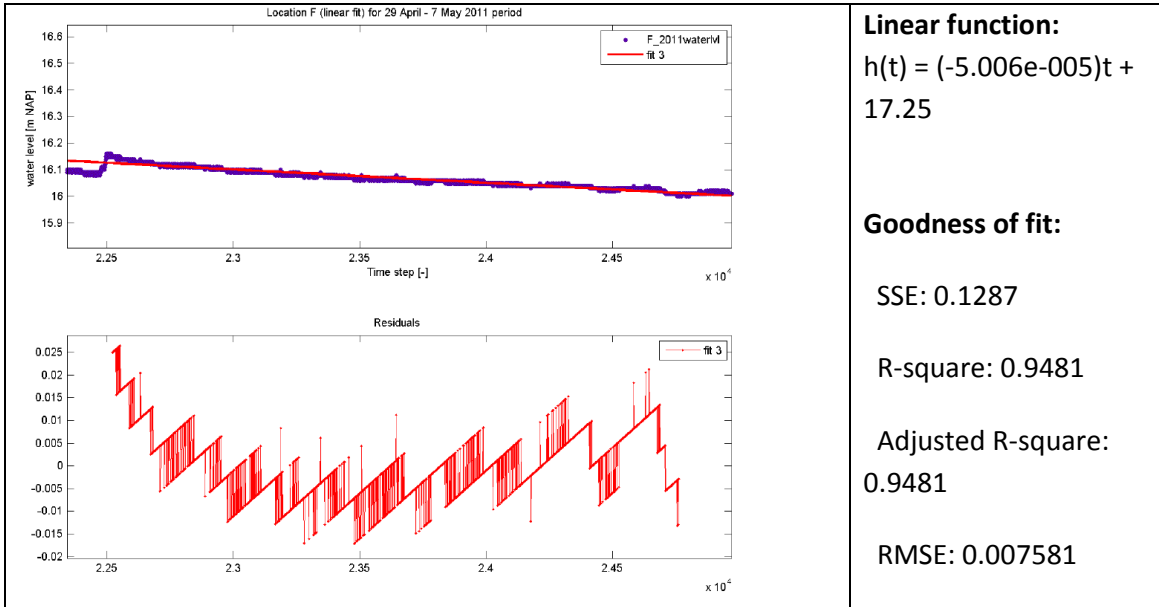
Using the linear function, we are able to achieve less than 0.01m of Root Mean Squared Error (except for one, the 3 – 11 April 2011 plot with RMSE of 0.0107m that is still acceptable) for our curve-fitting of the water trend observed at Location E in 2003 and 2011.

Curve-fitting using linear function at Location F



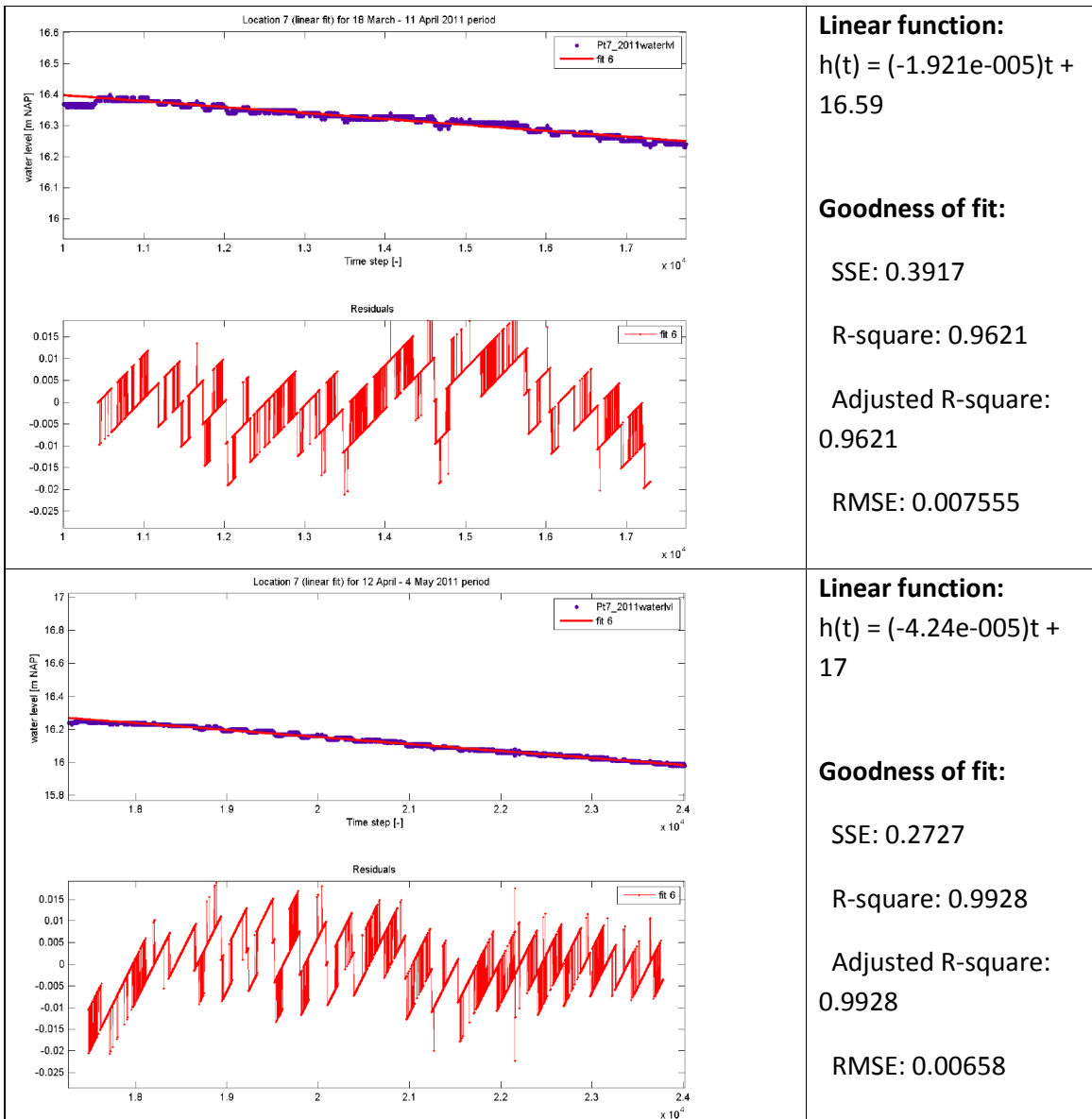






Using the linear function, we are able to achieve less than 0.01m of Root Mean Squared Error (except for one, the 3 – 11 April 2011 plot has a RMSE of 0.0106m which is still acceptable) for our curve-fitting of the water trend observed at Location F in 2003 and 2011.

Curve-fitting using linear function at Location 7 (surface water)



Using the linear function, we can achieve less than 0.01m of Root Mean Squared Error for our curve-fitting of the water trend observed at Location 7 (surface water) in 2011.

Appendix 13 Summary of the equations of water level trends derived from curve-fitting method

Monitoring location	2003	2011	Percentage difference in exfiltration rates (2011 – 2003)/2003
Location A	$h(t) = (-0.0001194)t + 16.89$ $h(t) = (-7.166e-005)t + 16.59$	$h(t) = (-2.682e-005)t + 16.67$ $h(t) = (-4.688e-005)t + 17.03$ $h(t) = (-4.633e-005)t + 17.06$ $h(t) = (-3.269e-005)t + 16.79$ $h(t) = (-4.985e-005)t + 17.23$	Upper range: -58.2% Lower range: -62.5%
	Average rate: -9.553e-05	Average rate: -4.051e-05	Average difference: 57.6% reduction
Location B	$h(t) = (-0.0001218)t + 17$ $h(t) = (-7.054e-005)t + 16.67$	$h(t) = (-2.883e-005)t + 16.72$ $h(t) = (-4.832e-005)t + 17.08$ $h(t) = (-4.432e-005)t + 17.05$ $h(t) = (-3.141e-005)t + 16.79$ $h(t) = (-5.197e-005)t + 17.31$	Upper range: -57.3% Lower range: -59.1%
	Average rate: -9.617e-05	Average rate: -4.097e-05	Average difference: 57.4% reduction
Location C	$h(t) = (-0.0001312)t + 16.94$ $h(t) = (-4.784e-005)t + 16.42$	$h(t) = (-2.749e-005)t + 16.58$ $h(t) = (-4.767e-005)t + 16.95$ $h(t) = (-3.236e-005)t + 16.71$ $h(t) = (-2.152e-005)t +$	Upper range: -64.6% Lower range: -55%

		16.5 $h(t) = (-4.646e-005)t + 17.12$	
	Average rate: -8.952e-05	Average rate: -3.51e-05	Average difference: 60.8% reduction
Location D	$h(t) = (-0.000123)t + 16.84$ $h(t) = (-5.748e-005)t + 16.45$	$h(t) = (-2.565e-005)t + 16.68$ $h(t) = (-3.628e-005)t + 16.89$ $h(t) = (-3.96e-005)t + 16.97$ $h(t) = (-2.032e-005)t + 16.59$ $h(t) = (-5.515e-005)t + 17.43$	Upper range: -55.2% Lower range: -64.6%
	Average rate: -9.024e-05	Average rate: -3.54e-05	Average difference: 60.8% reduction
Location E	$h(t) = (-0.0001244)t + 16.9$ $h(t) = (-6.93e-005)t + 16.54$	$h(t) = (-2.914e-005)t + 16.71$ $h(t) = (-4.845e-005)t + 17.07$ $h(t) = (-4.611e-005)t + 17.06$ $h(t) = (-3.018e-005)t + 16.75$ $h(t) = (-5.336e-005)t + 17.33$	Upper range: -57.1% Lower range: -58%
	Average rate: -9.685e-05	Average rate: -4.145e-05	Average difference: 57.2% reduction
Location F	$h(t) = (-0.0001235)t + 16.89$ $h(t) = (-7.176e-005)t + 16.56$	$h(t) = (-2.885e-005)t + 16.65$ $h(t) = (-4.582e-005)t + 16.99$ $h(t) = (-4.085e-005)t + 16.94$ $h(t) = (-1.944e-005)t + 16.51$ $h(t) = (-5.006e-005)t + 17.25$	Upper range: -59.5% Lower range: -72.9%

	Average rate: -9.763e-05	Average rate: -3.7e-05	Average difference: 62.1% reduction
Location Pt 7 (surface water)	-	h(t) = (-1.921e-005)t + 16.59 h(t) = (-4.24e-005)t + 17	Not applicable as this location was not monitored in 2003.
		Average rate: -3.1e-05	